MANIPULATING GROWTH AND DIFFERENTIATION OF EMBRYONIC INTESTINE IN ORGAN CULTURE

A thesis submitted to the University of Manchester from the degree of

Doctor in Philosophy

in the Faculty of Biology, Medicine and Health

2016

Riccardo Coletta

School of Biological Sciences

Division of Cell Matrix Biology and Regenerative Medicine

Table of contents

Word count: 44.027

List of figures

List of tables

Abstract

University of Manchester

Name: Riccardo Coletta

Degree Title: Doctor of Philosophy

Thesis title: Manipulating growth and differentiation of embryonic intestine in organ culture.

Date: 2016

Background. An *ex vivo* experimental strategy replicating *in vivo* intestinal development would provide an accessible setting to study normal and dysmorphic biology, and would be a test bed for tissue engineering. Previous studies implicated transforming growth factor β1 (TGFβ1) in postnatal gut maturation and regeneration following injury, but its potential role in intestinal development is poorly understood. I firstly hypothesised that embryonic small intestine is able to heal after physical injury. To test this idea, I aimed to create an organ culture model using explants of embryonic jejunum. I secondly hypothesised that TGFβ1 affects embryonic small intestine growth and differentiation. Accordingly, I aimed to use the same organ culture model to determine potential effects of exogenous TGFβ1.

Methods. Segments of mouse embryonic jejunum were isolated by dissection and placed on semipermeable platforms. They were fed with defined, serum free, media, in some cases supplemented with TGFβ1. Growth, differentiation and healing of explants were characterized and quantified using a battery of techniques that included whole mount imaging, histology, immunostaining and RNA arrays. TGFβ1 was measured in amniotic fluid by enzyme-linked immunosorbent assay. Groups were compared by statistical tests.

Results. After three days of culture, jejunal rudiments differentiated from simple tubes into a more complex structures containing smooth muscle surrounding newly formed villi. Pairs of rudiments, linked by a thread, fused and formed a continuous single lumen, as assessed by trajectories of fluorescent dextrans injected into their distal ends. Functional continuity was confirmed by spontaneous waves of peristalsis crossing the point of fusion. *In vivo*, TGFβ receptors I and II were detected in embryonic longitudinal smooth muscle cells and, in organ culture, exogenous TGFβ1 induced differentiation of longitudinal smooth muscle. Microarray profiling showed that TGFβ1 increased smooth muscle associated transcripts in a dose-dependent manner. TGFβ1 protein was detected in amniotic fluid at a time when the embryonic small intestine was physiologically herniated.

Conclusion. Embryonic jejunal segments can fuse to form a single functional organ when aided by a mechanical manipulation. By analogy with the requirement for exogenous TGFβ1 for smooth muscle differentiation in culture, the TGFβ1 protein that I demonstrated to be present in the amniotic fluid may enhance intestinal development when it is physiologically herniated in early gestation. Future studies of embryonic intestinal cultures should add TGFβ1 in the defined media to produce a more faithful model of *in vivo* muscle differentiation. In future, this model could be used to test whether other growth factors enhance intestinal growth, and so pave the way to novel biological treatments for short bowel syndrome, a devastating disease with a high mortality.

Declaration

No portion of the work referred to in this thesis has been submitted in support of an application for another degree or qualification of this or any other university or other institute learning.

Copyright statement

The following four notes on copyright and the ownership of intellectual property rights must be included as written below:

i. The author of this thesis (including any appendices and/or schedules to this thesis) owns certain copyright or related rights in it (the "Copyright") and he has given The University of Manchester certain rights to use such Copyright, including for administrative purposes.

ii. Copies of this thesis, either in full or in extracts and whether in hard or electronic copy, may be made **only** in accordance with the Copyright, Designs and Patents Act 1988 (as amended) and regulations issued under it or, where appropriate, in accordance with licensing agreements which the University has from time to time. This page must form part of any such copies made.

iii. The ownership of certain Copyright, patents, designs, trademarks and other intellectual property (the "Intellectual Property") and any reproductions of copyright works in the thesis, for example graphs and tables ("Reproductions"), which may be described in this thesis, may not be owned by the author and may be owned by third parties. Such Intellectual Property and Reproductions cannot and must not be made available for use without the prior written permission of the owner(s) of the relevant Intellectual Property and/or Reproductions.

iv. Further information on the conditions under which disclosure, publication and commercialisation of this thesis, the Copyright and any Intellectual Property and/or Reproductions described in it may take place is available in the University IP Policy (see http://documents.manchester.ac.uk/DocuInfo.aspx?DocID=2442 0), in any relevant Thesis restriction declarations deposited in the University Library, The University Library's regulations (see http://www.library.manchester.ac.uk/about/regulations/) and in The University's policy on Presentation of Theses

Acknowledgments

Thanks to my two supervisors' Professor Adrian S. Woolf and Professor Antonino Morabito for giving me this opportunity to work on this project.

Thanks to Professor Adrian S. Woolf, without his help this research would not have been possible. Professor Adrian S. Woolf has had a key role during this research; he has opened my mind, showing the importance to be critical, to be organized and to think as a scientist.

Thanks to Professor Antonino Morabito and his contagious dedication to the treatment of short bowel syndrome. He inspired me during my research and I am honoured to have worked alongside him. Thank you for supporting me through the idea to create an intestinal healing with no stitch and to study intestinal development.

Special thanks to Dr Neil A. Roberts and Dr Emma N. Hilton who worked alongside me and have taught me everything I know about hand-on laboratory. They made my years of research a really good experience "outside the lab".

Next, I would like to thank the Royal Manchester Children's Hospital and Short Bowel Charity for funding my research.

Thanks to all my friends in Italy because their encouragement supported me through these years abroad.

Finally and most importantly, I would like to thank my family: my father Francesco, my mother Maria Rita, my sister Francesca and my grandmother Vittorina. Your love supported me during these years abroad. A special thought goes to my grandfather Antonio. Even if you are no longer here, your memory will never leave me.

Preface – The Author

I am a paediatric surgeon trained at the Catholic University of Sacred Heart in Rome, Italy and I graduated as a medical doctor at the La Sapienza, University of Rome. I hold a clinical position as Senior Clinical Fellow (Registrar) at the Paediatric Autologous Bowel Reconstruction and Rehabilitation Unit in the Royal Manchester Children's Hospital in Manchester, UK since 2014.

During my surgical training, I have faced many newborn that undertake experience of massive intestinal resection due to catastrophic intestinal diseases. As a consequence, these patients will develop a condition known as Short Bowel Syndrome (SBS), a condition with poor prognosis and a reduction of quality of life. The challenge to find an effective treatment of this disease inspired me to gain further knowledge on intestinal development and to train myself with the most advanced surgical techniques for intestinal rehabilitation. These impulses motivated me to move to Manchester in 2013. Manchester gave me the opportunity to learn science, to open my mind and to improve as a surgeon.

During my PhD, my research was recognised by the Journal of Tissue Engineering and Regenerative Medicine and my works was published in the Journal (Coletta *et al.*, 2016; Coletta *et al.*, 2017). Copies of the papers are attached to the present thesis. For this research I had the honour to be awarded the prestigious Peter Paul Rickman Prize at the 61st British Association of Paediatric Surgery annual international congress in Edinburgh, July 2014. In 2013, 2014 and 2015 I was awarded best researcher at an Italian Conference of Paediatric Surgery. Furthermore, in 2014 I was awarded the best poster prize at the 8th Pediatric Intestinal Failure and Rehabilitation Symposium in Atlanta, USA.

Abbreviations

Ab	Antibody
α-SMA	α-Smooth muscle actin
AIP	Anterior intestinal portal
BABB	Benzyl alcohol/Benzyl benzoate
BAPS	British Association Paediatric Surgery
BMP	Bone morphogenetic proteins
BSA	Bovine serum albumin
C	Circular
CBCs	Crypt base columnar cells
cDNA	Complementary DNA
CDX	Caudal-type home-box factor
CD1	Cluster of differentiation 1
CM	Circular muscle
CIP	Caudal intestinal portal
CS	Carnegie stage
Ct	Cycle threshold
CTE	Controlled tissue expansion
DAPI	Diamidino phenylindole
DMEM	Dulbecco's modified eagle medium
E	Embryonic day
e	Epithelium
ECM	Extracellular matrix
EECs	Entero-endocrine cells

EGF	Epidermal growth factor
ELISA	Enzyme-linked immunosorbent assay
ENS	Enteric neuronal system
ESCs	Embryonic stem cells
FGF9	Fibroblast growth factor 9
Gapdh	Glyceraldehyde 3-phosphate dehydrogenase
GDF	Growth differentiation factor
GDNF	Glial cell line-derived neurotrophic factor
GO	Gene ontology
IFALD	Intestinal failure-associated liver disease
IHH	Indian hedgehog
im	Inner mesenchyme
ISCs	Intestinal stem cells
IST	Insulin, sodium selenite, transferrin
l	Longitudinal
LGR5	Leucine-rich repeat-containing G protein-coupled receptor 5
LILT	Longitudinal intestinal lengthening and tailoring
LM	Longitudinal muscle
LRCs	Label-retaining cells
MAD	Mothers against decapentaplegic
MAPK	Mitogen activated protein kinase
MOM	Mouse on Mouse
om	Outer mesenchyme
p	Phospho
PAS	Periodic acid-Schiff

PBS	Phosphate-buffered saline
PCA	Principal components analysis
PCR	Polymerase chain reaction
PDGF	Platelet derived growth factor
PSA	Penicillin G, streptomycin, amphotericin B
QPCR	Quantitative polymerase chain reactions
RET	Rearranged during transfection
SBS	Short bowel syndrome
SD	Standard deviation
SEM	Standard error of mean
SEM	Scanning electron microscopy
SHH	Sonic hedgehog
SILT	Spiral intestinal lengthening and tailoring
SM	Smooth muscle
SMA	Small body size
SOX	Sex-determining region Y-related high mobility group box
STEP	Serial transverse enteroplasty procedure
TESI	Tissue-engineered small intestine
TPN	Total parenteral nutrition
TGF	Transforming growth factor
TGFβR	Transforming growth factor β receptor
WNT	Wingless-related integration site

1 CHAPTER 1 - Background

1.1 Overview of this thesis

The small intestine is responsible for propelling, digesting and absorbing nutrients in vertebrate. Unfortunately, in humans, malformations during neonatal period or injury during later life can lead to profound reduction of intestinal length. As a consequence, the individual is unable to absorb enough nutrients for normal growth, generating the life threating condition called short bowel syndrome (SBS).

SBS has an estimated incidence of 25/100,000 live births (Wales *et al.*, 2004). Although medical and surgical approaches to treatment have been developed for SBS, new therapeutic approaches are needed to reduce its poor outcome and mortality.

Developmental biology of the gut is a field that has the potential for significant human impact by identifying novel treatments for congenital intestinal disease. Furthermore, understanding how the small bowel develops could hold the promise that this knowledge might be used to aid intestinal repair and regeneration approaches.

In the research presented in this thesis, a novel organ culture model has been designed to investigate two parallel themes that, in combination, may help in finding novel insights for the creation of new therapeutic approaches for intestinal diseases.

Using an embryonic mice model, the first theme was to explore whether the embryonic small bowel is able to restore continuity after mechanical injury. This is important not only to understand healing and regenerative capacity of the developing

intestine but also to address possible novel therapies for intestinal human disease. The healing capacity has been analysed at morphological and mechanical levels.

The second theme was to study the role of transforming growth factor β1 (TGFβ1) during intestinal embryonic differentiation. Previous studies had implicated TGFβ1 in postnatal gut maturation and tissue remodelling after injury. However, this growth factor had been little researched with regard to intestinal development. In this study, I went on to analyse the possible effects of TGFβ1 on cultured small intestine embryonic specimens.

Accordingly, I will now introduce the reader to the following major background topics: small intestinal development; methods to investigate small intestinal development; molecular control during small intestinal development; TGFβ signalling and it possible role in small intestinal development; and short bowel syndrome in children. Finally, this background section ends with the hypotheses and aims section of the thesis.

1.2 The small intestine

The small intestine is a component of the gastrointestinal system, which is a tube-like structure that extends from the mouth to the anus. The gastrointestinal system can be divided into the oesophagus, stomach, and small and large intestine in its adult form. The food enters in the mouth where it will be cut in to pieces and the first digestion starts. After the passage through the oesophagus, the gastric acid fluids process the food into the stomach and then the nutrients will be absorbed by the small intestine. Finally, the fluids are absorbed into the large intestine and colon to reach ultimately the rectum and to be sent out through the anus.

The small intestine features a unique structure. The epithelium and the mesenchyme create a finger-like structure facing into the lumen, the villus, and folding into the mesenchyme, called crypt, where the intestinal stems cells are preserved. Furthermore, the tissue around the epithelium contains two muscular structures, the circular and the longitudinal smooth muscular layer, which are fundamental for mixing and propulsion of gut contents. The lifelong supply of new intestinal cells is made possible by intestinal stem cells (ISCs) that are located at the bottom of crypts (Leedham *et al.*, 2005; Barker *et al.*, 2007) (Figure 1.1).

This section of the thesis will highlight how the small bowel acquires its characteristic features during development with an overview of its three main components, i.e. epithelium, muscle and neurons.

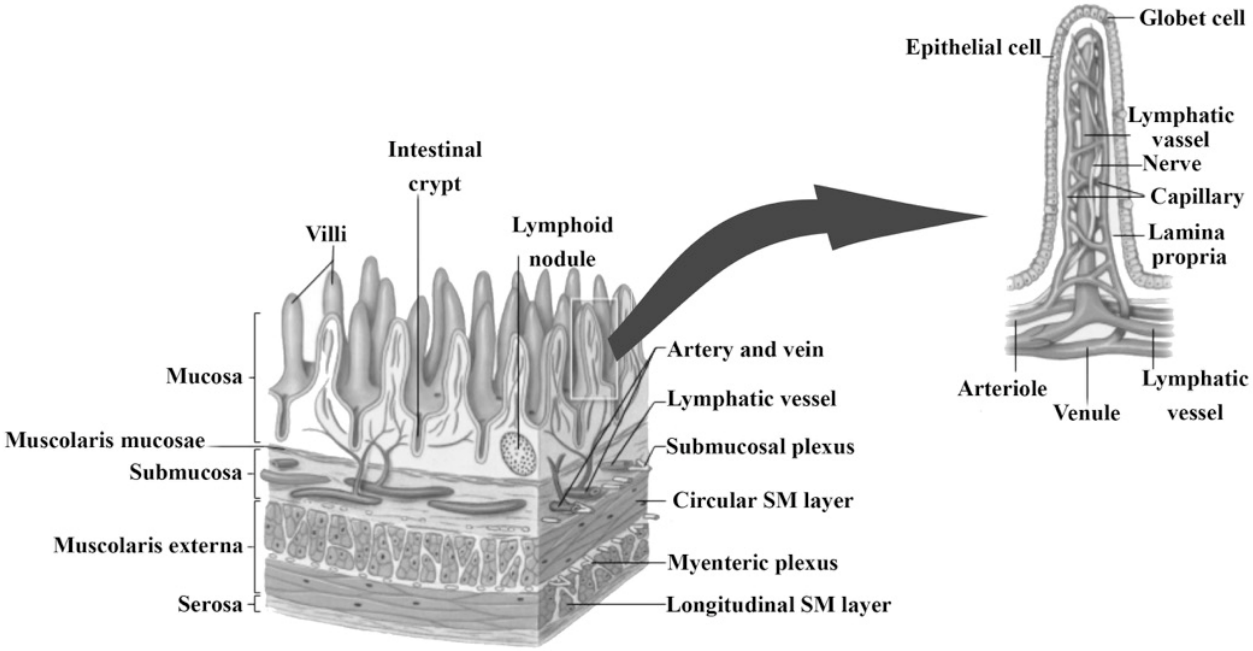

Figure 1.1 Organization of the mature small intestine

This diagrammatic picture shows the overall organization of the mature small intestine. Finger-like structures (highlighted on the right side of the picture) protruding into the lumen are villi, while crypts are the sites of intestinal stem cells. Note that below the mucosa and the muscularis mucosae are located two muscle layers (circular and longitudinal) intercalated by two neuronal plexus (submucosal and myenteric). This organization of muscles and neurons are fundamental for the creation of peristaltic waves. SM=smooth muscle. Picture adapted from (Martini *et al.*, 2015)

1.2.1 Morphological events during small intestinal development

The emergence of the gastrointestinal tract within the body cavity is one of the major innovations in vertebrate evolution, allowing the transition from an intracellular to an extracellular method of digestion (Stainier, 2005). Formation of specific segments is an important feature of the mammalian digestive tract because it optimizes digestion by enabling sequential functions, ranging from the uptake and processing of food, to absorption of nutrients and elimination of solid waste (Karasov *et al.*, 2011).

As shown previously in Figure 1.1, the human intestine reaches the mature state around 22 weeks post conception (Moxey and Trier, 1978), whereas mice gut development ends around two weeks after birth (Holmes *et al.*, 2006). Figure 1.2 shows a parallel from the main human and mouse developmental steps during intestinal development.

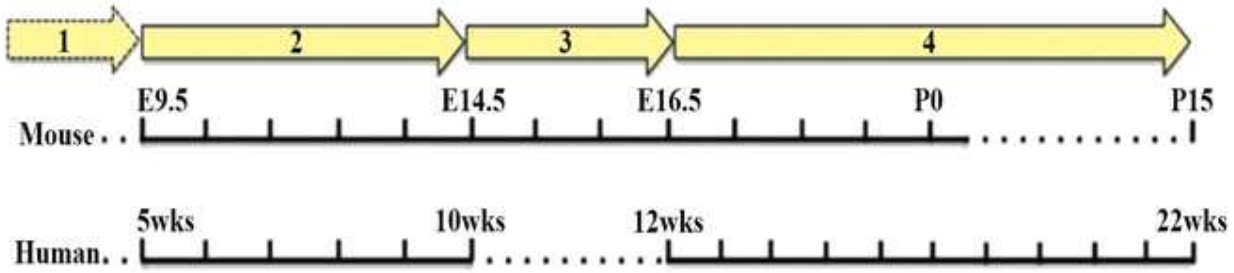

Figure 1.2 Human and mouse intestinal development

A parallel from the main human and mouse developmental step is proposed by the present timeline. (1) Pseudostratified epithelium formation and intestinal segment patterning. (2) Intestinal growth and elongation. (3) Epithelial reorganization and villification. (4) Crypt formation and acquisition of adult properties. Figure adapted from (Guiu and Jensen, 2015).

The mature intestine has been extensively characterized, but the mechanisms leading the development of its epithelium and muscle layers have received less attention. Furthermore, the observed transition from an immature foetal into an adult mature intestinal structures is believed to be tightly regulated by mechanical forces and signals from the surrounding environment, as I describe later in this Chapter, but insights are needed to understand how heterogeneous populations of cells in the epithelium, mesenchyme, and muscle interact during intestinal development.

The formation of the primitive gut tube is a result of symmetric and asymmetric cells division and reorganization during the transition from a zygote to a foetus. The development of the gut tube starts at embryonic day six (E6.0) in mice and at Carnegie stages (CS) six in humans (CS6), when the single layers of cells called the blastula differentiates into three layers named ectoderm, mesoderm, and endoderm (Gaivao *et al.*, 2014; Kojima *et al.*, 2014).

To understand the embryonic origin of the endoderm cells within the gut tube, endoderm cells of early somite stage mouse embryos were labelled with vital dyes (Tremblay and Zaret, 2005). After culturing the embryo to reach specific developmental stages, the tissue fate of dye-labelled cells was determined by immunofluorescence analysis. Such experimental chemical fate-mapping models have shown that, in embryonic mice, specific regions of the primitive endoderm contribute to specific domains of the gut tube, and in general, anterior endoderm cells contribute to the creation of the anterior intestinal portal (AIP), whereas posterior endoderm cells contribute to the caudal (posterior) intestinal portal (CIP) (Tremblay and Zaret, 2005; Franklin *et al.*, 2008). The lateral endoderm folds ventrally and the conjunction of the two lateral folds produce a closed gut tube as the

embryo is turning at E9.0 (Lewis and Tam, 2006; Zorn and Wells, 2009).

During the developmental time between E9.5 and E14 in mice and CS9-19 in humans, the gut tube starts to differentiate from a simple tube to a complex structure and epithelial cells are actively proliferating. The epithelium appears to be pseudo-stratified and the lumen first appear after apoptosis of the most distal epithelial cells (Matsumoto *et al.*, 2002). At E9.5 in the mouse (Kapur *et al.*, 1992) and prior to week four of human gestation (Fu *et al.*, 2003), neural crest-derived cells invade the foregut and begin their long rostro-caudal journey down the bowel to form the enteric nervous system.

As the primordial gut increases in length and in width, it protrudes into the extra embryonic coelom. This physiological herniation occurs because the gut grows faster than the abdominal cavity, which is occupied mainly by the liver at E14. Return of the gut into the abdominal cavity occurs in the tenth week of development in humans and E17 in mouse (Kluth *et al.*, 2003).

To better appreciate the normal process of midgut rotation, Metzger *et al.* produced an atlas of rat midgut development using scanning electron microscopy (SEM) (Metzger *et al.*, 2011). In this elegant study, the movement of the intestinal loop into the extra-embryonic coelom and its subsequent return into the abdominal cavity with an anticlockwise direction around the axis of the mesentery vessel was apparent. This process of rotation has also been proposed to occur in human where the midgut started its rotation at approximately week eight and complete its rotation at the tenth week of gestation (Rescorla *et al.*, 1990). The result of these two movements is a rotation of 270°. In a subsequent step, the caecum grows downwards from the upper quadrant of the right abdominal cavity into the right iliac fossa (Figure 1.3).

Unfortunately, these processes are still controversial, due in part to the differences in gut fixation after physiological herniation between human and rodents (Baoquan *et al.*, 1995; Pitera *et al.*, 2001).

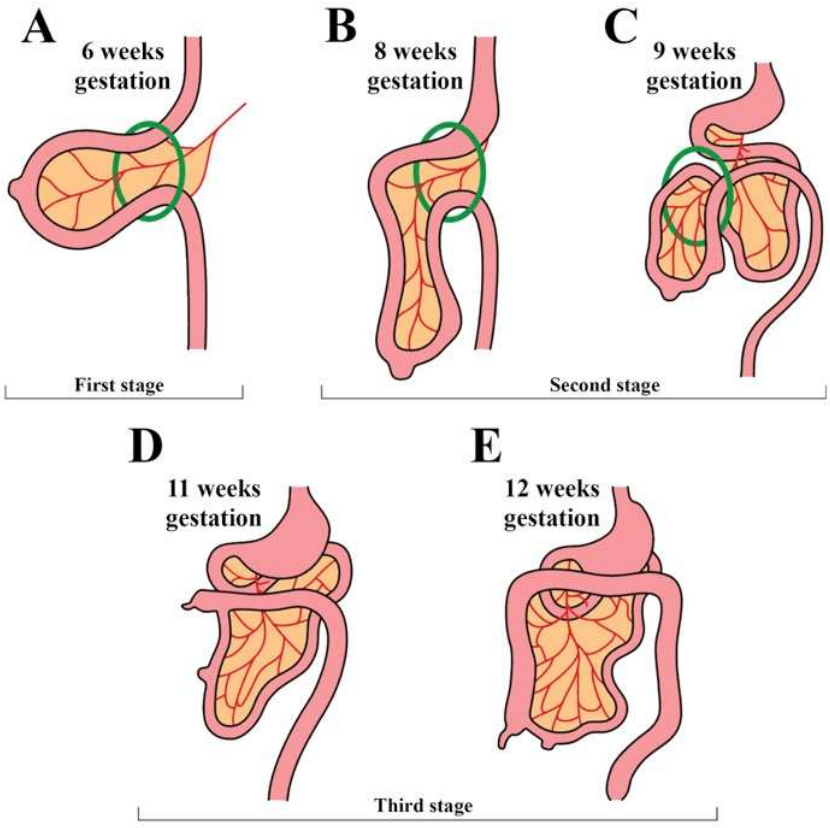

Figure 1.3 Representation of intestinal rotation

The picture illustrates a schematic representation of small intestinal rotation. (A, B) Primary intestinal loop before rotation. The superior mesenteric artery forms the axis of the loop and of subsequent rotation. (C-E) Counter-clockwise rotation of the gut occurs through 270° concomitantly with herniation of the small intestinal loops followed by return of the gut to the abdominal cavity. Figure adapted from (Filston and Kirks, 1981).

During these stages the mesenchymal compartment starts to differentiate creating the first muscular layer (circular muscular layer), and the epithelium differentiates forming the primordial lumen delimited by three main protrusions as a clover shape. By E14 in mice and week seven in humans (Fu *et al.*, 2004), neuronal migration is complete. In mice and humans, enteric neurons also undergo inward radial migration after initially colonizing the bowel (Jiang *et al.*, 2003), forming the two layers of ganglia that comprise the myenteric and submucosal plexuses (Figure 1.4).

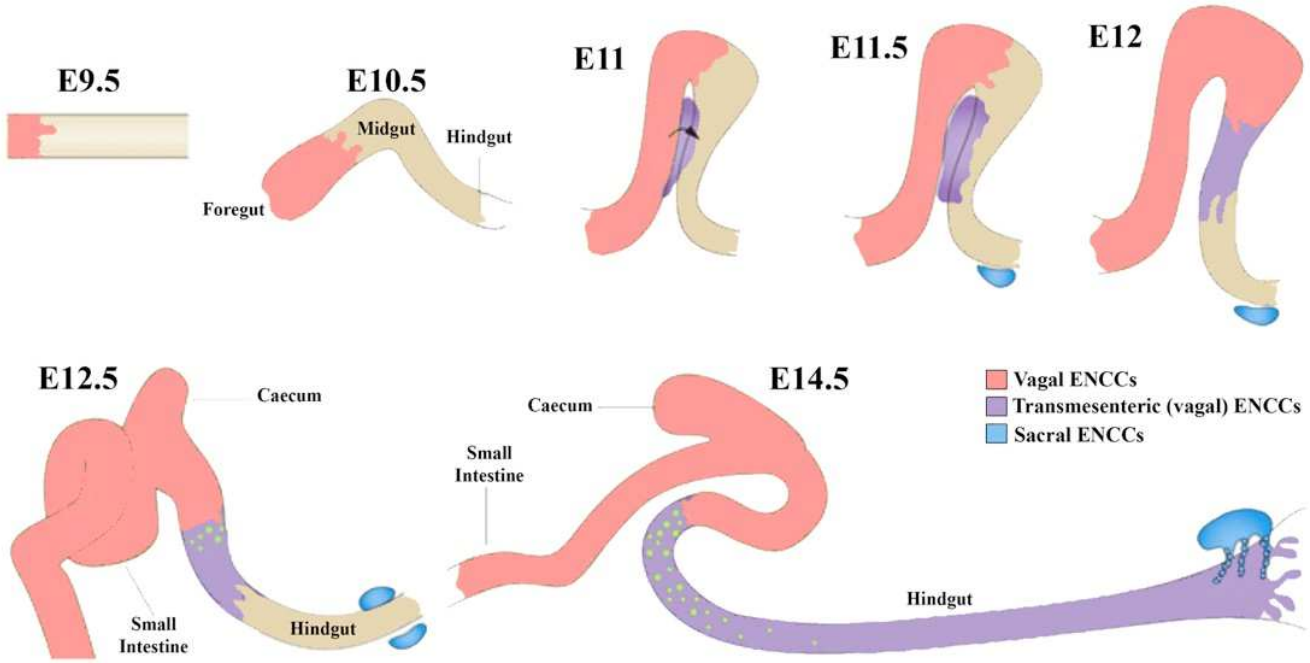

Figure 1.4 Neuronal distributions during intestinal differentiation

During early developmental stage (E9.5) the digestive system is a simple tube that starts to be popularized by vagal nerve. Since E10.5, the simple tube differentiates regionally creating the first fold (E11) and specializing in foregut, midgut and hindgut. Between E11.5 and E12.5, the trans mesenteric enteric system migrates into the fist portion of the hindgut till will reached the area of the sacral enteric nerves (E14.5).

From E14.5 in mice the pseudo-stratified epithelium becomes a simple columnar shape, while invaginations are developing within the mesenchyme. The interaction between epithelium and mesenchyme generate finger-like structures facing the intestinal lumen called villi (Grand *et al.*, 1976; Spence *et al.*, 2011).

In mice, from E16.5 to birth, the small intestine becomes organized into villi and intervillus regions. During the first two postnatal weeks, the intervillus region forms the mature crypt. An observational study of embryonic mice showed that the distance between the circular smooth muscle layer and the bottom of the crypts suggest that this process is not an invagination of the epithelium, but that the crypt-villus organization is promoted *via* expansion of the mesenchymal cell populations that move upward and encapsulate epithelial cells within the intervillus region (Calvert and Pothier, 1990). The appearance of crypts is a relatively late event, which ends the intestinal maturation (Schroder and Gossler, 2002; Guiu and Jensen, 2015) (Figure. 1.5).

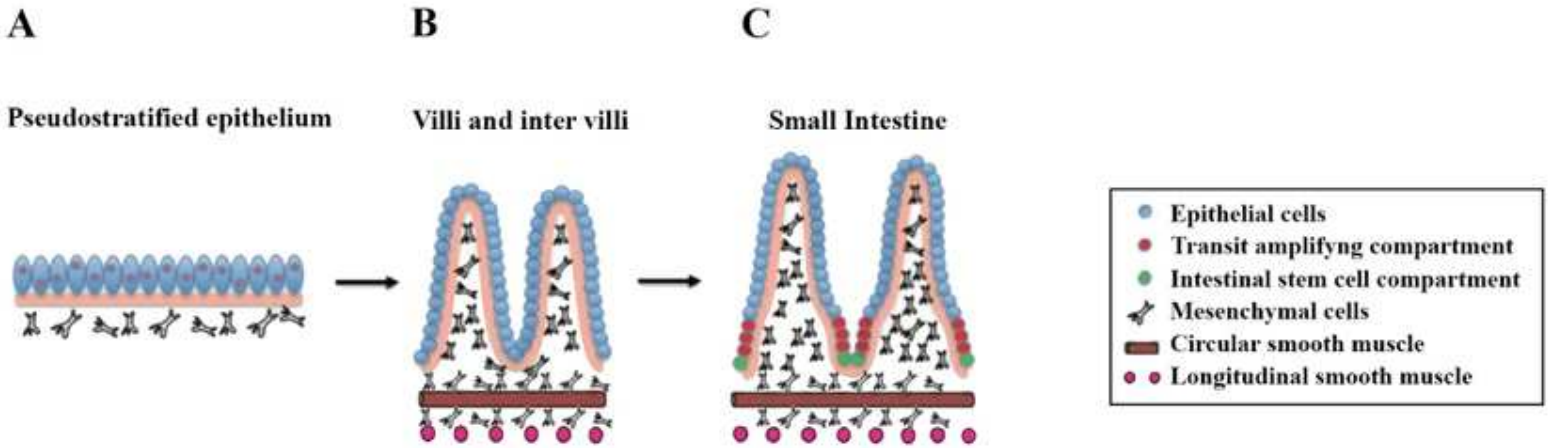

Figure 1.5 Epithelial differentiation in the small bowel

At early developmental stages, the intestine is a pseudostratified epithelium (A) that transits toward a simple epithelium composed of villi and inter-villi regions (B). This will eventually give rise to the crypt-villus structure in the small intestine and crypts. Figure adapted from (Guiu and Jensen, 2015).

In humans, the process of villus emergence in the gut starts at gestational week nine in a cranio-caudal direction (Moxey and Trier, 1978). The villus emergence process, called villification has been investigated experimentally in murine and avian models. Using a quantitative computational model of the mouse and avian developing gut, it has been shown that villification is tension-driven by the muscles in the outer layer of the intestine (Shyer *et al.*, 2013). Interestingly, in humans smooth muscle formation occurs at gestational week eight (Frid *et al.*, 1992), thereby preceding villification and the tension-driven mechanism could, therefore, be conserved through evolution.

In contrast, a recent study postulated that murine villification as well as human and other mammals, is not temporarily coordinated with development of smooth muscles layers (Walton *et al.*, 2016). Using an organ culture model of murine embryonic jejunum opened longitudinally, Walton *et al.* reported that after 38 hours of culture rudimentary villi were present despite the absence of the tension force of the circular muscle layer. Expanding previous researches postulating that bone morphogenetic proteins (BMP) are secreted ligands able to modelling tissues in many developmental contexts (Roberts *et al.*, 1995; Hogan, 1996), embryonic intestines from transgenic mice were cultured in the presence of an inhibitor of BMP signalling called dorsomorphin. After two days in culture the intestine showed alteration of villi morphology with no changes in muscular morphology, confirming that villification is not due to tension-driven mechanism generated by muscle layers.

Due to the controversy of these researches, it is still not clear whether the differentiation of the circular and longitudinal muscle layers played a fundamental role in driving villification during embryogenesis.

1.2.2 Circular and longitudinal muscle layers

The main function of smooth muscle in the gastrointestinal tract is to mix and propel intraluminal contents to enable efficient digestion of food, progressive absorption of nutrients, and evacuation of residues (Bitar, 2003).

The muscular layer is responsible for gut movement called peristalsis and it is characteristically organized into inner (circular) and in an outer (longitudinal) layer. Circular muscle tone generates radial pressure to create a local peristaltic wave (Huizinga and Lammers, 2009).

Research on small intestinal motility using perfusion techniques on adult rat intestine showed that the action of smooth muscle in the circular and longitudinal layers produces tonic contractions that preserve organ dimension against an imposed load such as a bolus of food, as well as forceful contractions that produce muscle shortening to propel the bolus along the gastrointestinal tract (Schreiber *et al.*, 2014).

Using a combination of intraluminal ultrasound with image analysis, it has been shown that local contraction of longitudinal muscle seems to shorten the longitudinal dimension of axial segments and increases the concentration of circular muscle fibres at the location of maximal circular muscle squeeze, thus reducing the force required by each circular muscle fibre. Moreover, the local axial motions of the mucosal surface induced by a peristaltic wave of local longitudinal shortening reduce the level of applied pressure required to locally close the lumen as a result of the local changes in fluid stresses within the lubrication layer (Brasseur *et al.*, 2007).

Interestingly, *in situ* hybridization analysis on whole mouse embryos for muscular marker using α smooth muscle actin (α-SMA) showed that the differentiation of smooth muscle tissues in the developing gastrointestinal tract, and in particular in the

small intestine, appear to begin by E13 (McHugh, 1995). Previous studies on mice gut demonstrated that circular smooth muscle layer initially forms in the middle of mesenchymal layer, and approximately 48 hours later the longitudinal smooth muscle layer develops in the peripheral mesenchyme (Kedinger *et al.*, 1990; McHugh, 1995).

Surprisingly, the most recent reviews (Noah *et al.*, 2011; Spence *et al.*, 2011) have placed little attentions on the muscle layer, in particular in the longitudinal muscle layer role during development. Furthermore, the molecular events that regulate longitudinal smooth muscle differentiation are still not clear (Faure and de Santa Barbara, 2011; Le Guen *et al.*, 2015).

Further researches are needed to clarify the developmental pattern of the gastro-enteric smooth muscle and the ontogeny of smooth muscle tissues during normal mammalian development.

1.2.3 Epithelial cells

The intestinal epithelium is a complex structure comprising villi and crypts (Figure 1.6). In the mouse, the adult epithelium undergoes renewal to maintain its optimal function (Watson and Hughes, 2012). The regenerative capacity of the mouse adult epithelium is established between E16.5 and postnatal day seven, when mature crypts develop from shallow pockets of proliferative cells that are restricted to the base of the embryonic villi (Gregorieff and Clevers, 2005).

Differentiated epithelial cells migrate upwards along the villi, an event that takes between three to five days, as demonstrated by an elegant study in which determination of whole population turnover time of mice intestinal epithelium was investigated using intra-peritoneal injection of tritiated thyamidine, a radioactive

substance able to be incorporated into the DNA and to mark permanently the nucleus of epithelial cells. This substance is taken up by the nuclei of cells in pre-mitotic stage (Creamer *et al.*, 1961). Using this strategy was passible to follow the epithelial cells from the crypts to the tip of the villi.

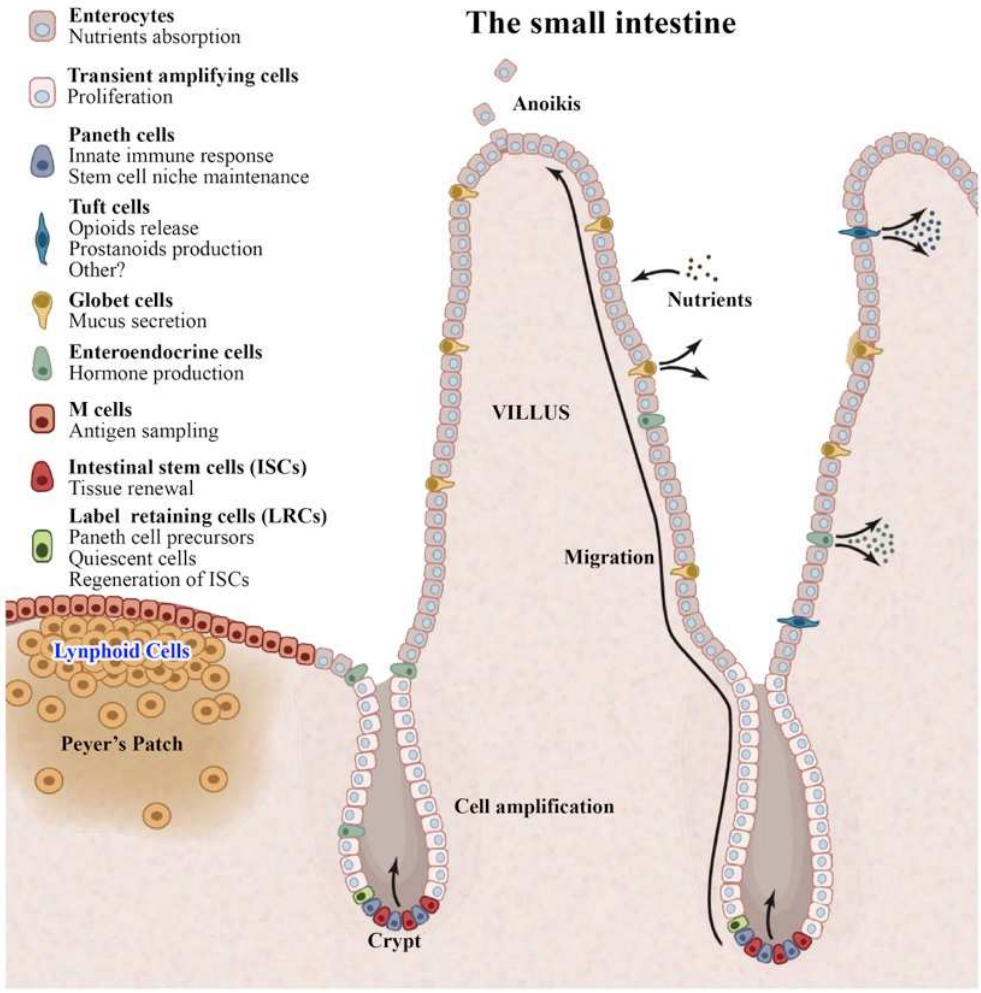

Figure 1.6 Epithelia in the villus/crypt axes

The intestinal epithelium is organized into finger-like structures called villi and into fold called crypt. The intestinal stem cells population are located into the crypt. ISC progeny are amplified through a series of very rapid divisions. When these cells migrate into the trans-amplification zone, they differentiate into one of six lineages that are present in the intestine. When one of the epithelial cells reaches the tip of the villi, the loss of integrin-mediated cell adhesion induces apoptosis by a process that is termed “anoikis”. Figure adapted from (Clevers and Batlle, 2013).

The intestinal crypts contain the ISCs, and the villi are a multi-differentiated system that simultaneously absorbs of nutrients and provides a barrier to the substantial bacterial burden (Figure 1.7A).

Enterocytes are polarized epithelial cells (Massey-Harroche, 2000), joined together by tight junctions (Assimakopoulos *et al.*, 2011). These cells are able not only to absorb macro and micronutrients (Daniel and Zietek, 2015; Thorsen *et al.*, 2014) but also to play a fundamental role in the host defence (Walker *et al.*, 2013) (Figure 1.7B). In mice, enterocytes were found to make up more than 80% of the entire epithelium in the small bowel (Cheng and Leblond, 1974). Once on the villous tip, enterocytes enter a death program called anoikis (Lugo-Martinez *et al.*, 2009) and are exfoliated from the villus apex into the intestinal lumen (Bertrand, 2011).

Entero-endocrine cells (EECs) are specialized epithelial cells that coordinate appropriate functional responses to a variety of stimuli from nutrients, food degradation products, toxic chemicals, microorganisms, and bacteria (Sternini *et al.*, 2008) (Figure 1.7C). EECs represent 1% of the total intestinal epithelial population (Rehfeld, 2004). Depending on the EECs position in the epithelial layers and on the morphology, these cells can be divided into *open type* with bottleneck shape and an apical surface covered by microvilli directly in contact with luminal contents, or *closed type* that are not in contact with the lumen but are located on the basal membrane and have no microvilli (Janssen and Depoortere, 2013).

Goblet cells are scattered throughout the epithelium and produce a protective mucus layer (Figure 1.7D). These cells act as an innate host defence producing secretory mucin glycoproteins and bioactive molecules (Andrianifahanana *et al.*, 2006). The goblet cell morphology is characterized by the presence of mucin granules located

below the apical membrane. The proportion of goblet cells increases from duodenum (4%) to distal colon (16%), similar to the pattern of microbial organisms present along the digestive system (Deplancke and Gaskins, 2001).

Microfold cells or M cells are highly specialized epithelial cells for the phagocytosis and transcytosis of gut lumen macromolecules, particulate antigens and pathogenic or commensal microorganisms across epithelium (Mabbott *et al.*, 2013). In mouse the M cells are localized into the follicle-associated epithelia and appeared to differentiate from leucine-rich repeat containing G protein-coupled receptor 5 positive ($LGR5^{+}$) cells (de Lau *et al.*, 2012), but the terminal differentiation of these cells seems to be regulated by a specific transcription factor as demonstrated by studies on Spi-B-deficient mice (Kanaya *et al.*, 2012; Nakato *et al.*, 2009). The optimal distribution of M cells in the intestinal epithelium seems to be important to guarantee efficient immune surveillance, while at the same time maintaining the integrity of the follicle-associated epithelia (Hsieh and Lo, 2012) (Figure 1.7E).

Paneth cells are specialized intestinal epithelial cells detected in the base of the crypt of Lieberkün, which is an invagination of the intestinal epithelial surface into the mesenchyme along the entire small bowel. Paneth cells have a distinctive morphology of pyramidal shaped columnar cells and they seem to originate from the adjacent $LGR5^{+}$ intestinal stem cells that are also present at the base of the crypts (Barker *et al.*, 2007; Snippert *et al.*, 2010). While the normal lifetime of the epithelial cells is estimated around three to five days, the Paneth cells live for 30 days (Clevers and Bevins, 2013) (Figure 1.7F). Although the first physiological function described for the Paneth cells has been about synthetize and secrete antimicrobial peptides and proteins (Wehkamp *et al.*, 2005; Bevins and Salzman,

2011), recent studies have suggested a fundamental role of these high-specialized cells to sustain intestinal epithelial stem cells (Bjerknes and Cheng, 2002; Sato *et al.*, 2011b).

Tuft cells, also known as brush cells, are specialized epithelial cells located in all digestive tract from simple vertebrate to humans (Jarvi and Keyrilainen, 1956) (Figure 1.7G). Tuft cells constitute a minor fraction (0.4%) of the adult mouse intestinal epithelium and present an unique shape, from pear-shaped, to barrel-shaped and goblet-shaped, apparently depending on the plane of section (Sato *et al.*, 2002). In humans tuft cells seem to differentiate in the small bowel around 20-22 weeks of gestation (Moxey and Trier, 1978). The role of tuft cells in the small bowel is still enigmatic, but several researches showed absorptive function (Sato and Miyoshi, 1997) and secretory function (Sato, 2007).

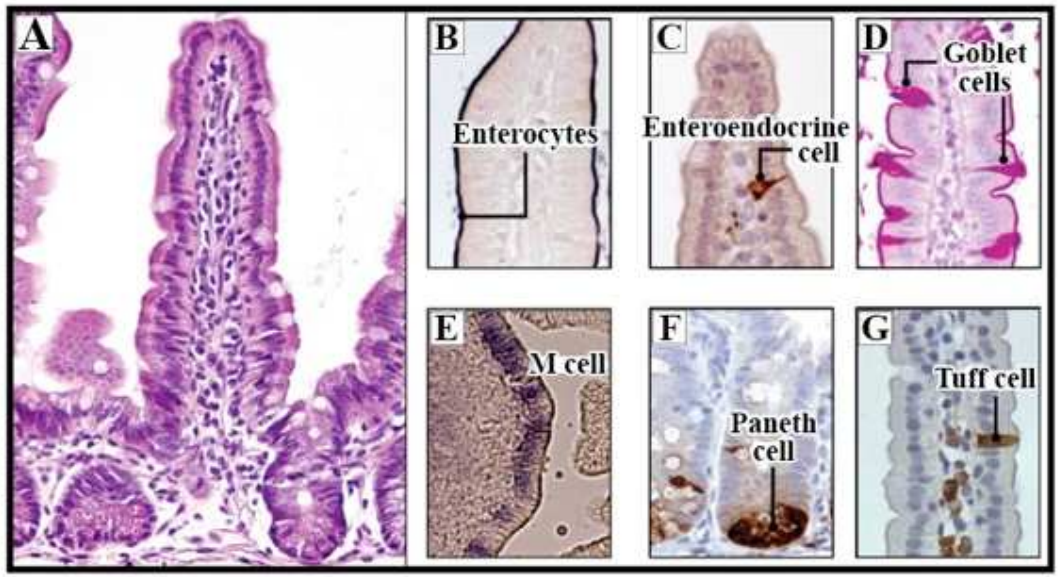

Figure 1.7 Epithelial cells types in the small intestine

(A) Haematoxylin and eosin staining showing the overall morphology of the mouse intestine. Immunohistochemical analysis for the main four differentiated cell types present in the intestinal epithelium: (B) alkaline phosphatase to stain enterocytes, (C) anti-synaptophysin to stain enteroendocrine cells (D) periodic acid–Schiff (PAS) to stain goblet cells, (E) Spi-B expression in microfold (M) cells. (F) Lysozyme to stain Paneth cells, and (G) doublecortin like kinase 1 (DCAMKL1) stained tuft cell. Figure adapted from (Clevers, 2013).

The function of ISCs is to maintain integrity of the intestinal epithelium (Hermiston *et al.*, 1993) which is in a constant state of renewal, replenishing every five to six days (Lipkin, 1985). Experimental studies based on animal models have sought to understand the development of the crypts in which the ISCs were discovered.

In 1981 and in 1999, Bjerknes and Cheng (Bjerknes and Cheng, 1981; Bjerknes and Cheng, 1999) proposed the existence of a stem cell-permissive microenvironment in crypt positions 1–4 by analysing mutant clones on a villus from SWR mouse. These cells, called crypt base columnar cells (CBCs), were interposed between Paneth cells at the crypt base and found to give rise to mutant clones containing multiple cell types. Similar evidence was reported from the result on neonatal mice embryo aggregation chimaeras (Schmidt *et al.*, 1988). Most recently using a transgenic mice, a second family of intestinal stem cell, called label-retaining cells (LRCs) or putative intestinal stem cells was identified, localised in a position 4 cells up (+4) from the crypt base, directly above the Paneth cell zone (Potten *et al.*, 2002).

ISCs are surrounded by a niche comprising mesenchymal cells that influence progenitor cells by direct cell-cell contact from the baso-lateral side and to the apical side. In a mouse model of mutation in β-catenin receptor, in wingless-related integration site (WNT) and hedgehog signals, that is one of the key pathway for regulating animal development (van den Brink, 2007), seems to interact inducing crypt formation (Korinek *et al.*, 1998).

To mark the ISCs, a study performed by Formeister in mice embryo found expression of sex determining region Y-box 9 (SOX9), a protein linked to the regulation of stem cell renewal in other tissues and in the regenerative intestinal epithelium (Formeister *et al.*, 2009). In 2008, Scoville *et al.* reviewed the literature

on intestinal stem cells and their signalling and postulated that under various conditions of stress or injury, +4 LRCs might undergo transient activation to generate progenitors as well as CBCs. However, CBCs may be able to rebuild lost +4 LRCs (Scoville *et al.*, 2008).

Although the crypt system seems to be anatomically simple, the signal pathways that regulate its life are still not clarified. WNT, BMP (He *et al.*, 2004), phosphatidylinositide 3-kinases (Cully *et al.*, 2006) and Notch (Schroder and Gossler, 2002) seem to co-ordinate and regulate ISCs and their progeny in controlling ISC self-renewal as well as lineage commitment and terminal differentiation. However, much of this information is influenced by +4 LRCs. In addition it is possible that both CBCs and +4 LRCs represent different populations of intestinal stem cell within the crypt, with CBCs perhaps more ready to respond to regenerative signals while +4 LRCs remain in a reserved quiescent state. Figure 1.8 summarizes the intestinal niche components.

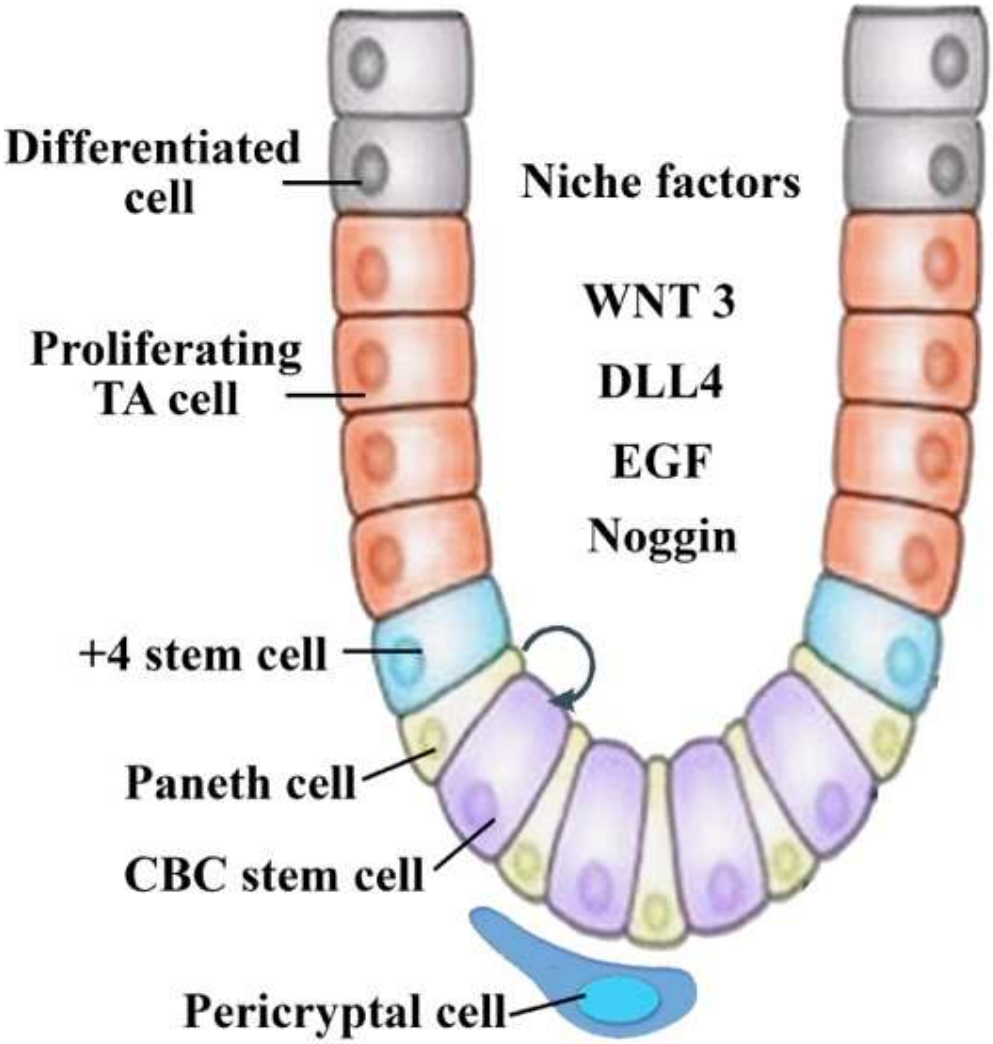

Figure 1.8 The crypt niche

Cartoon depicts the components of the CBC stem cell niche at the crypt base. Both Paneth cells and pericryptal stromal cells supply essential factors (including WNT, the Notch ligand Delta-like 1, epidermal growth factor (EGF) and Noggin) to regulate the survival and function of the CBC stem cells *in vivo*. Cartoon adapted from (Barker, 2014).

1.2.4 Enteric neuronal system

The enteric nervous system (ENS) is a division of the autonomic nervous system, dedicated to the control and regulation of the actions of the gut. The cells which comprise the ENS are organised into two distinct layers: the myenteric plexus (Auerbach's), located between the outer longitudinal and inner circular layers of the gut wall, and the submucosal plexus (Meissner's), situated deep to the gut mucosa (Heanue and Pachnis, 2007; Uesaka *et al.*, 2016).

The Auerbach's plexus provides motor innervation to both layers of the muscular layer of the gut, having both parasympathetic and sympathetic input (Dyachuk *et al.*, 2014), whereas the submucosal plexus has only parasympathetic fibres and provides secretive and motor innervation to the mucosa nearest the lumen of the gut (Uesaka *et al.*, 2015). Within these two plexi, neurons and glia are organised into interconnected clusters of cells known as ganglia (Grundy and Schemann, 2005) (Figure 1.9).

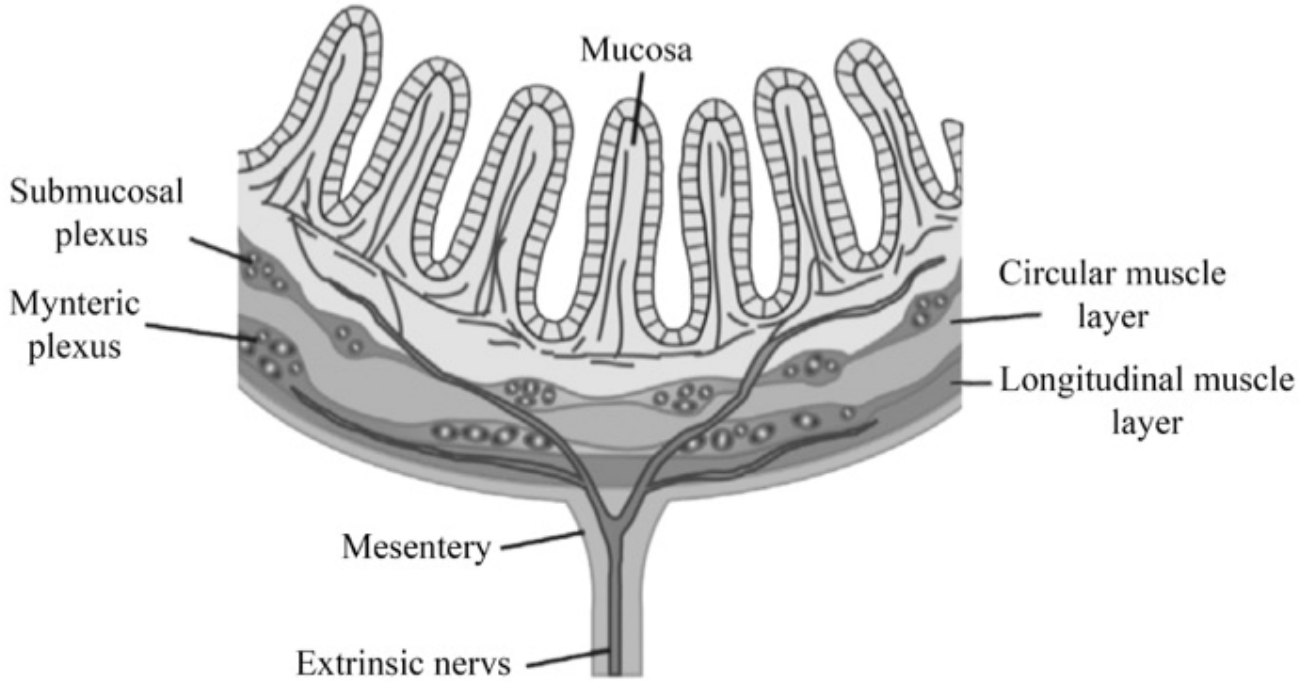

Figure 1.9 Innervation of gastrointestinal tract

The gastrointestinal tract is composed of two major plexuses and ganglia called myenteric and submucosal plexuses. Figure adapted from (Uesaka *et al.*, 2016).

1.3 Methods to investigate small intestinal development and differentiation

The present section aims to give an insight on the most common methodologies used to explore intestinal development. The animal models have been historically used to study macroscopic organogenesis, but the most recent research approaches seem to offer the possibility to investigate molecular pathways or gene expressions. These new approaches can direct developmental events trying to answer the unsolved molecular and morphological events of normal development.

The challenge for the future may be integrating data from modern research into a more complete understanding of the physiology of gastrointestinal development. Understanding the different research models was important to me in electing the experimental approach to be used in the studies described in this thesis.

1.3.1 *In vivo* models

In vivo refers to experimental studies using a whole, living organism. Animal studies and clinical trials are two forms of *in vivo* research. *In vivo* testing is often employed for observing the overall effects of an experiment on a living subject.

With both human and mouse genomes sequenced showing 99% of encoded sequences similarity (Waterston *et al.*, 2002), *in vivo* mice model, such as transgene expression and gene disruption, (Montgomery *et al.*, 1999; Ishikawa *et al.*, 2003; Gosalia *et al.*, 2015) has been confirmed to be an useful tool to elucidate mechanism of gene expression and has been used to understand morphological stages in human development.

In addition, the utility of model organisms such as the nematode *Caenorhabditis elegans* (McGhee, 2013), the fruitfly *Drosophila melanogaster* (Nakagoshi, 2005; Takashima *et al.*, 2011), and more experimentally accessible vertebrates such as *Xenopus laevis* (Henry *et al.*, 1996) and the zebrafish *Danio rerio* (Pack *et al.*, 1996; Schall *et al.*, 2015) for dissecting the mechanisms of gastrointestinal development are being increasingly appreciated.

Precisely targeted experiments are now possible and increasingly used as examples for study the epithelial composition of the intestinal villi (Hermiston *et al.*, 1993), the spatial differentiation process of the epithelial cell renewal and differentiation (Nyeng *et al.*, 2011), the molecular effects driving differentiation (Stringer *et al.*, 2012; Reeder *et al.*, 2014) and developmental mechanisms that normally regulate elongation of the small intestine (Geske *et al.*, 2008; Cervantes *et al.*, 2009).

1.3.2 *Ex vivo* models

Ex vivo means something that takes place outside an organism. In science, *ex vivo* refers to experimentation or measurements done in or on tissue from an organism in an external environment with the minimum alteration of natural conditions.

Ex vivo allows research on tissue (e.g. the organ culture model used in this study) to be completed under more controlled conditions than is often possible in *in vivo* experiments, albeit at the expense of possibly altering the natural environment. However, it is possible to harvest a cell (Hoffmann *et al.*, 2004) or stem cells (Choudhary and Capuco, 2012) from the organ and expand experimental interrogation outside the physiological control (for example on cell culture or petri dishes), a condition called *in vitro.*

Using an *in vitro* approach it has been possible to investigate which are the optimal growth factor combinations involved in self-renewal regulation, differentiation, and carcinogenesis of intestinal stem cells (Sato and Clevers, 2013b). Promotion of growth from a single stem cell expressing LGR5 to *in vitro* mini-gut was achieved (Sato and Clevers, 2013a), with the grafted organoids remaining healthy and functional for at least 6 months after transplantation (Li and Clevers, 2012; Yui *et al.*, 2012).

While *ex vivo* organ culture has been used extensively to investigate development and function of neurons (Sun *et al.*, 2016), kidney (Anders *et al.*, 2013), liver (de Graaf *et al.*, 2010), lung (Del Moral and Warburton, 2010), pancreas (Huotari *et al.*, 2002) and ureter (Bullock *et al.*, 2001), this approach has only been used three times to follow intestinal development (Hearn *et al.*, 1999; Abud *et al.*, 2005; Quinlan *et al.*, 2006).

1.4 Molecular control during small intestinal development

The process of gastrulation and creation of the primordial intestinal tube appears to be regulated by different and distinct molecular programs. These events can characterize not only the differentiation of the three primary germ layers, but also the cranio-caudal differentiation of the primordial intestine in foregut, mid-gut and hindgut (Sherwood *et al.*, 2009).

The following section of the thesis will highlight the fundamental molecular events during small intestinal development.

1.4.1 Molecular events during small intestinal development

How gut tubulogenesis is controlled and how the primordial layers are folded to create the intestinal portal is poorly understood. In mouse embryos, the lateral portion of the endoderm folds ventrally and joins together to form the primordial intestinal tube (Lewis and Tam, 2006). Although it is not clear how mesodermal movements guide gut tube morphogenesis, key transcription factors and signalling pathways in gut tube formation have been identified.

The elongation of the forming intestine is mediated by a number of different pathways that are most likely organized in complex regulatory networks. Recent studies have also provided insight into the molecular events that regulate the process by which the embryonic tissue converge along one axis and extend along a perpendicular axis during gut tube formation and elongation in mouse, an event called convergent extension (Garcia-Garcia *et al.*, 2008; Wen *et al.*, 2010).

In mice, sex determining region Y-box 2 (SOX2) and the caudal type homeobox factors (CDX) 1, 2, and 4 are expressed in the anterior and posterior part of the developing endoderm, respectively as showed by cell assay of transgenic mice,

where they coordinate and regulate midgut and hindgut regionalization and identity (Benahmed *et al.*, 2008; Grainger *et al.*, 2010).

Important roles in the developing gut tube have been found for WNT signalling. The WNT family comprises secreted lipid-modified glycoproteins involved in developmental processes including those in the lung (Caprioli *et al.*, 2015), trachea (Snowball *et al.*, 2015) and pancreas (Larsen *et al.*, 2015).

Knock out embryonic mice for the WNT activated transcription factor TCF1/TCF4 (Gregorieff *et al.*, 2004) have an abnormal intestine expressing ectopic level of transcription factors characteristic of the stomach, such as CDX2 and SOX2 demonstrated by *in situ* hybridizations analysis. Furthermore, WNT signalling is also important to sustain epithelial cell culture where the stimulation of this signalling mediated by a WNT agonist as R-Spondin1 appear to be essential for generate epithelial cell line culture (VanDussen *et al.*, 2015). R-spondin1 is a secreted protein that enhances WNT/β-catenin signalling and has pleiotropic functions in development and stem cell growth (Carmon *et al.*, 2011). The proliferative role of this protein was also exhibited in a mice study where rapid onset of crypt cell proliferation was observed after injection of R-spondin1 (Kim *et al.*, 2005).

An elegant study in embryonic mice demonstrated that the small intestinal morphogenesis is regulated by communication between the epithelium and the underlying mesenchyme, mediated by fibroblast growth factor 9 (FGF9) that is as an important epithelial-to-mesenchymal signal. In fact, mouse embryos that lack either FGF9 or the mesenchymal receptors for FGF9 contained a disproportionately shortened small intestine (Geske *et al.*, 2008). Analogously, WNT molecules seem to play a fundamental role in gut elongation. Knock out mice for WNT5a, a member of

the non-canonical WNT pathway expressed in the mouse gut mesenchyme from E9.5, shows reduced gut elongation but surprisingly leads to an increased girth of the intestine and post mitotic cells do not intercalate properly into the epithelium (Cervantes *et al.*, 2009).

1.4.2 Molecular events during small intestinal differentiation

Starting at E14.5 in the mouse (CS9 in humans), the stratified epithelium of the midgut and the hindgut endoderm begins to undergo extensive reorganization. Cross talk between the epithelium and mesenchyme is crucial for development of the primordial tube as a complex structure characterized by villi, crypts and two muscle layers.

Recent studies identified hedgehog pathway components (Ramalho-Santos *et al.*, 2000; Walton *et al.*, 2012), members of the BMP family (Walton *et al.*, 2016), and platelet-derived growth factor receptor α (PDGFR-α) (Karlsson *et al.*, 2000) as key pathways involved in the villification process.

Hedgehog signalling plays a fundamental role during animal development (Ingham and McMahon, 2001) and induces mesenchymal growth in the developing intestine. From early developmental stages, sonic hedgehog (SHH) and indian hedgehog (IHH), two key ligands of hedgehog signalling, are expressed by the endoderm of the mouse, rat and human gut (Madison *et al.*, 2005). While SHH production seems to be limited to the villus base during the villification, IHH is present in the differentiated epithelium (Kolterud *et al.*, 2009). Studies on knock out embryonic mice either for SHH or IHH have shown only limited anomalies on the gastrointestinal epithelium and villi structure, with *Shh* mutant mice exhibiting taller villi, and IHH knock out mice reduced numbers of villi suggesting opposing effects

of IHH and SHH (Ramalho-Santos *et al.*, 2000). In contrast, more severe alteration in mesenchymal differentiation has been reported, as demonstrated by reduced of circular smooth muscle thickness in removal of either *Shh* or *Ihh* in knockout mice (Mao *et al.*, 2010).

Perturbation of the BMP pathway in chicks leads to morphological anomalies of the gut due to abnormal differentiation of the three primordial layers. This was demonstrated by an experiment in which ectopic expression of *Bmp4* from an avian specific retroviral expression system showed abnormal development of the stomach and focally thin to absent smooth muscle in the gut. Furthermore, inhibition of BMP signalling pathway activation exhibited stenosis of the intestinal lumen (De Santa Barbara *et al.*, 2005). During gut development, the BMP pathway appears to be achieved mainly in the mesenchyme underneath nascent villi and has been demonstrate to be downstream the hedgehog pathway (Karlsson *et al.*, 2000; Walton *et al.*, 2016). In support of the role of BMP in villi development and crypt-villus axis creation, experimentally induced epithelial expression of the BMP2/4/7 antagonist Noggin causes abnormal villi formation in transgenic mice (Batts *et al.*, 2006). These experiments demonstrate an alteration of the sub epithelial mesenchymal condensation leading to larger but fewer villi compared to the wild type.

PDGF epithelial to mesenchymal signalling appears to function in parallel with the hedgehog pathway. PDGF-A and its receptor, PDGFR-α, are expressed in the endoderm and mesenchyme respectively, prior to villus emergence. In mice lacking PDGF-A or PDGFR-α, cellular proliferation remains restricted to the intervillus epithelium and crypts, resulting in fewer and thicker villi. Interestingly, thicker

circular muscle layer and early differentiation of the circular muscle layer was observed, which could explain the change in villification (Karlsson *et al.*, 2000).

During small bowel development, radial patterning results in the formation of distinctive concentric layers from the epithelium to the mesothelium. Considerable progress has been made in understanding the mechanisms regulating patterning of the gut along all axes during development (Roberts, 2000; Stainier, 2005). Roberts *et al.* (Roberts *et al.*, 1995; Roberts *et al.*, 1998) using viral misexpression of BMP4 and SHH in chick embryo showed that the epithelium of the developing gut produces SHH, which acts as a signal to influence the differentiation of the adjacent mesenchyme in a radial direction. Additionally, an elegant research on organ culture epithelial-mesenchymal recombination from embryonic intestinal chicken specimens showed that endodermal epithelium inhibits differentiation of smooth muscle and enteric neurons in adjacent mesenchyme by activating expression of BMP4 in adjacent non-smooth muscle mesenchyme, which later differentiates into the lamina propria and submucosa. This study also confirmed that SHH is expressed in endodermal epithelium and disruption of SHH-signalling induces differentiation of smooth muscle in the area adjacent to epithelium. (Sukegawa *et al.*, 2000).

In most of the above studies, intestinal smooth muscle was considered as a single entity. Surprisingly, all the most recent reviews of intestinal development or vertebral endoderm differentiation considers the muscle layer as a single entity (Spence *et al.*, 2011; Guiu and Jensen, 2015), and little is known about the complete differentiation of both circular and longitudinal intestinal muscle layers differentiation.

Interestingly, PDGF-α is expressed in the embryonic mice intestinal wall where smooth muscle is forming and has been functionally implicated in smooth muscle differentiation (Kurahashi *et al.*, 2008). Circular smooth muscle and interstitial cells of Cajal have been demonstrated to express PDGF-α and PDGF-β respectively (Kurahashi *et al.*, 2008; Torihashi *et al.*, 2009). These two factors were considered to act on longitudinal smooth muscle precursor cells that express PDGFR-α and β. According to the authors of these studies, the next step is to design *in vivo* functional experiments to investigate the role for PDGF protein and receptors in the development of the longitudinal muscle layer. However, this is likely to be very challenging as double knockout mutants for both PDGFR-α and PDGFR-β, as for TGFβ1 double knockout, are expected to be early embryonic lethal and appropriate conditional knock out lines have not been published.

Moving to the ENS, the pathways that guide morphogenesis are relatively poorly understood, but several classic morphogens are known to have important roles in ENS development. The hedgehog pathway is involved indirectly and directly in the developing ENS. Targeted mutation of SHH results in excessive numbers of enteric neurons and improper colonization of villi by enteric neuron cell bodies, whereas loss of IHH causes dilated segments of bowel and aganglionosis in parts of the gastrointestinal tract (Ramalho-Santos *et al.*, 2000).

A second role for hedgehog in the developing ENS seems to be indirect. Hedgehog signalling induces bowel mesenchyme to secrete bone BMP4. During initial enteric neuronal migration, BMP4 expression is induced in a ring of mesenchyme adjacent to the epithelium. Noggin, a BMP antagonist, is secreted by cells surrounding the BMP4-producing mesenchyme (Goldstein *et al.*, 2005) and presumably reduces the

effect of BMP4 on migratory enteric neuronal cells (Fu *et al.*, 2006).

Expression of the rearranged during transfection (RET) protein, a proto-oncogene that encodes a receptor tyrosine kinase for members of the glial cell line-derived neurotrophic factor (GDNF) family of extracellular signalling molecules, is detectable throughout the central neuronal system, peripheral neuronal system and renal tracts of the developing mouse (Pachnis *et al.*, 1993) and in a similar distribution in the human embryo (Tam *et al.*, 1996; Attie-Bitach *et al.*, 1998). The RET tyrosine kinase receptor has three domains, a cytoplasmic tyrosine kinase domain, a hydrophobic transmembrane domain and an extracellular binding domain (Schneider, 1992). Four RET ligands have been described: GDNF, the primary RET ligand in the gut, neurturin, artemin and persephin, which are secreted growth factors and part of the TGFβ superfamily (Durbec *et al.*, 1996a; Rosenthal, 1999). In migrating murine neuronal cell crest, RET is expressed from E10, as the cells enter the embryonic foregut (Durbec *et al.*, 1996b). Subsequently, expression is maintained in developing and adult neurons, but is down regulated during glial cell differentiation (Young *et al.*, 1999; Young *et al.*, 2003). GDNF is detectable in the mesenchyme of the murine gut at low levels from E10.5, just after the neuroblasts enter the foregut (Natarajan *et al.*, 2002). The levels then rise rapidly along the entire length of the gut, although there is a slight delay in hindgut expression (Mwizerwa *et al.*, 2011). Table 1.1 and 1.2 summarize the studies described in this section of the thesis.

Reference	Ligand	Species	Role
Hedgehog signalling			
(Kolterud *et al.*, 2009)	IHH and SHH	Mice	Control the amount of smooth muscle in villus cores. IHH and SHH regulate early development of villi
(Madison *et al.*, 2005)	IHH and SHH	Mice	Regulate early development of villi with paracrine effect
(Mao *et al.*, 2010)	IHH and SHH	Mice	Promote proliferation of mesenchymal progenitors in the gut
(Ramalho-Santos *et al.*, 2000)	IHH and SHH	Mice	Regulate the length of the gut. Regulate development of circular smooth muscle
(Roberts *et al.*, 1995)	SHH	Chick	Activates BMP4 during gut development
(Roberts *et al.*, 1998)	SHH	Chick	BMP4 prevents over-proliferation of the mesoderm during intestinal development due to SHH signalling
(Sukegawa *et al.*, 2000)	SHH	Chick	Inhibits differentiation of mesenchyme into smooth muscle in the area close to epithelium. Activate BMP4 during mesenchyme differentiation in smooth muscle

Table 1.1 Hedgehog signalling implications during small intestinal differentiation

The table above summarize the role of hedgehog signalling reported in literature.

Reference	Ligand	Species	Role
		BMP signalling	
(Batts *et al.*, 2006)	BMP4	Mouse	Differentiation of epithelial layers
(De Santa Barbara *et al.*, 2005)	BMP4	Chick	Inactivation of BMP4 alter intestinal mesoderm and neuronal migration and abnormal intestinal phenotype
(Fu *et al.*, 2006)	BMP4	Mice	BMP4 influences GDNF induced neuronal cell migration into gut
(Goldstein *et al.*, 2005)	BMP 4	Chick	Inhibition of BMP signalling leads to hindgut hypo-ganglionosis
(Walton *et al.*, 2016)	BMP4	Mice	Regulate villification after activation by SHH
		GDNF signalling	
(Attie-Bitach *et al.*, 1998)	GDNF	Human	Migration neuronal cells into gastrointestinal system
(Durbec *et al.*, 1996a)	GDNF	Xenopus	Differentiation and survival of neuronal system through RET
(Mwizerwa *et al.*, 2011)	GDNF	Chicken	Regulates the colonization of the neurones into the intestine
(Natarajan *et al.*, 2002)	GDNF	Mice	Induces a migratory response from pre-enteric neurones progenitors
		PDGF signalling	
(Karlsson *et al.*, 2000)	PDGF-α	Mice	Control the differentiation of the mucosa and the correct structuring of the mucosal lining of the intestine
(Kurahashi *et al.*, 2008)	PDGF-α	Mice	Critical roles in the development of longitudinal muscle cells.
(Torihashi *et al.*, 2009)	PDGF-β	Mice	Critical roles in the development of interstitial cells of Cajal.

Table 1.2 BMP, GDNF and PDGF signalling during small intestinal differentiation

The table above summarize the role of BMP, GDNF and PDGF signalling during intestinal differentiation reported in literature.

1.5 Why study transforming growth factor β signalling during small intestinal development?

There is a lack of direct evidence that TGFβ signalling contributes to differentiation of intestinal smooth muscle cells during embryonic development, although TGFβ appear to be one of the most important signalling pathways during development and normal physiology.

The next section will provide an overview of TGFβ signalling and showing the researches that suggest a TGFβ1 role during intestinal development.

1.5.1 Overview of TGFβ signalling

TGFβ superfamily signalling plays a critical role in the regulation of cell growth, differentiation, and development in a wide range of biological systems. In adult tissues, the TGFβ pathway is thought to regulate the dynamic interactions between immune, mesenchymal, and epithelial cells to maintain homeostasis in response to environmental stress (Blobe *et al.*, 2000).

Thirty three genes encode polypeptides within TGFβ superfamily, which are processed and secreted as homodimers or heterodimers (Wu and Hill, 2009). In mammals, there are three TGFβ ligands, termed TGFβ1, TGFβ2 and TGFβ3, which express differently in time and space (Millan *et al.*, 1991; Pelton *et al.*, 1991; Azhar *et al.*, 2003). TGFβ signals are conveyed through type I and type II receptors, which are transmembrane serine-threonine kinases, to specific intracellular mediators known as the SMAD proteins (Wrana, 2013). The name SMAD is a contraction between two homologues of both the protein *Drosophila* protein, mothers against decapentaplegic (MAD) and the *Caenorhabditis elegans* protein for small body size (SMA). Vertebrates have at least eight SMAD proteins that can be classified into

three functional groups: the receptor regulated SMADs (R-SMADs), common mediator SMADs (Co-SMADs), and the inhibitory SMADs (I-SMADs) (Yamada *et al.*, 2013). Using some intracellular protein called SMADs, the extracellular signals from TGFβ ligands will be transduced to the nucleus where they activate downstream gene transcription (Attisano and Wrana, 2002; Schmierer and Hill, 2007).

Ligand binding to the extracellular domain of the type II receptors induces a conformational change, resulting in the phosphorylation and activation of type I receptors. The activated type I receptor then phosphorylates the appropriate Smad and initiates the intracellular signalling cascade (Schmierer and Hill, 2007).

The TGFβ family can be divided into two groups based on their interaction with SMADs: the TGFs, activins, nodal and myostatin, which act through SMAD2 and SMAD3 (Piersma *et al.*, 2015) and the BMPs and growth differentiation factors (GDFs), which act through SMAD1, 5, and 8 (Hardwick *et al.*, 2004; O'Keeffe *et al.*, 2016) (Figure 1.10).

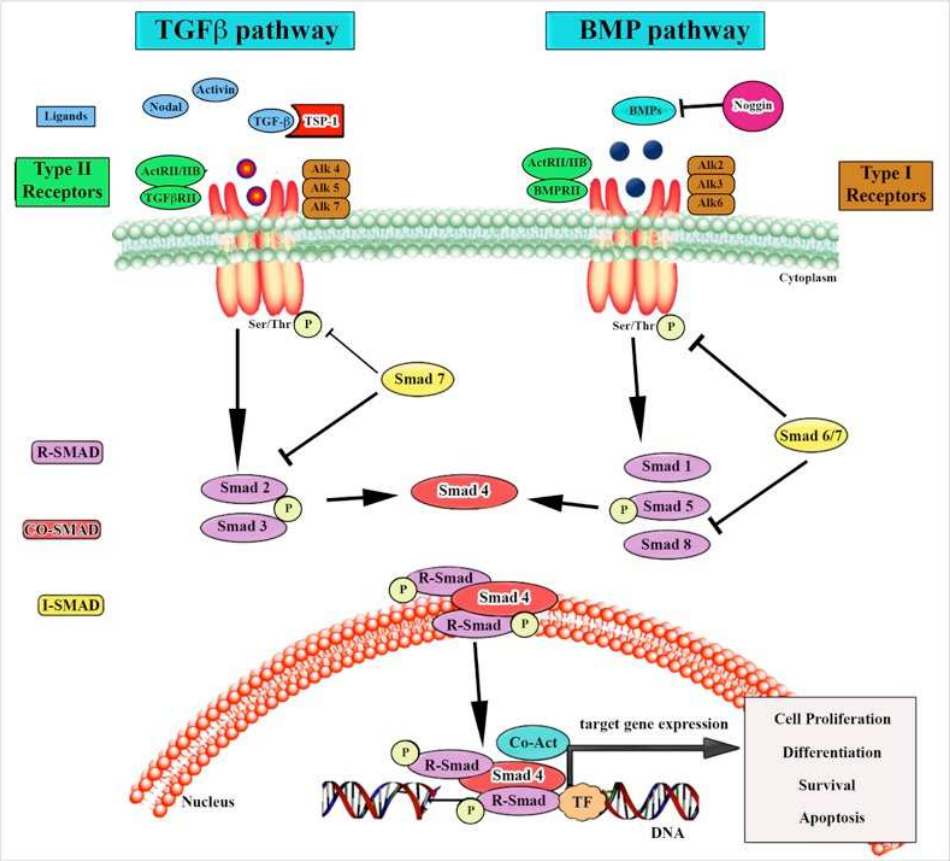

Figure 1.10 TGFβ/SMAD and BMP/SMAD signalling

Canonical signalling by TGFβ superfamily members can be divided into two main intracellular pathways according to the SMAD mediators: either SMAD2/3 or SMAD1/5/8. Members of the TGFβ family bind to specific Serine/Threonine protein kinase type II and type I receptors. Activated type I receptors induce the phosphorylation of specific receptor regulated SMADs, which are the intracellular effectors of TGFβ family members. In most cell types, TGFβ induces SMAD2/3 phosphorylation and BMPs induce SMAD1/5/8 phosphorylation. Activated R-SMADs form heteromeric complexes with SMAD4 that accumulate in the nucleus, where they regulate the expression of target genes.

In the canonical TGFβ pathway a ligand-receptor complex is formed, leading to SMAD proteins (pSMAD2-3) phosphorylation. These bind to SMAD4 to allow nuclear translocation and formation of complexes between transcription factors and co-activators/co-repressors on chromatin (Derynck and Zhang, 2003).

TGFβ pathways can also be activated in a non-canonical manner, in which the activated receptor complex interacts with different protein instead of phosphorylating directly SMAD proteins (Zhang, 2009). These non-SMAD pathways include various branches of mitogen-activated protein kinase (MAPK) pathways, Rho-like GTPase signalling pathways, and phosphatidylinositol-3-kinase/AKT pathways (Trojanowska, 2009; Iwata *et al.*, 2013). These enzymes modulate the activity of SMADs that activate a further enzyme to transmit the signal into the cell. Moreover, the receptor complex is able to activate several intracellular proteins by phosphorylation, which then transmit signals into the nucleus without direct cross-talk with the SMADs (Moustakas and Heldin, 2005).

Knockout of TGFβ pathway members often results in embryonic lethality. For example, using offspring from $TGF\beta1^{+/-}$ mice, 50% of mice embryos null for TGFβ1 and 25% of $TGF\beta1^{+/-}$ animals die at E10.5 showed defective haematopoiesis and endothelial differentiation of extra embryonic tissue with abnormal yolk sac vasculogenesis (Dickson *et al.*, 1995). Furthermore, mouse embryos null for *TGFβRII* show phenotypes similar to those of the *TGFβ1*–null embryos and also die at E10.5 because they exhibit severe defects in vascular development of the yolk sac and placenta, and an absence of circulating red blood cell (Oshima *et al.*, 1996; Larsson *et al.*, 2001), which suggests that this ligand-receptor combination acts at this stage in embryogenesis (Goumans and Mummery, 2000; Kulkarni *et al.*, 2002). In contrast, other researchers reported that mice homozygous for one disrupted

TGFβ1 allele survived for three to four week post-delivery (Shull *et al.*, 1992; Kulkarni *et al.*, 1993; Yang *et al.*, 2007). Interestingly, these studies identified progressive mononuclear cell infiltration in the vasculature that initiate a gradual inflammation of multiple tissues such as intestine, but no comments were found on alteration in intestinal morphology. The absence of an obvious phenotype in TGFβ1 null newborn has led to the suggestion that this grow factor is supplied to the foetus or newborn from maternal sources, as demonstrated by injected a ^{125}I-labeled mixture of active and latent TGFβ1, into the hearts of pregnant female mice that were TGFβ1 heterozygotes (Geiser *et al.*, 1993). This study suggested that maternal sources of TGFβ1 are vital for embryonic development. Table 1.3 summarize the phenotypes of TGFβ1 mutant mice described in this section of the thesis.

		Mutant Phenotype	
Reference	**Gene targeting**	**Embryonic**	**Adult**
(Dickson *et al.*, 1995) (Geiser *et al.*, 1993) (Kulkarni *et al.*, 1993) (Shull *et al.*, 1992)	TGFβ1	50 % die at E10.5 due to defective yolk sac vasculogenesis and haematopoiesis	Inflammation and autoimmune disorder and die at three to four weeks of age
(Larsson *et al.*, 2001)	TGFβRI	E.9.5: Mutants developed vascular abnormalities. Developmental retarded compared to wild type. E10.5: die	n/a
(Oshima *et al.*, 1996)	TGFβRII	Lethal around E10.5 Defect in yolk sac haematopoiesis and vasculogenesis	n/a

Table 1.3 Phenotypes of TGFβ1 ligand and TGFβ receptor deficient mice.

The table summarizes the most important articles describing the phenotypes of mice with anomalies of TGFβ1 ligand or receptor. Note that in TGFβ1 null mice only 50% of the embryos survive after birth but die after three to four week for extensive inflammation and wasting syndrome. Interestingly, embryos with deficit of TGFβ receptors die *in utero*. n/a=not applicable.

Loss of function phenotypes associated with disruption of TGFβ signalling genes is often dose-dependent. For instance, *SMAD4*$^{-/-}$ or *SMAD2*$^{-/-}$ mice die *in utero*, whereas heterozygotes survive without any identifiable defects at birth (Weinstein *et al.*, 2001). In non-transformed rat jejunal crypt cells, TGFβ1 has been shown to be implicated in the rapid cell turnover. In this model TGFβ1 seems to act as an auto-regulated growth inhibitor that potentially functions in an autocrine manner (Barnard *et al.*, 1989).

TGFβ may also acts as an injury/stress-activated messenger to recruit mesenchymal stem cells for tissue repair, regeneration, and pathological remodelling in various organs. In knockout mice, genetic deletion of TGFβ signalling mediators generate an alteration in the epithelia-mesenchymal transition mediated by SMAD2 (Nishimura, 2009). Moreover, TGFβ1 is known to be a key factor that intrinsically contributes to the restitution of injured intestinal epithelial cells, although it inhibits their proliferation as demonstrated in several models of intestinal inflammation (Paclik *et al.*, 2008).

A similar event is also reported in research investigating WNT signalling, a pathway that plays a critical role in the development of multicellular organisms and maintenance of adult tissue homeostasis (Clevers, 2006; Mohammed *et al.*, 2016). The multiple WNT ligands described in vertebrate animals act through two distinct mechanisms: the WNT/β catenin and the non-canonical WNT pathways (Veeman *et al.*, 2003). In human airway smooth muscle cell lines, non-canonical WNT pathway has been demonstrate to be involved in smooth muscle cell reorganization by TGFβ induced extracellular matrix production (Kumawat *et al.*, 2013). Furthermore, similar reciprocal signalling between TGFβ and WNT pathways has been found in vascular smooth muscle. Increased level of SMAD3 seems to stimulate the secretion

of canonical WNT proteins, which in turn enhances smooth muscle cells proliferation (DiRenzo *et al.*, 2016). The mutual interaction between these two highly conserved pathways has also been reported in a study investigating regeneration during injured colon, where TGFβ is stimulated by non-canonical WNT to establish new crypts containing quiescent epithelia (Miyoshi *et al.*, 2012).

Overall, TGFβ1 appears to regulate epithelial and mesenchymal cell proliferation, growth, differentiation and motility, but the activities of this molecule have been little investigated during embryonic gut development.

1.5.2 Could TGFβ signalling have a role in small intestinal development?

Previous studies have implicated TGFβ1 in postnatal gut maturation and also in regeneration following injury. By contrast, the possible roles of this molecule in embryonic gut development have been little studied. In the mature intestine, all three forms of TGFβ (TGFβ1-2-3) are detected in epithelia in the tips of villi (Barnard *et al.*, 1993) and TGFβ1 inhibits the proliferation of intestinal epithelia in cell culture (Yamada *et al.*, 2013).

In early mouse development, *in situ* hybridization for TGFβ1 showed this RNA to be expressed predominantly in the mesodermal components of the embryo. In fact, at E14 TGFβ1 appeared to be expressed in the gut predominantly in the mesodermal cell layers of the submucosa, but not in the intestinal epithelia, although it was visible at later stages of gut development at decreased levels (Schmid *et al.*, 1991).

Furthermore, analysing embryonic mouse gut from E15.5 to E17.5 by immunohistochemistry, TGFβ1 protein was localized in the smooth muscle layer and in the tip of the villi (Pelton *et al.*, 1991). Interestingly, an *in situ* hybridization study on TGFβRII localization in the E14 mouse embryo found this receptor in the muscle layer and in the mesenchyme but not in the endodermal epithelium of the developing intestine (Lawler *et al.*, 1994).

Considering the pathways regulating the rising of the villi, an intimate relationship between the muscle layer, the submucosa, and the epithelium seems to be clear and this bidirectional communication may drive intestinal morphogenesis. Although in this scenario TGFβ seems to have poorly defined roles, TGFβ proteins are expressed in the intestinal mucosa along with their receptors and have protective or reparative effects in various contexts (Pelton *et al.*, 1991; Hadjimichael *et al.*, 2016).

Components of the TGFβ pathway are also implicated in reciprocal signalling with other TGFβ superfamily members. TGFβRII localizes to villus enterocytes, especially at the tip (Winesett *et al.*, 1996), while BMP4 protein is observed in the mesenchyme of the villi and activates phospho (p) SMADs 1, 5, and 8 in the adjacent differentiated villus cells (Haramis *et al.*, 2004). In another study, a BMP receptor, BMPR1a, was observed in a gradient along the crypt-villus axis and in stem cells, but not in proliferative cells. Mice with knockouts of mesenchymal factors were noted to have decreased in BMP expression, developmental delays from a lack of epithelial proliferation, and adult survivors that developed extended hyper proliferative crypts and large villi (Kaestner *et al.*, 1997). Madison *et al.* also exposed intestinal mesenchyme of transgenic mice to a SHH ligand and observed the induction of BMP4 to analyse its role in the epithelial-mesenchymal transition. BMP signalling appears to involve cross-talk with the hedgehog pathway, and functions to maintain the proper polarity of the crypt-villus axis by inhibiting inappropriate epithelial proliferation in the villus (Madison *et al.*, 2005).

Moreover, embryonic intestinal small bowel epithelia secrete FGF9 that drives gut growth, enhancing mesenchymal proliferation (Geske *et al.*, 2008) and this protein seems to down regulate TGFβ signalling to prevent premature differentiation of the intestinal smooth muscle layers. Furthermore in the injured colon, TGFβ is also implicated in establishing new crypts containing quiescent epithelia (Miyoshi *et al.*, 2012). Notably, intestines of mice that lack FGF9 display premature myogenesis and excessive TGFβ signalling (Geske *et al.*, 2008).

TGFβ signalling is involved in endoderm differentiation, modulating proliferation, inducing extracellular matrix proteins expression, and stimulating intestinal epithelial cell migration along the villus axes (Sturm and Dignass, 2008). Using an

intestinal epithelial cell line *in vitro* model, TGFβ1 has been found to have potent effects on the intestinal epithelium, promoting rapid healing of the monolayers through stimulation and migration of cells across the wound margin (Ciacci *et al.*, 1993).

In an interesting review on the epithelial healing in inflammatory bowel disease, the TGFβ pathways seems to act from the baso-lateral site of the epithelial surface enhancing epithelial cell proliferation in the healing area margins (Sturm and Dignass, 2008). In contrast, members of the trefoil factor family appear to stimulate epithelial restitution in conjunction with mucin glycoproteins through a TGFβ independent mechanism from the apical site of the intestinal epithelium (Dignass *et al.*, 1994).

Although the role of TGFβ signalling has been investigated in vasculature smooth muscle cells (Hu *et al.*, 2015; Kofler and Simons, 2016; Zhang *et al.*, 2016b) and smooth muscle cells in the airways (Howell and McAnulty, 2006; Qu *et al.*, 2012; Li *et al.*, 2015b), but little is known about the role of TGFβ signalling in intestinal smooth muscle cells (Table 1.4). Interestingly TGFβ signalling increases premature myogenesis and fibrosis of intestinal smooth muscle cells in mice lacking FGF9 (Geske *et al.*, 2008).

Paper	Developmental age	Experiments performed
(Pelton *et al.*, 1991)	E15.5/E17.5	Immunohistochemical localization
(Schmid *et al.*, 1991)	E12.5/14.5	Northern analysis and in situ hybridisation
(Lawler *et al.*, 1994)	E14	In situ hybridization

Table 1.4 Literature summary of TGFβ1 roles in intestinal smooth muscle layers differentiation during mouse embryonic development

The present table highlights the paucity of papers that investigated the expression and localization of TGFβ1 in the smooth muscle layers during mouse embryonic development. Interestingly, these papers did not discriminate between circular and longitudinal muscle layers.

1.6 Short bowel syndrome in children

The present section describes the clinical background, which provided the clinical motivation of this research.

SBS in children is a multi-systemic disorder caused by inadequate length of small bowel usually less than half the expected for gestational age. SBS can occur as a congenital condition (Mandal *et al.*, 2016) or because patients develop conditions in which large section of bowel has to be removed surgically (Thompson, 2014).

Due to this syndrome, the child's growth rate is inefficient because the intestines cannot absorb the right amount of nutrients. Until now the treatment of this disease has been targeted towards nutritional support and surgical care (Coletta *et al.*, 2014).

Surgical treatment of SBS aims to increase intestinal absorptive capacity of the existing intestine using non-transplant surgical procedures improving not only the function of remaining bowel but also increasing the area of absorption (Ueno and Fukuzawa, 2010).

Future studies undertaken on intestinal development and increasing knowledge of intestinal stem cells may be the source for future therapy of SBS. Promoting appropriate intestinal length is far from being complete and more researches is needed to achieve a comprehensive understanding of intestinal growth. Critical analysis of the SBS disease, its management and the modern researches to treat this condition will be presented in the following paragraphs.

1.6.1 Aetiology and epidemiology

SBS has an estimated incidence of 25/100,000 live births (Wales *et al.*, 2004). The overall incidence and prevalence of SBS considering children and adult patients are estimated to be 3 per million and 4 per million, respectively (Bakker *et al.*, 1999)

Intriguingly, 44 cases of congenital SBS have been reported in literature so far (Huysman *et al.*, 1991; Schalamon *et al.*, 1999; Ordonez *et al.*, 2006; Hasosah *et al.*, 2008). Congenital SBS seems to be caused by homozygous or compound heterozygous mutation in the coxsackievirus and adenovirus receptor-like membrane protein (CLMP) gene on chromosome 11q24 as shown by homozygosity mapping using DNA from 5 patients from 4 families with congenital short bowel syndrome (Van Der Werf *et al.*, 2012). This gene is a type I transmembrane proteins within the immunoglobulin superfamily that localize to junctional complexes between endothelial and epithelial cells and may play a role in cell-cell adhesion (Raschperger *et al.*, 2004).

Developmental abnormalities of the small bowel (intestinal atresia, gastroschisis, malrotation and volvulus) and major abdominal disease in the postnatal period (necrotizing enterocolitis, midgut volvulus and inflammatory bowel disease) are the most important causes of SBS (Table 1.5) (Quiros-Tejeira *et al.*, 2004).

Infants	Children
Necrotizing enterocolitis	Cancer
Intestinal Atresia	Postoperative complication
Gastroschisis	Trauma
Midgut volvulus	Motility disorders

Table 1.5 Causes of short bowel syndrome in childhood

The present table showed the most common disease underlining SBS. Table adapted from (Quiros-Tejeira *et al*., 2004).

The debate on the correct definition of SBS is still on-going but is recognised that bowel length <100 cm in the first year of life is abnormal. Less than 40 cm traditionally requires therapy according to the practice of most centres (Soden, 2010; Khalil *et al.*, 2012). When the residual bowel less than 20 cm, this condition is called ultra-short bowel syndrome (Coran *et al.*, 1999).

The severity of intestinal resection and the absorptive condition of the remaining bowel determine the amount of total parenteral nutrition (TPN) required (Wales *et al.*, 2010). The complications emerging from SBS reported in the literature are: recurrent sepsis, catheter related sepsis, metabolic disturbances, hyperglycaemia, electrolyte imbalances, hypertriglyceridemia, gastric hyper secretion, diarrhoea, and organ dysfunction (Heine and Bines, 2002). Thus to consider the anatomical and physiological problems, a multidisciplinary treatment of SBS called intestinal rehabilitation programme focuses on the union of the correct enteral re-feeding and the best surgical technique for intestinal reconstruction (Khalil *et al.*, 2012).

1.6.2 Medical treatments

TPN is a method of feeding a person intravenously, bypassing the usual process of eating and digestion. TPN is considered a gold standard practice in SBS treatment because it is a solution for infants and children who are unable to eat or to absorb provided nutrients enterally (Kudsk, 2002; Wiles and Woodward, 2009).

After the introduction of TPN, the prognosis of infants and children with SBS has changed. As a result of an increased need for central venous access in order to administer the TPN, line sepsis and loss of venous access has been considered one of the most challenging complications (Goulet *et al.*, 2013).

When the TPN is required for more than three months the risk significantly increases to develop an intrahepatic cholestasis (Beale *et al.*, 1979; Kaufman *et al.*, 2003). Kelly defines the sequelae of SBS treatment as intestinal failure associated lived disease (IFALD) (Kelly, 2006; Kelly, 2010) (Table 1.6). Reducing the incidence of IFALD requires control of TPN composition as decreased dextrose, decreased fat emulsion, avoiding continuous infusion), maximization of enteral intake, treatment of small intestinal bacterial overgrowth, and pharmacotherapy with ursodeoxycholic acid.

Aetiology
Prematurity and low birth weight
Duration of TPN
Length of bowel remnant
Reduced enterohepatic circulation
Lack of enteral feeding
Recurrent sepsis
Deficiency of • Essential fatty acid • Chlorine
Excess of • Dextrose • Lipid emulsion >1 g/kg/die

Table 1.6 Aetiology of intestinal failure associated liver disease

The table above list the most common causes for the developing of intestinal failure associated liver disease in patients suffering from SBS. Table adapted from (Kelly, 2006).

1.6.3 Surgical treatments

The final aim of autologous gastro-intestinal reconstructive surgery is to return intestinal length and functional capacity equal to the age of the patient.

The first procedure to reduce the anatomical and functional problem of SBS was performed in Manchester in 1980 (Bianchi, 1980). Bianchi designed a technique called longitudinal intestinal lengthening and tailoring (LILT), a procedure that involves a longitudinal resection of a dilated segment of small bowel between the peritoneal leaves of the mesentery, which gives to two hemi loops sutured longitudinally with its own blood supply. The result is a loop of bowel doubled in length (Figure 1.11) (Bianchi, 1984; Bianchi, 1985).

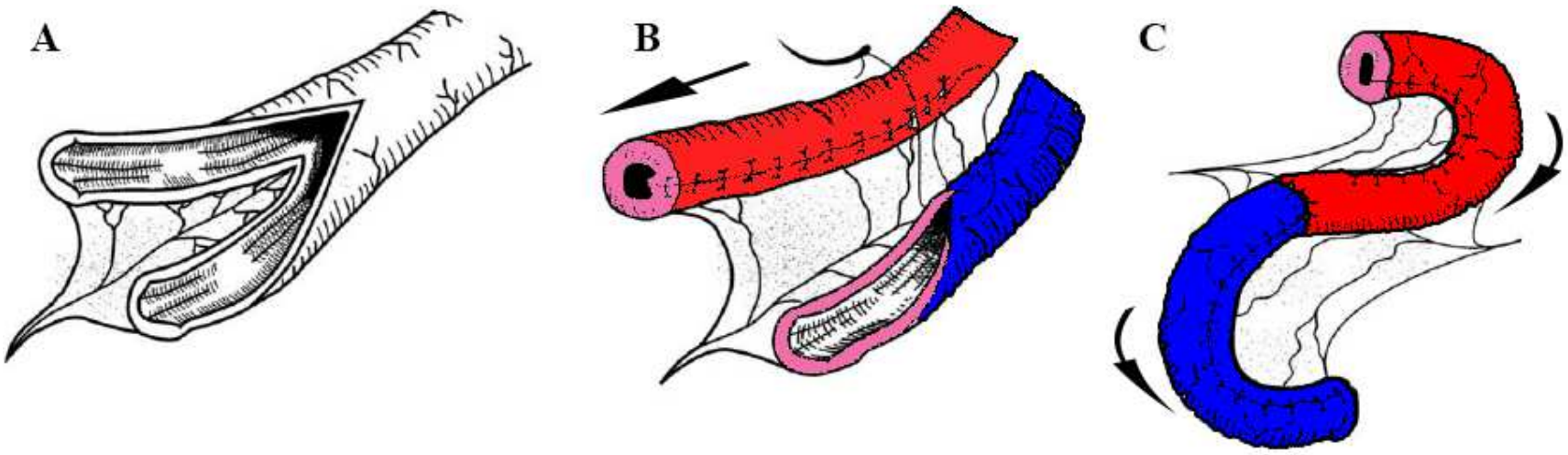

Figure 1.11 Longitudinal intestinal lengthening and tailoring (LILT)

(A). Blunt dissection between the peritoneal leaves of the mesentery, with development of a midline intravascular plane. (B) Formation of hemiloops by manual suturing inverts the bowel edges and preserves all mucosa. (C) Iso-peristaltic anastomosis between hemiloops in S shape. Diagram adapted from (Bianchi, 1984).

The second most remarkable procedure was designed in Boston where Kim *et al.* proposed an alternative approach to treat SBS called serial transverse enteroplasty procedure (STEP) (Figure 1.12) (Kim *et al.*, 2003a). This first human report (Kim *et al.*, 2003b) described the STEP lengthening procedure in a child who had previously undergone the established longitudinal technique of lengthening described by Bianchi. The STEP has been rapidly and widely adopted as an alternative intestinal lengthening procedure to the LILT proposed by Bianchi.

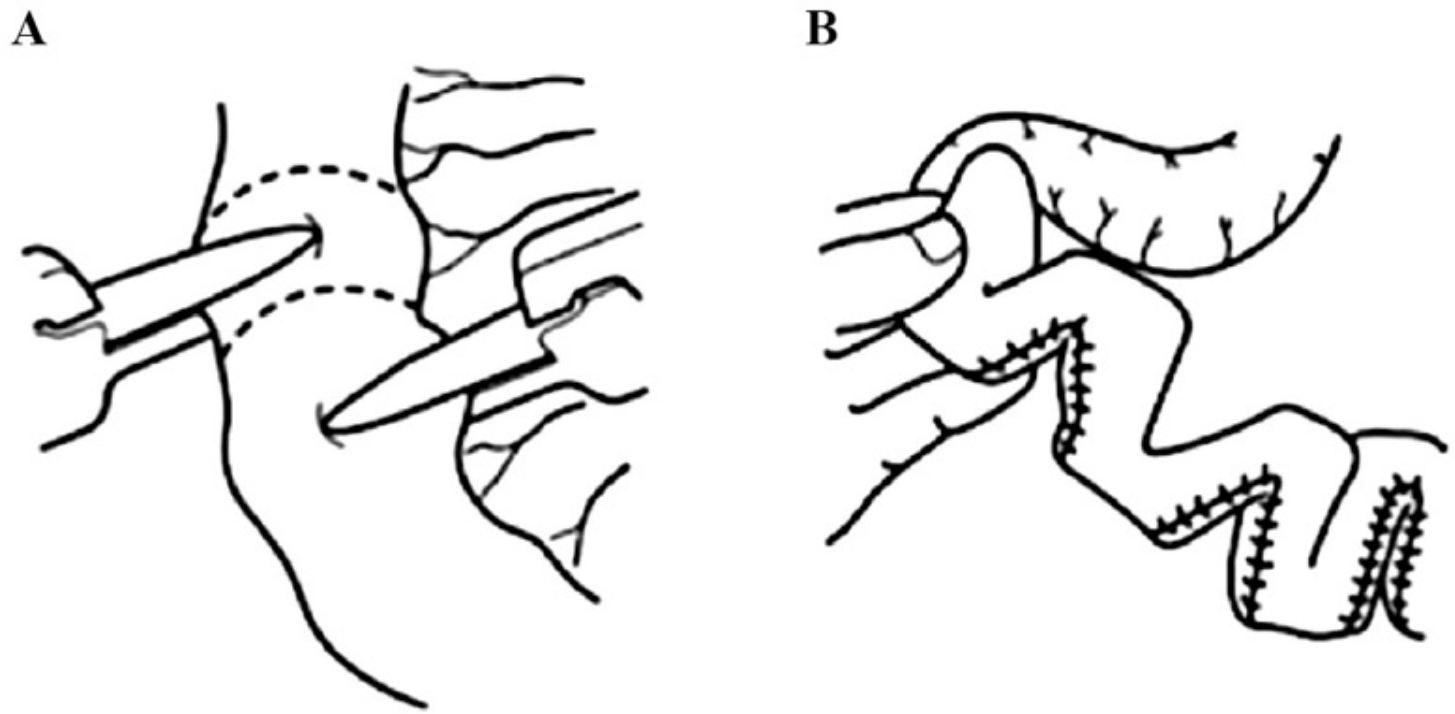

Figure 1.12 Serial transverse enteroplasty procedure (STEP)

(A) The small arrows show the direction of stapler and the sites of the mesenteric defects. (B) The staplers are placed in the 90^{o} and 270^{o} orientations using the mesentery as the 0^{o} reference point. Figure adapted from (Kim *et al.*, 2003a) and (Coletta *et al.*, 2014).

In 2013 a systematic review (King *et al.*, 2013) has proven no significant difference between the LILT and STEP procedures. The STEP has a higher rate of complications, while the Bianchi procedure has a higher rate of weaning patients from TPN. However the Bianchi procedure was associated with a higher rate of patients receiving transplants.

The latest proposed surgical technique for intestinal lengthening comes from Cserni *et al.* in 2011 (Figure 1.13) (Cserni *et al.*, 2011). In a double layer intestinal simulator and in porcine model, a section of bowel was lengthened and tailored in a spiral fashion replacing the longitudinal sectioned technique proposed in the LILT procedure. Cserni called this alternative technique spiral intestinal lengthening and tailoring (SILT), reporting the first human use of the SILT in 2013 (Cserni *et al.*, 2014). Although SILT shows great potential in selected cases of ultra-short non-dilated bowel, this new procedure still required further long-term studies.

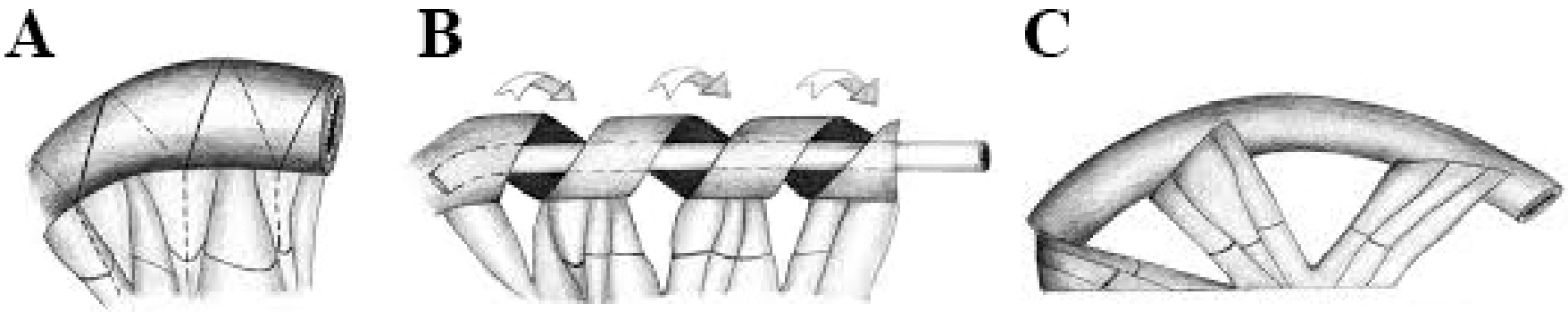

Figure 1.13 Spiral intestinal lengthening and tailoring (SILT)

(A) Bowel is cut at 60^{o} and tabularized. (B) Spiral lengthening and tailoring translation of intestine over a support to drive perfect orientation during suture time. The mesentery is gently split to facilitate spiral rotation. (C) SILT final result. Diagram adapted from (Cserni *et al.*, 2013).

In the event of failed adaptation and in the condition of liver failure and reduced venous access, transplantation becomes the only hope for children with SBS (Nayyar *et al.*, 2010). In this group of patients transplantation involves combined liver and small bowel. In some cases in which the liver has not undergone irreversible damage, isolated intestinal transplant could be performed.

With improvements in immunosuppression treatments, operative techniques and critical care, patient and graft survival have steadily increased. Graft and patient survival both vary from 64% to 89% at one year based on age category falling to 31% to 69% at five years for graft survival, and 33% to 76% for patient survival at five years. In larger centres, however, results are improved with one-year patient survival around 80% for both isolated intestine and combined liver-intestine grafts, dropping to around 60% at five years (Grant *et al.*, 2005).

Transplant should be the last resort, if patients fail to adapt once surgical options have been exhausted, develop irreversible liver failure or are about to lose all central venous access. Reconstructive surgery rather than transplantation is growing in frequency as a first line treatment, evidenced by the reduction in number of intestinal transplantations (Abu-Elmagd, 2015; Cohran, 2015).

1.7 Future treatment of short bowel syndrome

The modern approach to SBS has been considered to be multidisciplinary (Khalil *et al.*, 2012), but there are still cases where the only solution remains transplantation. However, the low number of donors, postoperative complications, the reduction of lifestyle and the low five years patient's survival data after intestinal transplantation (survival near 67%) suggest the need for alternative techniques. Motivated by these problems, researchers have placed their focus on finding non-transplant therapies to SBS since the end of the twentieth century.

The next section will provide a summary of the most recent research approaches for SBS disease like regenerative medicine, tissue engineering and distraction enterogenesis.

1.7.1 Regenerative medicine and tissue engineering

Tissue engineering refers to the practice of combining scaffolds, cells, and biologically active molecules into functional tissues. This technique has been applied successfully in the clinical arena for the production of different tissues such as bladder (Atala, 2014) or trachea (Fishman *et al.*, 2014) or by decellularization of native intestine (Totonelli *et al.*, 2012).

Regenerative medicine is a broad field that includes tissue engineering but also incorporates research on self-healing where the body uses its own systems, sometimes with help foreign biological material to recreate cells and rebuild tissues and organs. The terms tissue engineering and regenerative medicine have become largely interchangeable, as the field hopes to focus on cures instead of treatments for complex, often chronic, diseases (Zhang *et al.*, 2014). Regenerative medicine aims to use autologous human products to regenerate tissue damaged from congenital

diseases and to repair or replace injured organs (Kemp, 2006; Orlando *et al.*, 2011; Zhang *et al.*, 2014).

The development of bioengineering techniques and molecular medicine has focused researchers' attention on the possibility to use tissue-engineered small intestine (TESI). In 1988 the pioneering study of Vacanti described a method to attach cell preparations to biodegradable artificial polymers in organ culture and implanting this polymer-cell scaffold into rodent animals (Vacanti *et al.*, 1988). In 1997, Choi and Vacanti described a tissue-engineered small intestine on biodegradable scaffolds by transplanting intestinal epithelial organoid units in the rat model (Choi and Vacanti, 1997). Histological analysis of the neo-intestine showed formation of neo-mucosa characterized by columnar epithelium with goblet and Paneth cells (Choi *et al.*, 1998). Subsequently, Kim and the Vacanti's group investigated the effects of anastomosis between TESI to native small bowel alone or combined with small bowel resection on neo-intestinal regeneration (Kim *et al.*, 1999). When TESI was anastomosed to the side of the proximal small intestine of the rodents these animals improved weight gain, suggesting a role for TESI in the management of SBS (Grikscheit *et al.*, 2004).

Using detergent-enzymatic treatment on tissues like muscle (De Coppi *et al.*, 2006), trachea (Kutten *et al.*, 2015) or intestine (Totonelli *et al.*, 2012) is possible to generate a scaffold able to preserve the architecture of the native tissue and the extracellular matrix that is needed for cell proliferation. Due to the recent advantage in this technique used recently in clinical practice (Hamilton *et al.*, 2015), the decellularized scaffold seems to open new prospective in the treatment of intestinal disease as SBS. In future this approach could avoid the need of intestinal

transplantation but the transition to human therapy requires reliable techniques (De Coppi, 2013).

Using a mouse intestinal epithelial cell culture, the possibility to isolate epithelial pluripotent stem cell has been explored (Sato and Clevers, 2013b), leading the possibility to create mouse intestinal organoid, called also mini-gut (Sato and Clevers, 2013a). Recently, the methods used with the mouse pluripotent stem cell was tested with human pluripotent stem cell (Sato *et al.*, 2011a), creating long term expansion of human intestinal organoid.

The possibility to create intestinal organoid could have the potential to offer a personalized and scalable source of intestine for regenerative therapies. Recently, the possibility of human intestine embryonic stem cells or human intestinal organoids to repopulate scaffold, porcine or synthetic, was investigated with a primary output the ability of matrix/scaffolds to thrive when transplanted *in vivo* (Finkbeiner *et al.*, 2015). Although this study showed that human intestinal organoids in combination with a synthetic scaffold seems to offer a promising approach to generating tissue engineered human intestine, more studies are needed to create a fully functional tissue.

Reproduction of the three-dimensional structure of the single intestinal functional unit (the crypt with the respective villus) still represents one of the major challenges for the development of functional intestine. To solve this issue, the research group coordinated by De Coppi postulated a new bioengineering protocol to create an intestinal tissue-engineering model by using detergent-enzymatic treatment making a natural intestinal scaffold, as a base for developing functional intestinal tissue (Totonelli *et al.*, 2012). After the enzymatic treatment, the acellular matrix showed

its cylindrical structure with mesentery on the side (Figure 1.14). In addition they postulated that the preserved crypt/villus structure after one treatment might facilitate the establishment of the regenerating unit. Unfortunately, no *in vivo* experiment has been yet published to consolidate these results.

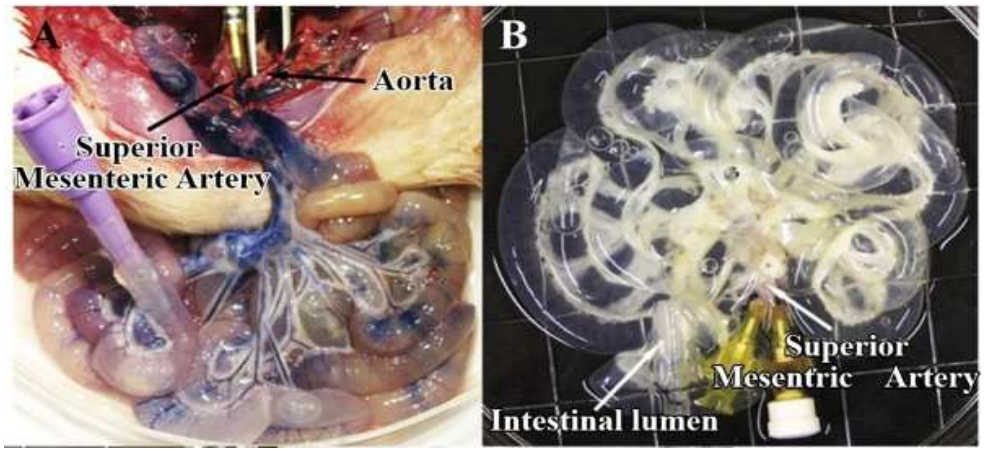

Figure 1.14 Decellularization of rat small intestine with detergent-enzymatic treatment

Macroscopic images prior (A) and following (B) decellularization. Complete decellularization of the rat intestine was obtained after one cycle of detergent-enzymatic treatment. Figure adapted from (Totonelli *et al.*, 2012).

Analysis of these models of treatment reveals two essential features. First, all the intestinal units were derived from newborn rodents. In the clinical setting it would be difficult, and sometimes impossible, to obtain human neonatal intestinal organoids, especially for autologous stem cell transplantation. Secondly, TESI is implanted in the omentum where it will form a cyst with all the intestinal layers. The omentum provides the vascular supply to the organoids and enables integration of the absorbed nutrients with the host portal circulation. The omentum, however, is often removed or scarred in patients with SBS because of prior surgeries. Even when present, the surface area of the omentum is not large enough to generate the area of intestinal tissue needed for clinically significant results.

The final point of controversy is the lack of peristalsis in the tissue-engineered bowel. Although tissues generated from intestinal organoids resemble the mucosa, functional smooth muscle layers and neural plexus are absent. However, in 2012 researchers directed by Bitar demonstrated the possibility of creating a bioengineered muscle by growing rabbit colonic circular smooth muscle cell on chitosan-coated plates (Zakhem *et al.*, 2012), opening new prospective in the future peristaltic movement of tissue engineered gut.

In future tissue-engineered treatments would avoid problems associated with intestinal transplantation, including donor availability and complications from immunosuppressive therapy but the transition to human therapy requires a reliable technique (De Coppi, 2013).

1.7.2 Distraction enterogenesis

In the last decade mechanical stretching has been used either to increase tissue surface or to stimulate its growth (Kraaijenga *et al.*, 2014; Rinker and Thornton, 2014; Charles and Leaver, 2015; Demehri *et al.*, 2015; Murphy *et al.*, 2011).

The idea of expanding bowel to create enough tissue in preparation for a lengthening procedure was introduced by Georgeson *et al.* in 1994 (Georgeson *et al.*, 1994). The authors described a nipple valve to occlude the lumen of the bowel. This process of creating a non-controlled bowel obstruction generates intestinal dilatation (Collins *et al.*, 1996). Bianchi introduced the concept of controlled tissue expansion (CTE) modifying the nipple valve idea of Georgeson and proposed this approach serially (Figure 1.15) (Bianchi, 2006).

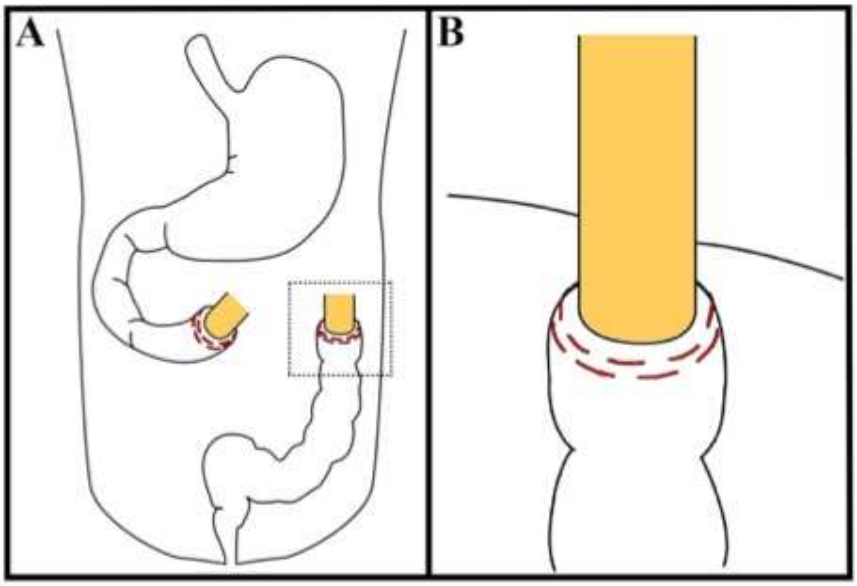

Figure 1.15 Controlled tissue expansion (CTE)

(A) Schematic representation of proximal and distal tube stomas. Malecot or Foley catheter is placed into the proximal and distal end of the remnant bowel. (B) Enlarged view of the tube stoma. The tube stoma is fashioned using purse string sutures to the abdominal wall. Tube is highlighted in yellow, purse string suture in red. Diagram adapted from (Murphy *et al.*, 2011).

The CTE proposed by Bianchi (Murphy *et al.*, 2011) uses a tube stoma clamping-recycling approach with the benefit to distend the proximal bowel by the natural content and to stimulate the mucosa of the distal epithelium by recycling chime (Pataki *et al.*, 2013). At the present time CTE appear to be the only strategy applicable in clinical practice.

Several approaches have been described to expand intestinal segments in a controlled way but all with some limitation. Recent studies reported the possibility to induce enterogenesis by different devices, which need distractive forces to elongate the bowel (Demehri *et al.*, 2016; Okawada *et al.*, 2011; Sullins *et al.*, 2014). However, these devices appear to be difficult to apply in a clinical scenario because the onset of the patients and the family is compulsory.

Recently a variety of devices and operative approaches have been used in animals, but none of these approaches have yet been translated into clinical use. While self-expanding shape-memory polymer cylinder (Fisher *et al.*, 2015), catheter device (Demehri *et al.*, 2015), telescopic hydraulic device (Demehri *et al.*, 2016) have all been tested, these have been limited by the need for complex activation mechanisms or the surgical risk associated with reoperation for removal of the device and consequent restoration of intestinal continuity.

The use of an osmotic expander has been popularised among plastic surgeons and has become the treatment method of choice for many congenital and acquired defects in a wide variety of diseases first adults and subsequently in children (Gronovich *et al.*, 2015; Yesilada *et al.*, 2013), but this approach has never been reported in the treatment of SBS so far.

1.8 Hypotheses and Aims

Molecular control of intestinal development has been extensively investigated *in vivo*, but little is known about the events controlled by TGFβ1. This lack of knowledge seems to be due mainly to the difficulties associated with *Tgfβ1* null mice model period because mutant embryos die at E9-E10 due to growth retardation, oedema, necrosis, vascular anomalies, endothelial instability, and loss of smooth muscle cells around the vessels.

The design of an organ culture *ex vivo* model could provide the opportunity to follow intestinal development and differentiation, and allows chemical manipulation. Furthermore, the ability to mechanically influence intestinal specimens *ex vivo* could provide an experimental model, which can be used to find new therapeutic strategies for catastrophic intestinal events such as the short bowel syndrome. These observations lead me to my hypotheses and aims.

Hypothesis 1: *Ex vivo* embryonic small bowel is able to restore continuity after an injury.

Aim 1: To develop a reliable and reproducible organ culture model capable of sustaining three-dimensional embryonic intestinal segments.

How I will do this: Using a hydrophilic polymeric membrane, on which the samples will be located, and by serum free defined medium the specimens will be cultured for a fixed time. Serial images will be obtained to detect architectural modifications and to monitor the specimens' viability. Furthermore, I will use immunofluorescence to determine whether this model can sustain normal development comparing the small bowel anatomies of specimens cultured in define media with embryonic jejuna

from E14 and E17. Finally, I will record the peristaltic movements of the specimens cultured *ex vivo* as supporting evidence that my model is reliable.

Aim 2: To test whether embryonic intestinal specimens will be suitable for physical manipulations aimed at enhancing continuity of embryonic gut segments, thus generating a single functional organ.

How I will do this: Using an *ex vivo* model I will create a gap between two consecutive specimens orientated by a thread into their lumen. The *ex vivo* system will be controlled daily to determine how the explants tolerate the growth with a thread into the lumen. Using opposite injection of two different dyes into the specimens lumen, I will determine the physical fusion of the explanted jejuna. Furthermore, to test the functional fusion, I will record real time movie to follow the intestinal contraction between the two consecutive explants after fusion. Finally, I will investigate whether the healed tissue is able to restore continuity of the neuronal network between the separated sections.

Hypothesis 2: Transforming growth factor β1 affects embryonic small bowel elongation and its architectural differentiation during development.

Aim: to identify the effects of TGFβ1 in an *ex vivo* model of intestinal development and to identify the source of TGFβ1 during development.

How I will do this: Using the model established to investigate the first hypothesis, I will create an *ex vivo* system in which I will add different concentrations of TGFβ1. Using immunofluorescence and morphological/anatomical analysis, I will determine the possible consequences that this growth factor can make *ex vivo.* I will collect the amniotic fluid of embryonic mice at E14 and E17 and the conditioned media of

tissue exposed for three days to TGFβ1. Using ELISA on these supernatants, I will measure the endogenous and the exogenous amount of TGFβ1. Furthermore, I will compare *in vivo* normal development versus specimens cultured in different condition of TGFβ1 *ex vivo* to determine how TGFβ1 influence intestinal development. Finally, using RNA microarray and QPCR, I will investigate how TGFβ1 can drive morphological events during intestinal development *ex vivo*.

2 CHAPTER 2 – Materials and Methods

2.1 Statement of experimental contributions

Many different experimental techniques were performed during this work. The author generated the majority of the data presented in this thesis. The scientific contributions to the present research will be stated on the present section.

I designed the study and the organ culture model, programmed the plug date of the mouse, performed the harvesting of the small bowel specimens, inserted the tread into the small bowel specimens, took the bright field pictures of the specimens during the culture, embedded the samples, sectioned the specimens, performed immunofluorescence and whole tissue staining, performed collection of specimens for the microarray and the QPCR, collected the amniotic fluid, the specimens and the conditioned media for the ELISA and interpreted all the statistical analysis.

Adrian S. Woolf helped me to design the research, to set up the organ culture model and to interpret the results.

Neil A. Roberts helped me to create an embedding medium for the specimens, to perform confocal and immunofluorescence images, to design ELISA and QPCR experiments and introduced myself to the use of ImageJ, Prism and Photoshop.

Emma N. Hilton helped me to design the ELISA and QPCR experiments and to interpret their data.

Parisa Ranjzad helped me to set up the organ culture model and to design the culture media.

Francesca Oltrabella performed the injection of the dyes into the specimens to investigate physical fusion of two consecutive explants.

Leo Zeef and Andy Hayes generated microarray data from the sample provided by myself.

Michael Randles undertook bioinformatics analyses of microarray data and generate corresponding graphs.

2.2 Animals and experimental design

At the beginning of the present research I undertook Home Office Modules covering mouse ethics and animal handling. The Institutional Review Board of the Registered Medical approved mouse experiments and Scientific Departments of the University of Manchester approved animal experiments. Populations of mice were housed at the University of Manchester, adhering to home office regulation and the Animal (Scientific Procedure) Act 1986. Wild type (CD1) mice were mated overnight in the University's Biological Services Facility. The morning of the vaginal plug was designated as E0. After Schedule 1 killing performed by those holding an appropriate home licence, the mouse was collected and placed on a semi-sterile bench in the dissection room for harvesting of the embryos.

To reduce the risk of contamination the abdomen was cleaned with 70% ethanol. The abdominal cavity was reached by midline incision through the muscles and peritoneum. The uterine horn was removed and separated from the other organs in the abdominal cavity.

The dissected uterine horn was placed in a Petri dish on ice containing cold dissection solution, Leibovitz-15 (GIBCO Dulbecco's Phosphate buffered saline 1x).

After separating the embryo from the uterus, the specimens were placed into a Petri dish contacting cold dissecting solution and transferred to a dissection microscope.

Amniotic fluid was collected from E14 and E17 embryos via a 16 - gauge needle and harvested in an Eppendorf tube at -80^{o} degrees. Dissection of the embryo was performed using microsurgical forceps (Micro Jewellers Forceps, Mercian, code JFL-5), scissors (Micro Scissors Flat Handle, Mercian, code SAS-11) and ophthalmic blade (Optimum Straight Knife 15o, BD Beaver, ref 370566).

The abdominal cavity of the embryo was opened and by gently blunt dissection the gastrointestinal system was explanted (Figure 2.1).

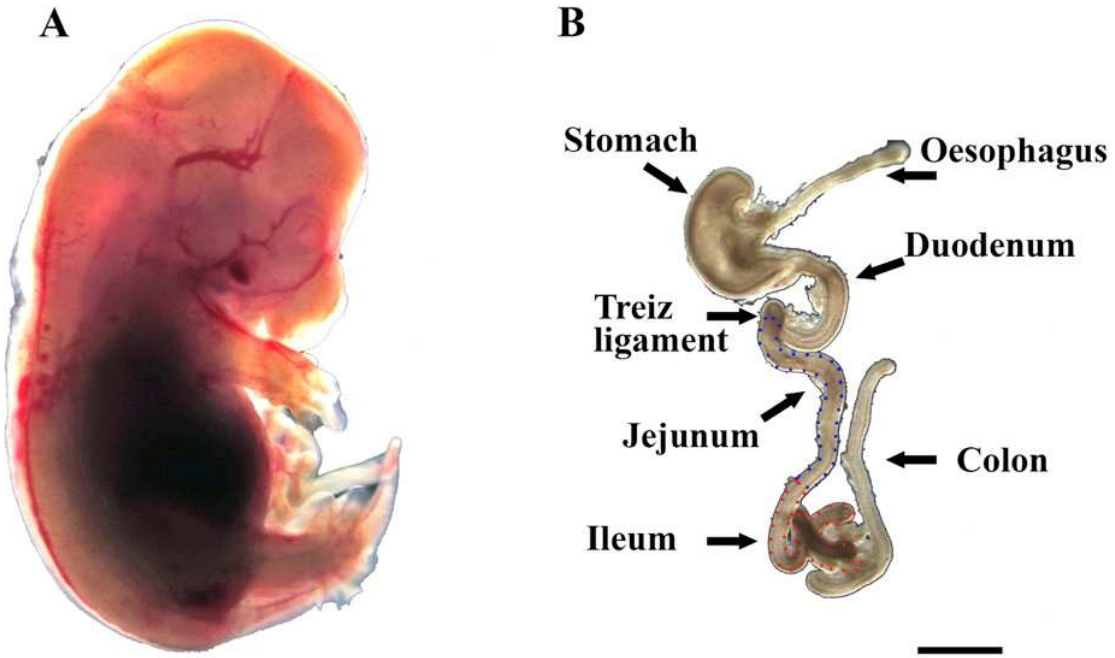

Figure 2.1 Macroscopic anatomy of embryonic day (E) 14 embryo and embryonic gastrointestinal system

Pictures from an animal used during the present research. (A) E14 embryonic mice. The small bowel appears to be herniated into the extra embryonic coelom. (B) E14 embryonic gastrointestinal system. All the compartmental sections are highlighted. Green dots: proximal small bowel. Red dots: distal small bowel. Scale bar is 500 μm.

After identification of the Treitz ligament, the embryonic jejunum was dissected and a 2-3 mm section used for histology or organ culture (Figure 2.2). In some experiments, a polyamide 10/0 suture (Ethicon) was threaded through the rudiment's lumen to keep the explant straight and ensure generation of precise transverse histological sections.

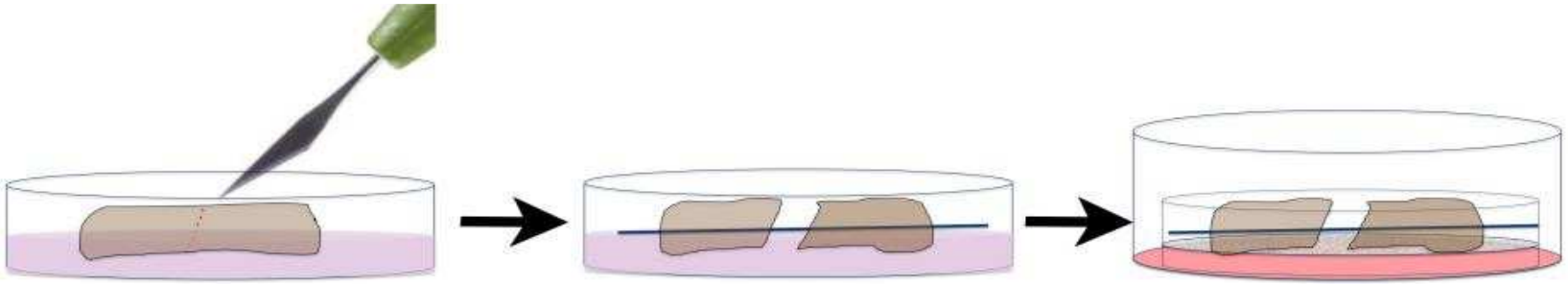

Figure 2.2 Organ culture: creation of intestinal gap bridged by a thread

An incision is performed in the middle portion of a proximal specimen. After the creation of iatrogenic gap between two contiguous pieces of intestine, a 10/0 Prolene thread is introduced thought the lumen of the embryonic bowel. Finally the specimen is located on a Millipore insert and is cultured in defined medium for three days. (Violet=Leibovitz-15; red=Defined serum free medium).

2.3 Organ culture

E14 rudiments were placed onto semipermeable 0.4 μm pore polytetrafluoroethylene culture plate inserts 0.4 μm Millicell, (Millipore, Bedford, MA, (cod. numb. PICM03050) and maintained at 37°C in an atmosphere of air/5% CO_2.

Defined serum-free media, placed underneath and touching the platform, fed explants. Basal media comprised Dulbecco's modified eagle medium (DMEM): with nutrient mixture F-12 (GIBCO BRL, prod. cod. 11320-033), insulin (10 mg/L), sodium selenite (5 mg/L), and transferrin (5.5 mg/L), penicillin G (100 units/mL), streptomycin (100 μg/mL) and amphotericin B (0.25 μg/mL) (Chan *et al.*, 2010).

For serum-free organ culture, a protocol was used which has been shown to support the differentiation of epithelial and mesenchymal/smooth muscle lineages in embryonic mouse bladders (Burgu *et al.*, 2006), ureters (Tai *et al.*, 2013) and metanephric kidneys (Anders *et al.*, 2013).

In some experiments, the medium was supplemented with recombinant human TGFβ1 (R&D Systems; cat. numb. 240-B-002) at 5 or 50 ng/mL, concentrations used previously in similar organ culture studies of embryonic mouse kidneys and salivary glands (Bush *et al.*, 2004; Janebodin *et al.*, 2013). The defined serum-free media or the media supplemented with growth factor was placed beneath the platform and touching the membrane of the Millicell insert.

In some other experiments, the medium was supplemented with R-spondin1 (Peprotech) a factor that promotes canonical WNT/β-catenin signalling and stimulates intestinal epithelial proliferation in postnatal mice (Kim *et al.*, 2005). The concentration used, 100 ng/mL, has previously been tested in experiments conducted on intestinal colonic and pancreatic culture (Huch *et al.*, 2013; Sato and Clevers,

2013a). Explants were cultured for three days because previous observations had shown that longer cultures were less viable (Quinlan *et al.*, 2006).

To determine whether embryonic intestinal lumens became continuous during culture, fluorescent fixable dextrans, 2 g/L in phosphate-buffered saline (PBS; Molecular Probes), were injected into opposite ends of adjacent explants, using a MPPI-2 Pressure Injector/BP15 Back Pressure Unit (Applied Scientific Instrumentation). Green fluorescent AlexaFluor 488 dextran (10 kDa) was injected into one end and Texas red (70 kDa) into the other.

In addition, 2 mm segments of E17 jejunum were placed into organ culture (basal medium only) and, after 1h, they were observed to determine whether they underwent peristalsis and to compare normal development with the specimens cultured for 3 days.

2.4 Enzyme-linked immunosorbent assay (ELISA)

To understand the concentration of TGFβ1 on the amniotic fluid, enzyme-linked immunosorbent assays (ELISAs) test was performed. The amniotic fluid was centrifuged first in $4^{o}C$ for 3 minutes and the supernatant used for the test.

For TGFβ1, the Abcam kit ab119557 was used. The ELISA was executed in accordance to the manufacturer protocols. For both the kit, the absorbance of both the samples and the standards was determined by a spectrophotometer using 450 nm as the primary wave length. Finally the data was analysed using Excel and GraphPad Prism 6.0.

2.5 Histology and Fluoroscopy

Tissues were fixed for 30 minutes in 4% paraformaldehyde, rinsed in 1% PBS, dehydrated in ice cold methanol and stored in -20^{o}C. After rehydration, samples were embedded in 25% fish gelatine and cryosectioned at 10 µm using -30^{o}C for the chamber and -32^{o}C for the object.

Transverse sections were fixed in acetone for five minutes, washed with ice cold 1% PBS and permeabilized in 1% PBS, 0.1% Triton X-100 for 10 minutes. Mouse on Mouse Blocking Reagent (MOM™, Vector Laboratories, cat. numb. BMK-2202) was used to block endogenous immunoglobulins.

Sections were incubated for 30 minutes with primary antibodies against: a-smooth muscle actin (αSMA; A2547, Santa Cruz Biotechnology: 1:200), a visceral muscle cytoskeletal protein (Wilm *et al.*, 2005); E-cadherin (ab76055, Abcam; 1:200), an epithelial cell-cell adhesion protein (Tai *et al.*, 2013); Ki67 (ab16667, Abcam; 1:100), a nuclear proliferation associated protein; SOX9 (Millipore, AB5535; 1/200), a transcription factor; TGFβ receptor I (TGFβRI; ab31013, Abcam; 1:200); and TGFβ receptor II (ab186838, Abcam; 1:200). Table 2.1 shows the detailed list of antibodies used.

After washing, fluorescent secondary antibodies (AlexaFluor 488, 568 or 599) were applied for one hour. Sections were counterstained with 4', 6-diamidino-2-phenylindole (DAPI) to detect nuclei for 10 seconds.

2.6 Whole tissue staining

Rudiments were rehydrated for two minutes in decreasing concentrations of methanol and then washed in 1% bovine serum albumin (BSA) in 1% PBS and 0.1% Triton X-100 for two hours. Then the specimens were transferred into glass tube and blocked with 1% BSA in 1% PBS, 0.1% Triton X-100 and 5% heat-treated goat serum for one hour.

After rinsing, they were incubated for 72 hours with 1:500 dilutions of primary antibodies to E-cadherin (ab76055, Abcam), an epithelial cell-cell adhesion protein (Tai *et al.*, 2013), and peripherin (1530, Millipore), an enteric neuron cytoskeletal protein (Ganns *et al.*, 2006). The incubation was performed rotating the vials in a dark room at 4^{o}C. Table 2.1 shows the detailed list of antibodies used.

After the first antibody step, the specimens were washed for four hours in 1% BSA in 1% PBS and 0.1% Triton X-100 to clean any excess of first antibody. Than the specimens were blocked again for one hour and finally they were incubated overnight with corresponding secondary antibodies (AlexaFluor). The second antibody step was performed rotating the vials in a dark room at 4^{o}C.

After three hours of wash in 1x PBS, 0.1% Tween-20, the specimens were incubated in 1x PBS, 0.1% Tween-20 for 48-72 hours to clean completely from any residual. Than the specimens were incubated in 75% glycerol overnight before be ready for confocal images. The 75% glycerol was used instead of 33% Benzyl Alcohol and 67% Benzyl Benzoate (BABB) solution because that shown to dissolve completely the embryonic intestine.

Before confocal investigation, the specimens were located into a handmade chamber prepared by solid resin and secured on a glass with high vacuum grease.

Ab specificity	Ab name and description	Source/supplier	Working dilution
SOX9	Ab5535, rabbit polyclonal	Millipore	1:200
pSMAD3 (Serine423/425)	Ab52903, rabbit monoclonal	Abcam	1:500
pSMAD2/3 (Serine423/425)	Sc-11769, goat polyclonal	Santa Cruz	1:100
TGFβ Receptor I	Ab31013, rabbit polyclonal	Abcam	1:200
TGFβ Receptor II	Ab186838, rabbit polyclonal	Abcam	1:200
E-cadherin [M168]	Ab76055, mouse monoclonal	Abcam	1:200
E-cadherin (H-108)	Sc-7870; rabbit polyclonal	Santa Cruz	1:200
α-Smooth Muscle actin	Ab21027, goat polyclonal	Abcam	1:200
α-Smooth Muscle actin	Sab2500963, goat polyclonal	Sigma-Aldrich	1:200
Ki67n [SP6]	Ab16667, rabbit monoclonal	Abcam	1:100
Peripherin	Ab1530, rabbit polyclonal	Millipore	1:500
Donkey, goat, mouse, rabbit	AlexaFluor 488, 566, 594	Life technologies	1:500

Table 2.1 List of primary antibodies

The present table lists the antibodies used for immunofluorescence and whole tissue staining. Ab=antibody.

2.7 RNA microarray and quantitative polymerase chain reaction

RNA was isolated from the specimens using the RNeasy Plus kit (QIAGEN). RNA quality was assessed, and concentrations measured, using a NanoDrop 2000 spectrophotometer. cDNA was generated using a High Capacity RNA-to-cDNA Kit (Applied Biosystems).

For whole transcriptome microarray expression analyses, amplified sense-strand cDNA (Ambion WT Expression Kit®) was generated from 100 ng of total RNA. Fragmentation and labelling (Affymetrix Genechip WT Terminal labelling kit®) and subsequent hybridization utilizing Affymetrix Genechip Mouse Exon 1.0 ST Array® was performed at the Genomic Technologies Core Facility at the University of Manchester.

Data were processed and analysed using Partek Genomics Solution (version 6.5, Copyright 2009, Partek Inc) with these options: probe sets of the core subset were quantile normalised and robust multi-array background correction applied. Exons were summarized to genes by calculating the mean of the exons (log 2).

Validation and gene enrichment strategies consisted of the following steps. Microarray data are available in the ArrayExpress database (www.ebi.ac.uk/arrayexpress) under accession number E-MTAB-4509. For reviewer access, please use username: Reviewer_E-MTAB-4509. Password: jeiuhaha.

To establish relationships and compare variability between replicate arrays and experimental conditions, principal components analysis (PCA) were used. PCA was chosen for its ability to reduce the effective dimensionality of complex gene-expression space without significant loss of information (Quackenbush, 2001). Next, differential expression in response to treatment was calculated using Cyber-T (Baldi

and Long, 2001). Correction for false discovery rates was done using the method of QVALUE (Storey and Tibshirani, 2003).

To validate array results, quantitative polymerase chain reaction (QPCR) TaqMan® Gene Expression assays were performed on cDNA gathered from RNA extraction and cDNA production stated above. TaqMan® Gene Expression protocol was applied according to the manufactory (Life Technologies). Each real-time PCR reaction was composed by 1:5 dilutions of cDNA, 2x TaqMan® Gene Expression Mastermix (Life Technologies cat. numb.4369016) and RNase-free H_2O.

TaqMan® Gene Expression probes for target genes were introduced at 500nM each. Alongside an endogenous housekeeping prove as Gapdh (glyceraldehyde 3 phosphate dehydrogenase) and for selected transcripts (Table 2.2) altered by 5 ng/mL of TGFβ1. Similar analysis by the same transcripts was made also for specimens cultured in 50 ng/mL of TGFβ1. QPCR was also undertaken for Tgfβ1 and Tgfβ2. Components were combined in a stepwise manner into a PCR 96-well multi plate (Sigma cat. numb. Z374903) in triplicate.

The assay plate was placed in the StepOnePlus™ Real Time PCR-system (Applied Biosystems). Samples were heated to 50^{o}C for 2 minutes followed by 95^{o}C for 10 minutes. Cycling conditions were: 95^{o}C for 15 minutes followed by 60^{o}C for one minute for 40 cycles. Samples were analysed using comparative Ct (ΔΔCt) method in the accompanying StepOnePlus™ software package.

UniGene Symbol	UniGene Name	TaqMan
Krt17	Keratin 17	Mn00495207_m1
Ctsw	Cathepsin W	Mn00515599_m1
Anpep	Aminopeptidase M	Mn00476227_m1
Col8a1	Collagen, type VIII, alpha 1	Mn01344185_m1
Lgr5	Leucine-rich repeat containing G protein-coupled receptor 5	Mn00495207_m1
Eln	Elastin	Mn00514670_m1
Angpt1	Angiopoietin 1	Mn00456503_m1
Sfrp1	Secreted frizzled-related protein 1	Mn00489161_m1
Fxyd2	FXYD domain containing ion transport regulator 2	Mn00446358_m1
Gpm6a	Glycoprotein M6A	Mn00463812_m1
Mlxipl	MLX interacting protein-like	Mn02342723_m1
Pten	Phosphatase and tensin homolog	Mn00477208_m1
Sfrp2	Secreted frizzled-related protein 2;	Mn01213947_m1
Tgfβ1	Transforming growth factor β1	Mn01178820_m1
Tgfβ2	Transforming growth factor β2	Mn00436955_m1
Gapdh	Glyceraldehyde 3 phosphate dehydrogenase	Mn99999915_m1

Table 2.2 List of TaqMan® probes used for QPCR

The present list showed the custom TaqMan® probes used in the present research. Mn = mouse.

2.8 Clustering and gene ontology enrichment analysis

Z-transformed mean normalised intensities were used for hierarchical clustering of microarray data. Agglomerative hierarchical clustering was performed using MultiExperiment Viewer (version 4.8.1) (Saeed *et al.*, 2003).

Normalised probeset intensities were hierarchically clustered on the basis of Euclidean distance, and distances between probesets were computed using a complete-linkage matrix. Clustering results were visualized using MultiExperiment Viewer (version 4.8.1).

Gene clusters identified by hierarchical clustering were analysed using DAVID GOEA (Huang da *et al.*, 2009b; Huang da *et al.*, 2009a). Keywords with fold enrichment ≥1.5, Bonferroni-corrected *P* value <0.05, EASE score (modified Fisher's exact test) <0.05 and at least two transcripts per keyword were considered significantly over-represented. These data were imported into Cytoscape (version 2.8.1) (Shannon *et al.*, 2003) and analysed using the Enrichment Map plugin (Merico *et al.*, 2010).

The following criteria were used to generate the networks: false discovery rate (Benjamini–Hochberg) cut-off <0.01 and similarity cut-off >0.6. The networks generated were subjected to a Markov Cluster Algorithm to generate distinct sub networks. Transcripts with significantly altered expression in the microarray were searched against Jackson laboratory MGI-Mouse gene expression database to identify 'jejunum' (TS23-28) and 'muscle tissue' (TS12-28) markers.

To identify smooth muscle specific transcripts, a following data query was used: 'find genes where expression is detected in smooth muscle tissue (TS20-28) and expression is not detected or analysed in skeletal muscle (TS20-28)'.

2.9 Imaging

Intestinal explants were imaged and measured daily until day three by an inverted microscope (Leica) using magnification 5x, exposition 50.6 milliseconds, gain 1.4x, saturation 1.70 and gamma 1.06.

Immunofluorescence images were collected with Fluoview FV1000 confocal (Olympus) using a 10x and 20x/1.40 Plan Apo objective on an inverted IX81 (Olympus) inverted microscope equipped with the perfect focus system to eliminate focus drift. Green and red channel were excited with the 488 nm and 594 nm laser lines respectively. Images were acquired through the Fluoview ver. 3.1b software (Olympus).

For confocal images, dextrans were visualized through an Olympus BX51 microscope and images captured with a Coolsnap ES camera (Photometrics) through MetaVue Software (Molecular Devices).

Images were processed and analysed using ImageJ (http://rsb.info.nih.gov/ij) and Adobe Photoshop CS6. Specific band pass filter sets were used to prevent bleed between channels.

2.10 Statistical analysis

In order to test whether there is a difference between populations of mean, three assumptions have been tested: populations have the same variance, populations are normally distributed and values are sampled independently from each other value.

Although previous studies have begun to culture intact embryonic gut rudiments (Abud *et al.*, 2005; Quinlan *et al.*, 2006), the peculiarity of the model designed for

the present research requested pilot experiments to determine how many number of pregnant mice to use.

To understand the increase in length and in area of the explants, the segment line and freehand selection tools of ImageJ were used to process the daily high magnification pictures of the explants (Figure 2.4 and Figure 2.5).

Figure 2.3 Method to measure the lengths of jejunal explants

The present figures taken from ImageJ explain the method used to measure intestinal length of the explants. Using ImageJ was possible to draw a line (yellow) within the middle area of the explant starting and finishing from the cut end. The software was able to calculate length in pixel and to convert these data in μm. Bar =500 μm.

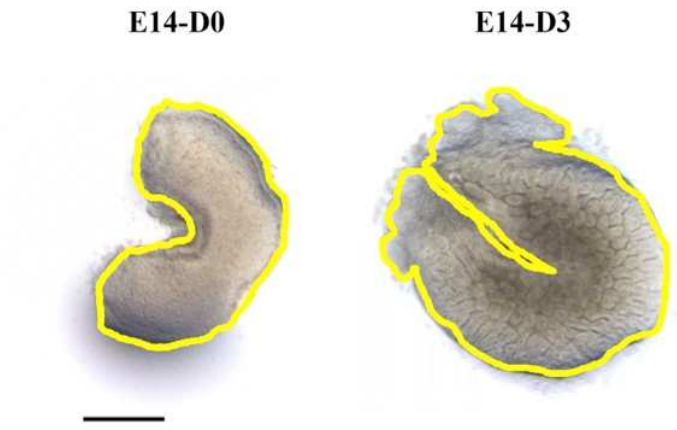

Figure 2.4 Method to measure the areas of jejunal rudiments

The area of the explants was measured daily using the software ImageJ. After sectioned the tool "Freehand selection", a yellow line was drawn around the specimens. This tool was able to measure the area occupied within the selection. Bar =500 μm.

In a typical organ culture experiment used in this research, the jejunal rudiments in 0, 5 and 50 ng/mL TGFβ1 originated from three embryo littermates so that the data were paired for statistical analyses.

For individual parameters analysed by immunofluorescence, the value for each rudiment was the average of measurements made in three sections approximately 50 mm apart.

All the analysis originated from immunofluorescence involved the area defined as a floor of the explant, which it is the portion of the explant onto the insert, extending from the first crypt to the last crypt on the abovementioned floor.

Datasets were subjected to the Shapiro-Wilk test to determine whether or not they were compatible with a normal distribution; thereafter, parametric (t-test two tailed) or non-parametric (Wilcoxon two tailed) analyses were applied, as appropriate. Fisher's exact test (two-tailed) was used to compare proportions of organs containing a longitudinal smooth muscle layer.

All the data was inserted in a Microsoft Excel database and statistical analysis was conducted with GraphPad Prism 6.0 and 7.0.

3 CHAPTER 3 – Bridging the gap: functional healing of embryonic small intestine *ex vivo*.

3.1 Overview

The ability to grow embryonic organs *ex vivo* provides opportunities to follow their differentiation in a controlled environment, with resulting insights into normal development. In addition, *ex vivo* organ culture can be used to assess the effects on organogenesis of physical manipulations or the addition of exogenous chemicals, such as growth factors.

This study aimed to create an organ culture model with which to test physical manipulations to enhance healing of small intestinal rudiments, thus generating a single functional organ. Using whole tissue staining, intraluminal injection of dyes and real time movies, I demonstrate that jejunal explants separated by a gap linked by a threaded through their lumens have the capacity to form a single functional unit. The key to success was to preserve tissue orientation using the thread.

In organ culture models, R-spondin1, a WNT agonist, seems to have an essential role in preserving tissue vitality, promoting epithelial proliferations (Sato *et al.*, 2011a; Sato and Clevers, 2013b) or restoring epithelial integrity after an injury (Miyoshi *et al.*, 2012). Therefore, I supplemented the organ cultures with this factor with the intention of promoting growth and potentially healing. However, the addition of R-spodin1 did not result in an increase in the frequency of fusion or in the length of the rudiments.

3.2 Organ Culture of embryonic jejunum

I made preliminary experiments to explore the optimal time to grow explanted jejunum into the *ex vivo* system. These observations showed that extended culture periods, for up to one week, were incompatible with tissue viability, probably because the organs had become too large to be optimally sustained by the culture system. Therefore, all further experiments used explants grown for three days.

E14 proximal small bowel contains a simple epithelium without villi, surrounded by a mesenchymal layer, the outermost cells of which are αSMA^{+} (Figure 3.1, left upper frame), showing that they are being to differentiate into visceral muscle. From E14, the jejunum presents changes in epithelial cell shape and apical surface expansion over time. This pseudostratified epithelium is highly proliferative and its epithelial cells grow in height, elongating towards the lumen just prior to villus formation.

After three days in culture, rudiments grown in basal medium had elongated and the histology showed intact tissue with the formation of rudimentary villi (Figure 3.1, right upper frame). The tissue organization of E14 explants cultured for three days was similar to that observed in the freshly-dissected E17 jejunum (Figure 3.1 left bottom frame).

In freshly dissected E14 and E17 intestine and in the rudiments cultured for three days, the epithelia immunostained for E-cadherin. Circular muscle layer was present in all three conditions but the cultured samples lacked longitudinal smooth muscle layer, as demonstrated by the paucity αSMA^{+} in the outer mesenchymal area (Figure 3.1 right upper frame).

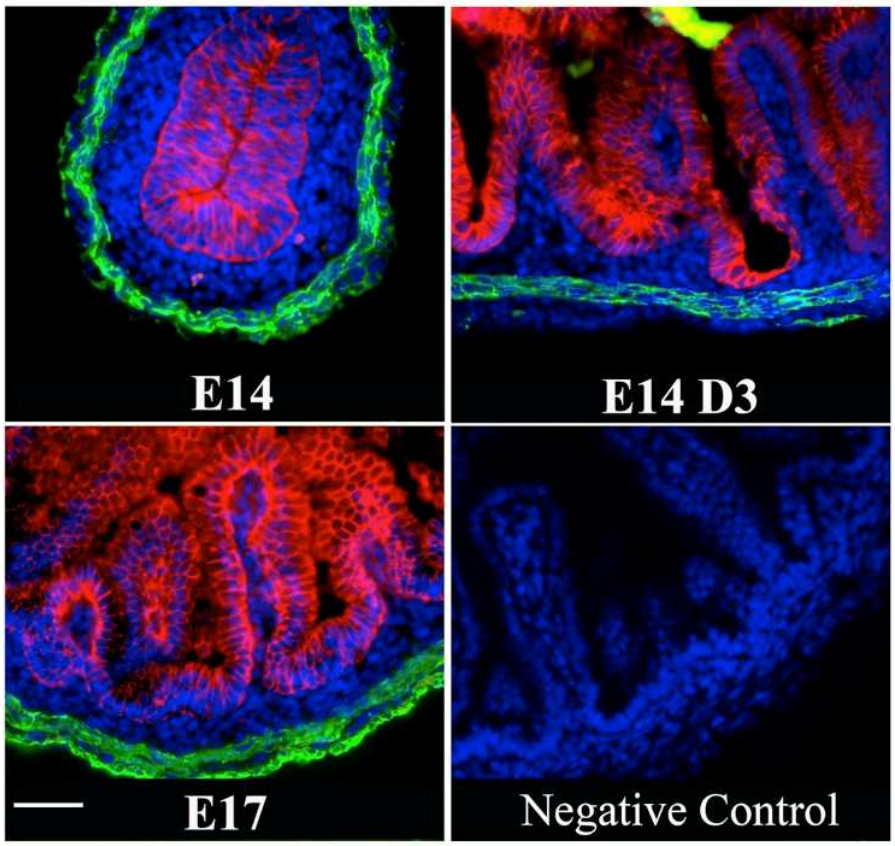

Figure 3.1 Histology of embryonic jejunum double immunostained for αSMA and E-cadherin

The images situated above are cross sections of intestinal tubes. All nuclei were counterstained with DAPI (blue). αSMA immunostaining appears green and E-cadherin immunostaining appears red. On the day when it was explanted (E14), the rudiment consisted of an E-cadherin^{+} epithelial core, which lacked villi; it was surrounded by mesenchyme, the outermost layers of which were αSMA^{+}. On day three of culture (E14 D3), rudimentary E-cadherin^{+} villi had formed and smooth muscle was maintained. At this time point, the explant resembled freshly dissected embryonic day 17 jejunum that also contain villi (E17). The lower right frame (No primary antibodies) depicts a tissue section from and E17 specimen in which the αSMA and E-cadherin antibodies were omitted. Bar indicates 50 μm.

In order to increase the proliferation rate of the explants and encouraging the healing, some rudiments were cultured in media supplemented by 100 ng/ml of R-spondin1, a WNT agonist acting as an epithelial cells proliferation. The cut ends of rudiments exposed to this exogenous growth factor displayed sheet-like extensions by day three of culture and these were not found in rudiments grown in basal medium alone (Figure 3.2).

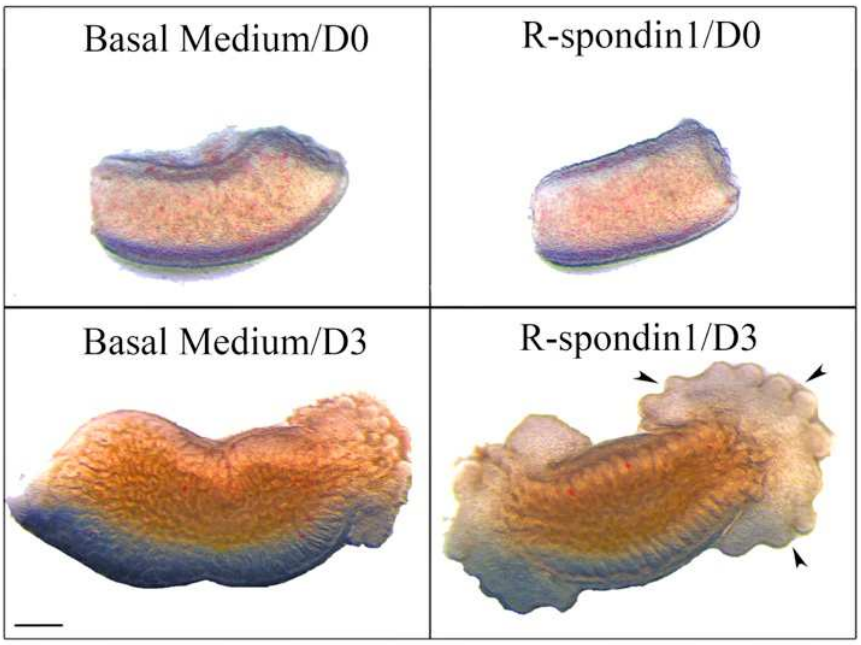

Figure 3.2 Effects of R-spondin1

Jejunal explants were cultured for three days in basal media alone or this media supplemented with R-spondin1. Note that, in the latter condition, there was exuberant growth of tissue from the ends of explants. Bar specifies 250 μm.

Although R-spondin1 altered the shapes of the ends of the explants, their lengths at day three of culture was not significantly different (unpaired Student's t-test) from explants fed basal medium alone (Figure 3.3).

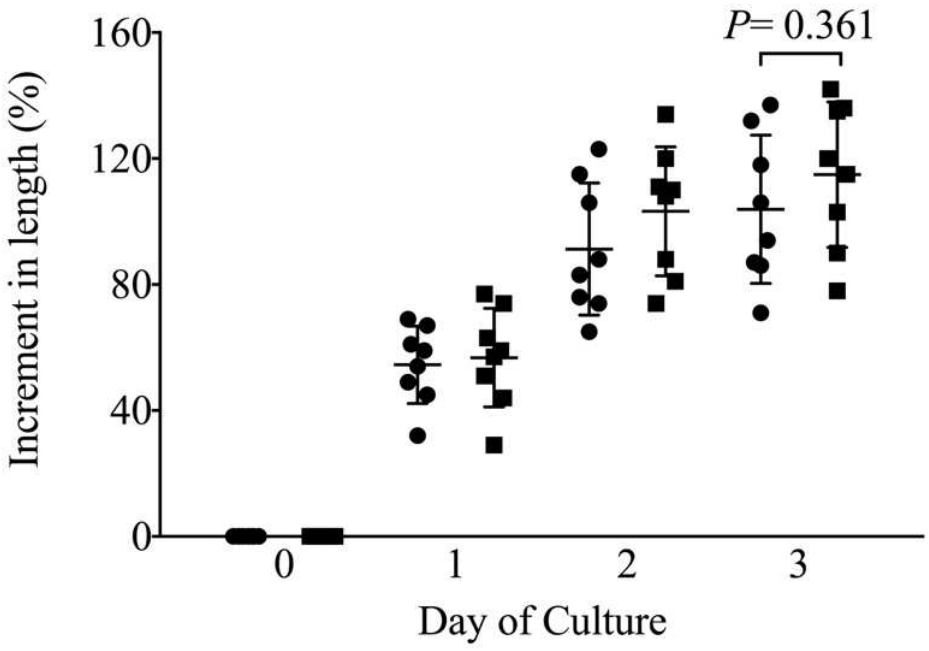

Figure 3.3 Intestinal increase in length of explanted embryonic jejunum

The scatter dot plot graph shows daily increase in length of specimens cultured in basal medium and in media supplemented with R-spondin1. Although R-spondin1 altered the shapes of explants (previously shown in Figure 3.2), the linear growth of the specimens was not significantly different (P=0.316) (as assessed by unpaired Student's *t*-tests) from explants fed basal media alone. Round shape= specimens cultured in defined media; square shape=specimens cultured in media supplemented by R-spondin1. Bars represent mean±SD (n=8 for each condition) % increase in organ lengths over three days in culture.

3.3 Physical fusion of explanted embryonic jejunum

I sought to determine whether two explants, comprising adjacent segments *in vivo*, placed near each other in the same proximal–distal orientation as found *in vivo*, might fuse in culture. However, preliminary experiments demonstrated that the rudiments curved as they grew (Figure 3.4), with the presumed mesenteric side in the concavity.

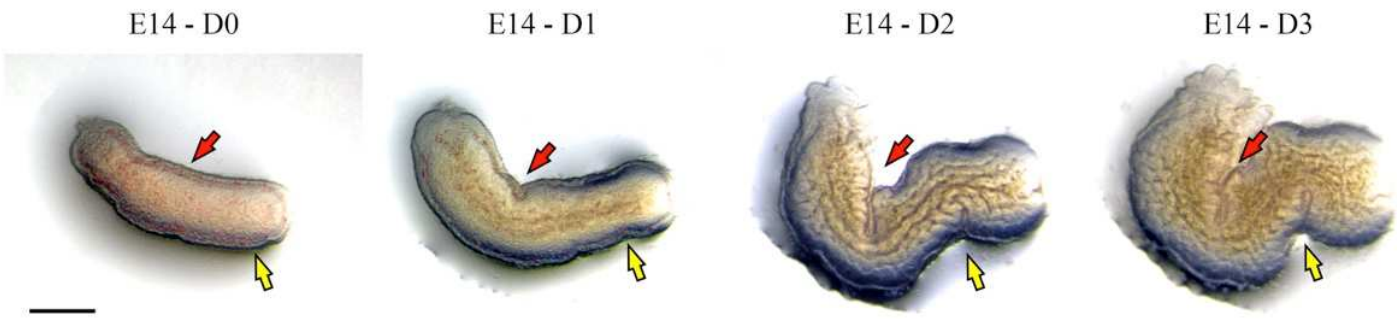

Figure 3.4 From a straight tube to a looped tube

Daily pictures of an E14 jejunal rudiment cultured for three day in defined media. At D0 the specimen is a straight tube that progressively acquires the characteristic loop shape as per normal jejunum. The arrows highlighted the area in which the tissue folds. Note also how the tissue elongates after three days and how the inner structure morphology changes due to the rising of the villi. E=embryonic age. D=day. Scale bar is 500 μm.

Furthermore, culturing two contiguous segments of embryonic small intestine separated by a gap showed that the proximate ends of adjacent explants became poorly aligned and the closure of the cut end was not permissive for fusion (Figure 3.5).

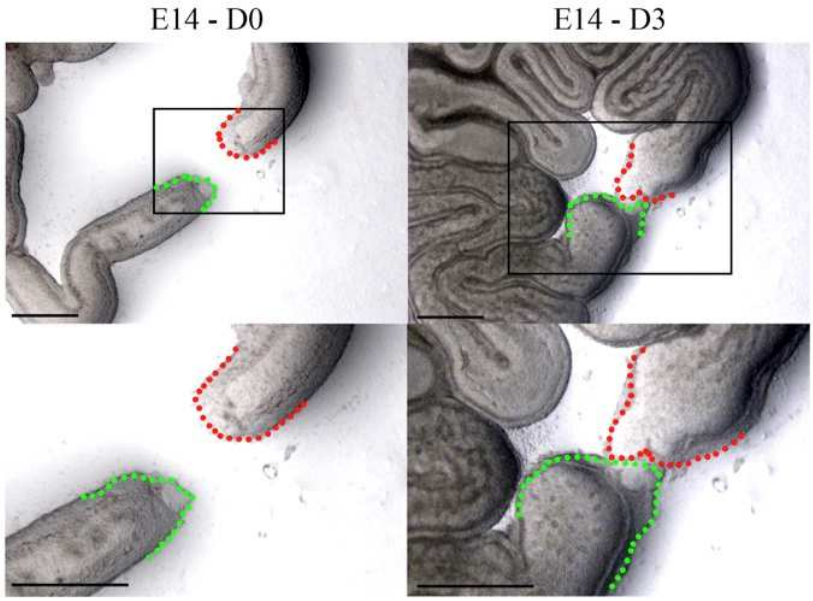

Figure 3.5 *Ex vivo* unguided embryonic jejunum does not restore continuity

Pictures of explanted segments of jejunum separated by a gap and cultured for three days. The dot lines (green and red) highlight the two consecutive specimen's ends. Upper frames show high magnification pictures of the explanted jejunum. The area of interest is identified by the box and magnified on the bottom frames. After three days in culture, the rudiments increased in length allowing the cut ends to touch spontaneously, but no complete fusion was reported. Scale bar=500 μm.

Due to this evidence and to maintain orientation of the specimens, upon being explanted the rudiment pairs were linked with a single suture threaded through their lumens as previously shown in Figure 2.2.

Using this strategy, as assessed by observations through an inverted microscope, the explants grew as linear tubes. On day three of culture, 25 (74%) of 34 such rudiment pairs were noted to be touching, with well-aligned central epithelial zones (Figure 3.6).

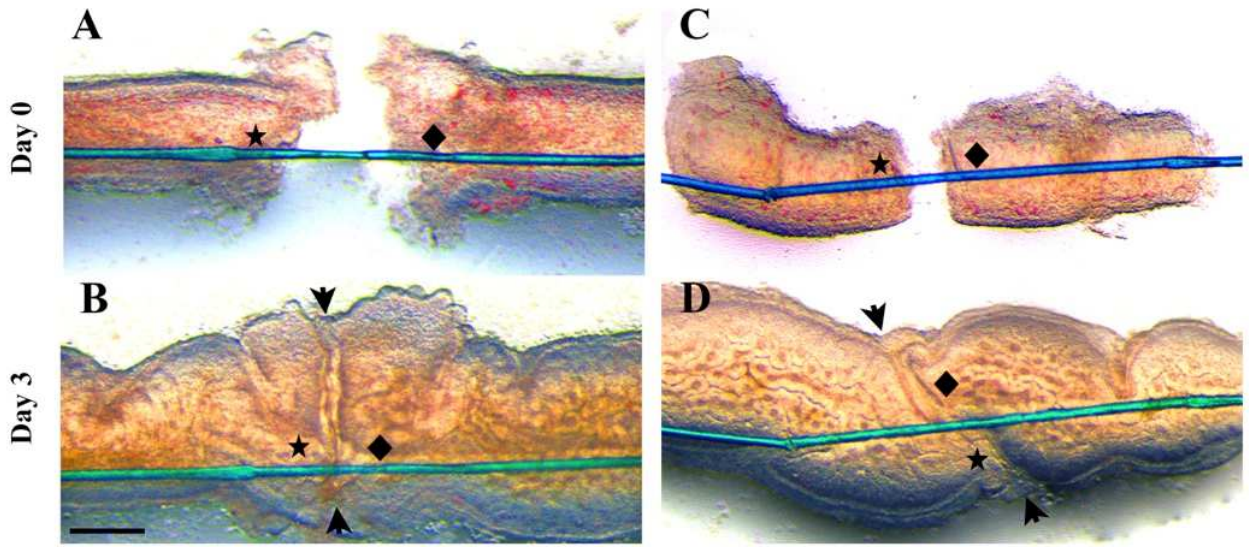

Figure 3.6 Physical fusion of explanted embryonic jejunum.

Images from explants at 0 (A, C) and 3 (B, D) days of culture. (A, C) Pairs of rudiments, which fused in culture. (A) Image of rudiments when they were explanted (day 0); note the bridging thread (blue) and the points (indicated by asterisk and diamond) where it enters nearby ends of the rudiments. (B) The same rudiment pair after 3 days of organ culture (day 3); note that the rudiments are well aligned in the border (arrowheads) where they touched. (C, D) Complementary views of a rudiment pair which failed to form a continuous lumen: after 3 days of culture, although the ends of the explants touched, they were poorly aligned (note the dislocation of asterisk and diamond). Bar=250 μm.

In 80% of such well-aligned pairs (equivalent to 59% of the total explanted pairs), a single patent lumen was confirmed by visualizing the trajectories of injected fluorescent dextrans, which crossed the midline of the fused rudiments (Figure 3.7 A-C).

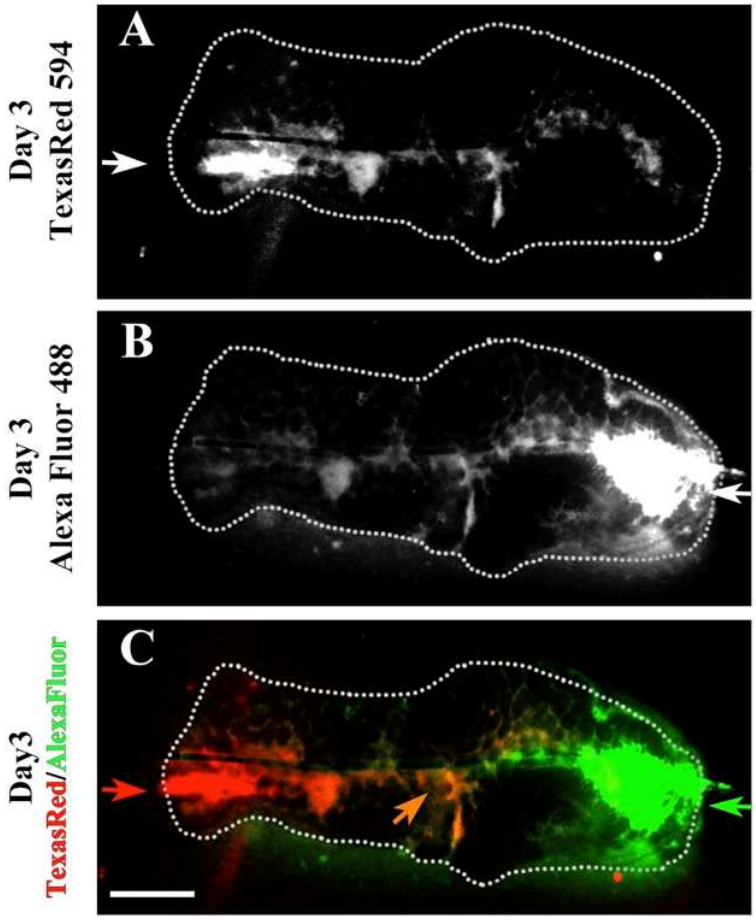

Figure 3.7 Continuity of lumens of fused explants.

Red fluorescent dextran (Texas red) was injected into the left end of the fused organ and green fluorescent dextran (AlexaFluor) injected into the right end; the respective trajectories of the probes are depicted (white) in (A, B); note that, in each case, the probes flow into the opposite rudiment; (C) merged colour image, with the zone of mixing visible as an orange colour (orange arrow). Bar=500 μm.

By contrast, on day three of culture, nine (26%) of 34 rudiment pairs either still had a gap between them or, if their ends touched, the epithelial zones of the two organs were not well aligned (as previously showed in Figure 3.6 C, D). In the latter cases, fluorescent dye was confined within the lumen of the single rudiment into which it had been injected (Figure 3.8 A-C). Figure 3.9 summarises the results of the healing experiments.

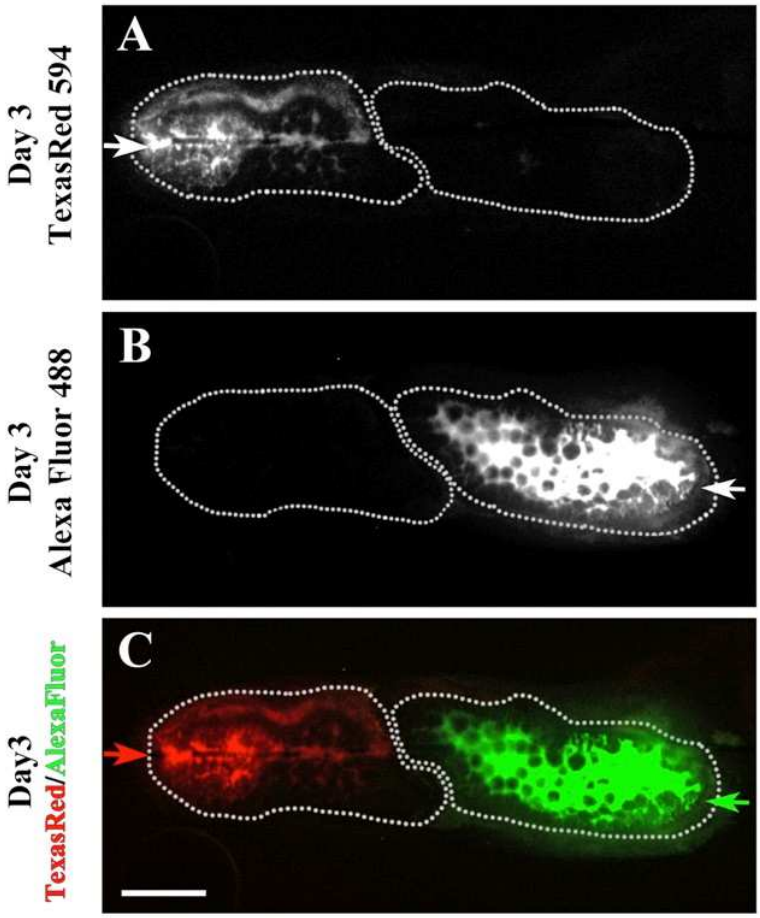

Figure 3.8 Failure of intestinal fusion

(A, B, C) The immunofluorescence pictures showed a rudiment pair, which failed to form a continuous lumen. Red fluorescent dextran (Texas red) was injected into the left end of the fused organ and green fluorescent dextran (AlexaFluor) The two dextrans failed to mix and were retained in separate lumens. Bar=500 μm.

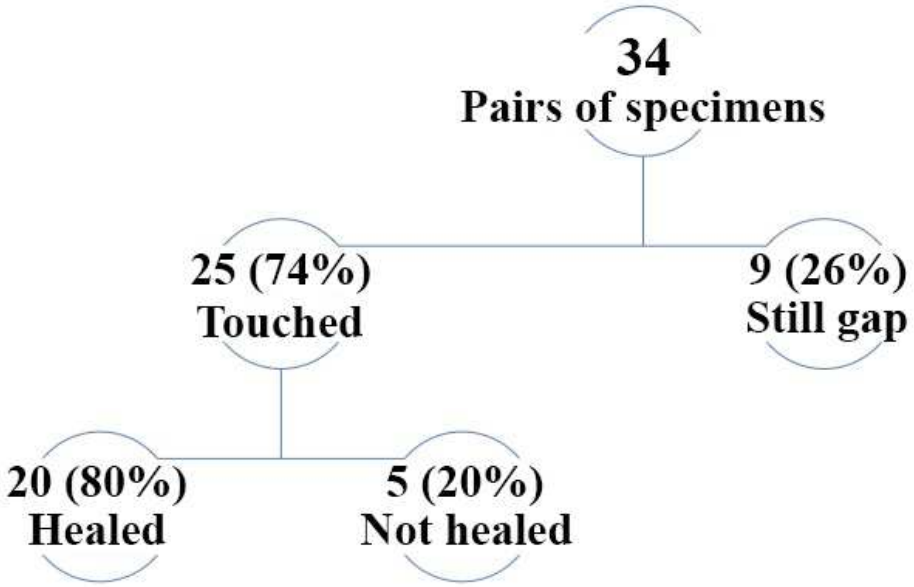

Figure 3.9 Summary of results from healing experiment

The smart-art graphic shows that, from 34 pairs of specimens, 74% of the rudiments were well aligned at the border where they touched. Interestingly, 80% of these fused specimens showed continuity of lumen, as demonstrated by dyes injection.

The average distance between adjacent rudiment pairs on the day they were explanted tended to be lower in well aligned (n=25; 181±24 μm, mean±SEM) versus nonaligned (n=9; 242±46 μm) pairs but these values were not significantly different (*P*=0.21; unpaired Student's t-test) (Figure 3.10).

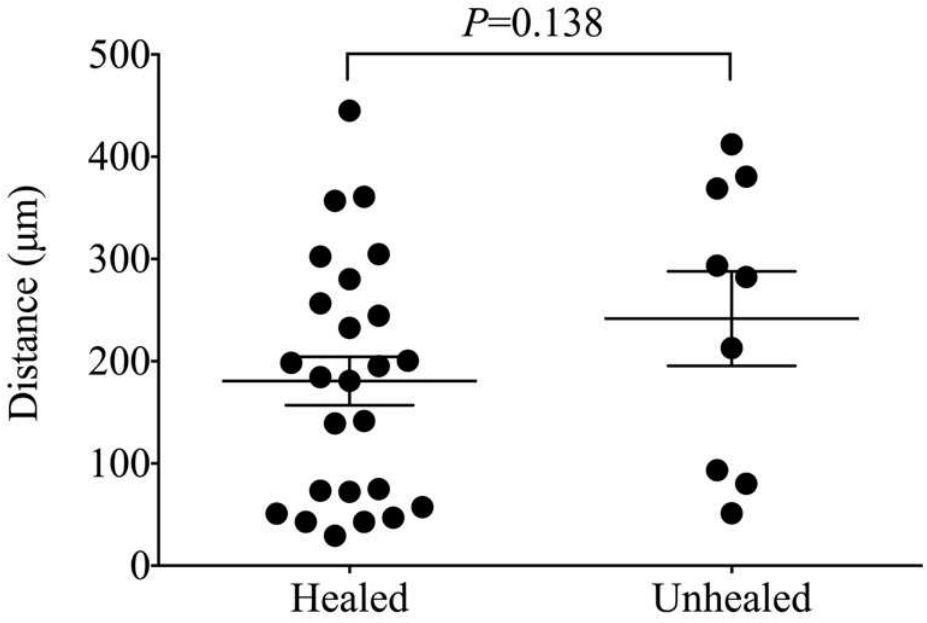

Figure 3.10 Distances between rudiment pairs at the time of being explanted

After organ culture in basal medium for three days, a subset of explant pairs were healed. There was no significant difference in the starting distances between healed and unhealed pairs, suggesting that initial placement of the rudiments onto the insert did not dictate whether the healing event is achievable. Bars indicated mean±SEM.

In experiments when rudiments were grown as pairs in the presence of R-spondin1, 14 (67%) of 21 of these pairs were seen to be well aligned and touch after 3 days of culture; this result was not significantly different from that measured in basal medium alone (P=0.76, Fisher's exact test, two-tailed). In specimens cultured with R-spondin1, no statistical difference was reported in the starting distance (P = 0.582) (Figure 3.11).

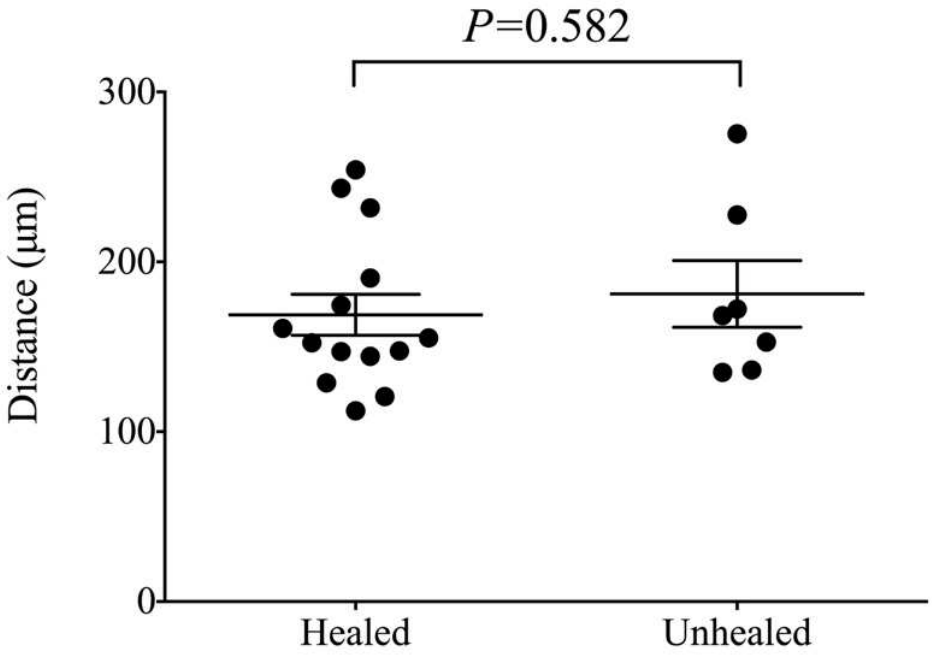

Figure 3.11 Distances between rudiment pairs at the time of being explanted in media supplemented with R-spondin1.

After three days of organ culture with medium fed by R-spondin1 a subset of explant pairs were healed (n=14; 67%). There was no significant difference in the starting distances between healed and unhealed pairs, confirming that initial placement of the rudiments onto the insert did not dictate whether the healing event is achievable. Bars indicated mean±SEM

Finally to investigate whether there was any bias related to the methodology used in these experiments, which could account have obscured any difference in healing ability between the basal medium only vs. R-spondin1 treated rudiments, the average starting distance between adjacent rudiment pairs was analysed. However, no significant difference was reported in the creation of the starting gap (P=0.845; unpaired Student's t-test; Figure 3.12).

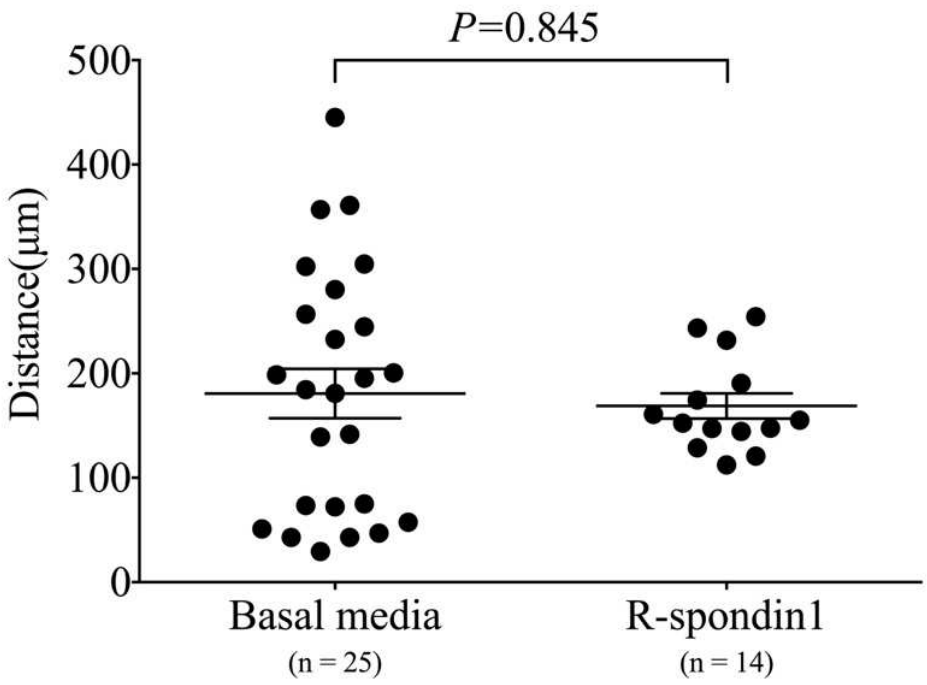

Figure 3.12 Distance between rudiment pairs that healed, on the day they were explanted

The present analysis compare the starting gap in specimens cultured in basal media or in media supplemented by R-spondin1, when the specimens were able to create a healing when the cut ends were aligned. This data highlight the reproducibility of the methods because there was no significant difference in the starting distances between the healed rudiments cultured in basal media or in media supplemented by R-spondin1. Interestingly, the specimens cultured in R-spondin1 appeared to have a more consistent starting gap. This could be addressed to the learning curve in the introduction of the tube into the specimens' lumen and in the setting of the methods. This result suggests that the tissue orientation is the major features for creating a feasible healing *ex vivo*. Bars indicated mean±SEM

3.4 Functional fusion of jejunal explants

After one day in culture, explanted rudiments began to undergo spontaneous peristalsis, with an average time between the start of contractions of 46±6 seconds.

Strikingly, in healed rudiment pairs, peristaltic waves were visualized to pass from one rudiment to the other. Sequential still images of a typical wave are shown in Figure 3.13 A-D, with a video of this process included in attached CD of this thesis (Video 1). Whole mount immunostaining for Peripherin revealed a reticular pattern of enteric nerves in rudiments cultured for three days.

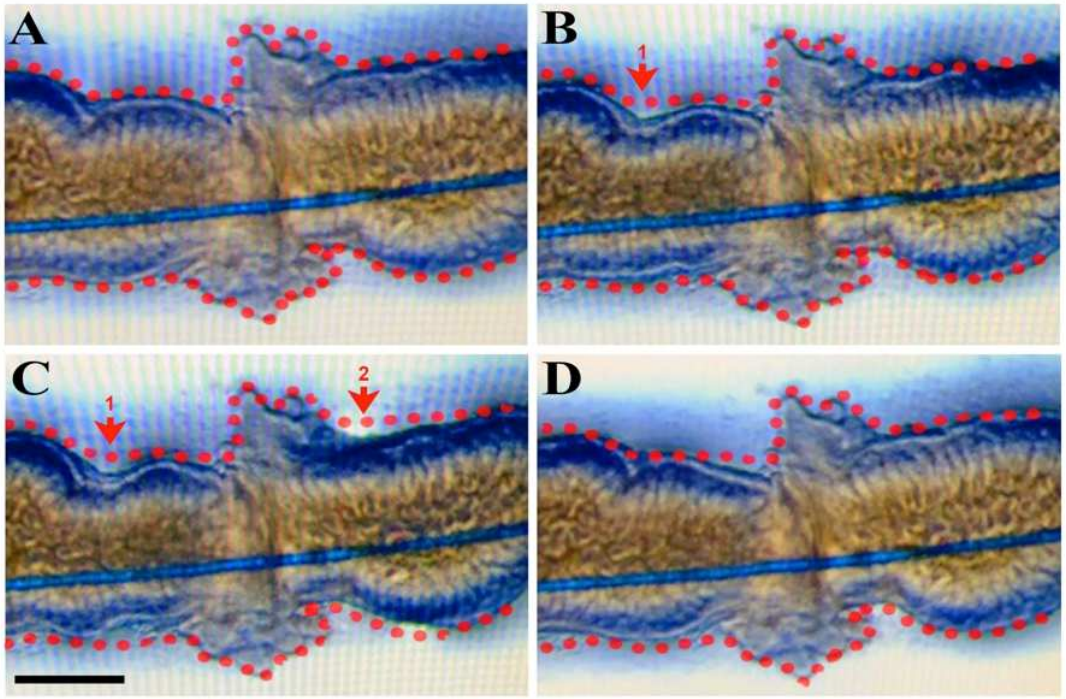

Figure 3.13 Functional fusion in organ culture.

Images from explants at the third day of culture. (A–D) These four frames are stills, spanning 6 s. The fused organ was initially relaxed (starting perimeter is traced by the dotted red lines in A–D). A contraction was spontaneously initiated (red arrow in B) and the wave travelled across the fusion zone, so that both sides of the explant were seen to be contracted (red arrows in C). (D) Finally, the organ relaxed. Bar=250 μm.

In healed intestines, a subset of Peripherin^{+} neurons formed a nexus in the fusion zone between rudiment pairs (Figure 3.14, Figure 3.15). This observation could explain how contraction waves are directed to pass along the fused organ in an uninterrupted manner.

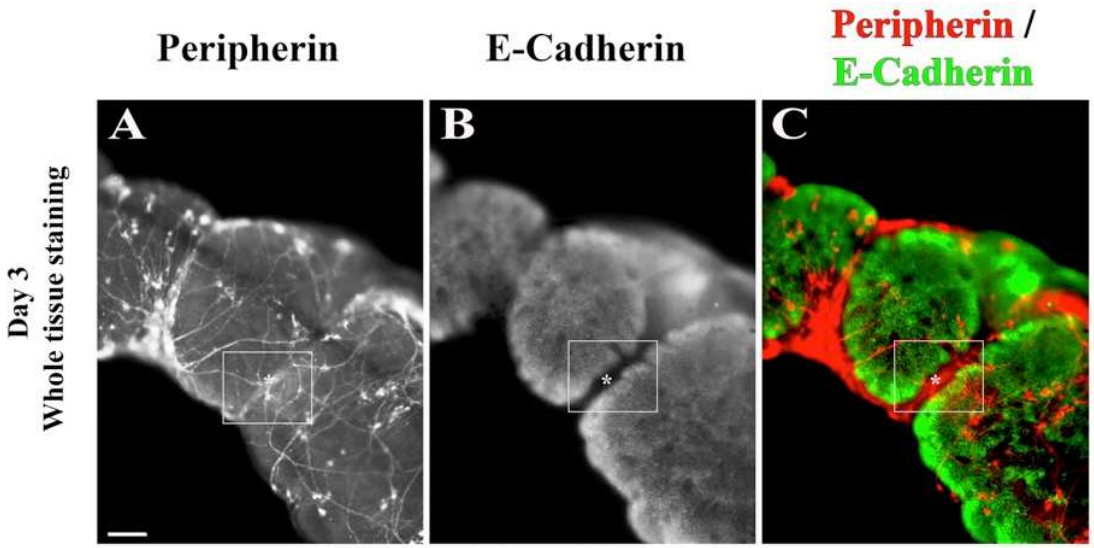

Figure 3.14 Continuity of the intestinal enteric networks after fusion.

Confocal images showing immunodetection of a Peripherin+ neural network [white in (A), red in the merged image in (C)] in the wall of a fused explant pair, and the epithelial compartment, which is E-cadherin [white in (B) and green in the merged image in (C)]. The boxed area shows that the neural network traverses the zone where adjacent explants touch, white asterisk, neural nexus. Bar=250 μm.

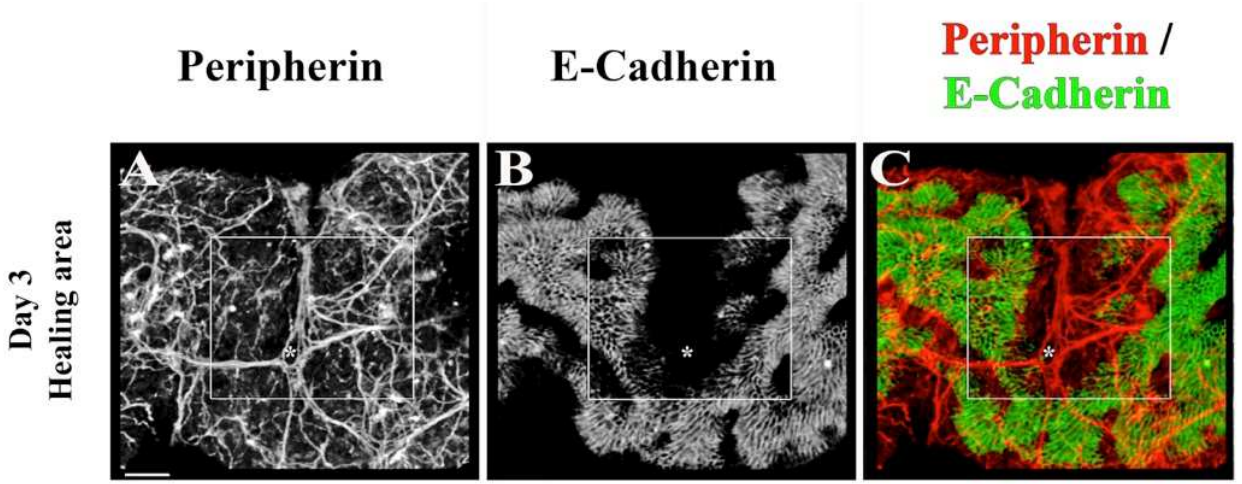

Figure 3.15 Creation of a neuronal network in the area of healing

High magnification pictures of the healing area in fused specimens. Confocal images show immunodetection of a Peripherin+ (white in A, red in C) in the area of healing. Asterisk identifies the area of healing. Interestingly, the E-cadherin (white in B and green in C) is not completely present in the healing area. This picture can suggest that the neuronal network and the mesenchyme can drive the intestinal healing in *ex vivo*. Bar=40 μm.

Although I do not currently have a method for live imaging of embryonic guts *in vivo*, I recorded (Video 2) similar peristaltic waves in E17 jejunum segments that had been explanted in organ culture and then recorded one hour later. Moreover, a network of Peripherin^{+} neurons was detected in the walls of freshly dissected E17 jejunum (Figure 3.16).

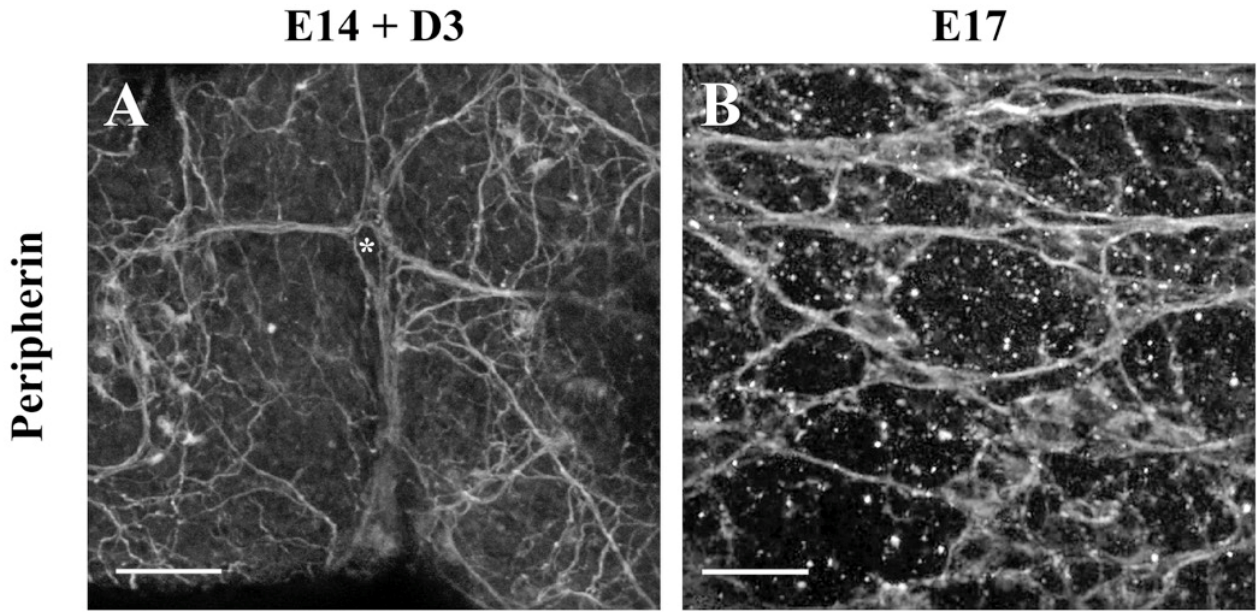

Figure 3.16 Neural networks in the wall of embryonic jejunum

Confocal image shows a Peripherin^{+} neural network in the wall of a freshly dissected embryonic day 14+3 cultured day (A) and 17 (B) mouse jejunum. (A) The boxed area shows that the neural network traverses the zone where adjacent explants touch, white asterisk, neural nexus. (B) E17 mouse jejunum showed a similar neuronal pattern compared to the E14 +3 days in culture. Bars indicate 100 μm.

3.5 Discussion

Surgery to elongate remnant bowel can be undertaken in SBS patients (Bianchi, 2006), and these treatments can be developed from pioneering surgical techniques in large animal models (Cserni *et al.*, 2013). The ability to tissue-engineer guts *ex vivo* is beginning to provide a source of gut tissues that can be used to complement the refashioning of aberrant gut by surgery (Sala *et al.*, 2009; Saxena *et al.*, 2010). One aspect that hither has been little explored is how to elicit optimal functional fusion of the adjacent ends of resected guts.

The current results confirm reports (Abud *et al.*, 2005; Quinlan *et al.*, 2006) that embryonic murine intestine can be maintained in organ culture, an environment permitting growth and differentiation. Abud *et al.* (2005) used this system to implement signalling through the epidermal growth factor in stimulation of epithelial growth and survival. Quinlan *et al.* (2006) showed that reporter genes could be virally transduced into cultured embryonic intestinal explants.

In my experiments, I explored whether paired bowel rudiments could fuse in organ culture to form a single functional unit, as assessed by the formation of a single patent lumen and spontaneous peristaltic waves that spanned the point of fusion of the two rudiments. The key to successful fusion was to span the gap between adjacent rudiments with a thread, which likely provided a bridge along which the nearby ends of adjacent organs could grow and ultimately fuse. In addition, this thread traversed the lengths of adjacent rudiment pairs, keeping them optimally aligned.

Not every rudiment pair was observed to functionally fuse and I hypothesized that the addition of R-spondin1 (Kim *et al.*, 2005) might increase the frequency of fusion.

Although R-spondin1 produced outgrowths from the ends of explanted guts, the frequency of fusion was not enhanced, possibly because these extensions had irregular, rather than normal tubular, shapes. Moreover, R-spondin1 did not significantly increase the lengths of the explants.

In the future I will hope to use the current system as a test bed to assess the effects of other growth factors (Krishnan *et al.*, 2011) on the efficacy of gut fusion.

Having established this model, I went into test the role of TGFβ1 during jejunal development in the following chapter.

4 CHAPTER 4 – Effect of TGFβ1 on embryonic jejunum differentiation

4.1 Overview

An *ex vivo* experimental strategy that replicates *in vivo* intestinal development could in theory provide an accessible setting with which to study normal and dysmorphic gut biology.

The previous chapter showed that over three days in organ culture, explants form villi and undergo spontaneous peristalsis. Nevertheless the wall of the explanted gut fails to form a robust longitudinal smooth muscle (SM) layer, matching not completely the *in vivo* counterpart.

Previous studies have implicated TGFβ1 in postnatal gut maturation and in regeneration following injury. In the mature intestine, TGFβ1 is detected in the tips of villi (Barnard *et al.*, 1993) and exogenous TGFβ1 inhibits the proliferation of intestinal epithelia in cell culture (Yamada *et al.*, 2013). Furthermore, TGFβ1 has also been implicated in supporting SM differentiation in diverse other tissues including urinary bladder mesenchyme (Liu *et al.*, 2010), amniotic stem cells (Ghionzoli *et al.*, 2013) and neural crest cells (Huang *et al.*, 2011).

In this study, I hypothesized that exogenous TGFβ1 would enhance SM differentiation in embryonic mouse jejunal explants. Using whole mount imaging, immunohistochemistry and RNA microarrays, I found that exogenous TGFβ1 promoted differentiation of longitudinal SM. At the level of the transcriptome, TGFβ1 showed effects correlating with the observed tissue changes. Moreover, I highlight that, *in vivo*, the physiologically herniated intestine is in close proximity to amniotic fluid, which could provide an important source of TGFβ1 proteins.

4.2 Jejunal development *in vivo* and *ex vivo*

I first clarified the tissue layers in the experimental model. Freshly dissected E14 jejunum appeared as a semi-translucent cylinder (Figure 4.1A). On histology (Figure 4.1B-D), it contained an epithelial core immunostaining for E-cadherin. This multi-layered epithelium had indentations on its apical surface but lacked villi.

Three sequential layers surrounded the epithelial tube: mesenchymal-like cells, a circular SM layer that immunostained for αSMA, and finally another mesenchymal-like layer. Hereafter, the term ‘inner mesenchyme’ is used to identify cells between epithelium and circular muscle, and ‘outer mesenchyme’ for cells outside the circular SM layer.

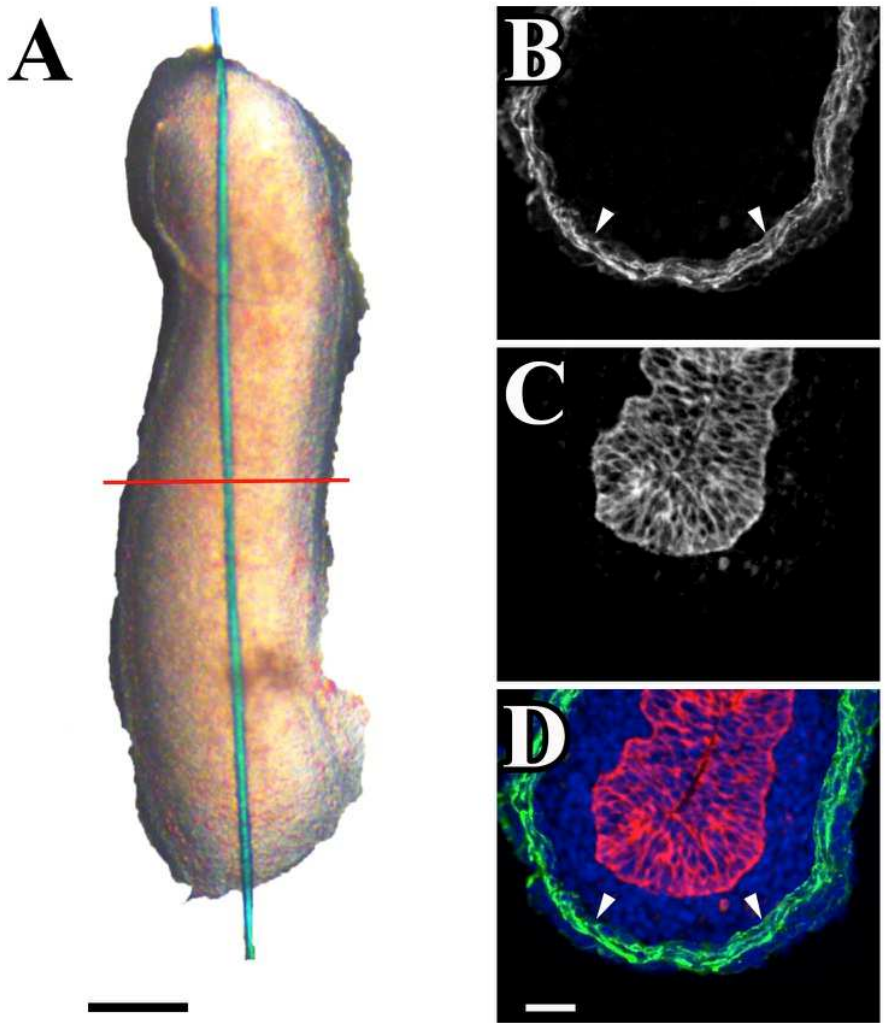

Figure 4.1 E14 embryonic jejunum

(A) E14 jejunum on the day it was explanted. The segment is kept straight by a suture threaded through the lumen. The red line represents the plane of sectioning used to generate histology. (B-D) Transverse sections of this rudiment show immunostaining for αSMA (white in B and green in the merged image in D) and E-cadherin (white in C and red in the merged image in D). White arrowheads depict the circular SM layer. Note there is no longitudinal SM layer. Scale bars are 250 μm.

Over three days in culture, and fed with basal media alone, the E14 explant increased in length and width (Figure 4.2A). A transverse section revealed a prominent ‘floor zone’ (Figure 4.2B-D) adjacent to the platform. This zone contained villi accounting for the ridge-like pattern evident in whole mounts. Inner mesenchyme, circular SM, and outer mesenchyme were present in the floor. Although scattered cells in the outer mesenchyme expressed αSMA, typically a robust longitudinal SM layer was absent. By contrast, the explant ‘roof’, abutting air, was a simple structure lacking villi. Floor and roof zones were continuous and enclosed a lumen.

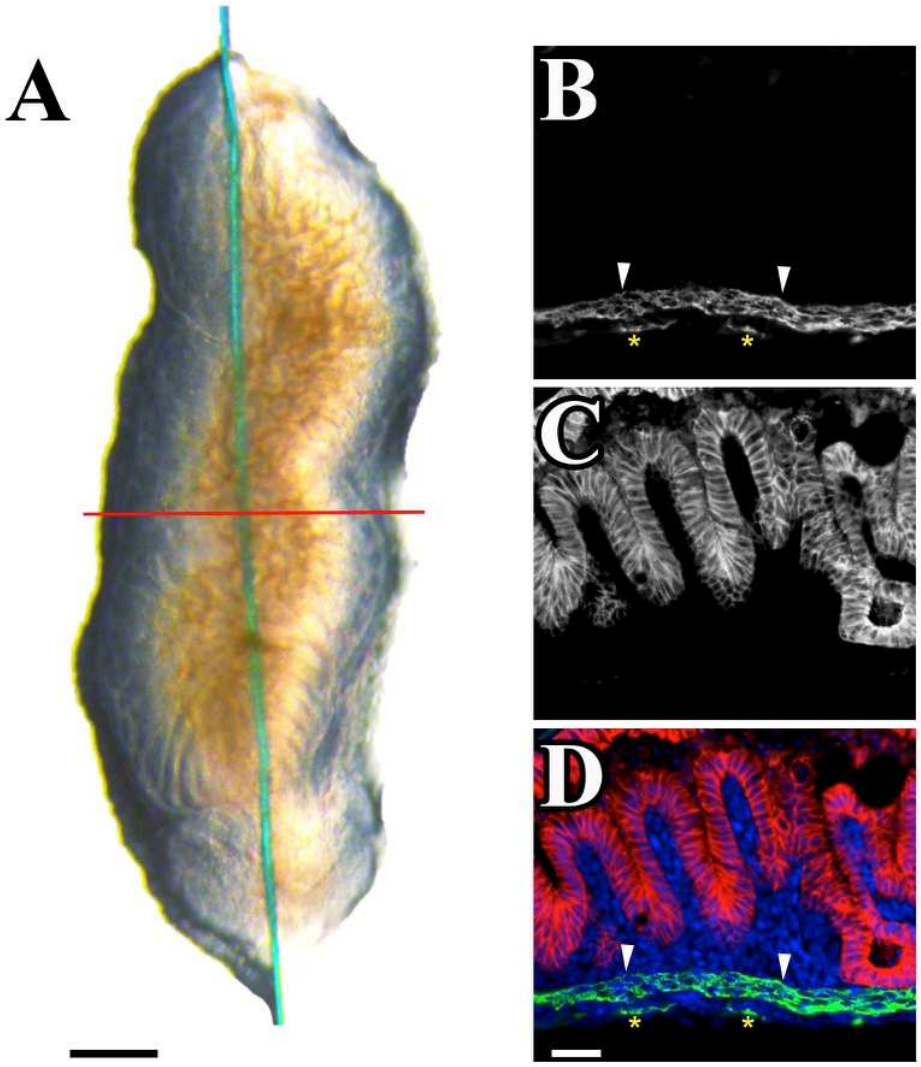

Figure 4.2 Organ culture of embryonic jejunum

(A) Embryonic jejunum cultured for three days. The segment is kept straight by a suture threaded through the lumen. The red line represents the plane of sectioning used to generate histology. (B-D) Note the formation of villi and the presence of a circular SM layer (with arrowheads); outside the latter, only a few scattered cells (yellow asterisks) express αSMA. Note there is no defined longitudinal SM layer. Scale bars are 250 μm.

A freshly dissected E17 jejunum is shown in Figure 4.3A. A transverse section (Figure 4.3B-D) revealed villi, an inner (circular) SM layer and an outer (longitudinal) SM layer. These observations show that, in organ culture, rudiments undergo a degree of differentiation and contain epithelial, mesenchymal and muscle cells. However, no defined longitudinal muscle layer is differentiated in specimens cultured with defined media (Figure 4.4).

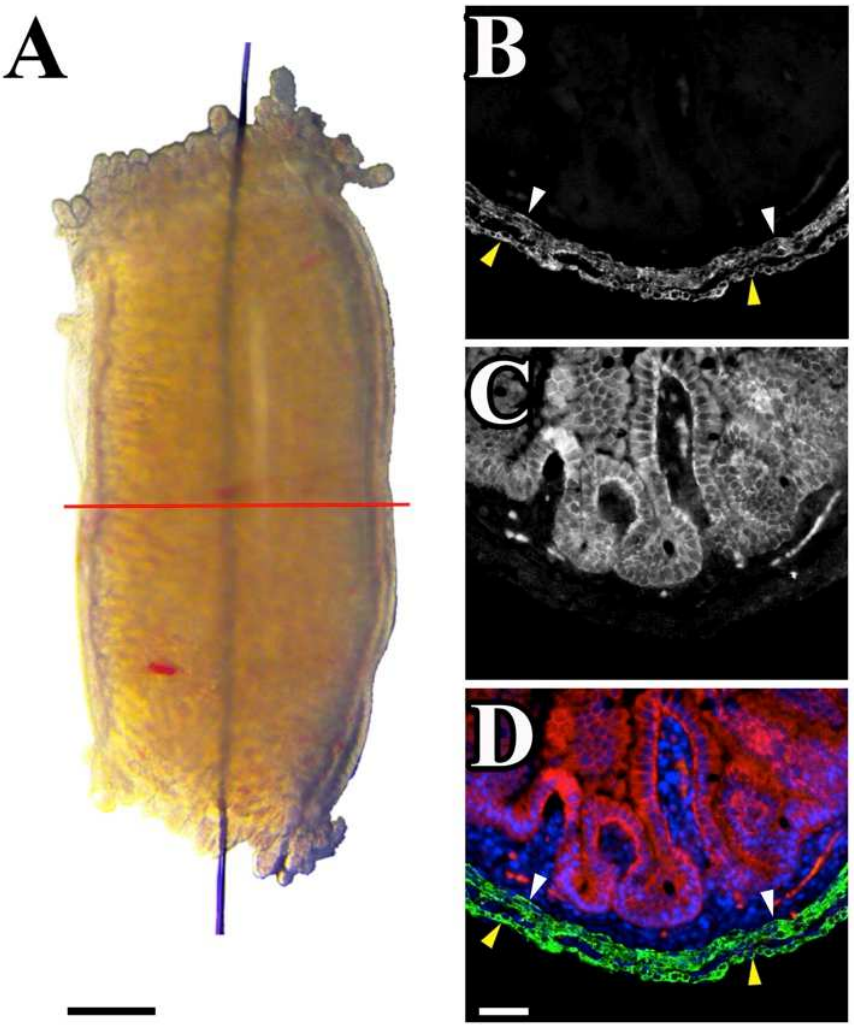

Figure 4.3 E17 embryonic jejunum

(A) Image on left is a whole E17 embryo and inset on right (B-D) Immunofluorescence pictures highlight the two αSMA^{+} layers (white in B, green in D) and the epithelium E-cadherin^{+} (white in C, red in D). Note the presence of villi and both a circular and longitudinal (yellow arrowheads) layer. White arrowheads indicate circular smooth muscle layer. Yellow arrowheads=longitudinal muscle layer. Scale bars=250 μm.

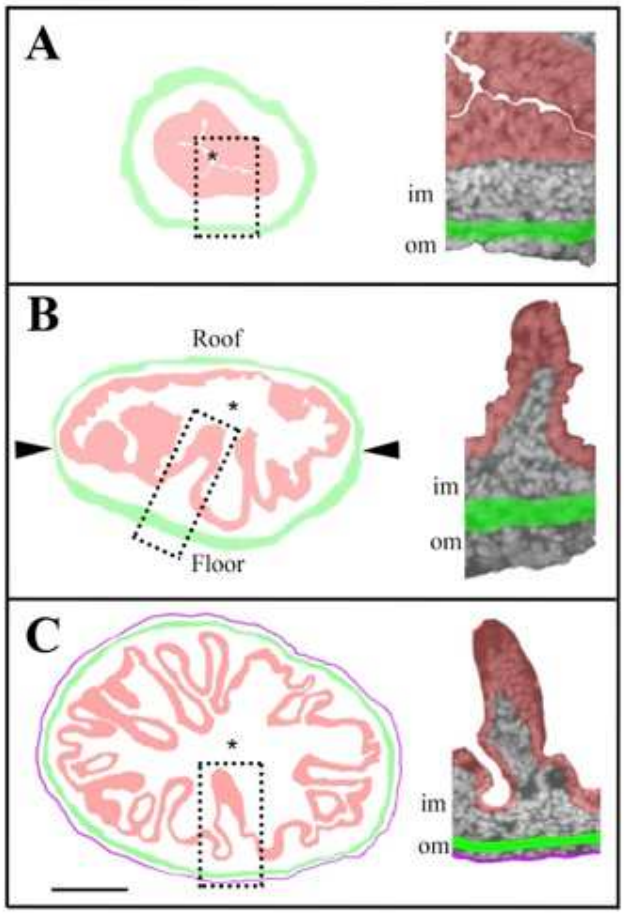

Figure 4.4 Schematic representation of embryonic jejunum *in vivo* and *ex vivo*

(A) Diagrammatic transverse section of E14 jejunum. The asterisk denotes the lumen. The epithelium (red) has yet to form villi, and the circular SM layer is green. The area in the black rectangle is enlarged on the right. Note the 'inner mesenchyme' (im; grey) between epithelium and the SM, and the 'outer mesenchyme' (om; grey) representing the most peripheral cell layers. (B) Diagrammatic transverse section through an E14-D0 explant fed basal medium alone. The explant's thick floor contains villi and is continuous with the thin roof (arrows indicate boundaries). (C) Diagrammatic transverse section through the E17 jejunum shows villi and the presence of a longitudinal SM layer (purple) that has formed within the outer mesenchyme. Scale bar is 250 μm.

4.3 Explant growth

I determined whether supplementing media with TGFβ1 altered growth by measuring explant length and area over three days in culture (Figure 4.5). To account for small variations in starting sizes, percentage increases were calculated for each rudiment (Figure 4.6). In basal media alone there was an average 69.3% increase in length and a 99.9% increase in area. Organs exposed to 5 or 50 ng/mL TGFβ1 also increased in size. With 5 ng/mL TGFβ1, there was no significant difference in length versus rudiments fed basal media alone, although their areas were modestly decreased (P=0.05). By contrast, rudiments exposed to 50 ng/mL TGFβ1 had marked decreases in growth versus controls in both lengths (P<0.0001) and areas (P=0.0004). Despite these concentration dependent effects of TGFβ1 on overall growth, in all three experimental conditions organs contained a floor and a roof, as assessed by histology (Figure 4.7).

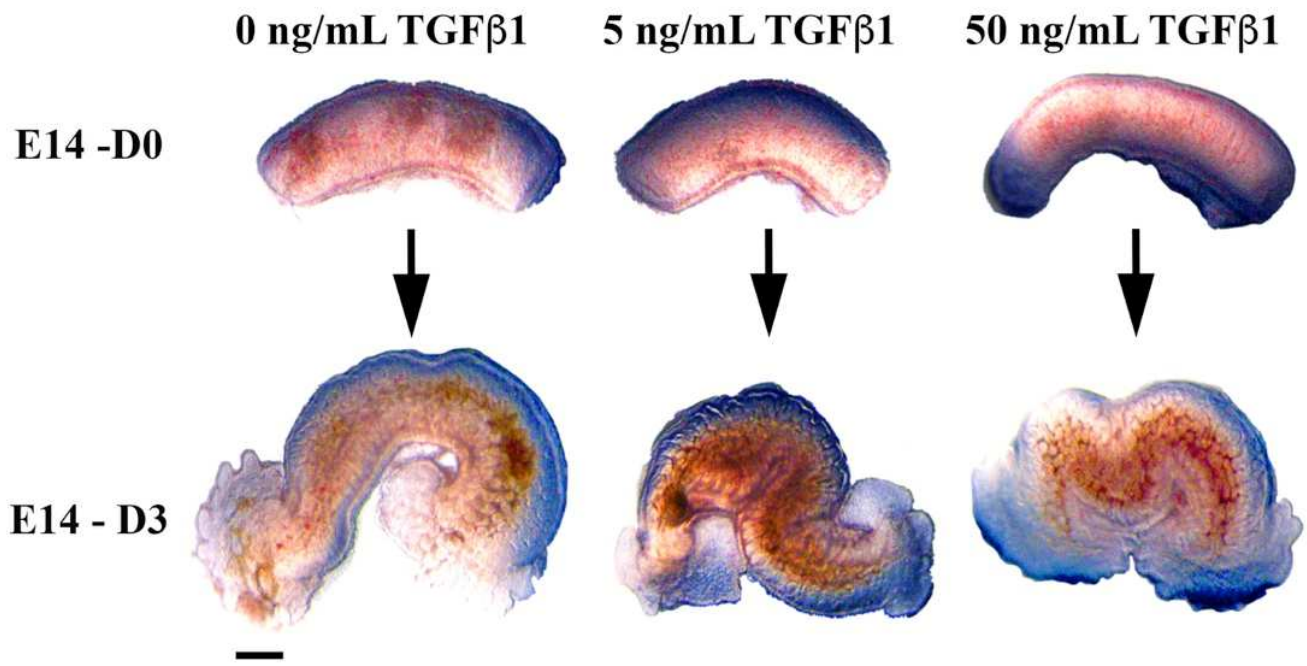

Figure 4.5 Effect of TGFβ1 on explant growth

Three rudiments when they were explanted (E14-D0). They were respectively fed basal media alone, or media supplemented with 5 or 50 ng/mL TGFβ1. As depicted in the lower images, all three organs grew over three days. Note that the explants have a tendency of looping as per normal intestinal development. Scale bar is 250 μm

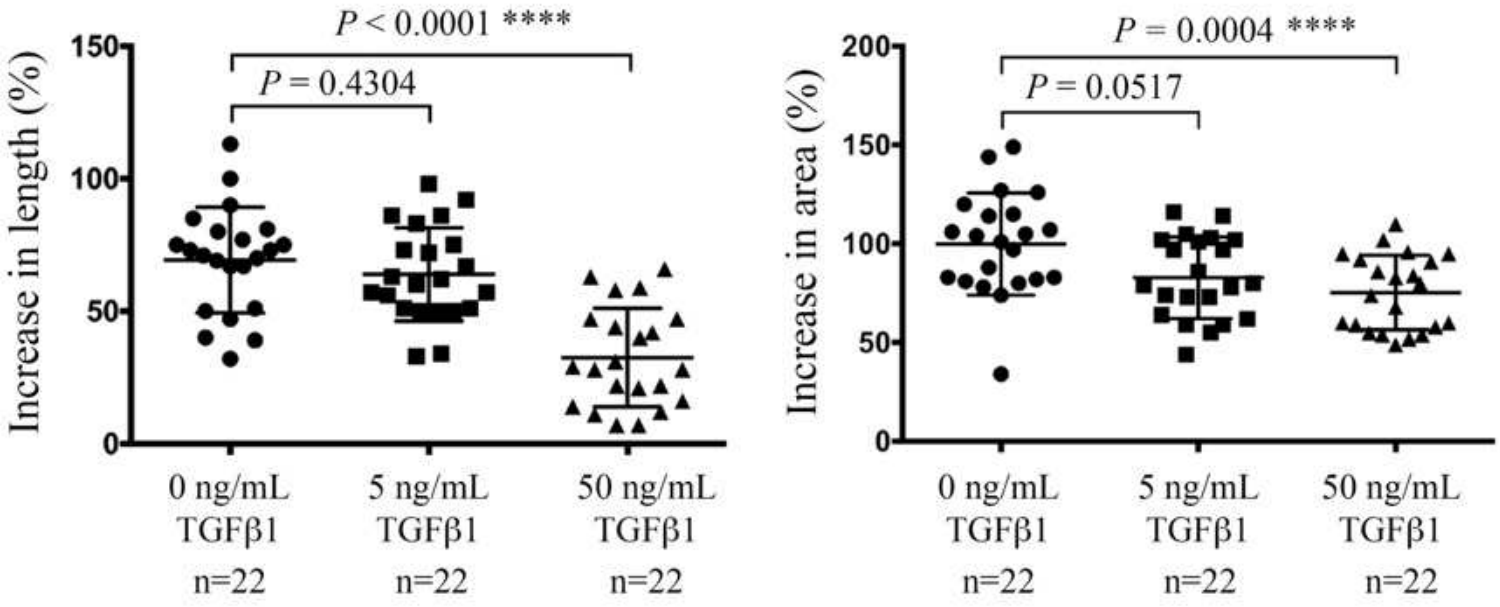

Figure 4.6 Statistical analyses of organ culture in different conditions

(A) Increases in length analysis showed that high concentration of TGFβ1 revealed a significant reduction in the length of the explant and (B) Increase in area investigation depicts a trend of effect due to the dose of TGFβ1. Even in this case high concentration of TGFβ1 appeared to reduce significantly the area of the specimens. Overall the statistical analysis indicated that the higher concentration of TGFβ1 retarded growth. Bars indicate mean±SD.

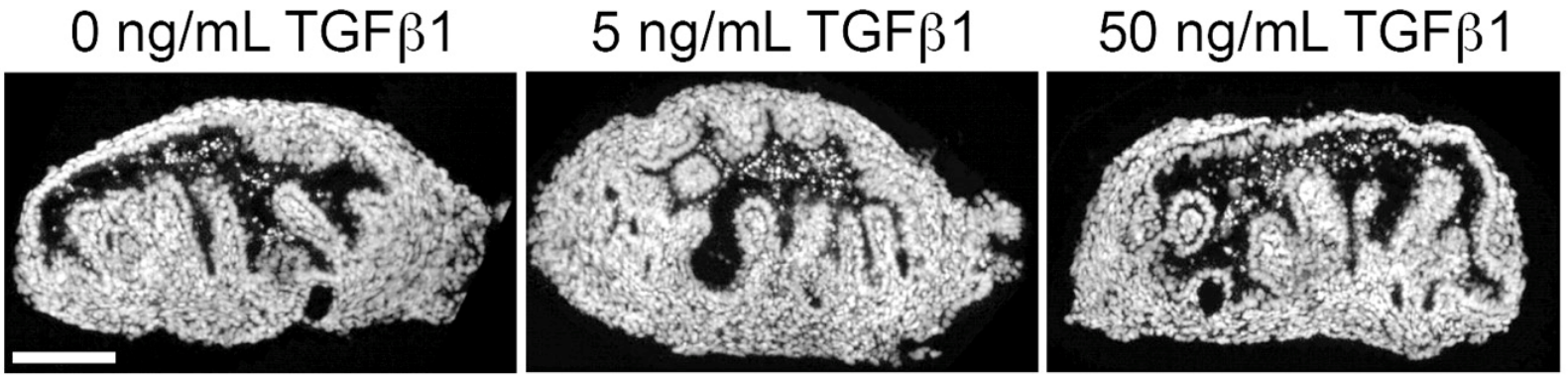

Figure 4.7 Effects of TGFβ1 on explant growth differentiation

Transverse sections of rudiments maintained for three days in organ culture, with nuclei stained (white) with DAPI. Each floor contained villi; these appeared less 'finger-like' in explants exposed to the higher concentration of TGFβ1. Scale bar is 250 μm.

4.4 Effects of TGFβ on embryonic muscle layers

Next, I focused on the detailed patterns of αSMA immunostaining within rudiments, comparing organ cultures with freshly isolated E14 and E17 jejuna. Transverse sections of E14 organs (Figure 4.8, left panel) showed a band of circular SM two to three cells thick but no longitudinal muscle layer. By contrast, E17 organs *in vivo* contained both a circular and a longitudinal SM layer (Figure 4.8, right panel).

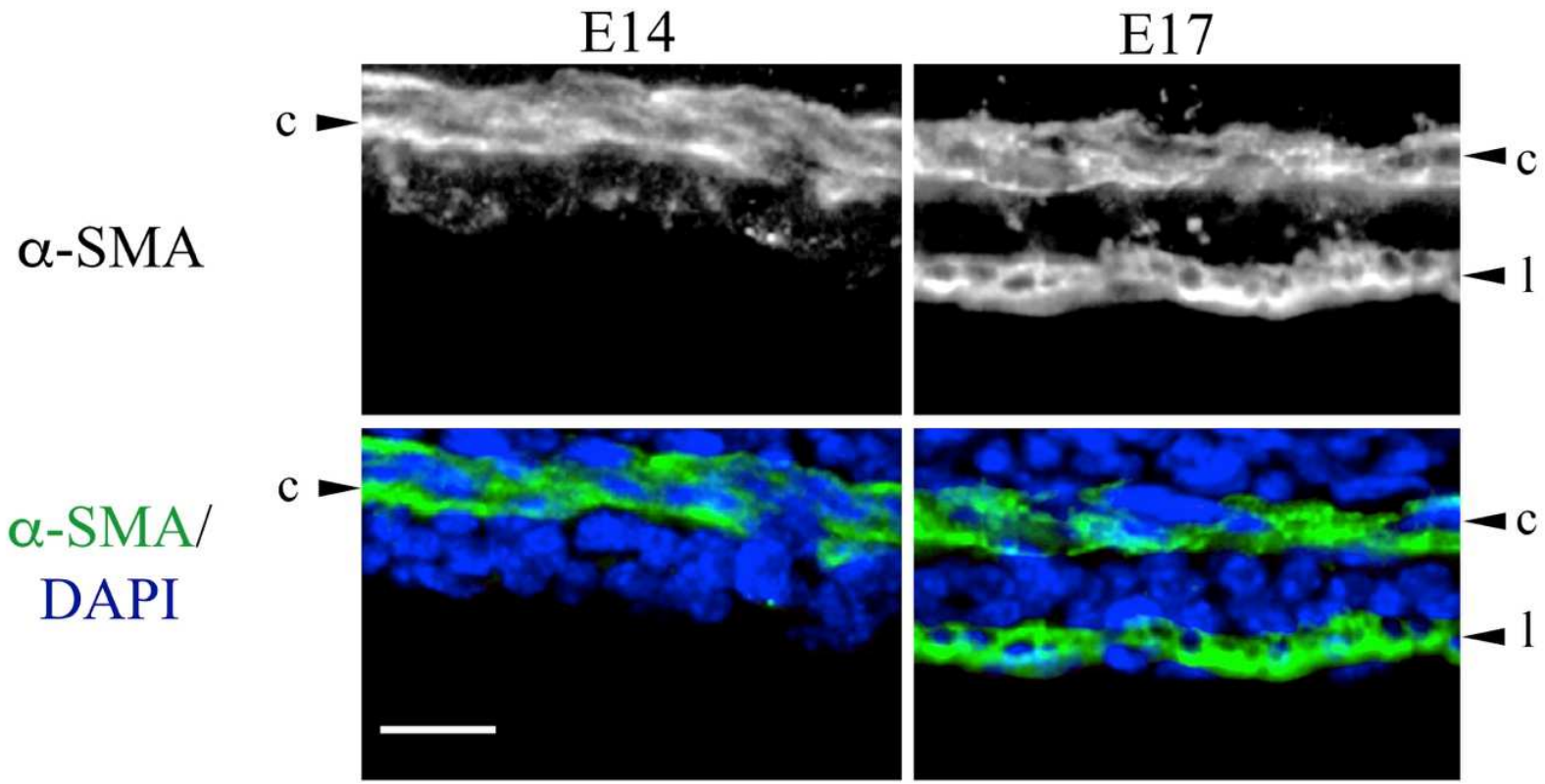

Figure 4.8 Muscle in embryonic jejunum *in vivo*

High power images of transverse sections from freshly isolated intestines from E14 and E17 *in vivo*. Upper frames show αSMA immunostaining (white); lower frames are the same sections with DAPI stained nuclei (blue) and αSMA in green and nuclei in blue. Note that a circular SM layer (c) is present at both times but only the E17 organ contains a longitudinal (l) layer. Scale bar is 10 μm.

Figure 4.9 shows representative histology images of organs cultures grown in basal media alone (left panel), 5 ng/mL TGFβ1 (middle panel) and 50 ng/mL TGFβ1 (right panel).

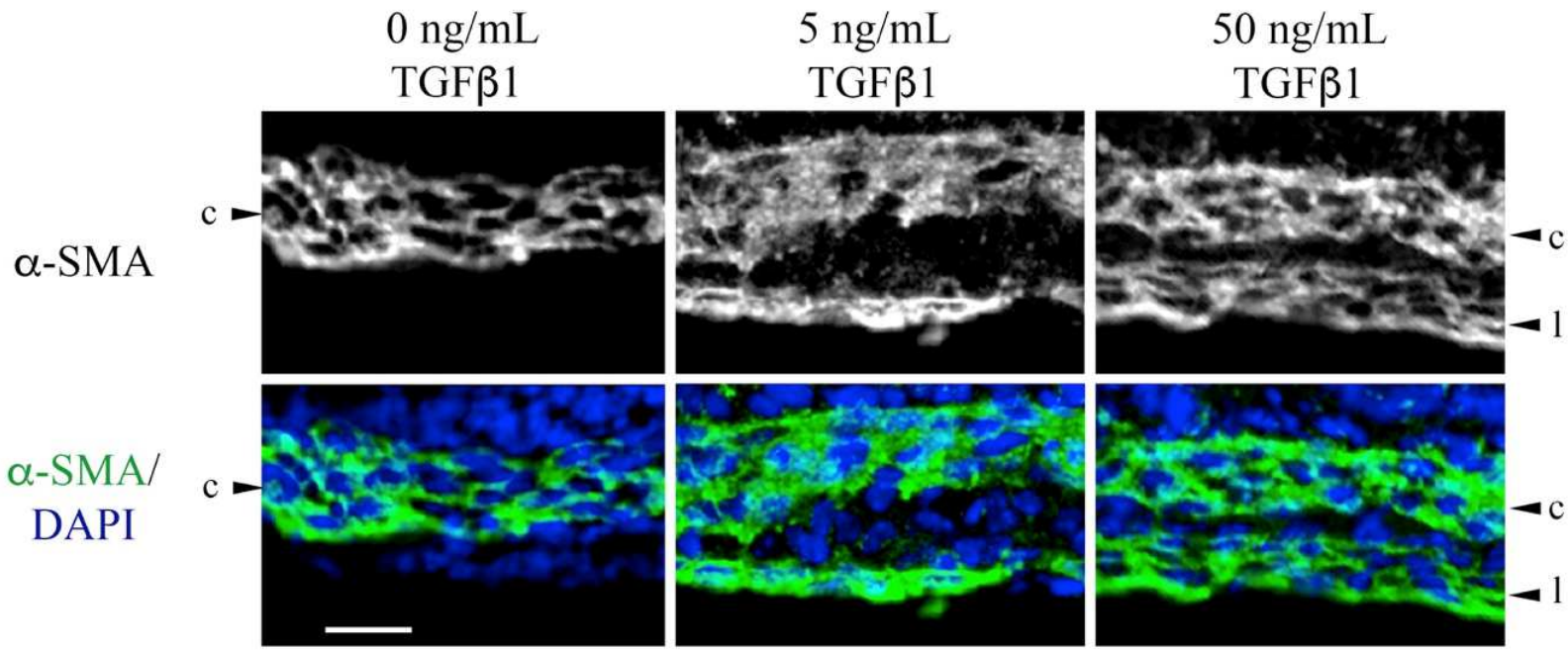

Figure 4.9 Muscle in embryonic jejunum in organ culture

High power images of transverse sections of floor zones of E14 rudiments (E14-D3, *ex vivo*) cultured for three days. Similar sequences for explants fed basal media alone (left panels), or media supplemented with 5 (middle panels) or 50 (right panels) ng/mL TGFβ1. Note that longitudinal muscle is only present in the latter two conditions. Scale bar is 10 μm.

Quantitative investigation on the presence of the longitudinal muscle layer into the study group showed that only the latter two have a longitudinal muscle layer. Only one of eight explants in basal media alone had a discrete longitudinal muscle layer, whereas seven of eight explants in 5 ng/mL TGFβ1, and all eight explants in 50 ng/mL TGFβ1, contained longitudinal SM (respectively, P=0.01 and P=0.001 versus explants in basal media) (Figure 4.10).

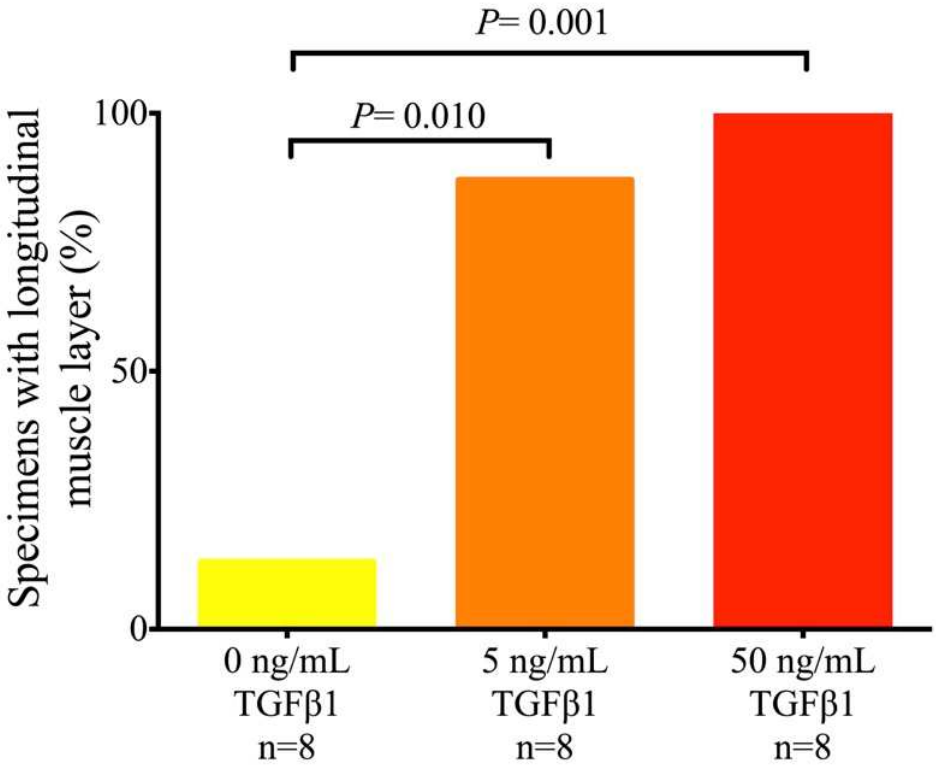

Figure 4.10 Percentage of longitudinal muscle layer in organ culture

Data from eight sets of organ cultures specimens. Each comprised rudiments from three embryos in the same litter, one explant fed basal media alone, and littermate rudiments fed 5 or 50 ng/mL TGFβ1. The bar graph shows the proportions of explant containing a longitudinal SM layer. Note that the longitudinal muscle layers seem to not differentiate in specimens cultured with no growth factor.

The two TGFβ1 concentrations caused step-wise increases in percentages of the total floor area occupied by longitudinal SM (Figure 4.11). All rudiments contained circular SM, and 50 ng/mL of TGFβ1 significantly increased the proportion of floors occupied by this layer (Figure 4.12).

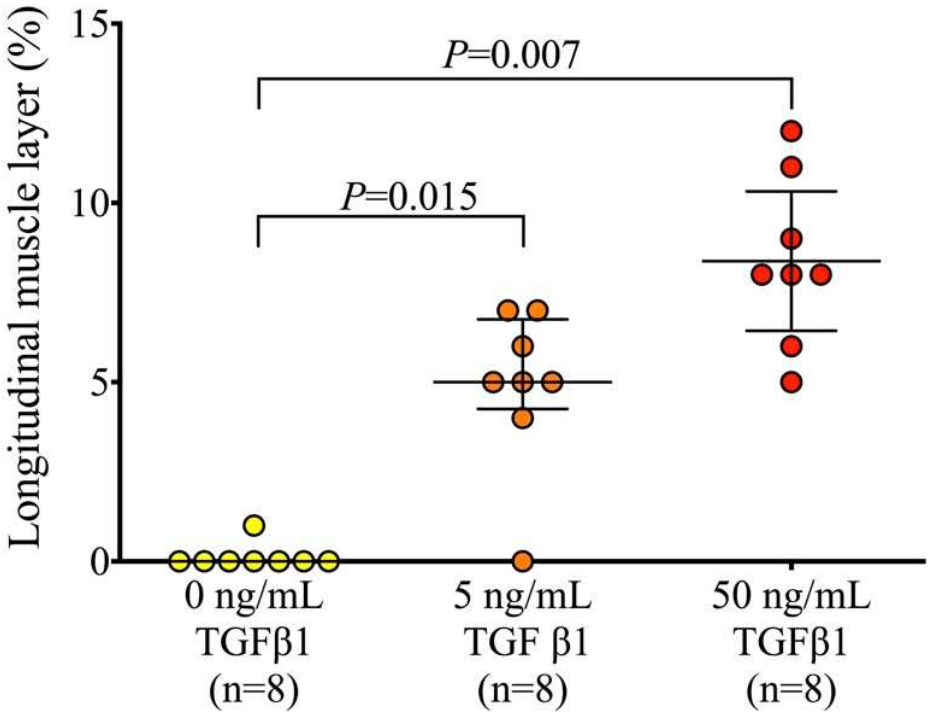

Figure 4.11 Percentage of explants floors occupied by longitudinal muscle layer

Data from eight sets of organ cultures rudiments. Each comprised rudiments from three embryos in the same litter, one explant fed basal media alone, and littermate rudiments fed 5 or 50 ng/mL of TGFβ1. The graph demonstrates a step-wise increase in percentages of the total floor area occupied by longitudinal SM due to the two different concentrations of TGFβ1. Bars indicate mean±SD. Yellow=specimens cultured in defined media; orange=specimens cultured in media supplemented by 5 ng/mL of TGFβ1; red= specimens cultured in media supplemented by 50 ng/mL of TGFβ1.

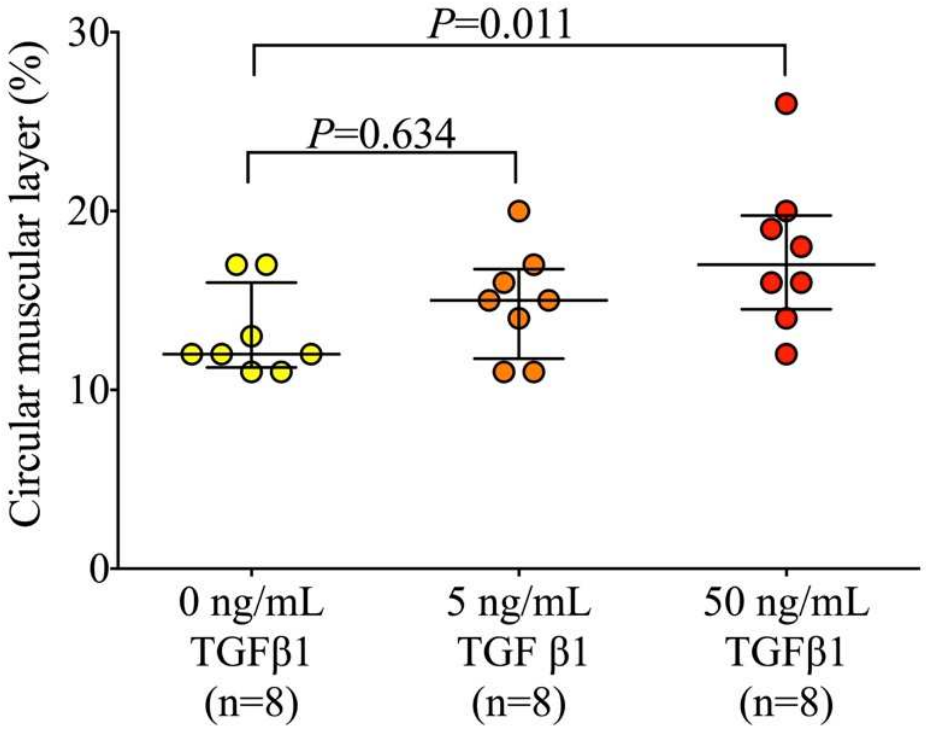

Figure 4.12 Percentage of explants floors occupied by circular muscle layer

Data from eight sets of organ cultures specimens. Each comprised rudiments from three embryos in the same litter, one explant fed basal media alone, and littermate rudiments fed 5 or 50 ng/mL of TGFβ1. The graph demonstrates that all the rudiments contained the circular muscle layer. Note that specimens cultured with 50 ng/mL of TGFβ1 significantly increased in the proportion of floors occupied by this layer. Bars indicate mean±SD. Yellow=specimens cultured in defined media; orange=specimens cultured in media supplemented by 5 ng/mL of TGFβ1; red= specimens cultured in media supplemented by 50 ng/mL of TGFβ1

4.5 Detection of TGFβ receptors

In vivo, at E14, TGFβRI was detected in the circular SM, and, at E17, it was detected in circular and longitudinal SM layers (Figure 4.13). No co-localisation of TGFβRII with αSMA was identified in the circular muscle layer of E14 while in E17 specimens TGFβRII was detected the mesenchyme between the two muscle layers and only partially co-localised in the longitudinal muscle layer (Figure 4.14)

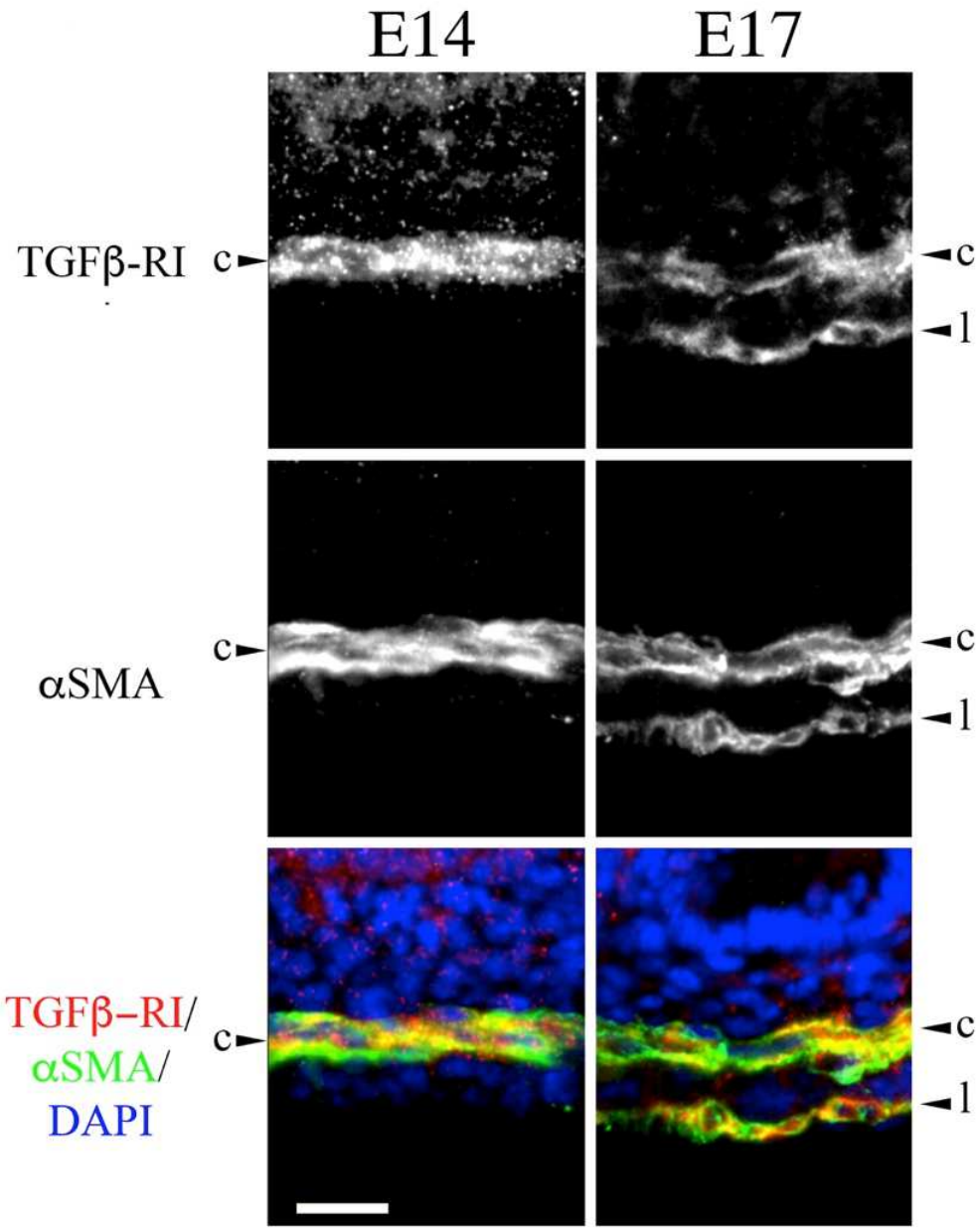

Figure 4.13 Immunohistochemistry of TGFβ receptor I *in vivo*

The figure shows transverse histology sections of freshly isolated jejuna (E14 and E17 *in vivo*). Frames in the top row show TGFβRI immunostaining (white); middle row shows the same sections immunostained for αSMA (white); the bottom row shows merged images with TGFβRI in red, αSMA in green, and nuclei in blue. This receptor was detected in circular muscle (c) at E14 and in this and also the longitudinal (l) layer at E17. Note that longitudinal muscle is absent at E14. Scale bar is 20 μm.

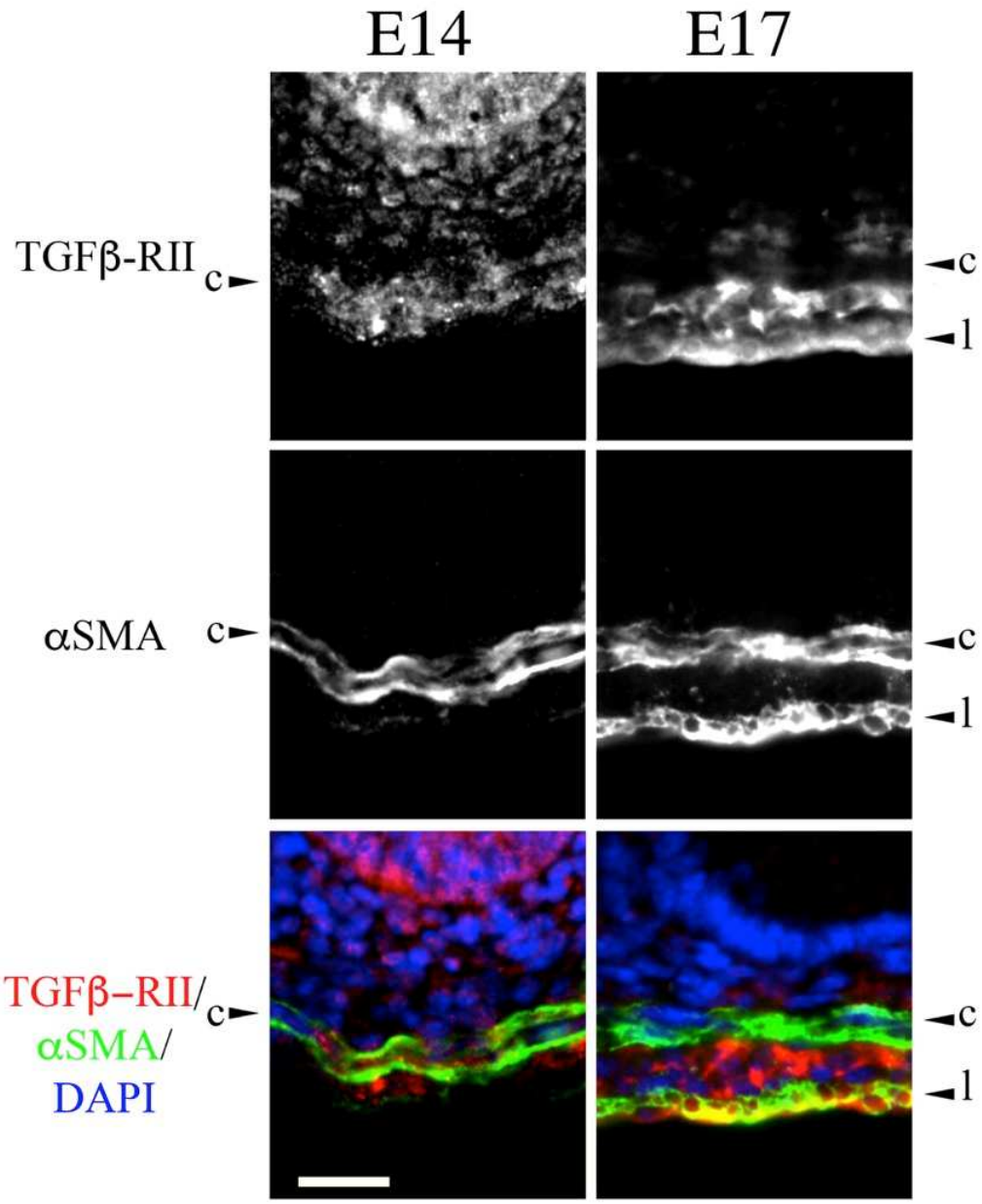

Figure 4.14 Immunohistochemistry of TGFβ receptor II *in vivo*

Transverse histology sections of freshly isolated jejuna (E14 and E17 *in vivo*) are presented in this figure. Frames in the top row show TGFβRII immunostaining (white); middle row shows the same sections immunostained for αSMA (white); the bottom row shows merged images with TGFβRII in red, αSMA in green, and nuclei in blue. TGFβRII was not detected in circular muscle at E14 but only in the mesenchyme after the circular smooth muscle layer. Interestingly in E17, TGFβRII is prominent in the mesenchyme below the circular muscle layer and partial co-localized with the αSMA^{+} cells of the longitudinal muscle layer. Scale bar is 20 μm.

In explanted organs cultured without exogenous TGFβ1, the outer mesenchyme expressed TGFβRII but not TGFβRI, in contrast with rudiments cultured with TGFβ1 where both receptors were identified. Moreover, similar to E17, in the rudiments exposed to exogenous TGFβ the newly formed longitudinal smooth muscle layer expressed both receptors. Table 4.1 summarizes the localization of TGFβRI and II in E14 and E17 jejunal sections.

Interestingly, there is evidence that TGFβ proteins initiate signalling only after binding to TGFβ receptors I and II (Akhurst and Hata, 2012). Therefore, the outer mesenchyme and the longitudinal muscle have the appropriate receptors to respond to TGFβ1 after E14, while by E17 (or three days in culture) the circular muscle is no longer competent to respond to TGFβ signalling.

Condition	Circular SM		Mesenchyme		Longitudinal SM	
	TGFβRI	TGFβRII	TGFβRI	TGFβRII	TGFβRI	TGFβRII
E14	Y	N	N	Y	n/a	n/a
E17	Y	N	N	Y	Y	Y

Table 4.1 Localization of TGFβ receptors *in vivo*

The table above describes the localization of TGFβRI and II detected by immunofluorescence analysis. In the circular muscle layers *in vivo*, both TGFβRI and II seems to be expressed in E14, while in E17 this receptor appear to be not localized. Although in E14 and E17, TGFβRI and II appeared to be localized in the outer mesenchyme oppositely in both condition, only E17 revealed a longitudinal muscle layer αSMA^{+}. n/a=not applicable due to no presence of longitudinal layer. SM=smooth muscle.

4.6 Jejunal villi

In vivo, between E14 and 17, the average width of the E-cadherin expressing epithelium fell from 38.2 to 18.5 μm, correlating with diminished cell multi-layering during formation of villi (Figure 4.15; Figure 4.16).

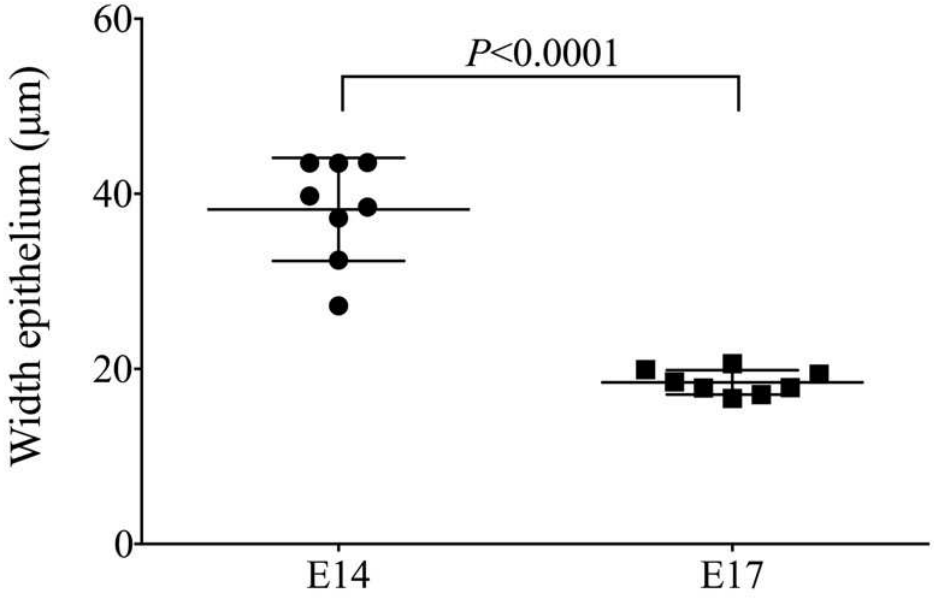

Figure 4.15 Width of epithelia layer *in vivo.*

Measurement of epithelial width showed that *in vivo* there is a significant change in the epithelial layer corresponding to the differentiation between the pluristratified epithelium in E14 to the pseudostratified in E17. During the developmental time between E14 to E17, proto-lumen is at the beginning fully occupied by the epithelium, but then the rise of villi with synchronous with the development of the pseudostratified epithelial layer creates a functional lumen. Bars indicate mean±SD.

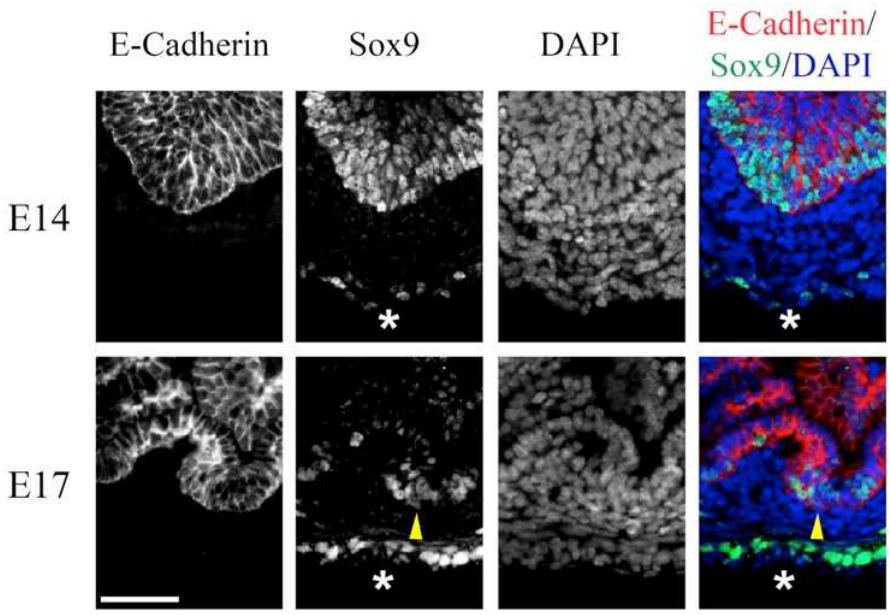

Figure 4.16 Embryonic jejunal epithelium differentiation *in vivo*

Transverse sections of freshly isolated jejuna (E14 and E17 *in vivo*) are presented in this panel. Left column=E-Cadherin (white); second column=SOX9 (white); third column shows nuclei (white); the right column is a merged image with E-cadherin in red, SOX9 in green and nuclei in blue. SOX9 was expressed in the basal layers of epithelium in the E14 jejunum *in vivo*. At E17, SOX9 was localized to clusters of epithelial cells (yellow arrowheads) between villi, with similar appearances in organ culture (see Figure 4.18). SOX9 was also detected in isolated cells in outer mesenchyme (asterisks), presumed enteric ganglia. Scale bar=40 μm.

E14 rudiments cultured in basal media alone also contained an epithelial layer with an average of width of 19.9 μm, similar to E17 jejunum *in vivo*. In explants exposed to TGFβ1, the average width was significantly decrease in specimens exposed to 5 ng/mL of TGFβ1 (P=0.02) but the epithelial width of rudiments exposed to 50 ng/mL of TGFβ1 was similar to controls (P=0.09) (Figure 4.17; Figure 4.18).

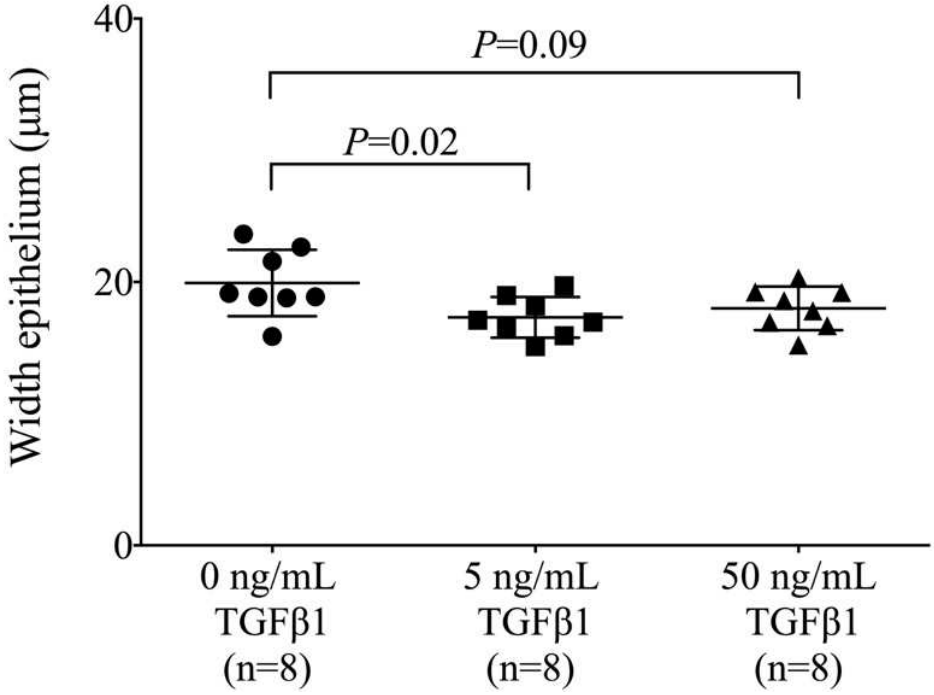

Figure 4.17 Effects of TGFβ1 in epithelial differentiation organ culture

After three days in culture, the rudiments exposed to exogenous TGFβ1 express a reduction of epithelial width as per normal epithelial differentiation (E17 mean epithelial width 18.47 μm; E14-D3 5ng/mL TGFβ1, 17.31 μm; E14-D3 5ng/mL TGFβ1, 17.99 μm). Interestingly, specimens cultured in defined media presented a wider epithelial layer compared to the 5ng/mL TGFβ1 (*P*= 0.02), but no difference were reported to 50 ng/mL TGFβ1. Bars indicate mean±SD.

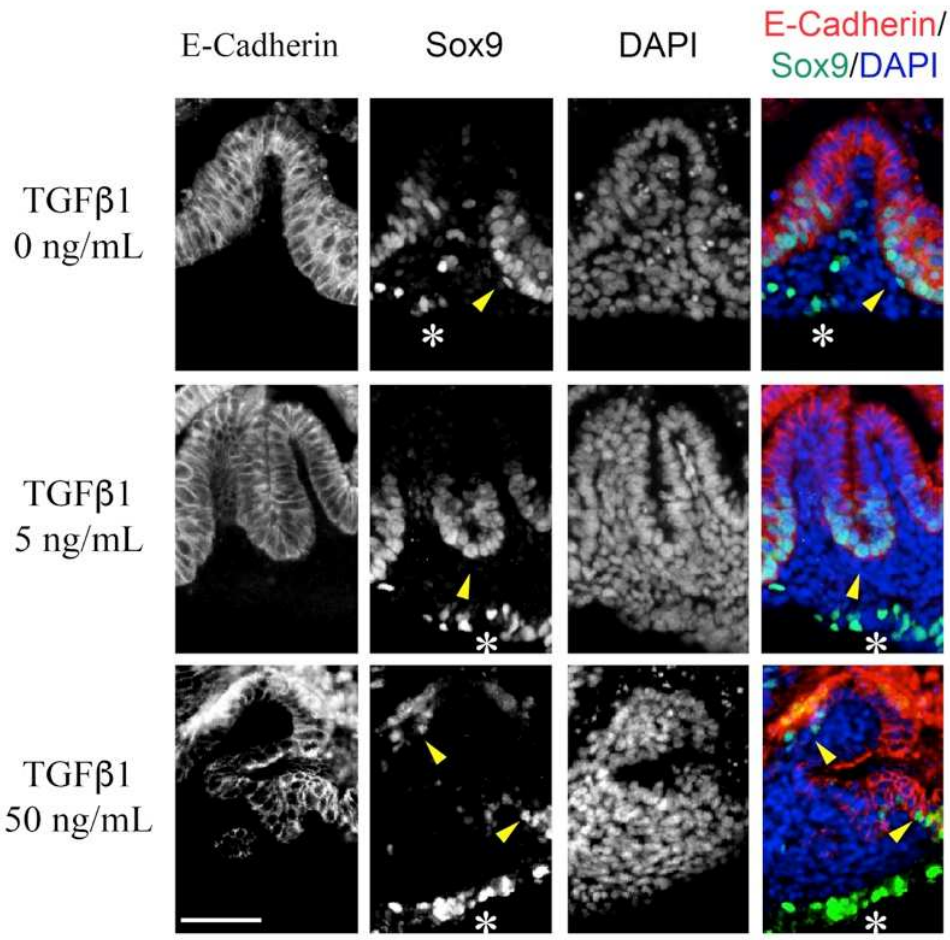

Figure 4.18 Embryonic jejunal epithelium differentiation organ culture

This panel shows transverse sections of E14 rudiments (E14-D3 *ex vivo*) floors. Left column=E-cadherin (white); second column=SOX9 (white); third column shows nuclei (white); the right column is a merged image with E-cadherin in red, SOX9 in green and nuclei in blue. During three days in organ culture the intestinal epithelium differentiate in finger like structure as per *in vivo*. Interestingly, high concentration of TGFβ1 showed dysmorphic villi, alteration of the E-cadherin pattern and lower amount of SOX9 in the area of the crypt. Scale bar=40 μm.

Villi formed in control explants and those exposed to TGFβ1; however, explants exposed to the higher TGFβ1 concentration appeared stunted. Transverse sections of explants in basal media alone contained an average of 5.2 villi (Figure 4.19). There was a significant (P=0.010) increase to an average of 6.5 villi in 5 ng/mL TGFβ1 but rudiments fed 50 ng/mL TGFβ1 tended to have fewer (average of 4.19) villi than controls.

The SOX9 transcription factor is expressed in proliferative epithelia in the intervillus area. In E14 organs that have yet to form villi, the basal cell layers of the epithelium expressed SOX9 (Figure 4.16). In E17 organs, in specimens cultured in defined medium and the explants exposed to TGFβ1, epithelial SOX9 expression was confined to regions between villi. SOX9 was also detected in non-smooth muscle cells in the outer mesenchyme; these are probably enteric glial cells, known to express SOX9 (Figure 4.16 and Figure 4.18).

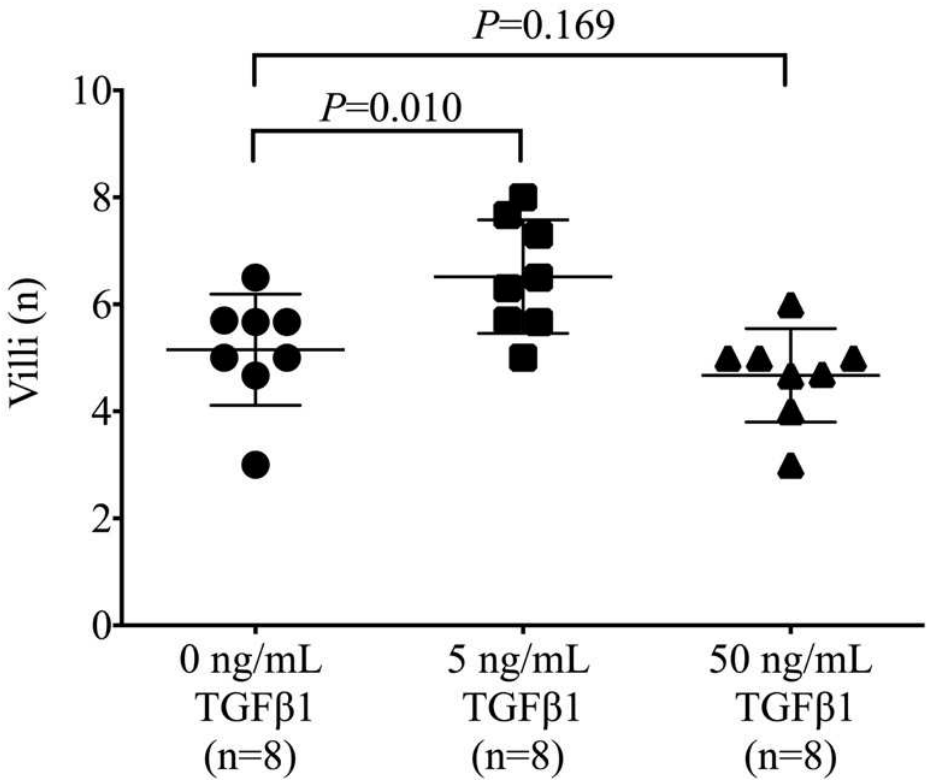

Figure 4.19 Effect of TGFβ1 on number of villi

The graph shows the numbers of villi in transverse sections of floors. Eight sets of organ cultures were analysed. In each set, the large bar indicates the mean; flanked by one SD. Explants in 5 ng/mL TGFβ1 contained significantly more villi than controls. Interestingly, immunohistochemistry showed that the shape of the villi is abnormal in specimens cultured in 50 ng/mL TGFβ1. Bars indicate mean±SD.

4.7 Jejunal transcriptome

To define molecular changes elicited by TGFβ1 in an unbiased manner, we undertook microarray analyses on organ culture samples and we validated the microarray data with QPCR for 13 of the most changed transcripts altered by 5 ng/mL of TGFβ1 (Table 4.2). The most deregulated transcripts resulted from microarray analysis are shown in Tables 4.2 and 4.3, with the full list available at Array-Express database (www.ebi.ac.uk/arrayexpress accession number E-MTAB-450). Ingenuity pathway analysis confirmed the observed changes were consistent with activated TGFβ1 pathways. Figure 4.20 and Figure 4.21 showed changes in levels of transcripts assessed by microarray and validated by QPCR analyses.

UniGene Symbol	UniGene Name	FC	*P*
Up regulated in 5 ng/mL TGFβ1			
Krt17	Keratin 17	2.07	0.0006
Ctsw	Cathepsin W	2.27	0.0001
Anpep	Aminopeptidase M	2.02	0.01
Col8a1	Collagen, type VIII, alpha 1	2.10	0.0001
Lgr5	Leucine-rich repeat containing G protein-coupled receptor 5	1.90	0.004
Eln	Elastin	1.82	0.005
Angpt1	Angiopoietin 1	1.81	0.0008
Sfrp1	Secreted frizzled-related protein 1	1.54	0.01
Down regulated in 5 ng/mL TGFβ1			
Fxyd2	FXYD domain containing ion transport regulator 2	-2.53	0.04
Gpm6a	Glycoprotein M6A	-2.05	0.0007
Mlxipl	MLX interacting protein-like	-1.84	0.01
Pten	Phosphatase and tensin homolog	-1.88	0.003
Sfrp2	Secreted frizzled-related protein 2;	-1.53	0.009

Table 4.2 Expression of selected genes from microarray analysis

These selected genes were used to validate microarray data using QPCR. All gene expression changes shown are statistically significant with $P<0.05$ using Student's paired *t* test and n=4 for each gene tested. Data from specimens cultured in 5 ng/mL of TGFβ1. FC=average fold change.

UniGene Symbol	UniGene Name	Fold change	*P*
Upregulated in 5 ng/ml TGFβ1 versus basal media			
Car6	Carbonic anhydrase 6	3.02	0.02
Pigr	Polymeric immunoglobulin receptor	3.01	0.01
Anxa10	Annexin A10	2.89	0.01
Ifit1	Interferon-induced protein with tetratricopeptide repeats1	2.64	0.04
Ctsw	Cathepsin W	2.27	0.0001
Mfap5	Microfibrillar associated protein 5	2.11	0.002
Col8a1	Collagen, type VIII, alpha 1	2.10	0.0001
Krt17	Keratin 17	2.07	0.0006
Lgr5	Leucine-rich repeat containing G protein-coupled receptor 5	1.90	0.004
Eln	Elastin	1.82	0.005
Downregulated in 5 ng/ml TGFβ1 versus basal media			
Cdh16	Cadherin 16	-3.80	0.03
Dppa5a	Developmental Pluripotency associated 5a	-2.89	0.02
Akp3	Alkaline phosphatase 3, intestine, not Mn requiring	-2.63	0.04
Fxyd2	FXYD domain containing ion transport regulator 2	-2.53	0.04
Paqr5	Progestin and adipoQ receptor family member V	-2.41	0.04
Tufm	Tu translation elongation factor, mitochondrial	-2.33	0.01
Hsd3b2	Hydroxyl-delta-5-steroid dehydrogenase, 3 beta- and steroid delta-isomerase 2	-2.31	0.02
Agmo	Alkylglycerosl monooxygenase	-2.25	0.03
Adam4	A disintegrin and metallopeptidase domain 4	-1.78	0.001

Table 4.3 Deregulated transcripts in organs exposed to 5 ng/ml TGFβ1

List of significant transcripts up and down regulated in specimens cultured with 5 ng/ml TGFβ1.

UniGene Symbol	UniGene Name	Fold change	*P*
Upregulated in 50 ng/ml TGFβ1 versus basal media			
C1qtnf3	C1q and tumor necrosis factor related protein 3	5.68	1.69E-05
Adamts16	A disintegrin-like and metallopeptidase with thrombospondin type 1, motif 16	3.93	5.67E-06
Akr1c18	Aldo-keto reductase family 1, member C18	3.73	0.0006
Adamtsl2	ADAMTS-like2	3.10	1.53E-05
Ibsp	Integrin binding sialoprotein	3.10	0.003
Mfap5	Microfibrillar associated protein 5	3.08	0.0001
Cilp	Cartilage intermediate layer protein, nucleotide pyrophosphohydrolase	3.02	0.007
Ctsw	Cathepsin W	2.96	4.97E-05
Col8a1	Collagen, type VIII, alpha 1	2.88	0.0004
Eln	Elastin	2.73	2.18E-05
Downregulated in 50 ng/ml TGFβ1 versus basal media			
Gpm6a	Glycoprotein m6a	-2.87	3.95E-05
Dppa5a	Developmental Pluripotency associated 5a	-2.50	0.03
Tufm	Tu translation elongation factor, mitochondrial	-2.21	0.0008
Gpx2	Glutathione peroxidase 2	-2.13	0.01
Kcne3	Potassium voltage-gated channel. Isk-related family, member 3	-1.80	0.002
Kcnn3	Potassium intermediate/small conductance calcium-activated channel, subfamily N, member 3	-1.79	0.01
Upk1b	Uroplakin 1B	-1.77	0.0004
Pten	Phosphatase and tensine homolog	-1.76	0.01
Celf1	CUGBP, Elav-like family member 1	-1.69	0.005
Sema3d	Sema domain, immunoglobulin domain, short basic domain, secreted 3D	-1.62	0.02

Table 4.4 Deregulated transcripts in organs exposed to 50 ng/ml TGFβ1

List of significant transcripts up and down regulated in specimens cultured with 5 ng/ml TGFβ1.

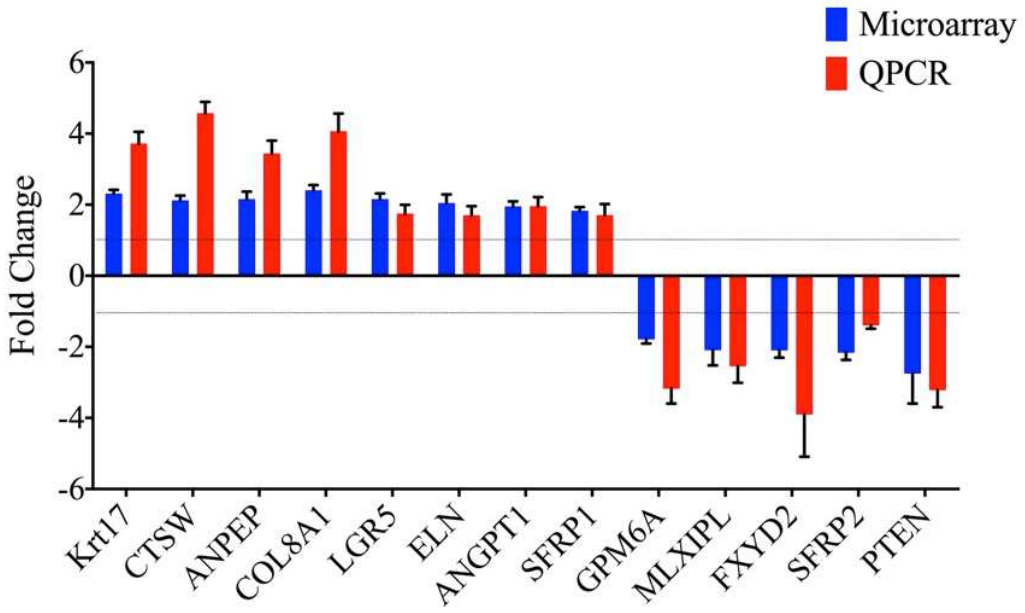

Figure 4.20 Comparison of changes in levels of selected transcripts measured by microarray versus QPCR (5ng/mL TGFβ1)

Changes in levels of transcripts (presented in table 4.2) were assessed by microarray (blue) and QPCR (red) analyses. Each bar is the average value of four experimental replicates of organs exposed to 5 ng/mL of TGFβ1 versus organs exposed to basal media alone. Note that the patterns generated by the two assays are broadly similar. Area between dot lines indicates FC ±1. Bars indicate SEM.

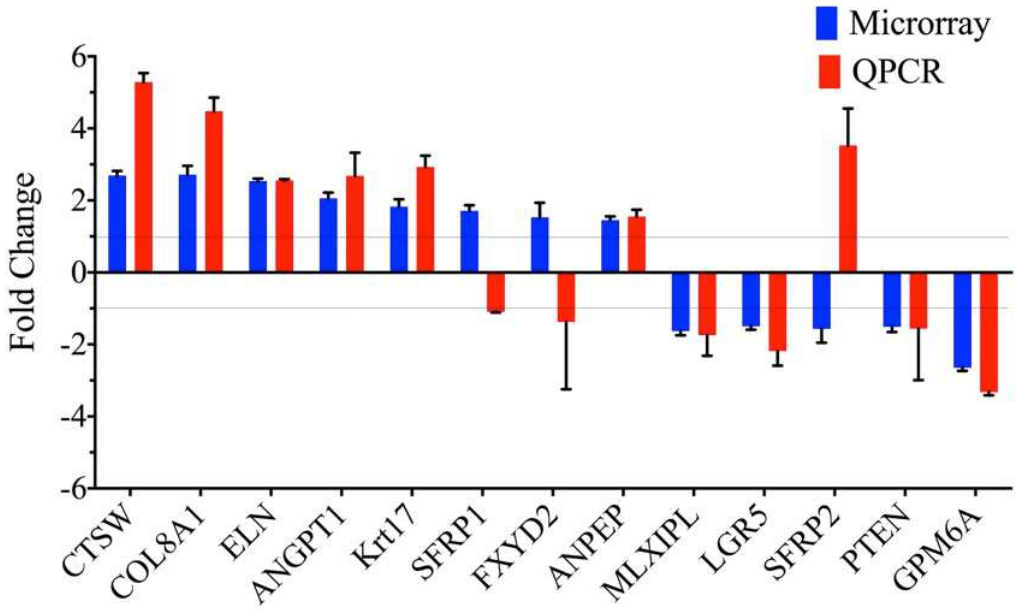

Figure 4.21 Comparisons of changes in levels of selected transcripts measured by microarray versus QPCR (50 ng/mL TGFβ1)

Changes in levels of transcripts (presented in table 4.2) were assessed by microarray (blue) and QPCR (red) analyses. Each bar is the average value of four experimental replicates of organs exposed to 50 ng/mL of TGFβ1 versus organs exposed to basal media alone. Area between dot lines indicates FC ±1. Bars indicate SEM.

In those exposed to 5 ng/mL TGFβ1, 176 transcripts were increased and 130 were decreased >1.4 fold and *P* value <0.005. In 50 ng/mL TGFβ1, 246 transcripts were increased and 76 were decreased >1.4 fold and *P* value <0.005.

In rudiments exposed to 5 ng/mL TGFβ1, there were '*TGFβ1growth factor-related changes'* (*P*-value of overlap, 2.81E-06; activation z-score, 2.50), and '*SMAD3-related changes*' (*P*-value of overlap, 6.75E-04; activation z-score, 2.38). The latter indicates activation of the canonical TGFβ signalling pathway (Akhurst and Hata, 2012).

In rudiments exposed to 50 ng/mL TGFβ1, there were '*TGFβ1growth factor-related changes'* (*P*-value of overlap, 2.07E-22; activation z-score, 3.91) and '*P38 mitogen activated protein kinase (MAPK)-related changes*' (*P*-value of overlap, 1.02E-10; activation z-score, 3.67). The latter indicates activation of a SMAD independent/non-canonical signalling TGFβ pathway (Akhurst and Hata, 2012).

Unsupervised hierarchical clustering (Figure 4.22) revealed three major gene expression patterns, *Clusters 1-3*. Cluster 1 comprised 90 unique transcripts with reduced expression in explants exposed to exogenous TGFβ1. GO enrichment analysis revealed that most encoded transmembrane proteins, including ion channels (Figure 4.23).

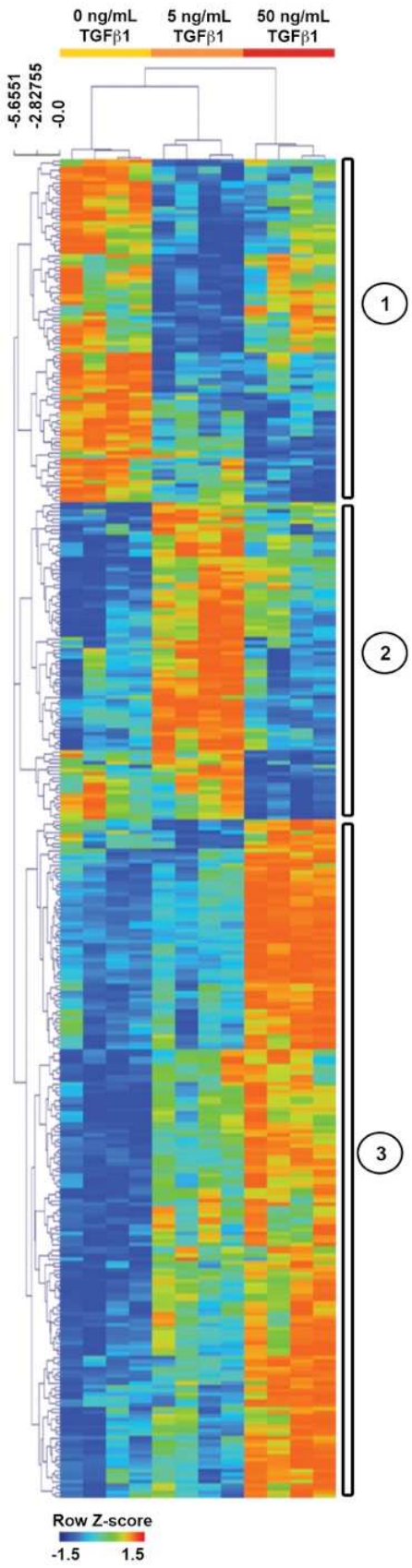
0 ng/mL TGFβ1
5 ng/mL TGFβ1
50 ng/mL TGFβ1
-5.6551
-2.82755
-0.0
1
2
3
Row Z-score
-1.5
1.5

Figure 4.22 Microarray analyses reveals TGFβ1 dose dependent effects

The heat map located in the previous page shows unsupervised hierarchical clustering by transcript expression. Rows are expression levels denoted as the Z-score, displayed in a high-low (red-blue) colour scale. Transcripts grouped into three Clusters: (1) reduced in response to TGFβ1, (2) increased in response to 5 ng/mL TGFβ1 and (3) increased in response to 50 ng/mL TGFβ1.

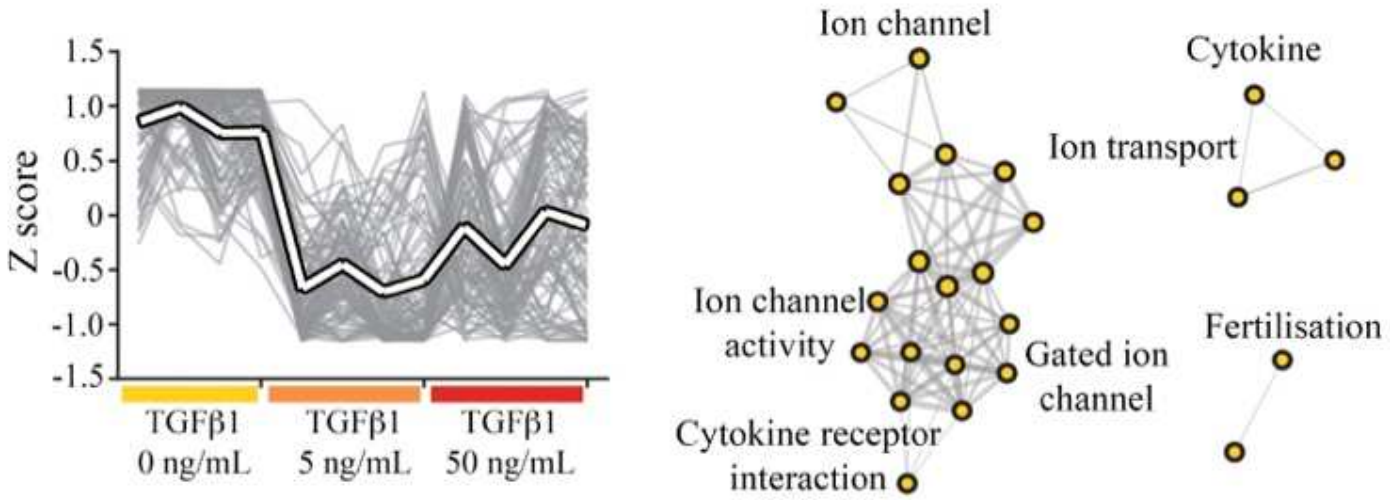

Figure 4.23 Cluster 1 profile plots and network analysis of transcriptomic data

Profile plot of Cluster 1 is shown, with the mean profile indicated by a white line. Overrepresented biological terms from each cluster are displayed as GO enrichment maps. Nodes represent GO terms and lines represent the degree of overlap. Cluster 1 revealed ion channels and membrane transcripts that were underrepresented following treatment with TGFβ1.

Cluster 2 contained 66 transcripts increased in explants exposed to 5 ng/mL TGFβ1, but not in those exposed to 50 ng/mL TGFβ1. These transcripts prominently encoded proteins involved in the cell cycle. (Figure 4.24)

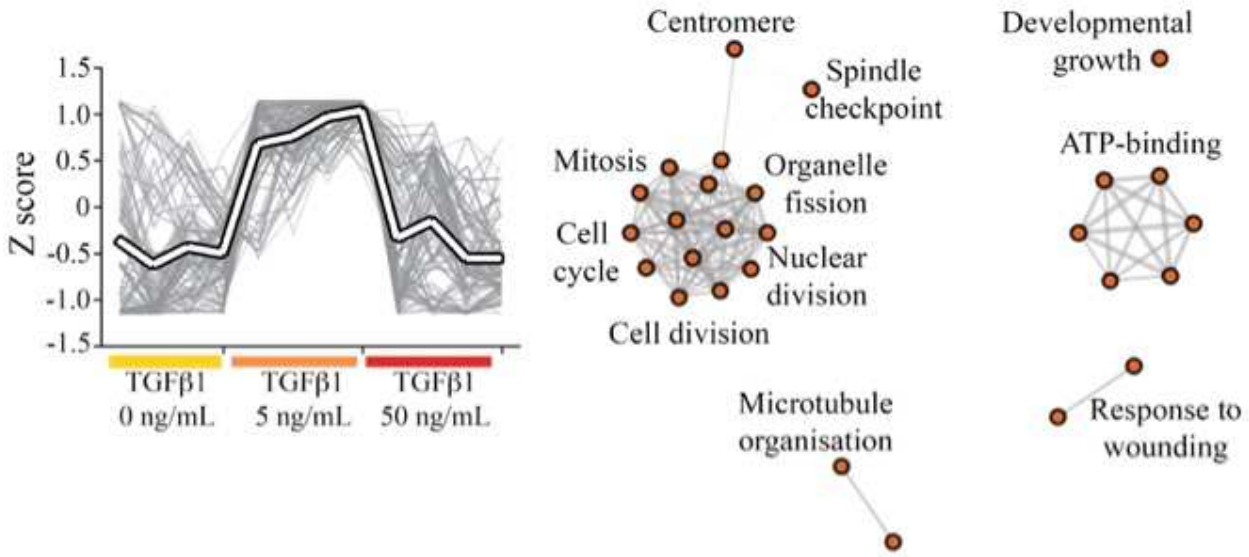

Figure 4.24 Cluster 2 profile plots and network analysis of transcriptomic data

Profile plot of Cluster 2 is shown, with the mean profile indicated by a white line. Overrepresented biological terms from each cluster are displayed as GO enrichment maps. Nodes represent GO terms and lines represent the degree of overlap. Cluster 2 revealed cell cycle and microtubule process transcripts that were overrepresented following 5 ng/mL TGFβ1.

Cluster 3 contained 170 increased transcripts with the highest expression in explants exposed to 50 ng/mL TGFβ1. They prominently encoded extracellular matrix (ECM), cellular adhesion and focal adhesion proteins (Figure 4.25).

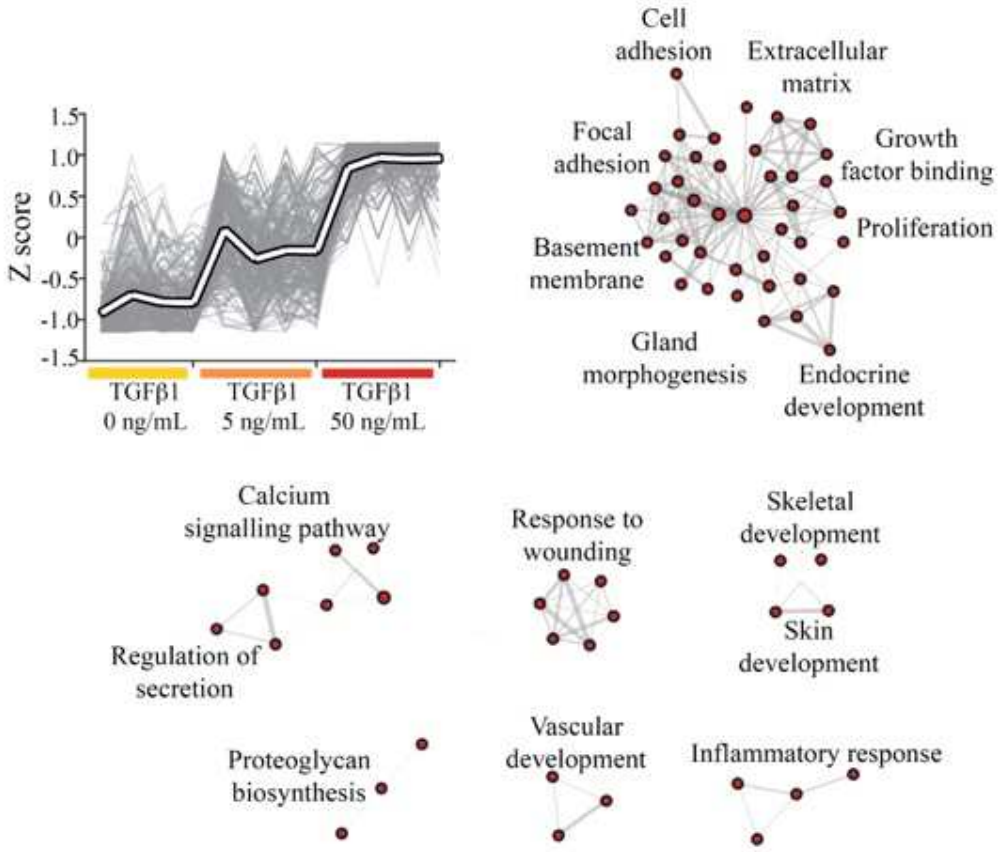

Figure 4.25 Cluster 3 profile plots and network analysis of transcriptomic data

Profile plot of Cluster 3 is shown, with the mean profile indicated by a white line. Overrepresented biological terms from each cluster are displayed as GO enrichment maps. Nodes represent GO terms and lines represent the degree of overlap. Cluster 3 revealed transcripts involved in ECM and focal adhesion type processes that were overrepresented after exposure to TGFβ1.

Using the Jackson laboratory MGI-Mouse gene expression database, we analysed tissue specific transcript sets. SM markers (Table 4.4) displayed a TGFβ1 concentration-dependent increase (Figure 4.26), whereas less specific muscle markers (Table 4.5) were only marginally increased (Figure 4.27).

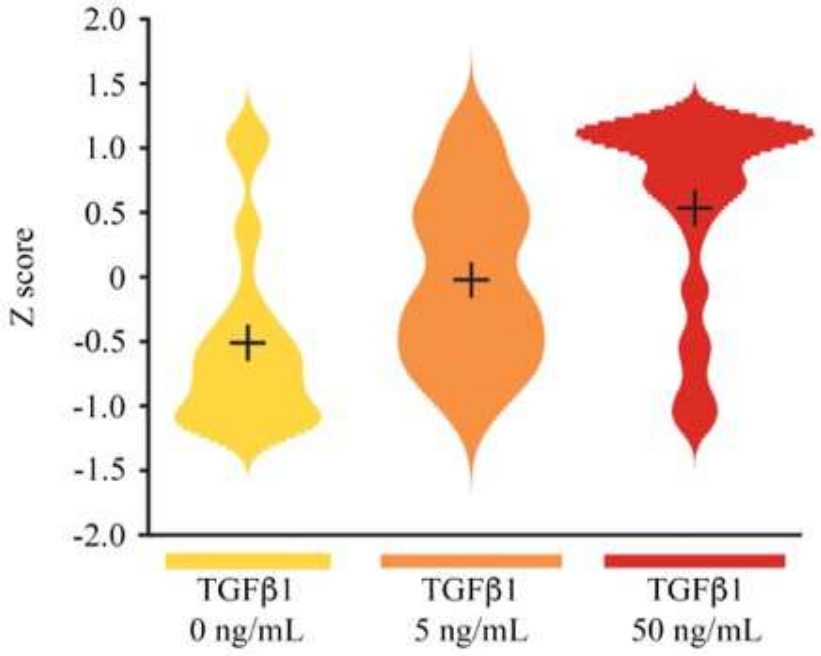

Figure 4.26 Violin plots of transcriptomic data for smooth muscle transcripts

Violin plot of Z-scores shows the expression levels of SM specific transcript. The violin plot combines box plot and kernel density trace to describe the distribution pattern of a vector of data. Note that SM specific transcript increased in a stepwise manner with increasing TGFβ1 concentrations. The symbol + indicate median of the data.

Gene name
Akr1b7
Ano1
Col5a2
Erg
H2-T10
Mfap4
Msln
Myocd
Sfrp1
Sncaip
Susd2
Wif1

Table 4.5 Smooth muscle transcripts used to generate correspondent violin plot

The table above listed the smooth muscle transcripts significantly changed by TGFβ1 and used to create the violin plot graph presented on Figure 4.26.

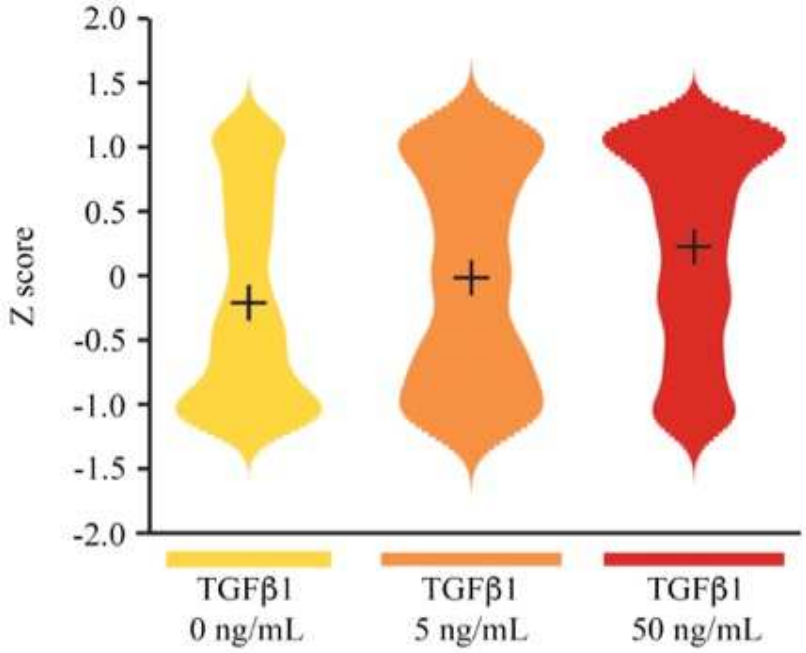

Figure 4.27 Violin plots of transcriptomic data for all muscle transcripts

A violin plot of Z-scores shows levels of transcripts along vertical axes. General muscle transcripts showed little change with TGFβ1. The symbol + indicate median of the data.

Gene name						
Abca9	Chrd	G0s2	Mb	Nrap	Rpl37	Tceb2
Acta1	Chrna1	Gli1	Meox1	Nxph4	Rpl3l	Thsd1
Actn2	Ckm	Gprasp1	Mpp4	Obscn	Ryr1	Tmod4
Actn3	Ckmt2	Habp2	Mybpc1	Obscn	S100a1	Tnnc1
Adamdec1	Coro6	Helb	Mybpc2	Pcdh18	Sag	Tnnc2
Adra1b	Cox6a2	Hfe2	Myf6	Pde10a	Sardh	Tnni1
Adssl1	Cryab	Hhip	Myh2	Pde6a	Scara5	Tnni2
Ak1	Csrp3	Hint2	Myh7	Pdk4	Scn4a	Tnnt3
Ankrd2	Des	Hrc	Myl1	Pdlim5	Sema6b	Tomm7
Ankrd23	Dgcr6	Hspb2	Myl2	Pdlim5	Sgca	Tpm1
Art3	Dido1	Hspb6	Mylpf	Pebp4	Shmt2	Tpm2
Asb5	Dido1	Hspb7	Myod1	Pgam2	Slc25a34	Trhde
Atp2a2	Dusp13	Impg2	Myom1	Pipox	Sln	Trim54
Atp5d	Eno3	Inhbe	Myom2	Pkia	Smpx	Tuba8
Cacna1s	Eya4	Itga10	Myot	Pln	Smr3a	Txlnb
Camk2d	Fbf1	Jph1	Myoz1	Ppara	Smyd1	Ucp3
Casq2	Fbp2	Krtap4-7	Myoz2	Ppp1r1a	St13	Vamp5
Ccrn4l	Fgf10	Ldb3	Ndufa1	Ppp1r3a	Stac3	Vamp5
Ccrn4l	Fgfr4	Lmod1	Nell1	Pygm	Sult1e1	Wnt5b
Cd7	Fhl1	Lpo	Nexn	Rabep2	Synpo2l	
Cdh15	Fhl3	Lrrc39	Nipsnap3b	Rapsn	Tacr2	
Cdk4	Fut2	Mapk12	Nos1	Rdh5	Tcap	
Cfl2	Fxyd1	Mars	Nr2e3	Rgma	Tcea3	

Table 4.6 Muscle transcripts used to generate correspondent violin plot

The table presented depicts muscle transcripts used to generate the graph showed in Figure 4.27.

Similar to muscle markers, jejunal transcript (Table 4.6) did not show TGFβ1 concentration-dependent increase (Figure 4.28). Collectively, these results demonstrate complex sets of changes in gene expression in response to exogenous TGFβ1, with both concentration-dependent and concentration-specific effects.

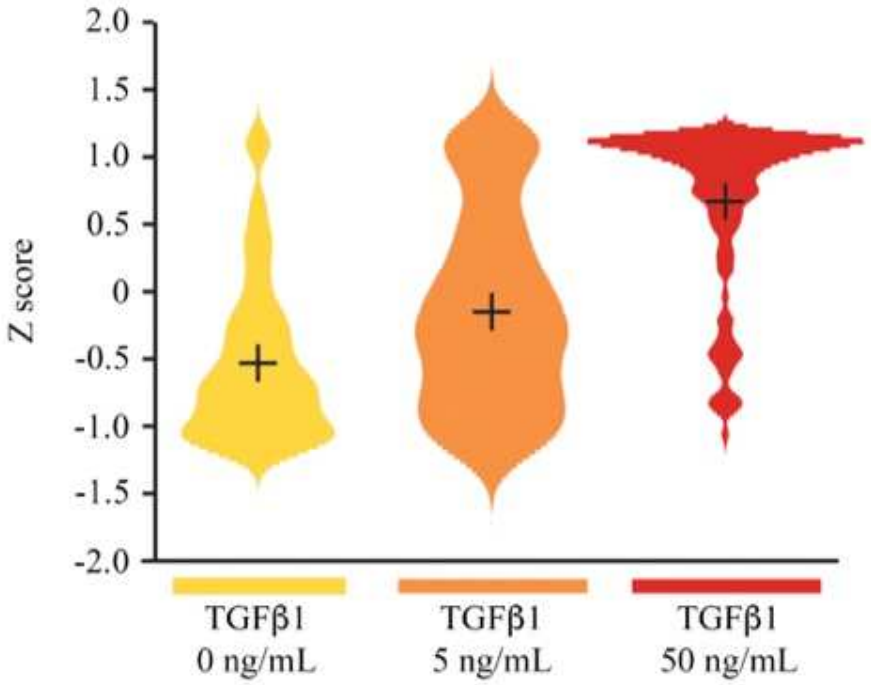

Figure 4.28 Violin plots of transcriptomic data for jejunal transcripts

Violin plots of Z-scores show levels of transcripts along vertical axes. Jejunal transcripts increased in a stepwise manner with increasing TGFβ1 concentrations. The symbol + indicate median of the data.

Gene name	
Ace	Htr2b
Ada	Htr2b
Arg1	Il2rg
Art1	Kcnma1
Ccl9	Kcnma1
Cd4	Laptm5
Cd53	Liph
Eno3	Myh11
Gas1	Nt5e
Grik2	Nt5e
Hoxc8	Slc6a12
Hspa4l	Tac2
Htr1d	Wnt5a
Htr2a	

Table 4.7 Jejunum transcripts used to generate correspondent violin plot

The table shows the list of transcripts related on jejunum and significantly altered on the microarray produced from experiment presented in Chapter 4. These data were used to create the violin plot graph in Figure 4.28.

4.8 Proliferation in explants

Given that the microarray data showed an increase in cell cycle transcripts following exposure to TGFβ1, I analysed either normal proliferation rate in *in vivo* rudiments and cell number and proliferation in tissue sections *ex vivo*. In normal development between E14 and E17, the intestine is normally subjected to extensive re-organization of the epithelial, mesenchymal and muscular compartment. As demonstrated by Figure 4.29, E17 jejunum is involved in higher proliferation rate compared to E14, as demonstrated from the anatomical differentiation from a single tube to a complex structure. Interestingly, inner and outer mesenchyme of the E17 jejunum tends to reach the highest point of proliferation, whereas in the E14 the proliferation rate constantly increases in a radial direction.

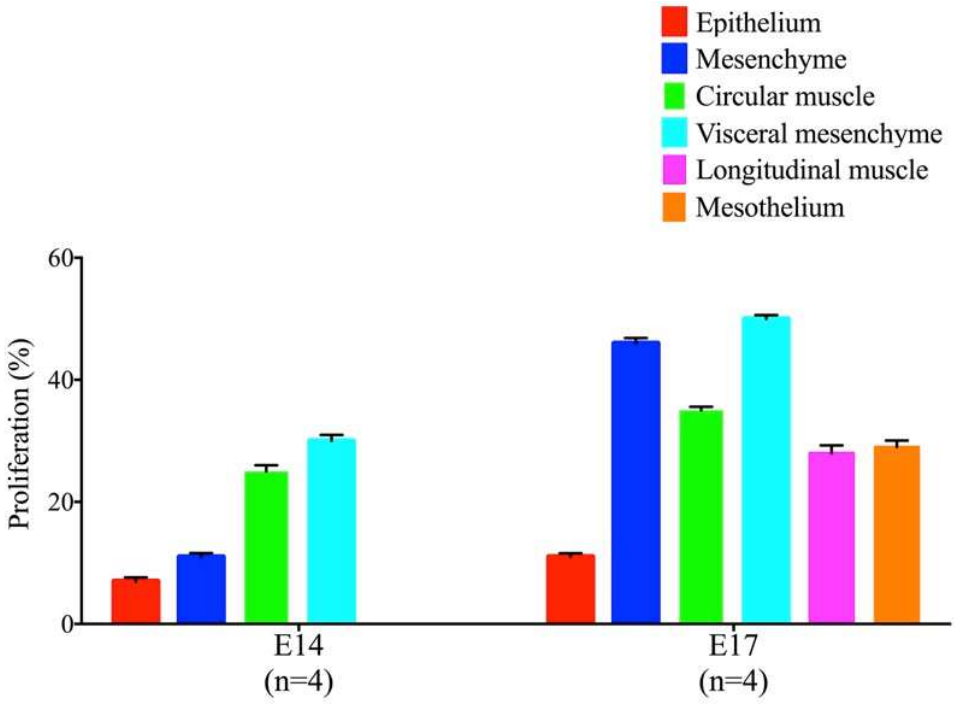

Figure 4.29 Proliferation in embryonic jejunum *in vivo*

The graph bar shows the rate of proliferation comparing E14 and E17 *in vivo* assessed by Ki67 immunohistochemistry. In E14 rudiments no longitudinal muscle layer or mesothelium was identified, whereas E17 exhibited all the intestinal layers. Although E14 explants presented a hyperbolic trend in proliferation rate per layers, the two mesenchymal layers of E17 rudiments showed the peak of proliferation, with an associated proliferative reduction of the epithelial layers. Bar=SEM.

Although the floors areas seem to growth slightly with increasing TGFβ1 concentrations (Figure 4.30), floors of rudiments exposed to 5 ng/mL TGFβ1 tended to have more nuclei (P=0.077) than controls (Figure 4.31).

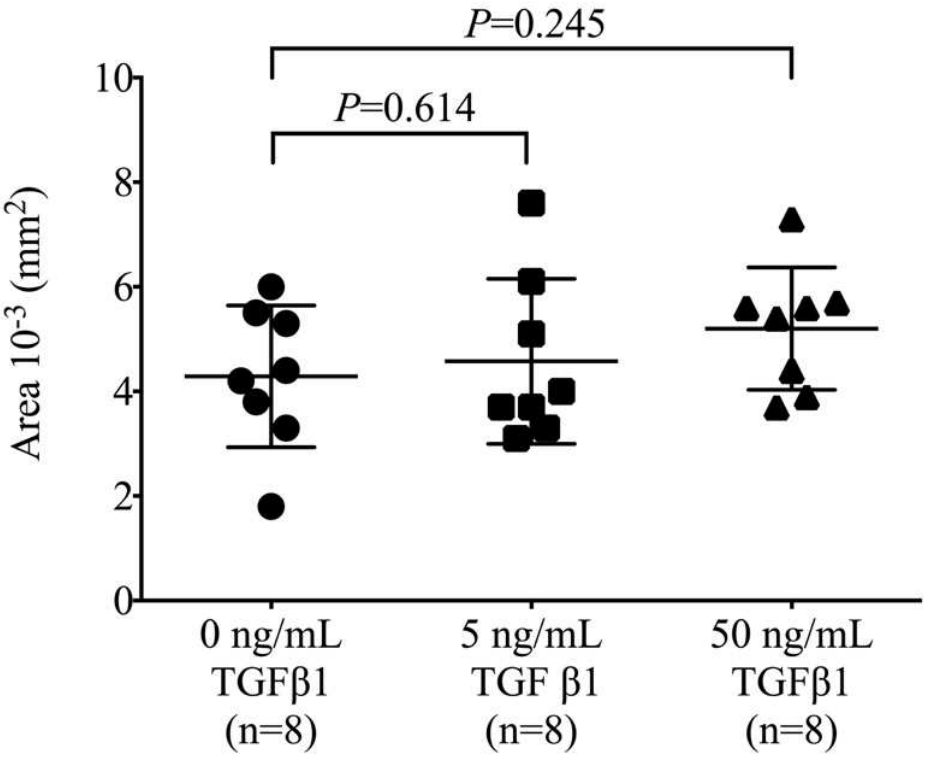

Figure 4.30 Cross-section areas of explants in organ culture

The graph depicts area of explant floors after three days in organ culture. There was no significant difference between TGFβ1 and control cultures. Bars indicate mean±SD.

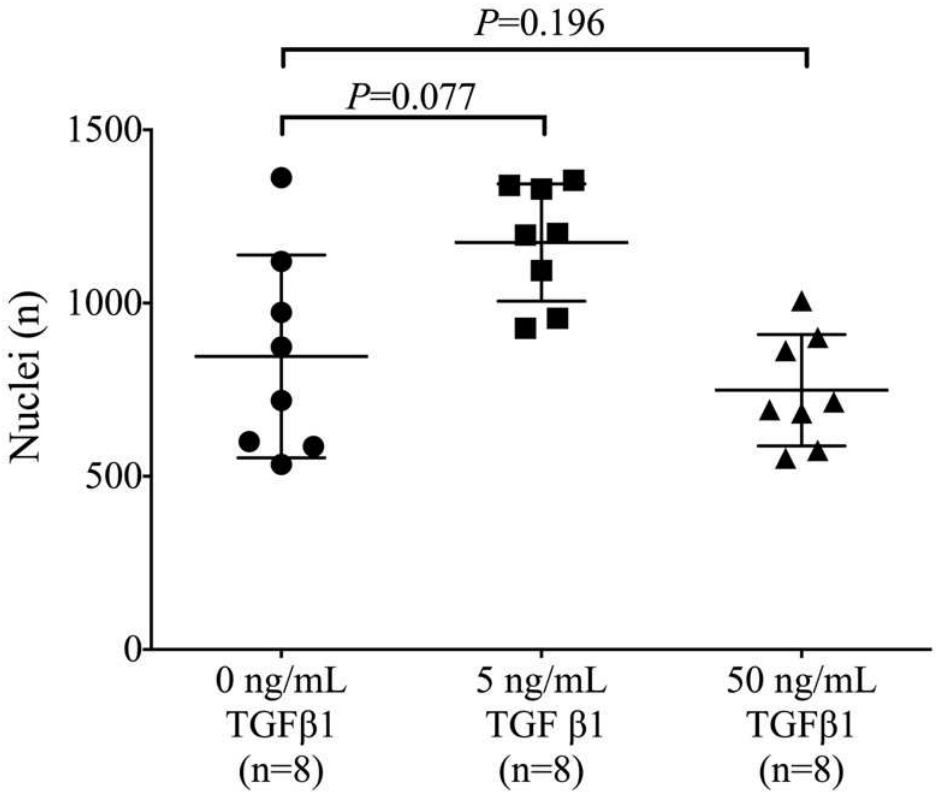

Figure 4.31 Numbers of cell nuclei in organ cultures

The graph illustrates the total number of nuclei in explant floors after three days in organ culture. There was no significant difference between TGFβ1 and control cultures. Bars indicate mean±SD.

Immunofluorescence for E-cadherin and αSMA showed that specimens cultured in defined media did not exhibit a defined longitudinal smooth muscle layers (Figure 4.32), but the percentage of floor αSMA^{+} between inner and outer mesenchyme stayed at the same level as specimens exposed to 5 ng/mL TGFβ1. Interestingly, 50 ng/mL TGFβ1 seems to increase the percentage of both circular and longitudinal smooth muscle layer. Figure 4.33 shows that proliferation was most prominent in inner mesenchymal and longitudinal muscle layers in rudiments exposed to 5 ng/mL TGFβ1.

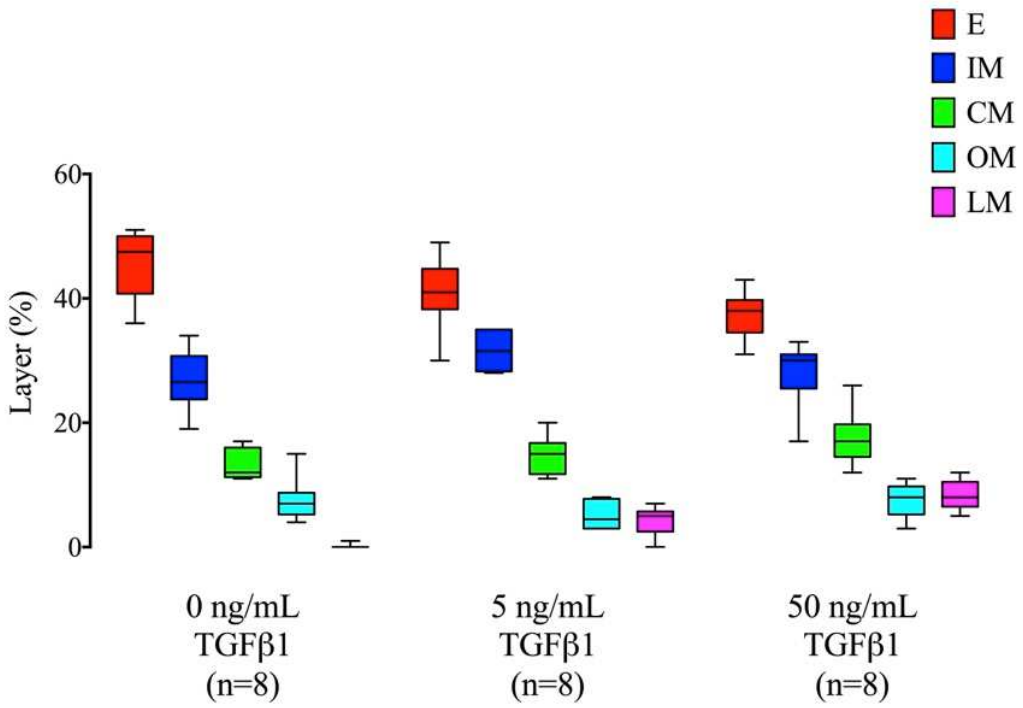

Figure 4.32 Distribution of layers in organ cultures

The box and whisker graph illustrate the distribution of the epithelium (E; red), inner mesenchyme (IM; dark blue), circular muscle (CM; green), outer mesenchyme (OM; light blue) and longitudinal muscle (LM; pink) in the floor of explant assessed by immunofluorescence for E-cadherin and αSMA. Although the layers distribution is conserved in all the condition, explants cultured in conditioned media do not present defined longitudinal muscle layers. Interestingly, rudiments cultured in 50 ng/ml of TGFβ1 exhibited ticked circular and longitudinal muscle layers. E=epithelium; IM=inner mesenchyme; CM=circular muscular layer; OM=outer mesenchyme; LM=longitudinal muscle layer. Box plot shows the inter quartile range, whiskers, and max/min outliers. Bar into the box indicates median.

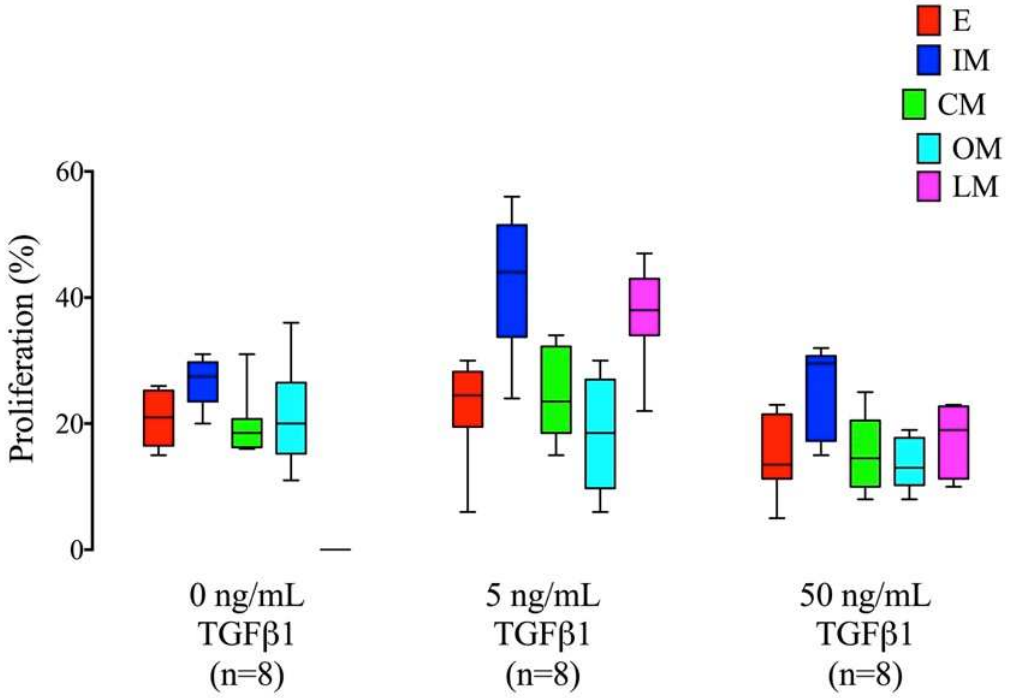

Figure 4.33 Proliferation in organ cultures

Percentages of proliferating cells (assessed by Ki67 immunohistochemistry) in explant floors: epithelium (E; red), inner mesenchyme (IM; dark blue), circular muscle (CM; green), outer mesenchyme (OM; light blue) and longitudinal muscle (LM; pink). Overall, the highest proportions of proliferative cells were noted in inner mesenchyme and the longitudinal muscle layer, both in the group of explants exposed to 5 ng/mL TGFβ1. Note that, n=8 for all layers in all three conditions apart from the longitudinal SM layer for which n=1 in 0 ng/mL TGFβ1 and n=7 in 5 ng/mL TGFβ1 (because only one of eight and seven of eight explants formed this layer in these respective conditions). E=epithelium; IM=inner mesenchyme; CM=circular muscular layer; OM=outer mesenchyme; LM=longitudinal muscle layer. Box plot shows the inter quartile range, whiskers, and max/min outliers. Bar into the box indicates median.

4.9 TGFβ in jejunum and amniotic fluid

In the E14 embryo, herniated intestine protruded into the extraembryonic coelom of the umbilicus (Figure 4.34, left paned). At E17 *in vivo*, the intestine had returned into the abdominal cavity (Figure 4.35). Note that the intestine had a close spatial relation with the amniotic fluid.

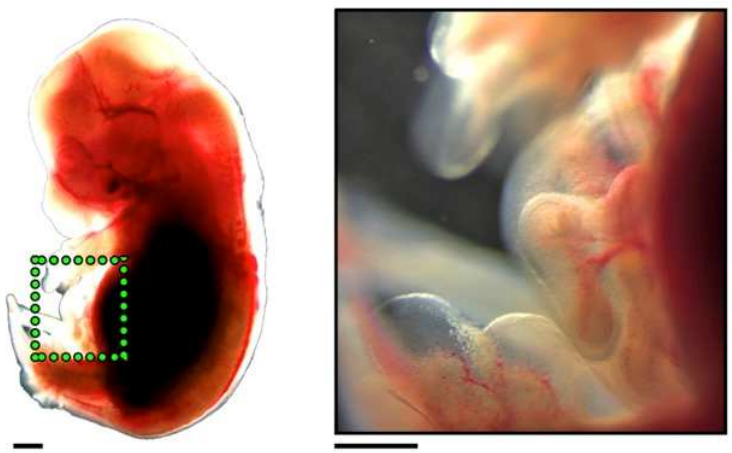

Figure 4.34 Whole mount of E14 mouse

Image on left is a whole E14 embryo and inset on right is a high power of the boxed area showing intestine protruding into the extraembryonic coelom. Scale bars=250 μm.

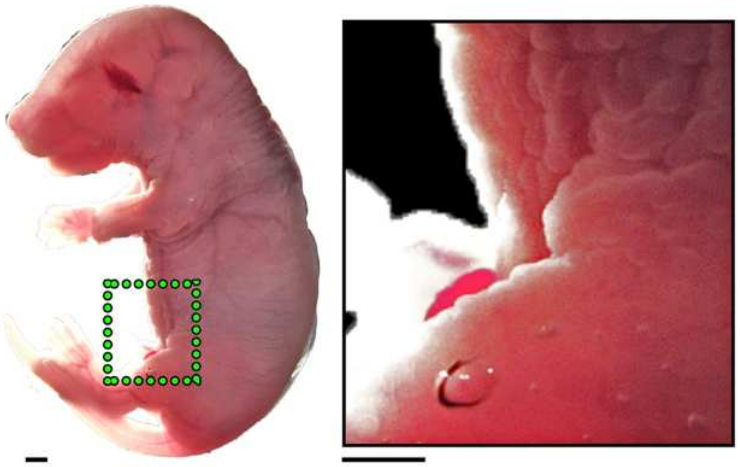

Figure 4.35 Whole mount of E17 mouse

Image on left is a whole E17 embryo and inset on right is a high power image of the boxed area showing that the intestine has returned into the body cavity Scale bars=250 μm.

Amniotic fluid contained TGFβ1 at E14 (1.39±0.31 ng/mL; mean±SD, n=3) and E17 (2.73±1.72). Next we sought TGFβ in the gut itself. As assessed by QPCR both the E14 and E17 jejunum expressed *Tgfβ1*, with levels falling between these embryonic stages (Figure 4.36). E14 explants, cultured for three days with basal media alone, contained levels of *Tgfβ1* similar to E17 organs *in vivo*.

Despite the detection of *Tgfβ1* transcripts in explants, there was no detectable TGFβ1 protein in organ culture conditioned media (lower limit of detection being 0.03 ng/mL).

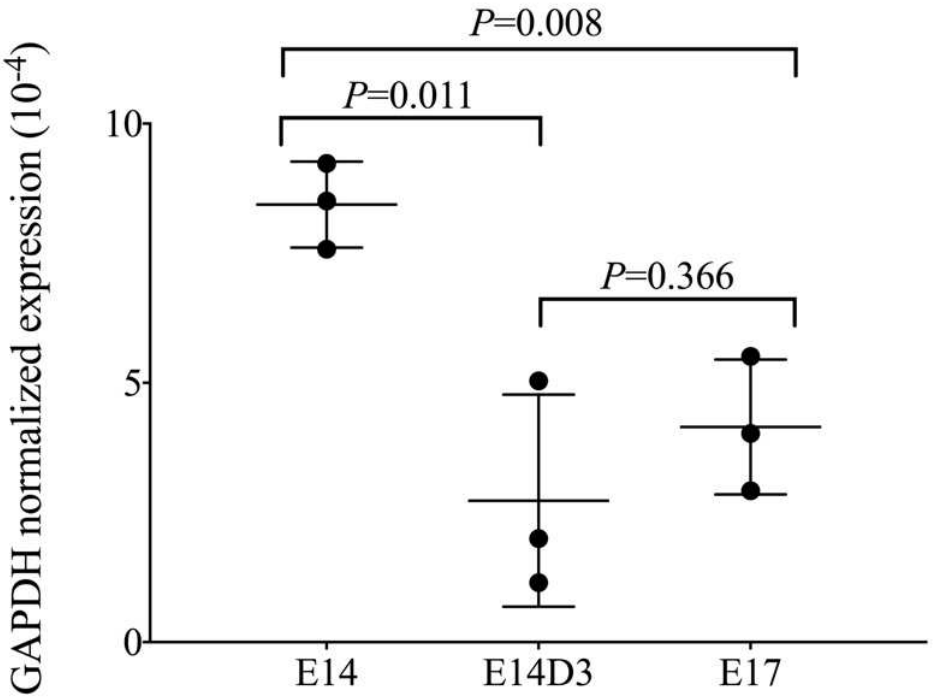

Figure 4.36 QPCR of endogenous TGFβ1

QPCR measurements for *Tgfβ1*, factored for *Gapdh*, expressed as the average of three samples of freshly dissected E14 jejunum (yellow, E14-D0), freshly dissected E17 jejunum (orange, E17), and E14 rudiments cultured for three days in basal media alone (red, E14-D3). Bars define mean±SD.

4.10 Discussion

The current study reveals marked effects of exogenous TGFβ1 on the muscularization of embryonic small intestine.

RNA microarrays of cultured organs showed that TGFβ1 increased SM specific transcripts in a concentration-dependent manner. Moreover, detailed examination of histology sections within explants revealed that exogenous TGFβ1 increased the proportions of the tissue occupied by SM.

I found that in the embryonic mouse small intestine, as reported in rats (Kedinger *et al.*, 1990), circular SM is present before longitudinal SM has formed. Strikingly, in the current *ex vivo* model, exogenous TGFβ1 was essential for differentiation of longitudinal SM. Moreover, the detection of TGFβRI and II in differentiating muscle cells is consistent with a direct effect of TGFβ1 in this process.

In fact, diverse growth factors have been implicated in controlling gut differentiation, as assessed by experiments in diverse vertebrate species (Rubin, 2007), and our results should be considered in relation to this body of knowledge. Embryonic gut endodermal cells secrete SHH that stimulates visceral mesoderm to form SM (Apelqvist *et al.*, 1997). BMP, a SHH target (Roberts *et al.*, 1995), and PDGF are expressed in the gut wall where SM is forming and have themselves been functionally implicated in SM differentiation (Kurahashi *et al.*, 2008; Torihashi *et al.*, 2009). As well as being a signalling centre for SHH, embryonic intestinal epithelia secrete FGF9 that drives gut growth, enhancing mesenchymal proliferation (Geske *et al.*, 2008). Here, FGF9 also prevents premature differentiation of intestinal SM cells in association with down regulated TGFβ signalling (Geske *et al.*, 2008).

In most of the above studies, gut SM was considered as a single entity. An exception is the report by Kurahashi *et al.* (2008) (Kurahashi *et al.*, 2008) that concluded that PDGF-A is expressed by circular SM, and that PDGF-β is expressed by interstitial cells of Cajal, and that these factors acted on longitudinal SM precursor cells expressing PDGFRα and β. In our RNA array, we found a significant up-regulation of *Pdgfa* (1.33 fold change in 5 ng/mL and 1.22 in 50 ng/mL TGFβ1) and *Pdgfc* (1.38 fold change in 5 ng/mL and 1.66 in 50 ng/mL TGFβ1).

There was no significant change in *Fgf9* transcripts after exposure to 5 ng/mL TGFβ1 but in rudiments exposed to 50 ng/mL TGFβ1, *Fgf9* levels were significantly lower (0.82) than controls. Thus, as well as having a direct effect of longitudinal SM differentiation may indirectly enhance embryonic intestinal muscle differentiation via alterations of these growth factors. No significant changes were noted in *Pdgfb, Pdgfd* or the receptors *Pdgfrα* and *Pdgfrβ,* nor in the HH pathway transcripts *Shh*, *Ptch1*, *Ptch2, Bmp2,* and *Bmp4*.

Whereas longitudinal muscle differentiated in the small intestine *in vivo* between E14 and E17, it failed to do so in explants fed with basal media alone. Strikingly, however, longitudinal SM differentiation was rescued by the addition of exogenous TGFβ1. As assessed by QPCR, *Tgfβ1* transcript was detected in the embryonic jejunum, with levels tending to fall between E14 and E17. Moreover, these transcripts, at levels similar to those found at E17 *in vivo*, were detected in E14 jejunal rudiments cultured for three days. On the other hand, conditioned media of explants fed basal media alone did not contain detectable levels of *Tgfβ1*.

At mouse E14, anatomically equivalent to week seven of human gestation (Sadler, 1990), I found that the elongating intestine protrudes into the extraembryonic celom

of the umbilicus where it is in close proximity to the amniotic cavity. By mouse E17, anatomically equivalent to week nine of human gestation (Sadler, 1990), the small intestine has become tightly coiled and has returned to the body cavity. Amniotic fluid has previously been shown to contain TGFβ, at least some of which is derived from the mother (Letterio *et al.,* 1994; McLennan and Koishi, 2004).

In the current study, I showed that amniotic fluid contained TGFβ1 in concentrations between about 1-2 ng/mL, at a time when the intestine is physiologically herniated. Thus, by analogy with the organ culture results, we suggest that fluid bathing the intestine may enhance its differentiation *in vivo*. This concept, that exogenous TGFβ supplements endogenous gut TGFβ, is similar to one proposed by Penttila *et al.* (Penttila *et al.,* 1998) who found that maternal milk was rich in this growth factor.

A recent mouse study by Zhang *et al* (Zhang et al., 2016a) used QPCR to measure levels of a variety of growth factor receptors in small intestine between E13 and postnatal day 60. They found that transcripts encoding TGFβRI were highest at E13, and fell later in gestation, then rose to a smaller peak at two weeks after birth. Transcripts encoding TGFβRII rose between E13 and two weeks after birth, and then decreased. The study reported that milk contained an average of 900 ng/ml of TGFβ1 at birth, with levels of TGFβ2 approximately an order of magnitude less Zhang *et al* (Zhang et al., 2016a). In the first few postnatal weeks, the authors contended that TGFβ proteins in milk might affect epithelial terminal differentiation, and play an anti-inflammatory effect, in the small intestine.

While TGFβ1 appeared to facilitate jejunal development, especially in relation to muscularization, my results point to the additional conclusion that the higher TGFβ1

concentration seems to have additional deleterious effects. Scrutiny of the array data revealed that some transcripts were up regulated between 50 and 5 ng/mL TGFβ1 that were unchanged between 5 and 0 ng/mL TGFβ1. They included metalloproteases Adamts16, Adamts20, a skeletal collagen Col24a1, integrin Itga9 and laminin Lama1. Furthermore, the array indicated that SMAD independent/non-canonical TGFβ1 signalling became activated at the higher concentration of TGFβ1.

TGFβ1 secreted by smooth muscle cells seems also to be involved in the modulation of cell phenotype also during postnatal process like chronic inflammation. *In vitro* study of human smooth muscle cell indicated that in the later phases of inflammation, a relative upswing of pro-fibrotic factors such as the TGFβ might modulate the expression collagen production. In this way, the repetitive events of chronic relapsing inflammation might drive stricture formation or increase in muscle width (Graham *et al.*, 1990). Furthermore, smooth muscle cells both secrete and respond to extracellular matrix factors and decreased expression of collagen I and III, with increased collagen VIII and ICAM-1 reflects the modulated smooth muscle cell phenotype (Alexander and Owens, 2012).

My current study cannot answer the question of whether Tgfβ1 transcripts expressed in the embryonic intestine play a biological role in gut development. TGFβ1 null mutant die either at E10–11 with defects in yolk sac vasculature (Dickson *et al.*, 1995), or in the first few postnatal weeks where they suffer a wasting disorder accompanied by multi-organ inflammation and ‘mild colonic and gastric necrosis’ (Kulkarni *et al.*, 1993). A similar embryonic phenotype was observed in homozygous *Tgfβr2* mutant mice (Oshima *et al.*, 1996) and *Tgfβr2*/wild type

chimeric mice progressed through the foetal period but suffered postnatal wasting accompanied and their ‘organs were smaller’ than normal.

5 CHAPTER 5 – General discussion

5.1 Summary of findings

The work presented in this thesis has applied physical and chemical manipulation to an *ex vivo* embryonic intestinal culture system.

The results presented in Chapter 3 establish that the mouse embryonic jejunum differentiates from a simple tube to a complex structure with villi, crypts and muscles between E14 to E17. Moreover, explanted jejunum broadly follows normal differentiation in an *ex vivo* organ culture using defined media for three days.

Demonstrating the possibility of culturing jejunal specimens in defined medium over a thread inserted into the lumen, with no damage or alteration of normal development, is one of the innovations of this study. Interestingly, after three days in organ culture, I observed that consecutive jejunal segments are able to restore physical and functional continuity when bridged by a thread. This is important because it demonstrates that in an *ex vivo* organ culture the jejunum is able to restore a functional contiguity following injury.

Chapter 4 details aspects of intestinal differentiation with particular focus of longitudinal muscle layers using a comparison between developmental events *in vivo* and *ex vivo*. Furthermore, chemical manipulation of defined media was applied to enhance differentiation *ex vivo*. Strikingly, this study shows that in *ex vivo* jejunum, exogenous TGFβ1 promotes the differentiation of smooth muscle layer, as revealed by the absence of the longitudinal muscle layer in specimens cultured in defined media without growth factor. Additionally, I noticed that in *ex vivo* tissue, a high concentration of TGFβ1 was deleterious to normal differentiation as demonstrated

by alterations in villi structure and an increase in circular smooth muscle layer thickness. Transcriptome analysis revealed complex sets of changes in gene expression in response to exogenous TGFβ1, with both concentration dependent and concentration specific effects. Finally, I was able to confirm that the embryonic jejunum is bathed in amniotic fluid between E14 to E17, which contains increasing concentrations of TGFβ1 as assessed by ELISA.

In conclusion, this study reveals that embryonic jejunum explants can be maintained in organ culture. Using this *ex vivo* model, I demonstrate that intestinal explants have the ability to restore functional continuity after an injury and I show the important function of exogenous TGFβ1 in the development of small intestinal muscularization *ex vivo*. In this contest, TGFβ1 protein that is present in the amniotic fluid may be crucial for the normal development of the gut when it is physiologically herniated.

5.2 Culturing embryonic jejunum *ex vivo*

The intestine represents a complex tissue, which is important for human growth due to its capacity in digesting and absorbing nutrients. Several congenital or acquired diseases can limit the intestinal length resulting in an inadequate absorptive surface. Furthermore, similar consequences are found in diseases that alter bolus transit time, a condition known as motility disorder. Studying intestinal development is important as it could offer the opportunity to restore tissue and organ physiology.

Although organ culture models have been extensively used for solid organs, the opportunity to explore intestinal development using a three dimensional culture system have not yet been extensively explored. Furthermore, there is also a parallel between mouse (E14) and human intestinal development (nine weeks gestational age) in morphological events such as the physiological herniation of bowel before its

return to the intestine into the abdominal cavity. Finally, my decision to use jejunum at E14 was also due to the striking elongation and differentiation events that occur from that particular age.

In order to define whether the *ex vivo* model can sustain intestinal development, I adopted several strategies including tissue sectioning, whole tissue staining and real time recording to compare *in vivo* versus *ex vivo* jejunal specimens. The results shown in Chapter 3 confirm reports (Wilm *et al.*, 2005; Shyer *et al.*, 2013) that between E14 and E17 the mouse jejunum differentiate from a tube with a virtual lumen to a complex structure with finger-like structures facing a lumen and crypts. Furthermore, daily measurement of cultured specimens demonstrated a constant growth both in length and in the area during the cultured time. More strikingly the peristaltic movement recorded by real time movies supported the evidence of explants viability.

The success of this organ culture model has allowed me to study the embryonic gut in a new way. In contrast with previous studies of intestine using an *ex vivo* approach (Hearn *et al.*, 1999; Reeder *et al.*, 2014; Walton and Kolterud, 2014) the application of a three dimensional organ culture strategy, the physical manipulation of the specimens (Chapter 3) and finally chemical manipulation (Chapter 4) allowed me to identify novel characteristics of the embryonic intestine.

5.3 Embryonic intestinal healing

Intestinal diseases can drastically shorten intestinal length, creating in the most dramatic scenario a condition called short bowel syndrome (Thompson, 2014). Its management is challenging and, despite advances in medical and surgical therapies, a significant morbidity and mortality in the first years after diagnosis is still reported

(Coletta *et al.*, 2014). Accordingly, novel treatments are still required to treat intestinal diseases. This thesis hypothesised that the bowel could be encouraged to grow such that it would bridge the gap between two short segments. Translating this idea into clinical practice, if this conditioned new bowel was morphologically intact and functional, it could obviate the need for other therapies.

As demonstrated by a study on neonatal lambs (Hadidi, 2007), it seems to be possible to physically manipulate the growth of gastrointestinal tissue. Subsequently, the same group used a similar procedure in babies with long gap oesophageal atresia where this part of the foregut is congenitally absent in its mid part (Hadidi *et al.*, 2007). Interestingly, trans-anastomotic tube to preserve gut length has been used in clinical practice for the treatment of intestinal atresia or necrotizing enterocolitis (Yardley *et al.*, 2008; Romao *et al.*, 2011), but no gap is left between the consecutive sections of bowel. Moreover, an intestinal anastomosis without using stitches between the two cut ends is currently technically unattainable.

In Chapter 3, I hypothesised that the embryonic bowel has the capacity for restoring continuity after injury. The first challenge I found was to create a model in which two consecutive jejunal rudiments were located onto an insert divided by a fixed gap. A second challenge was to explore the possibility of inserting a material through the embryonic lumen without creating damage to the tissue.

In order to combat these difficulties, I introduced a very fine hydrophilic thread into the virtual lumen of E14 of two consecutive specimens of jejunum. Moreover, this thread traversed the lengths of adjacent rudiment pairs, keeping them optimally aligned. Finally, I cultured the specimens in the designed organ culture model, feeding some of them by R-spondin1, an intestinal growth factor (Kim *et al.*, 2005)

reported to be important in intestinal regeneration, aiming to accelerate intestinal growth and consequently facilitate intestinal fusion.

Surprisingly, the vast majority of the explants exhibited not only a physical but more importantly a functional healing as demonstrated by confocal images, healing patency tested by bilateral injection of dyes and real time videos. Interestingly, the addition of R-spondin1 was able to generate an epithelial outgrowth from the cut ends of the explanted jejuna but fusion was not enhanced.

In contrast with previous studies, in which synthetic materials were stitched on the cut ends of tissue (Ike *et al.*, 1989; Hadidi, 2007), no anastomosis between the thread and the jejuna specimens was used during my experiments. Using this approach, the specimens seem to grow over the tube with no spatial limitation as demonstrated by the looping shape adopted over three days in culture. Continually, I demonstrate that the fusion is possible only when the orientation of the two specimens is preserved, a condition that appear to be possible by the use of the thread as bridge.

Open questions remain on the identification of the optimal gap between the two consecutive specimens, or whether it is possible to locate the specimens in a less permissive environment such as the abdominal cavity. Further investigations are needed to assess the possibility to culture post-natal jejuna and to assess the effects of other growth factors (Krishnan *et al.*, 2011) on the efficacy of gut fusion.

5.4 TGFβ1 enhances smooth muscle differentiation

TGFβ1 is known to play a key role in smooth muscle cells development, in particular in vasculature as demonstrated by an *in vivo* study in which 50% of TGFβ1-null mice die in utero at days 10.5-11.5 with defects in the yolk sac vasculature, including decreased vessel wall integrity and reduced contact between

endothelial and mesenchymal cells (Dickson *et al.*, 1995). Furthermore, a similar phenotype was reported in mice lacking the TGFβRII (Oshima *et al.*, 1996). Recently, a study on embryonic stem cells (ESCs)-derived embryoid bodies transfected by an adenovirus provided evidence that inhibition of TGFβ1 decreased expression of SMC-specific markers as a specific effect of loss of TGFβ1 signalling (Sinha *et al.*, 2004).

There is also compelling evidence that TGFβ1 co-ordinately up regulates a variety of smooth muscle cell differentiation marker genes including smooth muscle-actin, smooth muscle myosin heavy chain, and h1-calponin in cultured smooth muscle cells derived from mature blood vessels (Bjorkerud, 1991; Hautmann *et al.*, 1997).

Because smooth muscle cell differentiation is characterized by the up-regulation of these and other smooth muscle-specific genes, it has been postulated that TGFβ1 may promote smooth muscle cell development from pluri-potential precursors. This hypothesis was initially investigated *in vitro*, with primary cultures of neural crest cells (Shah *et al.*, 1996) and more recently with neural crest-derived Monc-1 cells (Chen and Lechleider, 2004). These studies provided evidence that addition of TGFβ1 induced these cells to express several smooth muscle cell markers, including SMA and calponin. However, although the cells were able to respond to exogenous growth factor by expressing smooth muscle cell differentiation marker genes, no loss of function studies were done to determine whether endogenous TGFβ1 signalling was a component of the normal developmental pathway of smooth muscle cells derived from the neural crest.

The organ culture model used in Chapter 4 revealed that specimens cultured in defined media are not able to complete differentiation of the longitudinal muscle

layer. Remarkably, TGFβ1 appears to rescue the longitudinal layers differentiation, and also to increase the number of villi.

TGFβ1 null newborn is indistinguishable from littermates that are homozygous or heterozygous for the normal allele (Millan *et al.*, 1991), and show histological abnormalities only after birth (Geiser *et al.*, 1993; Kulkarni *et al.*, 1993). An explanation could be that TGFβl is supplied to the foetus from maternal sources, as demonstrated in a study using a labelled mixture of active and latent TGFβl injected into the hearts of pregnant female TGFβ1 heterozygotes mice. Time-dependent trans-placental transit by TGFβ1 was observed after injection of pregnant mice in tissue like foetal lung, muscle and liver (Letterio *et al.*, 1994).

The result from Latterio *et al.* prompted me to use ELISA analysis of amniotic fluid from E14 mouse, which is the time when the intestine is physiologically herniated. This test demonstrates that amniotic fluid contained TGFβ1 in concentrations between about 1-2 ng/mL. Thus, by analogy with the organ culture results, we suggest that fluid bathing the intestine may enhance its differentiation *in vivo*.

QPCR shows that *Tgfβ1* transcripts were detected in the embryonic jejunum (Chapter 4), with levels tending to fall between E14 and E17. Moreover, these transcripts were detected in the cultured jejunal rudiments at level similar to E17 cultured for three days, but interestingly conditioned media of explants did not contain detectable levels of TGFβ1. Figure 5.1 shows a proposed timeline of muscular differentiation according to the results presented in Chapter 4.

The results from Chapter 4 suggest that embryonic bowel may require exogenous growth factor from the amniotic fluid to fully develop the longitudinal muscle layers,

and future studies of embryonic intestine *ex vivo* should include TGFβ1 in the defined media to produce a more faithful model of *in vivo* muscle differentiation.

In terms of morphology, the higher concentration of TGFβ1 caused an overall retardation in growth. This effect recalls those reported in embryonic organ cultures of mouse kidneys (Rogers *et al.*, 1993; Clark *et al.*, 2001) and salivary glands (Hardman *et al.*, 1994) exposed to exogenous TGFβ. Thus, there may be a parallel with a variety of human diseases in which excessive TGFβ signalling has been associated with aberrant development and differentiation.

As examples, TGFβ deregulation has been implicated in metaplastic SM formation within malformed kidneys (Yang *et al.*, 2000), aberrant ECM modelling within aortic aneurysms in Marfan syndrome (Nataatmadja *et al.*, 2006), and the formation of fibrotic strictures in Crohn's disease (Li *et al.*, 2015a). Chapter 4 also demonstrate that specimens cultured in high concentration of TGFβ1 exhibited increase in muscular width and alteration of villi structure.

Looking at the data generated from my research, I can speculate that in the malformation called gastroschisis, where herniated gut fails to return to the abdominal cavity, the intestine would suffer overexposure to growth factors in the amniotic fluid including TGFβ1. Furthermore, a recent communication in the British Association of Paediatric Surgery (BAPS) annual congress report an elegant study in which specimens from gastroschisis patients were compared to resected small bowel segment from other intestinal disease (Carnaghan *et al.*, 2016). Similar to the results presented in Chapter 4, the histological investigation presented i at the BAPS showed that in gastroschisis circular and longitudinal layers are significantly thickened (Carnaghan *et al.*, 2016).

For these reasons, a better understanding of the impact of TGFβ1 during intestinal development could potentially represent a target to treat intestinal dysmotility disorder in human, although better understanding of TGFβ1 in human amniotic fluid and TGFβ receptors in human intestine has yet to be confirmed.

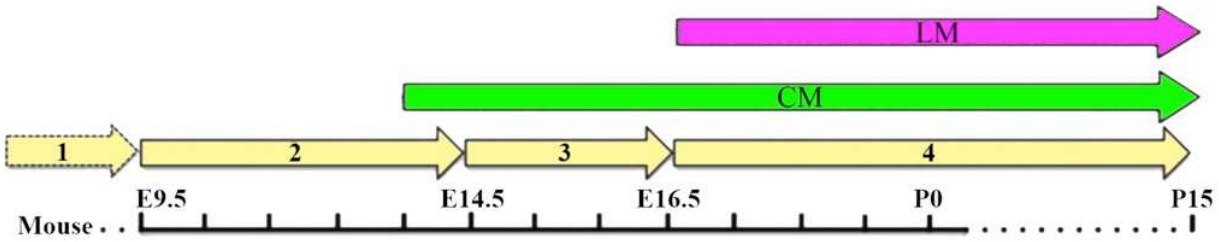

Figure 5.1 Mouse intestinal smooth muscle differentiation during small bowel development

The diagram presents a proposed timeline of intestinal circular and longitudinal smooth muscle differentiation in mice during small bowel development. According on the experiments performed in Chapter 4, the circular muscle layers appeared to be differentiated around E14, day of explant. After three days in culture and fed by TGFβ1, the longitudinal muscle layers start to differentiate as demonstrated by α-SMA^{+} immunofluorescence. CM=circular muscle layer. LM=longitudinal muscle layer. Figure modified from Figure 1.1 and adapted from (Guiu and Jensen, 2015).

5.5 Limitations of the study

The *ex vivo* organ culture model used in this research presents some limitations. In particular, I noticed that transverse section of the specimens revealed a prominent 'floor zone' adjacent to the platform, a morphological change that may be associated with the air-fluid environment in which the specimens are cultured for three days. The floor zone contained villi accounting for the ridge-like pattern evident in the whole mount analysis. Inner mesenchyme, circular smooth muscle, and outer mesenchyme were also present in the floor. By contrast, the explant 'roof', abutting air, was a simple structure lacking villi.

The specimens were cultured only for three days because I found that after five days of culture the surrounding mesenchyme of the epithelial tube had spread to form a monolayer, confirming data reported previously (Quinlan *et al.*, 2006). This can be considered a limitation of the present study because it is still not clear which is the best media or substrate to use for preserving tissue integrity for longer periods in organ culture.

The high mortality of the TGFβ1 null embryonic mice at E10 appears to be a major limitation for investigating the role of TGFβ1 during bowel development. Moreover, the alterations of the embryonic intestinal epithelial, muscular and neuronal compartments remain to be described in the absence of TGFβ1 signalling and interestingly no TGFβ1 inhibitor experiments have been reported in intestinal embryonic tissue *ex vivo* yet.

The final limitation implicates the source of tissue used in the present study in which only the events related on a particular embryonic age (from E14 to E17) were investigated. For this reason, it is still not clear whether the results provided of this

research can be translated in postnatal tissue or whether is possible to use this model as an exemplary of intestinal disease comparable to short bowel syndrome.

5.6 Perspectives and future work

The opportunity to investigate intestinal development and its physiology using animal models has opened new challenges. The existing descriptions of intestinal morphogenesis governed by growth and transcription factors need to be elaborated upon with the re-inclusion and re-consideration of other factors, such as mechanics, in intestinal growth. Furthermore, understanding the innate regenerative possibility that small bowel hold seems to be critical to discover and design new treatment for intestinal diseases. Finally, a modern comprehension of the signalling regulating intestinal homeostasis could be used to drive regenerative events after injury.

In future the *ex vivo* model proposed in this research could be used not only to test different growth factors, such as epithelial, vascular or neuronal growth factors, but also to investigate physical manipulation of embryonic intestine. Additionally, the results presented in this thesis may open potential works not only in the creation of a more faithful model of *in vivo* intestinal differentiation, but also to test possible therapeutic models for intestinal disease.

Due to the novelty of the methodological approach presented in this thesis, several additional experimental works can provide a better understanding of the two main results described. The capacity of this model to support three-dimensionally embryonic jejunum suggests the possibility of investigating the intestinal epithelium, musculature and neurons from a different perspective.

The identification of the crypts after three days of culture as demonstrated by $Sox9^{+}$ cells (previously shown in Figure 4.20) could provide new insights into the study of

epithelial stem cell niche. This model can be also used to identify the cellular progeny of the intestinal stem cells called +4 cells by immunostaining the rudiments for antibodies such as Lrig1, Lgr5, Oft4. Furthermore, this model can be use in future to investigate secretory lineages versus absorptive lineage of the epithelial cells. Different epithelial markers as villin, mucin, synaptophysin or lysozyme can be useful to identify the different developed epithelial cell within the villi. A possible future work would it be to growth postnatal intestine onto the Millipore insert *ex vivo* to investigate the speed of growth.

To methodologically improve the model, the postnatal intestine could be opened on its length and cultured as an open tube. This *ex vivo* three-dimensional opened intestine may allow the researcher not only to investigate the percentage of growth in a controlled time but also to investigate the speed of growth. Thereafter, two consecutive specimens of postnatal bowel can be located on the membrane divided by different gaps looking to find the optimal distance in which the bowel is able to fuse and finally this model could be used to explore whether different growth factors (as beads located onto the insert or as aliquot into the conditioned media) could accelerate intestinal length and fusion.

As demonstrated in Chapter 3, this model permits physical and mechanical manipulations that can drive intestinal healing. In order to better understand these properties, propagation of calcium waves within the healing area could be studied to confirm the restoration of peristaltic waves.

This model could be used to test how intestinal cells could migrate into a decellularized scaffold *ex vivo* looking to create a functional healing in gastrointestinal diseases or to create an autologous synthetic bowel starting from the

biopsy of the patient. Using transgenic embryonic rudiments, the migration of jejunal cells across the healing area can be followed confirming the physical fusion.

Moreover, 30-50 μm sagittal sections of the healing area could be immunostained and processed by light sheet microscopy or by high contrast microstructural visualization with x-ray phase contrast computed tomography. This investigation can provide three-dimensional high-quality images of the intestinal microarchitecture of the healed tissue.

Interestingly, Chapter 4 indicated that exogenous TGFβ1 seems to be fundamental for the optimal growth of the intestine in terms of muscular development. It is still not clear what effect exogenous TGFβ1 has in postnatal intestine, when both epithelium and muscular layers are developing. By contrast, the TGFβ1-TGFβRI and II system plays a pivotal role in mediating pro-inflammatory intestinal disease, where it may act to regulate cell growth and proliferation.

Future studies of embryonic intestinal cultures should include TGFβ1 in the defined media to produce a more faithful model of *in vivo* muscle differentiation. Finally, it is notable that human pluripotent stem cells can be induced to form intestinal organoids in culture (Wells and Spence, 2014). While most attention has been given to epithelial morphogenesis in this model, the organoids can also contain mesenchyme that forms SM and fibroblasts. In future, it will be informative to determine whether TGFβ affects the differentiation of these mesenchyme-derived cells.

In order to better understand the TGFβ role in intestinal development and in post-natal intestinal tissue, TGFβ inhibitor experiments would be needed to identify

whether exogenous TGFβ could restore normal intestinal morphology during development, and to investigate the potential clinical implications of this growth factor in intestinal diseases.

With particular interest in paediatric disease, future studies could be designed to investigate whether the over exposure of prenatal intestine to amniotic fluid, which has been demonstrated to be a source of TGFβ1, could be physiological relevant in the sequelae of gastroschisis, a congenital disease characterised by a defect in the anterior abdominal wall through which the abdominal contents freely protrude. These future studies could improve our understanding of the intestinal hypo-peristaltic disorders presented in gastroschisis, and eventually design possible treatments.

Taking into account all these potential works, the creation of *in vivo* model to study human therapies for intestinal diseases, such as SBS, seems to be plausible. In this contest, it is possible to hypothesise a model in which isolate two consecutive segments of small bowel bridged by a scaffold embedded by growth factors and secured to the peritoneal surface. This isolated system could allow the intestine segments to growth into the scaffold while the surface attached to the peritoneum can create a vascularized support as demonstrate by reconstructive gastrointestinal procedure as the Kimura (Kimura and Soper, 1993). At the time of harvesting, the new elongated and vascularized segment could be used for a lengthening procedure in which it will be possible to divide into three vascularized segments that anatomize together to generate a segment length three times more than the original (Figure 5.2). This significant increase in length can reduce the need of TPN and dramatically reduce the patient referred to intestinal transplant.

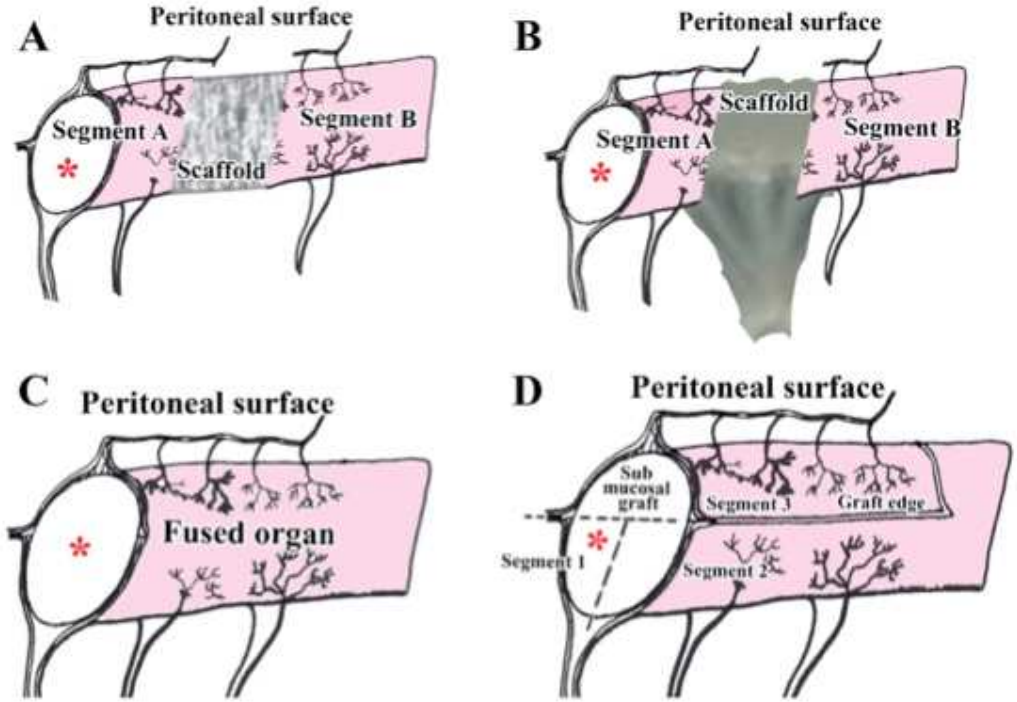

Figure 5.2 Triple lengthening procedure after intestinal regeneration over scaffold

(A) Two consecutive segment of bowel (Segment A-B) bridged by synthetic scaffold and secured to the peritoneal surface. (B) The similar methods can be adapted to decellularized scaffold. (C) The scaffold will help the tissue to growth over or into it generating a fused organ. (D) The neo tissue can be divided in three segments to perform a triple longitudinal intestinal lengthening and tailoring. Asterisk=intestinal lumen.

5.7 Conclusion

The aim of this thesis was to use an *ex vivo* model to study the healing potential of the embryonic intestine after an injury and to investigate the effect of TGFβ1 on its development. Although these studies were performed in embryonic intestine and the results are difficult to translate in post-natal environment, what it is truly exciting about this experimental model is the potential versatility for studying intestinal biology and potential new chemical and physical therapies.

Overall the data generated in this thesis forms an insight for further study of intestinal development and intestinal regeneration. Moreover, these *ex vivo* approaches could be easily reproduced and applied to inform the design of novel therapies for human disease.

References

Abu-Elmagd, K. (2015) The concept of gut rehabilitation and the future of visceral transplantation. *Nat Rev Gastroenterol Hepatol,* 12(2)**,** 108-20.

Abud, H. E., Watson, N. & Heath, J. K. (2005) Growth of intestinal epithelium in organ culture is dependent on EGF signalling. *Exp Cell Res,* 303(2)**,** 252-62.

Akhurst, R. J. & Hata, A. (2012) Targeting the TGFbeta signalling pathway in disease. *Nat Rev Drug Discov,* 11(10)**,** 790-811.

Alexander, M. R. & Owens, G. K. (2012) Epigenetic control of smooth muscle cell differentiation and phenotypic switching in vascular development and disease. *Annu Rev Physiol,* 74**,** 13-40.

Anders, C., Ashton, N., Ranjzad, P., Dilworth, M. R. & Woolf, A. S. (2013) Ex vivo modeling of chemical synergy in prenatal kidney cystogenesis. *PLoS One,* 8(3)**,** e57797.

Andrianifahanana, M., Moniaux, N. & Batra, S. K. (2006) Regulation of mucin expression: mechanistic aspects and implications for cancer and inflammatory diseases. *Biochim Biophys Acta,* 1765(2)**,** 189-222.

Apelqvist, A., Ahlgren, U. & Edlund, H. (1997) Sonic hedgehog directs specialised mesoderm differentiation in the intestine and pancreas. *Curr Biol,* 7(10)**,** 801-4.

Assimakopoulos, S. F., Papageorgiou, I. & Charonis, A. (2011) Enterocytes' tight junctions: From molecules to diseases. *World J Gastrointest Pathophysiol,* 2(6)**,** 123-37.

Atala, A. (2014) Regenerative bladder augmentation using autologous tissue-when will we get there? *J Urol,* 191(5)**,** 1204-5.

Attie-Bitach, T., Abitbol, M., Gerard, M., Delezoide, A. L., Auge, J., Pelet, A., Amiel, J., Pachnis, V., Munnich, A., Lyonnet, S. & Vekemans, M. (1998) Expression of the RET proto-oncogene in human embryos. *Am J Med Genet,* 80(5)**,** 481-6.

Attisano, L. & Wrana, J. L. (2002) Signal transduction by the TGF-beta superfamily. *Science,* 296(5573)**,** 1646-7.

Azhar, M., Schultz Jel, J., Grupp, I., Dorn, G. W., 2nd, Meneton, P., Molin, D. G., Gittenberger-de Groot, A. C. & Doetschman, T. (2003) Transforming growth factor beta in cardiovascular development and function. *Cytokine Growth Factor Rev,* 14(5)**,** 391-407.

Bakker, H., Bozzetti, F., Staun, M., Leon-Sanz, M., Hebuterne, X., Pertkiewicz, M., Shaffer, J. & Thul, P. (1999) Home parenteral nutrition in adults: a european multicentre survey in 1997. ESPEN-Home Artificial Nutrition Working Group. *Clin Nutr,* 18(3)**,** 135-40.

Baldi, P. & Long, A. D. (2001) A Bayesian framework for the analysis of microarray expression data: regularized t -test and statistical inferences of gene changes. *Bioinformatics,* 17(6)**,** 509-19.

Baoquan, Q., Diez-Pardo, J. A. & Tovar, J. A. (1995) Intestinal rotation in experimental congenital diaphragmatic hernia. *J Pediatr Surg,* 30(10)**,** 1457-62.

Barker, N. (2014) Adult intestinal stem cells: critical drivers of epithelial homeostasis and regeneration. *Nat Rev Mol Cell Biol,* 15(1)**,** 19-33.

Barker, N., van Es, J. H., Kuipers, J., Kujala, P., van den Born, M., Cozijnsen, M., Haegebarth, A., Korving, J., Begthel, H., Peters, P. J. & Clevers, H. (2007)

Identification of stem cells in small intestine and colon by marker gene Lgr5. *Nature,* 449(7165)**,** 1003-7.
Barnard, J. A., Beauchamp, R. D., Coffey, R. J. & Moses, H. L. (1989) Regulation of intestinal epithelial cell growth by transforming growth factor type beta. *Proc Natl Acad Sci U S A,* 86(5)**,** 1578-82.
Barnard, J. A., Warwick, G. J. & Gold, L. I. (1993) Localization of transforming growth factor beta isoforms in the normal murine small intestine and colon. *Gastroenterology,* 105(1)**,** 67-73.
Batts, L. E., Polk, D. B., Dubois, R. N. & Kulessa, H. (2006) Bmp signaling is required for intestinal growth and morphogenesis. *Dev Dyn,* 235(6)**,** 1563-70.
Beale, E. F., Nelson, R. M., Bucciarelli, R. L., Donnelly, W. H. & Eitzman, D. V. (1979) Intrahepatic cholestasis associated with parenteral nutrition in premature infants. *Pediatrics,* 64(3)**,** 342-7.
Benahmed, F., Gross, I., Gaunt, S. J., Beck, F., Jehan, F., Domon-Dell, C., Martin, E., Kedinger, M., Freund, J. N. & Duluc, I. (2008) Multiple regulatory regions control the complex expression pattern of the mouse Cdx2 homeobox gene. *Gastroenterology,* 135(4)**,** 1238-1247, 1247 e1-3.
Bertrand, K. (2011) Survival of exfoliated epithelial cells: a delicate balance between anoikis and apoptosis. *J Biomed Biotechnol,* 2011**,** 534139.
Bevins, C. L. & Salzman, N. H. (2011) Paneth cells, antimicrobial peptides and maintenance of intestinal homeostasis. *Nat Rev Microbiol,* 9(5)**,** 356-68.
Bianchi, A. (1980) Intestinal loop lengthening--a technique for increasing small intestinal length. *J Pediatr Surg,* 15(2)**,** 145-51.
Bianchi, A. (1984) Intestinal lengthening: an experimental and clinical review. *J R Soc Med,* 77 Suppl 3**,** 35-41.
Bianchi, A. (1985) Lengthening a baby's gut. *Lancet,* 1(8432)**,** 819.
Bianchi, A. (2006) From the cradle to enteral autonomy: the role of autologous gastrointestinal reconstruction. *Gastroenterology,* 130(2 Suppl 1)**,** S138-46.
Bitar, K. N. (2003) Function of gastrointestinal smooth muscle: from signaling to contractile proteins. *Am J Med,* 115 Suppl 3A**,** 15S-23S.
Bjerknes, M. & Cheng, H. (1981) The stem-cell zone of the small intestinal epithelium. V. Evidence for controls over orientation of boundaries between the stem-cell zone, proliferative zone, and the maturation zone. *Am J Anat,* 160(1)**,** 105-12.
Bjerknes, M. & Cheng, H. (1999) Clonal analysis of mouse intestinal epithelial progenitors. *Gastroenterology,* 116(1)**,** 7-14.
Bjerknes, M. & Cheng, H. (2002) Multipotential stem cells in adult mouse gastric epithelium. *Am J Physiol Gastrointest Liver Physiol,* 283(3)**,** G767-77.
Bjorkerud, S. (1991) Effects of transforming growth factor-beta 1 on human arterial smooth muscle cells in vitro. *Arterioscler Thromb,* 11(4)**,** 892-902.
Blobe, G. C., Schiemann, W. P. & Lodish, H. F. (2000) Role of transforming growth factor beta in human disease. *N Engl J Med,* 342(18)**,** 1350-8.
Brasseur, J. G., Nicosia, M. A., Pal, A. & Miller, L. S. (2007) Function of longitudinal vs circular muscle fibers in esophageal peristalsis, deduced with mathematical modeling. *World J Gastroenterol,* 13(9)**,** 1335-46.
Bullock, S. L., Johnson, T. M., Bao, Q., Hughes, R. C., Winyard, P. J. & Woolf, A. S. (2001) Galectin-3 modulates ureteric bud branching in organ culture of the developing mouse kidney. *J Am Soc Nephrol,* 12(3)**,** 515-23.

Burgu, B., McCarthy, L. S., Shah, V., Long, D. A., Wilcox, D. T. & Woolf, A. S. (2006) Vascular endothelial growth factor stimulates embryonic urinary bladder development in organ culture. *BJU Int,* 98(1)**,** 217-25.

Bush, K. T., Sakurai, H., Steer, D. L., Leonard, M. O., Sampogna, R. V., Meyer, T. N., Schwesinger, C., Qiao, J. & Nigam, S. K. (2004) TGF-beta superfamily members modulate growth, branching, shaping, and patterning of the ureteric bud. *Dev Biol,* 266(2)**,** 285-98.

Calvert, R. & Pothier, P. (1990) Migration of fetal intestinal intervillous cells in neonatal mice. *Anat Rec,* 227(2)**,** 199-206.

Caprioli, A., Villasenor, A., Wylie, L. A., Braitsch, C., Marty-Santos, L., Barry, D., Karner, C. M., Fu, S., Meadows, S. M., Carroll, T. J. & Cleaver, O. (2015) Wnt4 is essential to normal mammalian lung development. *Dev Biol,* 406(2)**,** 222-34.

Carmon, K. S., Gong, X., Lin, Q., Thomas, A. & Liu, Q. (2011) R-spondins function as ligands of the orphan receptors LGR4 and LGR5 to regulate Wnt/beta-catenin signaling. *Proc Natl Acad Sci U S A,* 108(28)**,** 11452-7.

Carnaghan, H., Virasami, A., Pierro, A., De Coppi, P., AJ., B., Serbire, N. & Eaton, S. (2016) Smooth muscle actin expression is decreased in small bowel longitudinal muscle in human gastroschisis: possible implications for motility. *British Association of Paediatric Surgery (BAPS).* Amsterdam.

Cervantes, S., Yamaguchi, T. P. & Hebrok, M. (2009) Wnt5a is essential for intestinal elongation in mice. *Dev Biol,* 326(2)**,** 285-94.

Chan, S. K., Riley, P. R., Price, K. L., McElduff, F., Winyard, P. J., Welham, S. J., Woolf, A. S. & Long, D. A. (2010) Corticosteroid-induced kidney dysmorphogenesis is associated with deregulated expression of known cystogenic molecules, as well as Indian hedgehog. *Am J Physiol Renal Physiol,* 298(2)**,** F346-56.

Charles, L. & Leaver, J. (2015) Tissue expansion in burn reconstruction: what can the child and family expect? *Nurs Child Young People,* 27(4)**,** 22-8.

Chen, S. & Lechleider, R. J. (2004) Transforming growth factor-beta-induced differentiation of smooth muscle from a neural crest stem cell line. *Circ Res,* 94(9)**,** 1195-202.

Cheng, H. & Leblond, C. P. (1974) Origin, differentiation and renewal of the four main epithelial cell types in the mouse small intestine. V. Unitarian Theory of the origin of the four epithelial cell types. *Am J Anat,* 141(4)**,** 537-61.

Choi, R. S., Riegler, M., Pothoulakis, C., Kim, B. S., Mooney, D., Vacanti, M. & Vacanti, J. P. (1998) Studies of brush border enzymes, basement membrane components, and electrophysiology of tissue-engineered neointestine. *J Pediatr Surg,* 33(7)**,** 991-6; discussion 996-7.

Choi, R. S. & Vacanti, J. P. (1997) Preliminary studies of tissue-engineered intestine using isolated epithelial organoid units on tubular synthetic biodegradable scaffolds. *Transplant Proc,* 29(1-2)**,** 848-51.

Choudhary, R. K. & Capuco, A. V. (2012) In vitro expansion of the mammary stem/progenitor cell population by xanthosine treatment. *BMC Cell Biol,* 13**,** 14.

Ciacci, C., Lind, S. E. & Podolsky, D. K. (1993) Transforming growth factor beta regulation of migration in wounded rat intestinal epithelial monolayers. *Gastroenterology,* 105(1)**,** 93-101.

Clark, A. T., Young, R. J. & Bertram, J. F. (2001) In vitro studies on the roles of transforming growth factor-beta 1 in rat metanephric development. *Kidney Int,* 59(5)**,** 1641-53.
Clevers, H. (2006) Wnt/beta-catenin signaling in development and disease. *Cell,* 127(3)**,** 469-80.
Clevers, H. (2013) The intestinal crypt, a prototype stem cell compartment. *Cell,* 154(2)**,** 274-84.
Clevers, H. & Batlle, E. (2013) SnapShot: the intestinal crypt. *Cell,* 152(5)**,** 1198-1198 e2.
Clevers, H. C. & Bevins, C. L. (2013) Paneth cells: maestros of the small intestinal crypts. *Annu Rev Physiol,* 75**,** 289-311.
Cohran, V. (2015) Intestinal Failure: The Long and Short of the Matter. *J Pediatr,* 167(1)**,** 6-8.
Coletta, R., Khalil, B. A. & Morabito, A. (2014) Short bowel syndrome in children: surgical and medical perspectives. *Semin Pediatr Surg,* 23(5)**,** 291-7.
Coletta, R., Roberts, N. A., Oltrabella, F., Khalil, B. A., Morabito, A. & Woolf, A. S. (2016) Bridging the gap: functional healing of embryonic small intestine ex vivo. *J Tissue Eng Regen Med,* 10(2)**,** 178-82.
Coletta, R., Roberts, N. A., Randles, M. J., Morabito, A. & Woolf, A. S. (2017) Exogenous transforming growth factor-beta1 enhances smooth muscle differentiation in embryonic mouse jejunal explants. *J Tissue Eng Regen Med*.
Collins, J., 3rd, Vicente, Y., Georgeson, K. & Kelly, D. (1996) Partial intestinal obstruction induces substantial mucosal proliferation in the pig. *J Pediatr Surg,* 31(3)**,** 415-9.
Coran, A. G., Spivak, D. & Teitelbaum, D. H. (1999) An analysis of the morbidity and mortality of short-bowel syndrome in the pediatric age group. *Eur J Pediatr Surg,* 9(4)**,** 228-30.
Creamer, B., Shorter, R. G. & Bamforth, J. (1961) The turnover and shedding of epithelial cells. I. The turnover in the gastro-intestinal tract. *Gut,* 2**,** 110-8.
Cserni, T., Biszku, B., Guthy, I., Dicso, F., Szaloki, L., Folaranmi, S., Murphy, F., Rakoczy, G., Bianchi, A. & Morabito, A. (2014) The first clinical application of the spiral intestinal lengthening and tailoring (silt) in extreme short bowel syndrome. *J Gastrointest Surg,* 18(10)**,** 1852-7.
Cserni, T., Takayasu, H., Muzsnay, Z., Varga, G., Murphy, F., Folaranmi, S. E. & Rakoczy, G. (2011) New idea of intestinal lengthening and tailoring. *Pediatr Surg Int,* 27(9)**,** 1009-13.
Cserni, T., Varga, G., Erces, D., Kaszaki, J., Boros, M., Laszlo, A., Murphy, F., Foldvari, A., Morabito, A., Bianchi, A. & Rakoczy, G. (2013) Spiral intestinal lengthening and tailoring - first in vivo study. *J Pediatr Surg,* 48(9)**,** 1907-13.
Cully, M., You, H., Levine, A. J. & Mak, T. W. (2006) Beyond PTEN mutations: the PI3K pathway as an integrator of multiple inputs during tumorigenesis. *Nat Rev Cancer,* 6(3)**,** 184-92.
Daniel, H. & Zietek, T. (2015) Taste and move: glucose and peptide transporters in the gastrointestinal tract. *Exp Physiol,* 100(12)**,** 1441-50.
De Coppi, P. (2013) Regenerative medicine for congenital malformations. *J Pediatr Surg,* 48(2)**,** 273-80.
De Coppi, P., Bellini, S., Conconi, M. T., Sabatti, M., Simonato, E., Gamba, P. G., Nussdorfer, G. G. & Parnigotto, P. P. (2006) Myoblast-acellular skeletal

muscle matrix constructs guarantee a long-term repair of experimental full-thickness abdominal wall defects. *Tissue Eng,* 12(7)**,** 1929-36.
de Graaf, I. A., Olinga, P., de Jager, M. H., Merema, M. T., de Kanter, R., van de Kerkhof, E. G. & Groothuis, G. M. (2010) Preparation and incubation of precision-cut liver and intestinal slices for application in drug metabolism and toxicity studies. *Nat Protoc,* 5(9)**,** 1540-51.
de Lau, W., Kujala, P., Schneeberger, K., Middendorp, S., Li, V. S., Barker, N., Martens, A., Hofhuis, F., DeKoter, R. P., Peters, P. J., Nieuwenhuis, E. & Clevers, H. (2012) Peyer's patch M cells derived from Lgr5(+) stem cells require SpiB and are induced by RankL in cultured "miniguts". *Mol Cell Biol,* 32(18)**,** 3639-47.
De Santa Barbara, P., Williams, J., Goldstein, A. M., Doyle, A. M., Nielsen, C., Winfield, S., Faure, S. & Roberts, D. J. (2005) Bone morphogenetic protein signaling pathway plays multiple roles during gastrointestinal tract development. *Dev Dyn,* 234(2)**,** 312-22.
Del Moral, P. M. & Warburton, D. (2010) Explant culture of mouse embryonic whole lung, isolated epithelium, or mesenchyme under chemically defined conditions as a system to evaluate the molecular mechanism of branching morphogenesis and cellular differentiation. *Methods Mol Biol,* 633**,** 71-9.
Demehri, F. R., Freeman, J. J., Fukatsu, Y., Luntz, J. & Teitelbaum, D. H. (2015) Development of an endoluminal intestinal lengthening device using a geometric intestinal attachment approach. *Surgery,* 158(3)**,** 802-11.
Demehri, F. R., Utter, B., Freeman, J. J., Fukatsu, Y., Luntz, J., Brei, D. & Teitelbaum, D. H. (2016) Development of an endoluminal intestinal attachment for a clinically applicable distraction enterogenesis device. *J Pediatr Surg,* 51(1)**,** 101-6.
Deplancke, B. & Gaskins, H. R. (2001) Microbial modulation of innate defense: goblet cells and the intestinal mucus layer. *Am J Clin Nutr,* 73(6)**,** 1131S-1141S.
Derynck, R. & Zhang, Y. E. (2003) Smad-dependent and Smad-independent pathways in TGF-beta family signalling. *Nature,* 425(6958)**,** 577-84.
Dickson, M. C., Martin, J. S., Cousins, F. M., Kulkarni, A. B., Karlsson, S. & Akhurst, R. J. (1995) Defective haematopoiesis and vasculogenesis in transforming growth factor-beta 1 knock out mice. *Development,* 121(6)**,** 1845-54.
Dignass, A., Lynch-Devaney, K., Kindon, H., Thim, L. & Podolsky, D. K. (1994) Trefoil peptides promote epithelial migration through a transforming growth factor beta-independent pathway. *J Clin Invest,* 94(1)**,** 376-83.
DiRenzo, D. M., Chaudhary, M. A., Shi, X., Franco, S. R., Zent, J., Wang, K., Guo, L. W. & Kent, K. C. (2016) A crosstalk between TGF-beta/Smad3 and Wnt/beta-catenin pathways promotes vascular smooth muscle cell proliferation. *Cell Signal,* 28(5)**,** 498-505.
Durbec, P., Marcos-Gutierrez, C. V., Kilkenny, C., Grigoriou, M., Wartiowaara, K., Suvanto, P., Smith, D., Ponder, B., Costantini, F., Saarma, M. & et al. (1996a) GDNF signalling through the Ret receptor tyrosine kinase. *Nature,* 381(6585)**,** 789-93.
Durbec, P. L., Larsson-Blomberg, L. B., Schuchardt, A., Costantini, F. & Pachnis, V. (1996b) Common origin and developmental dependence on c-ret of subsets of enteric and sympathetic neuroblasts. *Development,* 122(1)**,** 349-58.

Dyachuk, V., Furlan, A., Shahidi, M. K., Giovenco, M., Kaukua, N., Konstantinidou, C., Pachnis, V., Memic, F., Marklund, U., Muller, T., Birchmeier, C., Fried, K., Ernfors, P. & Adameyko, I. (2014) Neurodevelopment. Parasympathetic neurons originate from nerve-associated peripheral glial progenitors. *Science*, 345(6192)**,** 82-7.

Faure, S. & de Santa Barbara, P. (2011) Molecular embryology of the foregut. *J Pediatr Gastroenterol Nutr,* 52 Suppl 1**,** S2-3.

Filston, H. C. & Kirks, D. R. (1981) Malrotation - the ubiquitous anomaly. *J Pediatr Surg,* 16(4 Suppl 1)**,** 614-20.

Finkbeiner, S. R., Freeman, J. J., Wieck, M. M., El-Nachef, W., Altheim, C. H., Tsai, Y. H., Huang, S., Dyal, R., White, E. S., Grikscheit, T. C., Teitelbaum, D. H. & Spence, J. R. (2015) Generation of tissue-engineered small intestine using embryonic stem cell-derived human intestinal organoids. *Biol Open,* 4(11)**,** 1462-72.

Fisher, J. G., Sparks, E. A., Khan, F. A., Dionigi, B., Wu, H., Brazzo, J., 3rd, Fauza, D., Modi, B., Safranski, D. L. & Jaksic, T. (2015) Extraluminal distraction enterogenesis using shape-memory polymer. *J Pediatr Surg,* 50(6)**,** 938-42.

Fishman, J. M., Wiles, K., Lowdell, M. W., De Coppi, P., Elliott, M. J., Atala, A. & Birchall, M. A. (2014) Airway tissue engineering: an update. *Expert Opin Biol Ther,* 14(10)**,** 1477-91.

Formeister, E. J., Sionas, A. L., Lorance, D. K., Barkley, C. L., Lee, G. H. & Magness, S. T. (2009) Distinct SOX9 levels differentially mark stem/progenitor populations and enteroendocrine cells of the small intestine epithelium. *Am J Physiol Gastrointest Liver Physiol,* 296(5)**,** G1108-18.

Franklin, V., Khoo, P. L., Bildsoe, H., Wong, N., Lewis, S. & Tam, P. P. (2008) Regionalisation of the endoderm progenitors and morphogenesis of the gut portals of the mouse embryo. *Mech Dev,* 125(7)**,** 587-600.

Frid, M. G., Shekhonin, B. V., Koteliansky, V. E. & Glukhova, M. A. (1992) Phenotypic changes of human smooth muscle cells during development: late expression of heavy caldesmon and calponin. *Dev Biol,* 153(2)**,** 185-93.

Fu, M., Lui, V. C., Sham, M. H., Cheung, A. N. & Tam, P. K. (2003) HOXB5 expression is spatially and temporarily regulated in human embryonic gut during neural crest cell colonization and differentiation of enteric neuroblasts. *Dev Dyn,* 228(1)**,** 1-10.

Fu, M., Tam, P. K., Sham, M. H. & Lui, V. C. (2004) Embryonic development of the ganglion plexuses and the concentric layer structure of human gut: a topographical study. *Anat Embryol (Berl),* 208(1)**,** 33-41.

Fu, M., Vohra, B. P., Wind, D. & Heuckeroth, R. O. (2006) BMP signaling regulates murine enteric nervous system precursor migration, neurite fasciculation, and patterning via altered Ncam1 polysialic acid addition. *Dev Biol,* 299(1)**,** 137-50.

Gaivao, M. M., Rambags, B. P. & Stout, T. A. (2014) Gastrulation and the establishment of the three germ layers in the early horse conceptus. *Theriogenology,* 82(2)**,** 354-65.

Ganns, D., Schrodl, F., Neuhuber, W. & Brehmer, A. (2006) Investigation of general and cytoskeletal markers to estimate numbers and proportions of neurons in the human intestine. *Histol Histopathol,* 21(1)**,** 41-51.

Garcia-Garcia, M. J., Shibata, M. & Anderson, K. V. (2008) Chato, a KRAB zinc-finger protein, regulates convergent extension in the mouse embryo. *Development,* 135(18)**,** 3053-62.

Geiser, A. G., Letterio, J. J., Kulkarni, A. B., Karlsson, S., Roberts, A. B. & Sporn, M. B. (1993) Transforming growth factor beta 1 (TGF-beta 1) controls expression of major histocompatibility genes in the postnatal mouse: aberrant histocompatibility antigen expression in the pathogenesis of the TGF-beta 1 null mouse phenotype. *Proc Natl Acad Sci U S A,* 90(21)**,** 9944-8.

Georgeson, K., Halpin, D., Figueroa, R., Vincente, Y. & Hardin, W., Jr. (1994) Sequential intestinal lengthening procedures for refractory short bowel syndrome. *J Pediatr Surg,* 29(2)**,** 316-20; discussion 320-1.

Geske, M. J., Zhang, X., Patel, K. K., Ornitz, D. M. & Stappenbeck, T. S. (2008) Fgf9 signaling regulates small intestinal elongation and mesenchymal development. *Development,* 135(17)**,** 2959-68.

Ghionzoli, M., Repele, A., Sartiani, L., Costanzi, G., Parenti, A., Spinelli, V., David, A. L., Garriboli, M., Totonelli, G., Tian, J., Andreadis, S. T., Cerbai, E., Mugelli, A., Messineo, A., Pierro, A., Eaton, S. & De Coppi, P. (2013) Human amniotic fluid stem cell differentiation along smooth muscle lineage. *FASEB J,* 27(12)**,** 4853-65.

Goldstein, A. M., Brewer, K. C., Doyle, A. M., Nagy, N. & Roberts, D. J. (2005) BMP signaling is necessary for neural crest cell migration and ganglion formation in the enteric nervous system. *Mech Dev,* 122(6)**,** 821-33.

Gosalia, N., Yang, R., Kerschner, J. L. & Harris, A. (2015) FOXA2 regulates a network of genes involved in critical functions of human intestinal epithelial cells. *Physiol Genomics,* 47(7)**,** 290-7.

Goulet, O., Olieman, J., Ksiazyk, J., Spolidoro, J., Tibboe, D., Kohler, H., Yagci, R. V., Falconer, J., Grimble, G. & Beattie, R. M. (2013) Neonatal short bowel syndrome as a model of intestinal failure: physiological background for enteral feeding. *Clin Nutr,* 32(2)**,** 162-71.

Goumans, M. J. & Mummery, C. (2000) Functional analysis of the TGFbeta receptor/Smad pathway through gene ablation in mice. *Int J Dev Biol,* 44(3)**,** 253-65.

Graham, M. F., Bryson, G. R. & Diegelmann, R. F. (1990) Transforming growth factor beta 1 selectively augments collagen synthesis by human intestinal smooth muscle cells. *Gastroenterology,* 99(2)**,** 447-53.

Grainger, S., Savory, J. G. & Lohnes, D. (2010) Cdx2 regulates patterning of the intestinal epithelium. *Dev Biol,* 339(1)**,** 155-65.

Grand, R. J., Watkins, J. B. & Torti, F. M. (1976) Development of the human gastrointestinal tract. A review. *Gastroenterology,* 70(5 PT.1)**,** 790-810.

Grant, D., Abu-Elmagd, K., Reyes, J., Tzakis, A., Langnas, A., Fishbein, T., Goulet, O., Farmer, D. & Intestine Transplant, R. (2005) 2003 report of the intestine transplant registry: a new era has dawned. *Ann Surg,* 241(4)**,** 607-13.

Gregorieff, A. & Clevers, H. (2005) Wnt signaling in the intestinal epithelium: from endoderm to cancer. *Genes Dev,* 19(8)**,** 877-90.

Gregorieff, A., Grosschedl, R. & Clevers, H. (2004) Hindgut defects and transformation of the gastro-intestinal tract in Tcf4(-/-)/Tcf1(-/-) embryos. *EMBO J,* 23(8)**,** 1825-33.

Grikscheit, T. C., Siddique, A., Ochoa, E. R., Srinivasan, A., Alsberg, E., Hodin, R. A. & Vacanti, J. P. (2004) Tissue-engineered small intestine improves recovery after massive small bowel resection. *Ann Surg,* 240(5)**,** 748-54.

Gronovich, Y., Binenboym, R., Retchkiman, M., Eizenman, N., Lotan, A., Stuchiner, B. & Tuchman, I. (2015) Reconstruction in plastic surgery using osmotic tissue expanders. *Harefuah,* 154(3)**,** 155-8, 213.

Grundy, D. & Schemann, M. (2005) Enteric nervous system. *Curr Opin Gastroenterol,* 21(2)**,** 176-82.
Guiu, J. & Jensen, K. B. (2015) From Definitive Endoderm to Gut-a Process of Growth and Maturation. *Stem Cells Dev,* 24(17)**,** 1972-83.
Hadidi, A. T. (2007) Long oesophageal gaps - a new surgical technique: an experimental study on lambs. *Eur J Pediatr Surg,* 17(4)**,** 229-35.
Hadidi, A. T., Hosie, S. & Waag, K. L. (2007) Long gap esophageal atresia: lengthening technique and primary anastomosis. *J Pediatr Surg,* 42(10)**,** 1659-62.
Hadjimichael, C., Nikolaou, C., Papamatheakis, J. & Kretsovali, A. (2016) MicroRNAs for Fine-Tuning of Mouse Embryonic Stem Cell Fate Decision through Regulation of TGF-beta Signaling. *Stem Cell Reports,* 6(3)**,** 292-301.
Hamilton, N. J., Kanani, M., Roebuck, D. J., Hewitt, R. J., Cetto, R., Culme-Seymour, E. J., Toll, E., Bates, A. J., Comerford, A. P., McLaren, C. A., Butler, C. R., Crowley, C., McIntyre, D., Sebire, N. J., Janes, S. M., O'Callaghan, C., Mason, C., De Coppi, P., Lowdell, M. W., Elliott, M. J. & Birchall, M. A. (2015) Tissue-Engineered Tracheal Replacement in a Child: A 4-Year Follow-Up Study. *Am J Transplant,* 15(10)**,** 2750-7.
Haramis, A. P., Begthel, H., van den Born, M., van Es, J., Jonkheer, S., Offerhaus, G. J. & Clevers, H. (2004) De novo crypt formation and juvenile polyposis on BMP inhibition in mouse intestine. *Science,* 303(5664)**,** 1684-6.
Hardman, P., Landels, E., Woolf, A. S. & Spooner, B. S. (1994) TGF-β1 Inhibits Growth and Branching Morphogenesis In Embryonic Mouse Submandibular and Sublingual Glands in Vitro. *Development, Growth & Differentiation,* 36(6)**,** 567–577.
Hardwick, J. C., Van Den Brink, G. R., Bleuming, S. A., Ballester, I., Van Den Brande, J. M., Keller, J. J., Offerhaus, G. J., Van Deventer, S. J. & Peppelenbosch, M. P. (2004) Bone morphogenetic protein 2 is expressed by, and acts upon, mature epithelial cells in the colon. *Gastroenterology,* 126(1)**,** 111-21.
Hasosah, M., Lemberg, D. A., Skarsgard, E. & Schreiber, R. (2008) Congenital short bowel syndrome: a case report and review of the literature. *Can J Gastroenterol,* 22(1)**,** 71-4.
Hautmann, M. B., Madsen, C. S. & Owens, G. K. (1997) A transforming growth factor beta (TGFbeta) control element drives TGFbeta-induced stimulation of smooth muscle alpha-actin gene expression in concert with two CArG elements. *J Biol Chem,* 272(16)**,** 10948-56.
He, X. C., Zhang, J., Tong, W. G., Tawfik, O., Ross, J., Scoville, D. H., Tian, Q., Zeng, X., He, X., Wiedemann, L. M., Mishina, Y. & Li, L. (2004) BMP signaling inhibits intestinal stem cell self-renewal through suppression of Wnt-beta-catenin signaling. *Nat Genet,* 36(10)**,** 1117-21.
Heanue, T. A. & Pachnis, V. (2007) Enteric nervous system development and Hirschsprung's disease: advances in genetic and stem cell studies. *Nat Rev Neurosci,* 8(6)**,** 466-79.
Hearn, C. J., Young, H. M., Ciampoli, D., Lomax, A. E. & Newgreen, D. (1999) Catenary cultures of embryonic gastrointestinal tract support organ morphogenesis, motility, neural crest cell migration, and cell differentiation. *Dev Dyn,* 214(3)**,** 239-47.
Heine, R. G. & Bines, J. E. (2002) New approaches to parenteral nutrition in infants and children. *J Paediatr Child Health,* 38(5)**,** 433-7.

Henry, G. L., Brivanlou, I. H., Kessler, D. S., Hemmati-Brivanlou, A. & Melton, D. A. (1996) TGF-beta signals and a pattern in Xenopus laevis endodermal development. *Development,* 122(3)**,** 1007-15.

Hermiston, M. L., Green, R. P. & Gordon, J. I. (1993) Chimeric-transgenic mice represent a powerful tool for studying how the proliferation and differentiation programs of intestinal epithelial cell lineages are regulated. *Proc Natl Acad Sci U S A,* 90(19)**,** 8866-70.

Hoffmann, P., Eder, R., Kunz-Schughart, L. A., Andreesen, R. & Edinger, M. (2004) Large-scale in vitro expansion of polyclonal human CD4(+)CD25high regulatory T cells. *Blood,* 104(3)**,** 895-903.

Hogan, B. L. (1996) Bone morphogenetic proteins in development. *Curr Opin Genet Dev,* 6(4)**,** 432-8.

Holmes, J. L., Van Itallie, C. M., Rasmussen, J. E. & Anderson, J. M. (2006) Claudin profiling in the mouse during postnatal intestinal development and along the gastrointestinal tract reveals complex expression patterns. *Gene Expr Patterns,* 6(6)**,** 581-8.

Howell, J. E. & McAnulty, R. J. (2006) TGF-beta: its role in asthma and therapeutic potential. *Curr Drug Targets,* 7(5)**,** 547-65.

Hsieh, E. H. & Lo, D. D. (2012) Jagged1 and Notch1 help edit M cell patterning in Peyer's patch follicle epithelium. *Dev Comp Immunol,* 37(2)**,** 306-12.

Hu, J. H., Wei, H., Jaffe, M., Airhart, N., Du, L., Angelov, S. N., Yan, J., Allen, J. K., Kang, I., Wight, T. N., Fox, K., Smith, A., Enstrom, R. & Dichek, D. A. (2015) Postnatal Deletion of the Type II Transforming Growth Factor-beta Receptor in Smooth Muscle Cells Causes Severe Aortopathy in Mice. *Arterioscler Thromb Vasc Biol,* 35(12)**,** 2647-56.

Huang da, W., Sherman, B. T. & Lempicki, R. A. (2009a) Bioinformatics enrichment tools: paths toward the comprehensive functional analysis of large gene lists. *Nucleic Acids Res,* 37(1)**,** 1-13.

Huang da, W., Sherman, B. T. & Lempicki, R. A. (2009b) Systematic and integrative analysis of large gene lists using DAVID bioinformatics resources. *Nat Protoc,* 4(1)**,** 44-57.

Huang, W. Y., Xie, W., Guo, X., Li, F., Jose, P. A. & Chen, S. Y. (2011) Smad2 and PEA3 cooperatively regulate transcription of response gene to complement 32 in TGF-beta-induced smooth muscle cell differentiation of neural crest cells. *Am J Physiol Cell Physiol,* 301(2)**,** C499-506.

Huch, M., Bonfanti, P., Boj, S. F., Sato, T., Loomans, C. J., van de Wetering, M., Sojoodi, M., Li, V. S., Schuijers, J., Gracanin, A., Ringnalda, F., Begthel, H., Hamer, K., Mulder, J., van Es, J. H., de Koning, E., Vries, R. G., Heimberg, H. & Clevers, H. (2013) Unlimited in vitro expansion of adult bi-potent pancreas progenitors through the Lgr5/R-spondin axis. *EMBO J,* 32(20)**,** 2708-21.

Huizinga, J. D. & Lammers, W. J. (2009) Gut peristalsis is governed by a multitude of cooperating mechanisms. *Am J Physiol Gastrointest Liver Physiol,* 296(1)**,** G1-8.

Huotari, M. A., Miettinen, P. J., Palgi, J., Koivisto, T., Ustinov, J., Harari, D., Yarden, Y. & Otonkoski, T. (2002) ErbB signaling regulates lineage determination of developing pancreatic islet cells in embryonic organ culture. *Endocrinology,* 143(11)**,** 4437-46.

Huysman, W. A., Tibboel, D., Bergmeijer, J. H. & Molenaar, J. C. (1991) Long-term survival of a patient with congenital short bowel and malrotation. *J Pediatr Surg,* 26(1)**,** 103-5.

Ike, O., Shimizu, Y., Okada, T., Natsume, T., Watanabe, S., Ikada, Y. & Hitomi, S. (1989) Experimental studies on an artificial esophagus for the purpose of neoesophageal epithelization using a collagen-coated silicone tube. *ASAIO Trans,* 35(3)**,** 226-8.

Ingham, P. W. & McMahon, A. P. (2001) Hedgehog signaling in animal development: paradigms and principles. *Genes Dev,* 15(23)**,** 3059-87.

Ishikawa, T. O., Tamai, Y., Li, Q., Oshima, M. & Taketo, M. M. (2003) Requirement for tumor suppressor Apc in the morphogenesis of anterior and ventral mouse embryo. *Dev Biol,* 253(2)**,** 230-46.

Iwata, J., Suzuki, A., Pelikan, R. C., Ho, T. V. & Chai, Y. (2013) Noncanonical transforming growth factor beta (TGFbeta) signaling in cranial neural crest cells causes tongue muscle developmental defects. *J Biol Chem,* 288(41)**,** 29760-70.

Janebodin, K., Buranaphatthana, W., Ieronimakis, N., Hays, A. L. & Reyes, M. (2013) An in vitro culture system for long-term expansion of epithelial and mesenchymal salivary gland cells: role of TGF-beta1 in salivary gland epithelial and mesenchymal differentiation. *Biomed Res Int,* 2013**,** 815895.

Janssen, S. & Depoortere, I. (2013) Nutrient sensing in the gut: new roads to therapeutics? *Trends Endocrinol Metab,* 24(2)**,** 92-100.

Jarvi, O. & Keyrilainen, O. (1956) On the cellular structures of the epithelial invasions in the glandular stomach of mice caused by intramural application of 20-methylcholantren. *Acta Pathol Microbiol Scand Suppl,* 39(Suppl 111)**,** 72-3.

Jiang, Y., Liu, M. T. & Gershon, M. D. (2003) Netrins and DCC in the guidance of migrating neural crest-derived cells in the developing bowel and pancreas. *Dev Biol,* 258(2)**,** 364-84.

Kaestner, K. H., Silberg, D. G., Traber, P. G. & Schutz, G. (1997) The mesenchymal winged helix transcription factor Fkh6 is required for the control of gastrointestinal proliferation and differentiation. *Genes Dev,* 11(12)**,** 1583-95.

Kanaya, T., Hase, K., Takahashi, D., Fukuda, S., Hoshino, K., Sasaki, I., Hemmi, H., Knoop, K. A., Kumar, N., Sato, M., Katsuno, T., Yokosuka, O., Toyooka, K., Nakai, K., Sakamoto, A., Kitahara, Y., Jinnohara, T., McSorley, S. J., Kaisho, T., Williams, I. R. & Ohno, H. (2012) The Ets transcription factor Spi-B is essential for the differentiation of intestinal microfold cells. *Nat Immunol,* 13(8)**,** 729-36.

Kapur, R. P., Yost, C. & Palmiter, R. D. (1992) A transgenic model for studying development of the enteric nervous system in normal and aganglionic mice. *Development,* 116(1)**,** 167-75.

Karasov, W. H., Martinez del Rio, C. & Caviedes-Vidal, E. (2011) Ecological physiology of diet and digestive systems. *Annu Rev Physiol,* 73**,** 69-93.

Karlsson, L., Lindahl, P., Heath, J. K. & Betsholtz, C. (2000) Abnormal gastrointestinal development in PDGF-A and PDGFR-(alpha) deficient mice implicates a novel mesenchymal structure with putative instructive properties in villus morphogenesis. *Development,* 127(16)**,** 3457-66.

Kaufman, S. S., Gondolesi, G. E. & Fishbein, T. M. (2003) Parenteral nutrition associated liver disease. *Semin Neonatol,* 8(5)**,** 375-81.

Kedinger, M., Simon-Assmann, P., Bouziges, F., Arnold, C., Alexandre, E. & Haffen, K. (1990) Smooth muscle actin expression during rat gut development and induction in fetal skin fibroblastic cells associated with intestinal embryonic epithelium. *Differentiation,* 43(2)**,** 87-97.

Kelly, D. A. (2006) Intestinal failure-associated liver disease: what do we know today? *Gastroenterology,* 130(2 Suppl 1)**,** S70-7.

Kelly, D. A. (2010) Preventing parenteral nutrition liver disease. *Early Hum Dev,* 86(11)**,** 683-7.

Kemp, P. (2006) History of regenerative medicine: looking backwards to move forwards. *Regen Med,* 1(5)**,** 653-69.

Khalil, B. A., Ba'ath, M. E., Aziz, A., Forsythe, L., Gozzini, S., Murphy, F., Carlson, G., Bianchi, A. & Morabito, A. (2012) Intestinal rehabilitation and bowel reconstructive surgery: improved outcomes in children with short bowel syndrome. *J Pediatr Gastroenterol Nutr,* 54(4)**,** 505-9.

Kim, H. B., Fauza, D., Garza, J., Oh, J. T., Nurko, S. & Jaksic, T. (2003a) Serial transverse enteroplasty (STEP): a novel bowel lengthening procedure. *J Pediatr Surg,* 38(3)**,** 425-9.

Kim, H. B., Lee, P. W., Garza, J., Duggan, C., Fauza, D. & Jaksic, T. (2003b) Serial transverse enteroplasty for short bowel syndrome: a case report. *J Pediatr Surg,* 38(6)**,** 881-5.

Kim, K. A., Kakitani, M., Zhao, J., Oshima, T., Tang, T., Binnerts, M., Liu, Y., Boyle, B., Park, E., Emtage, P., Funk, W. D. & Tomizuka, K. (2005) Mitogenic influence of human R-spondin1 on the intestinal epithelium. *Science,* 309(5738)**,** 1256-9.

Kim, S. S., Kaihara, S., Benvenuto, M. S., Choi, R. S., Kim, B. S., Mooney, D. J. & Vacanti, J. P. (1999) Effects of anastomosis of tissue-engineered neointestine to native small bowel. *J Surg Res,* 87(1)**,** 6-13.

Kimura, K. & Soper, R. T. (1993) A new bowel elongation technique for the short-bowel syndrome using the isolated bowel segment Iowa models. *J Pediatr Surg,* 28(6)**,** 792-4.

King, B., Carlson, G., Khalil, B. A. & Morabito, A. (2013) Intestinal bowel lengthening in children with short bowel syndrome: systematic review of the Bianchi and STEP procedures. *World J Surg,* 37(3)**,** 694-704.

Kluth, D., Jaeschke-Melli, S. & Fiegel, H. (2003) The embryology of gut rotation. *Semin Pediatr Surg,* 12(4)**,** 275-9.

Kofler, N. & Simons, M. (2016) The expanding role of neuropilin: regulation of transforming growth factor-beta and platelet-derived growth factor signaling in the vasculature. *Curr Opin Hematol,* 23(3)**,** 260-7.

Kojima, Y., Tam, O. H. & Tam, P. P. (2014) Timing of developmental events in the early mouse embryo. *Semin Cell Dev Biol,* 34**,** 65-75.

Kolterud, A., Grosse, A. S., Zacharias, W. J., Walton, K. D., Kretovich, K. E., Madison, B. B., Waghray, M., Ferris, J. E., Hu, C., Merchant, J. L., Dlugosz, A. A., Kottmann, A. H. & Gumucio, D. L. (2009) Paracrine Hedgehog signaling in stomach and intestine: new roles for hedgehog in gastrointestinal patterning. *Gastroenterology,* 137(2)**,** 618-28.

Korinek, V., Barker, N., Moerer, P., van Donselaar, E., Huls, G., Peters, P. J. & Clevers, H. (1998) Depletion of epithelial stem-cell compartments in the small intestine of mice lacking Tcf-4. *Nat Genet,* 19(4)**,** 379-83.

Kraaijenga, S., van der Molen, L., van Tinteren, H., Hilgers, F. & Smeele, L. (2014) Treatment of myogenic temporomandibular disorder: a prospective

randomized clinical trial, comparing a mechanical stretching device (TheraBite(R)) with standard physical therapy exercise. *Cranio,* 32(3)**,** 208-16.

Krishnan, K., Arnone, B. & Buchman, A. (2011) Intestinal growth factors: potential use in the treatment of inflammatory bowel disease and their role in mucosal healing. *Inflamm Bowel Dis,* 17(1)**,** 410-22.

Kudsk, K. A. (2002) Current aspects of mucosal immunology and its influence by nutrition. *Am J Surg,* 183(4)**,** 390-8.

Kulkarni, A. B., Huh, C. G., Becker, D., Geiser, A., Lyght, M., Flanders, K. C., Roberts, A. B., Sporn, M. B., Ward, J. M. & Karlsson, S. (1993) Transforming growth factor beta 1 null mutation in mice causes excessive inflammatory response and early death. *Proc Natl Acad Sci U S A,* 90(2)**,** 770-4.

Kulkarni, A. B., Thyagarajan, T. & Letterio, J. J. (2002) Function of cytokines within the TGF-beta superfamily as determined from transgenic and gene knockout studies in mice. *Curr Mol Med,* 2(3)**,** 303-27.

Kumawat, K., Menzen, M. H., Bos, I. S., Baarsma, H. A., Borger, P., Roth, M., Tamm, M., Halayko, A. J., Simoons, M., Prins, A., Postma, D. S., Schmidt, M. & Gosens, R. (2013) Noncanonical WNT-5A signaling regulates TGF-beta-induced extracellular matrix production by airway smooth muscle cells. *FASEB J,* 27(4)**,** 1631-43.

Kurahashi, M., Niwa, Y., Cheng, J., Ohsaki, Y., Fujita, A., Goto, H., Fujimoto, T. & Torihashi, S. (2008) Platelet-derived growth factor signals play critical roles in differentiation of longitudinal smooth muscle cells in mouse embryonic gut. *Neurogastroenterol Motil,* 20(5)**,** 521-31.

Kutten, J. C., McGovern, D., Hobson, C. M., Luffy, S. A., Nieponice, A., Tobita, K., Francis, R. J., Reynolds, S. D., Isenberg, J. S. & Gilbert, T. W. (2015) Decellularized tracheal extracellular matrix supports epithelial migration, differentiation, and function. *Tissue Eng Part A,* 21(1-2)**,** 75-84.

Larsen, B. M., Hrycaj, S. M., Newman, M., Li, Y. & Wellik, D. M. (2015) Mesenchymal Hox6 function is required for mouse pancreatic endocrine cell differentiation. *Development,* 142(22)**,** 3859-68.

Larsson, J., Goumans, M. J., Sjostrand, L. J., van Rooijen, M. A., Ward, D., Leveen, P., Xu, X., ten Dijke, P., Mummery, C. L. & Karlsson, S. (2001) Abnormal angiogenesis but intact hematopoietic potential in TGF-beta type I receptor-deficient mice. *EMBO J,* 20(7)**,** 1663-73.

Lawler, S., Candia, A. F., Ebner, R., Shum, L., Lopez, A. R., Moses, H. L., Wright, C. V. & Derynck, R. (1994) The murine type II TGF-beta receptor has a coincident embryonic expression and binding preference for TGF-beta 1. *Development,* 120(1)**,** 165-75.

Le Guen, L., Marchal, S., Faure, S. & de Santa Barbara, P. (2015) Mesenchymal-epithelial interactions during digestive tract development and epithelial stem cell regeneration. *Cell Mol Life Sci,* 72(20)**,** 3883-96.

Leedham, S. J., Brittan, M., McDonald, S. A. & Wright, N. A. (2005) Intestinal stem cells. *J Cell Mol Med,* 9(1)**,** 11-24.

Letterio, J. J., Geiser, A. G., Kulkarni, A. B., Roche, N. S., Sporn, M. B. & Roberts, A. B. (1994) Maternal rescue of transforming growth factor-beta 1 null mice. *Science,* 264(5167)**,** 1936-8.

Lewis, S. L. & Tam, P. P. (2006) Definitive endoderm of the mouse embryo: formation, cell fates, and morphogenetic function. *Dev Dyn,* 235(9)**,** 2315-29.

Li, C., Iness, A., Yoon, J., Grider, J. R., Murthy, K. S., Kellum, J. M. & Kuemmerle, J. F. (2015a) Noncanonical STAT3 activation regulates excess TGF-beta1 and collagen I expression in muscle of stricturing Crohn's disease. *J Immunol,* 194(7)**,** 3422-31.

Li, L. H., Lu, B., Wu, H. K., Zhang, H. & Yao, F. F. (2015b) Apigenin inhibits TGF-beta1-induced proliferation and migration of airway smooth muscle cells. *Int J Clin Exp Pathol,* 8(10)**,** 12557-63.

Li, V. S. & Clevers, H. (2012) In vitro expansion and transplantation of intestinal crypt stem cells. *Gastroenterology,* 143(1)**,** 30-4.

Lipkin, M. (1985) Growth and development of gastrointestinal cells. *Annu Rev Physiol,* 47**,** 175-97.

Liu, B., Feng, D., Lin, G., Cao, M., Kan, Y. W., Cunha, G. R. & Baskin, L. S. (2010) Signalling molecules involved in mouse bladder smooth muscle cellular differentiation. *Int J Dev Biol,* 54(1)**,** 175-80.

Lugo-Martinez, V. H., Petit, C. S., Fouquet, S., Le Beyec, J., Chambaz, J., Pincon-Raymond, M., Cardot, P. & Thenet, S. (2009) Epidermal growth factor receptor is involved in enterocyte anoikis through the dismantling of E-cadherin-mediated junctions. *Am J Physiol Gastrointest Liver Physiol,* 296(2)**,** G235-44.

Mabbott, N. A., Donaldson, D. S., Ohno, H., Williams, I. R. & Mahajan, A. (2013) Microfold (M) cells: important immunosurveillance posts in the intestinal epithelium. *Mucosal Immunol,* 6(4)**,** 666-77.

Madison, B. B., Braunstein, K., Kuizon, E., Portman, K., Qiao, X. T. & Gumucio, D. L. (2005) Epithelial hedgehog signals pattern the intestinal crypt-villus axis. *Development,* 132(2)**,** 279-89.

Mandal, K. C., Halder, P., Barman, S. & Mukhopadhyay, B. (2016) Congenital Short Bowel Syndrome due to Absent Midgut. *Indian J Pediatr*.

Mao, J., Kim, B. M., Rajurkar, M., Shivdasani, R. A. & McMahon, A. P. (2010) Hedgehog signaling controls mesenchymal growth in the developing mammalian digestive tract. *Development,* 137(10)**,** 1721-9.

Martini, F. H., Nath, J. L. & Bartholomew, E. F. (2015) *Fundamental of Anatomy & Physiology*. San Francisco: Benjamin Cummings.

Massey-Harroche, D. (2000) Epithelial cell polarity as reflected in enterocytes. *Microsc Res Tech,* 49(4)**,** 353-62.

Matsumoto, A., Hashimoto, K., Yoshioka, T. & Otani, H. (2002) Occlusion and subsequent re-canalization in early duodenal development of human embryos: integrated organogenesis and histogenesis through a possible epithelial-mesenchymal interaction. *Anat Embryol (Berl),* 205(1)**,** 53-65.

McGhee, J. D. (2013) The Caenorhabditis elegans intestine. *Wiley Interdiscip Rev Dev Biol,* 2(3)**,** 347-67.

McHugh, K. M. (1995) Molecular analysis of smooth muscle development in the mouse. *Dev Dyn,* 204(3)**,** 278-90.

McLennan, I. S. & Koishi, K. (2004) Fetal and maternal transforming growth factor-beta 1 may combine to maintain pregnancy in mice. *Biol Reprod,* 70(6)**,** 1614-8.

Merico, D., Isserlin, R., Stueker, O., Emili, A. & Bader, G. D. (2010) Enrichment map: a network-based method for gene-set enrichment visualization and interpretation. *PLoS One,* 5(11)**,** e13984.

Metzger, R., Metzger, U., Fiegel, H. C. & Kluth, D. (2011) Embryology of the midgut. *Semin Pediatr Surg,* 20(3)**,** 145-51.

Millan, F. A., Denhez, F., Kondaiah, P. & Akhurst, R. J. (1991) Embryonic gene expression patterns of TGF beta 1, beta 2 and beta 3 suggest different developmental functions in vivo. *Development,* 111(1)**,** 131-43.

Miyoshi, H., Ajima, R., Luo, C. T., Yamaguchi, T. P. & Stappenbeck, T. S. (2012) Wnt5a potentiates TGF-beta signaling to promote colonic crypt regeneration after tissue injury. *Science,* 338(6103)**,** 108-13.

Mohammed, M. K., Shao, C., Wang, J., Wei, Q., Wang, X., Collier, Z., Tang, S., Liu, H., Zhang, F., Huang, J., Guo, D., Lu, M., Liu, F., Liu, J., Ma, C., Shi, L. L., Athiviraham, A., He, T. C. & Lee, M. J. (2016) Wnt/beta-catenin signaling plays an ever-expanding role in stem cell self-renewal, tumorigenesis and cancer chemoresistance. *Genes Dis,* 3(1)**,** 11-40.

Montgomery, R. K., Mulberg, A. E. & Grand, R. J. (1999) Development of the human gastrointestinal tract: twenty years of progress. *Gastroenterology,* 116(3)**,** 702-31.

Moustakas, A. & Heldin, C. H. (2005) Non-Smad TGF-beta signals. *J Cell Sci,* 118(Pt 16)**,** 3573-84.

Moxey, P. C. & Trier, J. S. (1978) Specialized cell types in the human fetal small intestine. *Anat Rec,* 191(3)**,** 269-85.

Murphy, F., Khalil, B. A., Gozzini, S., King, B., Bianchi, A. & Morabito, A. (2011) Controlled tissue expansion in the initial management of the short bowel state. *World J Surg,* 35(5)**,** 1142-5.

Mwizerwa, O., Das, P., Nagy, N., Akbareian, S. E., Mably, J. D. & Goldstein, A. M. (2011) Gdnf is mitogenic, neurotrophic, and chemoattractive to enteric neural crest cells in the embryonic colon. *Dev Dyn,* 240(6)**,** 1402-11.

Nakagoshi, H. (2005) Functional specification in the Drosophila endoderm. *Dev Growth Differ,* 47(6)**,** 383-92.

Nakato, G., Fukuda, S., Hase, K., Goitsuka, R., Cooper, M. D. & Ohno, H. (2009) New approach for m-cell-specific molecules screening by comprehensive transcriptome analysis. *DNA Res,* 16(4)**,** 227-35.

Nataatmadja, M., West, J. & West, M. (2006) Overexpression of transforming growth factor-beta is associated with increased hyaluronan content and impairment of repair in Marfan syndrome aortic aneurysm. *Circulation,* 114(1 Suppl)**,** I371-7.

Natarajan, D., Marcos-Gutierrez, C., Pachnis, V. & de Graaff, E. (2002) Requirement of signalling by receptor tyrosine kinase RET for the directed migration of enteric nervous system progenitor cells during mammalian embryogenesis. *Development,* 129(22)**,** 5151-60.

Nayyar, N., Mazariegos, G., Ranganathan, S., Soltys, K., Bond, G., Jaffe, R., Sun, Q., Nucci, A., Kosmach, B., Squires, R., Abu-Elmagd, K. & Sindhi, R. (2010) Pediatric small bowel transplantation. *Semin Pediatr Surg,* 19(1)**,** 68-77.

Nishimura, S. L. (2009) Integrin-mediated transforming growth factor-beta activation, a potential therapeutic target in fibrogenic disorders. *Am J Pathol,* 175(4)**,** 1362-70.

Noah, T. K., Donahue, B. & Shroyer, N. F. (2011) Intestinal development and differentiation. *Exp Cell Res,* 317(19)**,** 2702-10.

Nyeng, P., Bjerke, M. A., Norgaard, G. A., Qu, X., Kobberup, S. & Jensen, J. (2011) Fibroblast growth factor 10 represses premature cell differentiation during establishment of the intestinal progenitor niche. *Dev Biol,* 349(1)**,** 20-34.

O'Keeffe, G. W., Gutierrez, H., Howard, L., Laurie, C. W., Osorio, C., Gavalda, N., Wyatt, S. L. & Davies, A. M. (2016) Region-specific role of growth differentiation factor-5 in the establishment of sympathetic innervation. *Neural Dev,* 11(1)**,** 4.

Okawada, M., Maria, H. M. & Teitelbaum, D. H. (2011) Distraction induced enterogenesis: a unique mouse model using polyethylene glycol. *J Surg Res,* 170(1)**,** 41-7.

Ordonez, P., Sondheimer, J. M., Fidanza, S., Wilkening, G. & Hoffenberg, E. J. (2006) Long-term outcome of a patient with congenital short bowel syndrome. *J Pediatr Gastroenterol Nutr,* 42(5)**,** 576-80.

Orlando, G., Wood, K. J., Stratta, R. J., Yoo, J. J., Atala, A. & Soker, S. (2011) Regenerative medicine and organ transplantation: past, present, and future. *Transplantation,* 91(12)**,** 1310-7.

Oshima, M., Oshima, H. & Taketo, M. M. (1996) TGF-beta receptor type II deficiency results in defects of yolk sac hematopoiesis and vasculogenesis. *Dev Biol,* 179(1)**,** 297-302.

Pachnis, V., Mankoo, B. & Costantini, F. (1993) Expression of the c-ret proto-oncogene during mouse embryogenesis. *Development,* 119(4)**,** 1005-17.

Pack, M., Solnica-Krezel, L., Malicki, J., Neuhauss, S. C., Schier, A. F., Stemple, D. L., Driever, W. & Fishman, M. C. (1996) Mutations affecting development of zebrafish digestive organs. *Development,* 123**,** 321-8.

Paclik, D., Lohse, K., Wiedenmann, B., Dignass, A. U. & Sturm, A. (2008) Galectin-2 and -4, but not galectin-1, promote intestinal epithelial wound healing in vitro through a TGF-beta-independent mechanism. *Inflamm Bowel Dis,* 14(10)**,** 1366-72.

Pataki, I., Szabo, J., Varga, P., Berkes, A., Nagy, A., Murphy, F., Morabito, A., Rakoczy, G. & Cserni, T. (2013) Recycling of bowel content: the importance of the right timing. *J Pediatr Surg,* 48(3)**,** 579-84.

Pelton, R. W., Saxena, B., Jones, M., Moses, H. L. & Gold, L. I. (1991) Immunohistochemical localization of TGF beta 1, TGF beta 2, and TGF beta 3 in the mouse embryo: expression patterns suggest multiple roles during embryonic development. *J Cell Biol,* 115(4)**,** 1091-105.

Penttila, I. A., van Spriel, A. B., Zhang, M. F., Xian, C. J., Steeb, C. B., Cummins, A. G., Zola, H. & Read, L. C. (1998) Transforming growth factor-beta levels in maternal milk and expression in postnatal rat duodenum and ileum. *Pediatr Res,* 44(4)**,** 524-31.

Piersma, B., Bank, R. A. & Boersema, M. (2015) Signaling in Fibrosis: TGF-beta, WNT, and YAP/TAZ Converge. *Front Med (Lausanne),* 2**,** 59.

Pitera, J. E., Smith, V. V., Woolf, A. S. & Milla, P. J. (2001) Embryonic gut anomalies in a mouse model of retinoic Acid-induced caudal regression syndrome: delayed gut looping, rudimentary cecum, and anorectal anomalies. *Am J Pathol,* 159(6)**,** 2321-9.

Potten, C. S., Owen, G. & Booth, D. (2002) Intestinal stem cells protect their genome by selective segregation of template DNA strands. *J Cell Sci,* 115(Pt 11)**,** 2381-8.

Qu, Z. H., Yang, Z. C., Chen, L., Lv, Z. D., Yi, M. J. & Ran, N. (2012) Inhibition airway remodeling and transforming growth factor-beta1/Smad signaling pathway by astragalus extract in asthmatic mice. *Int J Mol Med,* 29(4)**,** 564-8.

Quackenbush, J. (2001) Computational analysis of microarray data. *Nat Rev Genet,* 2(6)**,** 418-27.

Quinlan, J. M., Yu, W. Y., Hornsey, M. A., Tosh, D. & Slack, J. M. (2006) In vitro culture of embryonic mouse intestinal epithelium: cell differentiation and introduction of reporter genes. *BMC Dev Biol,* 6**,** 24.

Quiros-Tejeira, R. E., Ament, M. E., Reyen, L., Herzog, F., Merjanian, M., Olivares-Serrano, N. & Vargas, J. H. (2004) Long-term parenteral nutritional support and intestinal adaptation in children with short bowel syndrome: a 25-year experience. *J Pediatr,* 145(2)**,** 157-63.

Ramalho-Santos, M., Melton, D. A. & McMahon, A. P. (2000) Hedgehog signals regulate multiple aspects of gastrointestinal development. *Development,* 127(12)**,** 2763-72.

Raschperger, E., Engstrom, U., Pettersson, R. F. & Fuxe, J. (2004) CLMP, a novel member of the CTX family and a new component of epithelial tight junctions. *J Biol Chem,* 279(1)**,** 796-804.

Reeder, A. L., Zaremba, K. M., Liebl, R. M., Kowalkowski, A. & Nichol, P. F. (2014) Exogenous Sonic hedgehog protein does not rescue cultured intestine from atresia formation. *J Surg Res,* 187(1)**,** 14-8.

Rehfeld, J. F. (2004) A centenary of gastrointestinal endocrinology. *Horm Metab Res,* 36(11-12)**,** 735-41.

Rescorla, F. J., Shedd, F. J., Grosfeld, J. L., Vane, D. W. & West, K. W. (1990) Anomalies of intestinal rotation in childhood: analysis of 447 cases. *Surgery,* 108(4)**,** 710-5; discussion 715-6.

Rinker, B. & Thornton, B. P. (2014) Skin-sparing mastectomy and immediate tissue expander breast reconstruction in patients with macromastia using the Passot breast reduction pattern. *Ann Plast Surg,* 72(6)**,** S158-64.

Roberts, D. J. (2000) Molecular mechanisms of development of the gastrointestinal tract. *Dev Dyn,* 219(2)**,** 109-20.

Roberts, D. J., Johnson, R. L., Burke, A. C., Nelson, C. E., Morgan, B. A. & Tabin, C. (1995) Sonic hedgehog is an endodermal signal inducing Bmp-4 and Hox genes during induction and regionalization of the chick hindgut. *Development,* 121(10)**,** 3163-74.

Roberts, D. J., Smith, D. M., Goff, D. J. & Tabin, C. J. (1998) Epithelial-mesenchymal signaling during the regionalization of the chick gut. *Development,* 125(15)**,** 2791-801.

Rogers, S. A., Ryan, G., Purchio, A. F. & Hammerman, M. R. (1993) Metanephric transforming growth factor-beta 1 regulates nephrogenesis in vitro. *Am J Physiol,* 264(6 Pt 2)**,** F996-1002.

Romao, R. L., Ozgediz, D., de Silva, N., Chiu, P., Langer, J. & Wales, P. W. (2011) Preserving bowel length with a transluminal stent in neonates with multiple intestinal anastomoses: a case series and review of the literature. *J Pediatr Surg,* 46(7)**,** 1368-72.

Rosenthal, A. (1999) The GDNF protein family: gene ablation studies reveal what they really do and how. *Neuron,* 22(2)**,** 201-3.

Rubin, D. C. (2007) Intestinal morphogenesis. *Curr Opin Gastroenterol,* 23(2)**,** 111-4.

Sadler, T. W. (1990) *Champter 14. Digestive system. in Langman's medical embryology.* (6th edition; original illustrations by Jill Leland. ed.). Baltimore, USA: Williams & Wilkins.

Saeed, A. I., Sharov, V., White, J., Li, J., Liang, W., Bhagabati, N., Braisted, J., Klapa, M., Currier, T., Thiagarajan, M., Sturn, A., Snuffin, M., Rezantsev, A., Popov, D., Ryltsov, A., Kostukovich, E., Borisovsky, I., Liu, Z.,

Vinsavich, A., Trush, V. & Quackenbush, J. (2003) TM4: a free, open-source system for microarray data management and analysis. *Biotechniques,* 34(2)**,** 374-8.

Sala, F. G., Kunisaki, S. M., Ochoa, E. R., Vacanti, J. & Grikscheit, T. C. (2009) Tissue-engineered small intestine and stomach form from autologous tissue in a preclinical large animal model. *J Surg Res,* 156(2)**,** 205-12.

Sato, A. (2007) Tuft cells. *Anat Sci Int,* 82(4)**,** 187-99.

Sato, A., Hisanaga, Y., Inoue, Y., Nagato, T. & Toh, H. (2002) Three-dimensional structure of apical vesicles of tuft cells in the main excretory duct of the rat submandibular gland. *Eur J Morphol,* 40(4)**,** 235-9.

Sato, A. & Miyoshi, S. (1997) Fine structure of tuft cells of the main excretory duct epithelium in the rat submandibular gland. *Anat Rec,* 248(3)**,** 325-31.

Sato, T. & Clevers, H. (2013a) Growing self-organizing mini-guts from a single intestinal stem cell: mechanism and applications. *Science,* 340(6137)**,** 1190-4.

Sato, T. & Clevers, H. (2013b) Primary mouse small intestinal epithelial cell cultures. *Methods Mol Biol,* 945**,** 319-28.

Sato, T., Stange, D. E., Ferrante, M., Vries, R. G., Van Es, J. H., Van den Brink, S., Van Houdt, W. J., Pronk, A., Van Gorp, J., Siersema, P. D. & Clevers, H. (2011a) Long-term expansion of epithelial organoids from human colon, adenoma, adenocarcinoma, and Barrett's epithelium. *Gastroenterology,* 141(5)**,** 1762-72.

Sato, T., van Es, J. H., Snippert, H. J., Stange, D. E., Vries, R. G., van den Born, M., Barker, N., Shroyer, N. F., van de Wetering, M. & Clevers, H. (2011b) Paneth cells constitute the niche for Lgr5 stem cells in intestinal crypts. *Nature,* 469(7330)**,** 415-8.

Saxena, A. K., Baumgart, H., Komann, C., Ainoedhofer, H., Soltysiak, P., Kofler, K. & Hollwarth, M. E. (2010) Esophagus tissue engineering: in situ generation of rudimentary tubular vascularized esophageal conduit using the ovine model. *J Pediatr Surg,* 45(5)**,** 859-64.

Schalamon, J., Schober, P. H., Gallippi, P., Matthyssens, L. & Hollwarth, M. E. (1999) Congenital short-bowel; a case study and review of the literature. *Eur J Pediatr Surg,* 9(4)**,** 248-50.

Schall, K. A., Holoyda, K. A., Grant, C. N., Levin, D. E., Torres, E. R., Maxwell, A., Pollack, H. A., Moats, R. A., Frey, M. R., Darehzereshki, A., Al Alam, D., Lien, C. & Grikscheit, T. C. (2015) Adult zebrafish intestine resection: a novel model of short bowel syndrome, adaptation, and intestinal stem cell regeneration. *Am J Physiol Gastrointest Liver Physiol,* 309(3)**,** G135-45.

Schmid, P., Cox, D., Bilbe, G., Maier, R. & McMaster, G. K. (1991) Differential expression of TGF beta 1, beta 2 and beta 3 genes during mouse embryogenesis. *Development,* 111(1)**,** 117-30.

Schmidt, G. H., Winton, D. J. & Ponder, B. A. (1988) Development of the pattern of cell renewal in the crypt-villus unit of chimaeric mouse small intestine. *Development,* 103(4)**,** 785-90.

Schmierer, B. & Hill, C. S. (2007) TGFbeta-SMAD signal transduction: molecular specificity and functional flexibility. *Nat Rev Mol Cell Biol,* 8(12)**,** 970-82.

Schneider, R. (1992) The human protooncogene ret: a communicative cadherin? *Trends Biochem Sci,* 17(11)**,** 468-9.

Schreiber, D., Jost, V., Bischof, M., Seebach, K., Lammers, W. J., Douglas, R. & Schafer, K. H. (2014) Motility patterns of ex vivo intestine segments depend on perfusion mode. *World J Gastroenterol,* 20(48)**,** 18216-27.

Schroder, N. & Gossler, A. (2002) Expression of Notch pathway components in fetal and adult mouse small intestine. *Gene Expr Patterns,* 2(3-4)**,** 247-50.

Scoville, D. H., Sato, T., He, X. C. & Li, L. (2008) Current view: intestinal stem cells and signaling. *Gastroenterology,* 134(3)**,** 849-64.

Shah, N. M., Groves, A. K. & Anderson, D. J. (1996) Alternative neural crest cell fates are instructively promoted by TGFbeta superfamily members. *Cell,* 85(3)**,** 331-43.

Shannon, P., Markiel, A., Ozier, O., Baliga, N. S., Wang, J. T., Ramage, D., Amin, N., Schwikowski, B. & Ideker, T. (2003) Cytoscape: a software environment for integrated models of biomolecular interaction networks. *Genome Res,* 13(11)**,** 2498-504.

Sherwood, R. I., Chen, T. Y. & Melton, D. A. (2009) Transcriptional dynamics of endodermal organ formation. *Dev Dyn,* 238(1)**,** 29-42.

Shull, M. M., Ormsby, I., Kier, A. B., Pawlowski, S., Diebold, R. J., Yin, M., Allen, R., Sidman, C., Proetzel, G., Calvin, D. & et al. (1992) Targeted disruption of the mouse transforming growth factor-beta 1 gene results in multifocal inflammatory disease. *Nature,* 359(6397)**,** 693-9.

Shyer, A. E., Tallinen, T., Nerurkar, N. L., Wei, Z., Gil, E. S., Kaplan, D. L., Tabin, C. J. & Mahadevan, L. (2013) Villification: how the gut gets its villi. *Science,* 342(6155)**,** 212-8.

Sinha, S., Hoofnagle, M. H., Kingston, P. A., McCanna, M. E. & Owens, G. K. (2004) Transforming growth factor-beta1 signaling contributes to development of smooth muscle cells from embryonic stem cells. *Am J Physiol Cell Physiol,* 287(6)**,** C1560-8.

Snippert, H. J., van der Flier, L. G., Sato, T., van Es, J. H., van den Born, M., Kroon-Veenboer, C., Barker, N., Klein, A. M., van Rheenen, J., Simons, B. D. & Clevers, H. (2010) Intestinal crypt homeostasis results from neutral competition between symmetrically dividing Lgr5 stem cells. *Cell,* 143(1)**,** 134-44.

Snowball, J., Ambalavanan, M., Whitsett, J. & Sinner, D. (2015) Endodermal Wnt signaling is required for tracheal cartilage formation. *Dev Biol,* 405(1)**,** 56-70.

Soden, J. S. (2010) Clinical assessment of the child with intestinal failure. *Semin Pediatr Surg,* 19(1)**,** 10-9.

Spence, J. R., Lauf, R. & Shroyer, N. F. (2011) Vertebrate intestinal endoderm development. *Dev Dyn,* 240(3)**,** 501-20.

Stainier, D. Y. (2005) No organ left behind: tales of gut development and evolution. *Science,* 307(5717)**,** 1902-4.

Sternini, C., Anselmi, L. & Rozengurt, E. (2008) Enteroendocrine cells: a site of 'taste' in gastrointestinal chemosensing. *Curr Opin Endocrinol Diabetes Obes,* 15(1)**,** 73-8.

Storey, J. D. & Tibshirani, R. (2003) Statistical significance for genomewide studies. *Proc Natl Acad Sci U S A,* 100(16)**,** 9440-5.

Stringer, E. J., Duluc, I., Saandi, T., Davidson, I., Bialecka, M., Sato, T., Barker, N., Clevers, H., Pritchard, C. A., Winton, D. J., Wright, N. A., Freund, J. N., Deschamps, J. & Beck, F. (2012) Cdx2 determines the fate of postnatal intestinal endoderm. *Development,* 139(3)**,** 465-74.

Sturm, A. & Dignass, A. U. (2008) Epithelial restitution and wound healing in inflammatory bowel disease. *World J Gastroenterol,* 14(3)**,** 348-53.
Sukegawa, A., Narita, T., Kameda, T., Saitoh, K., Nohno, T., Iba, H., Yasugi, S. & Fukuda, K. (2000) The concentric structure of the developing gut is regulated by Sonic hedgehog derived from endodermal epithelium. *Development,* 127(9)**,** 1971-80.
Sullins, V. F., Wagner, J. P., Suwarnasarn, A. T., Lee, S. L., Wu, B. M. & Dunn, J. C. (2014) A novel biodegradable device for intestinal lengthening. *J Pediatr Surg,* 49(1)**,** 109-13; discussion 113.
Sun, G., Liu, W., Fan, Z., Zhang, D., Han, Y., Xu, L., Qi, J., Zhang, S., Gao, B. T., Bai, X., Li, J., Chai, R. & Wang, H. (2016) The Three-Dimensional Culture System with Matrigel and Neurotrophic Factors Preserves the Structure and Function of Spiral Ganglion Neuron In Vitro. *Neural Plast,* 2016**,** 4280407.
Tai, G., Ranjzad, P., Marriage, F., Rehman, S., Denley, H., Dixon, J., Mitchell, K., Day, P. J. & Woolf, A. S. (2013) Cytokeratin 15 marks basal epithelia in developing ureters and is upregulated in a subset of urothelial cell carcinomas. *PLoS One,* 8(11)**,** e81167.
Takashima, S., Adams, K. L., Ortiz, P. A., Ying, C. T., Moridzadeh, R., Younossi-Hartenstein, A. & Hartenstein, V. (2011) Development of the Drosophila entero-endocrine lineage and its specification by the Notch signaling pathway. *Dev Biol,* 353(2)**,** 161-72.
Tam, P. K., Gould, S. J., Martucciello, G., Biddolph, S., Takahashi, M. & Jasonni, V. (1996) Ret protein in the human fetal rectum. *J Pediatr Surg,* 31(4)**,** 568-71.
Thompson, J. S. (2014) Short Bowel Syndrome and Malabsorption - Causes and Prevention. *Viszeralmedizin,* 30(3)**,** 174-8.
Thorsen, K., Drengstig, T. & Ruoff, P. (2014) Transepithelial glucose transport and Na+/K+ homeostasis in enterocytes: an integrative model. *Am J Physiol Cell Physiol,* 307(4)**,** C320-37.
Torihashi, S., Hattori, T., Hasegawa, H., Kurahashi, M., Ogaeri, T. & Fujimoto, T. (2009) The expression and crucial roles of BMP signaling in development of smooth muscle progenitor cells in the mouse embryonic gut. *Differentiation,* 77(3)**,** 277-89.
Totonelli, G., Maghsoudlou, P., Garriboli, M., Riegler, J., Orlando, G., Burns, A. J., Sebire, N. J., Smith, V. V., Fishman, J. M., Ghionzoli, M., Turmaine, M., Birchall, M. A., Atala, A., Soker, S., Lythgoe, M. F., Seifalian, A., Pierro, A., Eaton, S. & De Coppi, P. (2012) A rat decellularized small bowel scaffold that preserves villus-crypt architecture for intestinal regeneration. *Biomaterials,* 33(12)**,** 3401-10.
Tremblay, K. D. & Zaret, K. S. (2005) Distinct populations of endoderm cells converge to generate the embryonic liver bud and ventral foregut tissues. *Dev Biol,* 280(1)**,** 87-99.
Trojanowska, M. (2009) Noncanonical transforming growth factor beta signaling in scleroderma fibrosis. *Curr Opin Rheumatol,* 21(6)**,** 623-9.
Ueno, T. & Fukuzawa, M. (2010) Current status of intestinal transplantation. *Surg Today,* 40(12)**,** 1112-22.
Uesaka, T., Nagashimada, M. & Enomoto, H. (2015) Neuronal Differentiation in Schwann Cell Lineage Underlies Postnatal Neurogenesis in the Enteric Nervous System. *J Neurosci,* 35(27)**,** 9879-88.

Uesaka, T., Young, H. M., Pachnis, V. & Enomoto, H. (2016) Development of the intrinsic and extrinsic innervation of the gut. *Dev Biol*.

Vacanti, J. P., Morse, M. A., Saltzman, W. M., Domb, A. J., Perez-Atayde, A. & Langer, R. (1988) Selective cell transplantation using bioabsorbable artificial polymers as matrices. *J Pediatr Surg,* 23(1 Pt 2)**,** 3-9.

van den Brink, G. R. (2007) Hedgehog signaling in development and homeostasis of the gastrointestinal tract. *Physiol Rev,* 87(4)**,** 1343-75.

Van Der Werf, C. S., Wabbersen, T. D., Hsiao, N. H., Paredes, J., Etchevers, H. C., Kroisel, P. M., Tibboel, D., Babarit, C., Schreiber, R. A., Hoffenberg, E. J., Vekemans, M., Zeder, S. L., Ceccherini, I., Lyonnet, S., Ribeiro, A. S., Seruca, R., Te Meerman, G. J., van Ijzendoorn, S. C., Shepherd, I. T., Verheij, J. B. & Hofstra, R. M. (2012) CLMP is required for intestinal development, and loss-of-function mutations cause congenital short-bowel syndrome. *Gastroenterology,* 142(3)**,** 453-462 e3.

VanDussen, K. L., Marinshaw, J. M., Shaikh, N., Miyoshi, H., Moon, C., Tarr, P. I., Ciorba, M. A. & Stappenbeck, T. S. (2015) Development of an enhanced human gastrointestinal epithelial culture system to facilitate patient-based assays. *Gut,* 64(6)**,** 911-20.

Veeman, M. T., Axelrod, J. D. & Moon, R. T. (2003) A second canon. Functions and mechanisms of beta-catenin-independent Wnt signaling. *Dev Cell,* 5(3)**,** 367-77.

Wales, P. W., de Silva, N., Kim, J., Lecce, L., To, T. & Moore, A. (2004) Neonatal short bowel syndrome: population-based estimates of incidence and mortality rates. *J Pediatr Surg,* 39(5)**,** 690-5.

Wales, P. W., Nasr, A., de Silva, N. & Yamada, J. (2010) Human growth hormone and glutamine for patients with short bowel syndrome. *Cochrane Database Syst Rev,* (6)**,** CD006321.

Walker, C. R., Hautefort, I., Dalton, J. E., Overweg, K., Egan, C. E., Bongaerts, R. J., Newton, D. J., Cruickshank, S. M., Andrew, E. M. & Carding, S. R. (2013) Intestinal intraepithelial lymphocyte-enterocyte crosstalk regulates production of bactericidal angiogenin 4 by Paneth cells upon microbial challenge. *PLoS One,* 8(12)**,** e84553.

Walton, K. D. & Kolterud, A. (2014) Mouse fetal whole intestine culture system for ex vivo manipulation of signaling pathways and three-dimensional live imaging of villus development. *J Vis Exp,* (91)**,** e51817.

Walton, K. D., Kolterud, A., Czerwinski, M. J., Bell, M. J., Prakash, A., Kushwaha, J., Grosse, A. S., Schnell, S. & Gumucio, D. L. (2012) Hedgehog-responsive mesenchymal clusters direct patterning and emergence of intestinal villi. *Proc Natl Acad Sci U S A,* 109(39)**,** 15817-22.

Walton, K. D., Whidden, M., Kolterud, A., S, K. S., Czerwinski, M. J., Kushwaha, J., Parmar, N., Chandhrasekhar, D., Freddo, A. M., Schnell, S. & Gumucio, D. L. (2016) Villification in the mouse: Bmp signals control intestinal villus patterning. *Development,* 143(3)**,** 427-36.

Waterston, R. H., Lindblad-Toh, K., Birney, E., Rogers, J., Abril, J. F., Agarwal, P., Agarwala, R., Ainscough, R., Alexandersson, M., An, P., Antonarakis, S. E., Attwood, J., Baertsch, R., Bailey, J., Barlow, K., Beck, S., Berry, E., Birren, B., Bloom, T., Bork, P., Botcherby, M., Bray, N., Brent, M. R., Brown, D. G., Brown, S. D., Bult, C., Burton, J., Butler, J., Campbell, R. D., Carninci, P., Cawley, S., Chiaromonte, F., Chinwalla, A. T., Church, D. M., Clamp, M., Clee, C., Collins, F. S., Cook, L. L., Copley, R. R., Coulson, A.,

Couronne, O., Cuff, J., Curwen, V., Cutts, T., Daly, M., David, R., Davies, J., Delehaunty, K. D., Deri, J., Dermitzakis, E. T., Dewey, C., Dickens, N. J., Diekhans, M., Dodge, S., Dubchak, I., Dunn, D. M., Eddy, S. R., Elnitski, L., Emes, R. D., Eswara, P., Eyras, E., Felsenfeld, A., Fewell, G. A., Flicek, P., Foley, K., Frankel, W. N., Fulton, L. A., Fulton, R. S., Furey, T. S., Gage, D., Gibbs, R. A., Glusman, G., Gnerre, S., Goldman, N., Goodstadt, L., Grafham, D., Graves, T. A., Green, E. D., Gregory, S., Guigo, R., Guyer, M., Hardison, R. C., Haussler, D., Hayashizaki, Y., Hillier, L. W., Hinrichs, A., Hlavina, W., Holzer, T., Hsu, F., Hua, A., Hubbard, T., Hunt, A., Jackson, I., Jaffe, D. B., Johnson, L. S., Jones, M., Jones, T. A., Joy, A., Kamal, M., Karlsson, E. K., et al. (2002) Initial sequencing and comparative analysis of the mouse genome. *Nature,* 420(6915)**,** 520-62.

Watson, A. J. & Hughes, K. R. (2012) TNF-alpha-induced intestinal epithelial cell shedding: implications for intestinal barrier function. *Ann N Y Acad Sci,* 1258**,** 1-8.

Wehkamp, J., Fellermann, K., Herrlinger, K. R., Bevins, C. L. & Stange, E. F. (2005) Mechanisms of disease: defensins in gastrointestinal diseases. *Nat Clin Pract Gastroenterol Hepatol,* 2(9)**,** 406-15.

Weinstein, M., Monga, S. P., Liu, Y., Brodie, S. G., Tang, Y., Li, C., Mishra, L. & Deng, C. X. (2001) Smad proteins and hepatocyte growth factor control parallel regulatory pathways that converge on beta1-integrin to promote normal liver development. *Mol Cell Biol,* 21(15)**,** 5122-31.

Wells, J. M. & Spence, J. R. (2014) How to make an intestine. *Development,* 141(4)**,** 752-60.

Wen, J., Chiang, Y. J., Gao, C., Xue, H., Xu, J., Ning, Y., Hodes, R. J., Gao, X. & Chen, Y. G. (2010) Loss of Dact1 disrupts planar cell polarity signaling by altering dishevelled activity and leads to posterior malformation in mice. *J Biol Chem,* 285(14)**,** 11023-30.

Wiles, A. & Woodward, J. M. (2009) Recent advances in the management of intestinal failure-associated liver disease. *Curr Opin Clin Nutr Metab Care,* 12(3)**,** 265-72.

Wilm, B., Ipenberg, A., Hastie, N. D., Burch, J. B. & Bader, D. M. (2005) The serosal mesothelium is a major source of smooth muscle cells of the gut vasculature. *Development,* 132(23)**,** 5317-28.

Winesett, M. P., Ramsey, G. W. & Barnard, J. A. (1996) Type II TGF(beta) receptor expression in intestinal cell lines and in the intestinal tract. *Carcinogenesis,* 17(5)**,** 989-95.

Wrana, J. L. (2013) Signaling by the TGFbeta superfamily. *Cold Spring Harb Perspect Biol,* 5(10)**,** a011197.

Wu, M. Y. & Hill, C. S. (2009) Tgf-beta superfamily signaling in embryonic development and homeostasis. *Dev Cell,* 16(3)**,** 329-43.

Yamada, Y., Mashima, H., Sakai, T., Matsuhashi, T., Jin, M. & Ohnishi, H. (2013) Functional roles of TGF-beta1 in intestinal epithelial cells through Smad-dependent and non-Smad pathways. *Dig Dis Sci,* 58(5)**,** 1207-17.

Yang, S. P., Woolf, A. S., Yuan, H. T., Scott, R. J., Risdon, R. A., O'Hare, M. J. & Winyard, P. J. (2000) Potential biological role of transforming growth factor-beta1 in human congenital kidney malformations. *Am J Pathol,* 157(5)**,** 1633-47.

Yang, Z., Mu, Z., Dabovic, B., Jurukovski, V., Yu, D., Sung, J., Xiong, X. & Munger, J. S. (2007) Absence of integrin-mediated TGFbeta1 activation in

vivo recapitulates the phenotype of TGFbeta1-null mice. *J Cell Biol,* 176(6)**,** 787-93.

Yardley, I., Khalil, B., Minford, J. & Morabito, A. (2008) Multiple jejunoileal atresia and colonic atresia managed by multiple primary anastomosis with a single gastroperineal transanastomotic tube without stomas. *J Pediatr Surg,* 43(11)**,** e45-6.

Yesilada, A. K., Akcal, A., Dagdelen, D., Sucu, D. O., Kilinc, L. & Tatlidede, H. S. (2013) The feasibility of tissue expansion in reconstruction of congenital and aquired deformities of pediatric patients. *Int J Burns Trauma,* 3(3)**,** 144-50.

Young, H. M., Bergner, A. J. & Muller, T. (2003) Acquisition of neuronal and glial markers by neural crest-derived cells in the mouse intestine. *J Comp Neurol,* 456(1)**,** 1-11.

Young, H. M., Ciampoli, D., Hsuan, J. & Canty, A. J. (1999) Expression of Ret-, p75(NTR)-, Phox2a-, Phox2b-, and tyrosine hydroxylase-immunoreactivity by undifferentiated neural crest-derived cells and different classes of enteric neurons in the embryonic mouse gut. *Dev Dyn,* 216(2)**,** 137-52.

Yui, S., Nakamura, T., Sato, T., Nemoto, Y., Mizutani, T., Zheng, X., Ichinose, S., Nagaishi, T., Okamoto, R., Tsuchiya, K., Clevers, H. & Watanabe, M. (2012) Functional engraftment of colon epithelium expanded in vitro from a single adult Lgr5(+) stem cell. *Nat Med,* 18(4)**,** 618-23.

Zakhem, E., Raghavan, S., Gilmont, R. R. & Bitar, K. N. (2012) Chitosan-based scaffolds for the support of smooth muscle constructs in intestinal tissue engineering. *Biomaterials,* 33(19)**,** 4810-7.

Zhang, C., Murphy, S. V. & Atala, A. (2014) Regenerative medicine in urology. *Semin Pediatr Surg,* 23(3)**,** 106-11.

Zhang, M., Liao, Y. & Lonnerdal, B. (2016a) Milk growth factors and expression of small intestinal growth factor receptors during the perinatal period in mice. *Pediatr Res.*

Zhang, P., Hou, S., Chen, J., Zhang, J., Lin, F., Ju, R., Cheng, X., Ma, X., Song, Y., Zhang, Y., Zhu, M., Du, J., Lan, Y. & Yang, X. (2016b) Smad4 Deficiency in Smooth Muscle Cells Initiates the Formation of Aortic Aneurysm. *Circ Res,* 118(3)**,** 388-99.

Zhang, Y. E. (2009) Non-Smad pathways in TGF-beta signaling. *Cell Res,* 19(1)**,** 128-39.

Zorn, A. M. & Wells, J. M. (2009) Vertebrate endoderm development and organ formation. *Annu Rev Cell Dev Biol,* 25**,** 221-51.